ISSN 1007-9327 (print)
ISSN 2219-2840 (online)

World Journal of *Gastroenterology*

World J Gastroenterol 2018 February 28; 24(8): 877-956

Published by Baishideng Publishing Group Inc

World Journal of Gastroenterology

Contents

Weekly Volume 24 Number 8 February 28, 2018

ABOUT COVER

Editorial board member of *World Journal of Gastroenterology*, Shuhei Komatsu, MD, PhD, Associate Professor, Division of Digestive Surgery, Department of Surgery, Kyoto Prefectural University of Medicine, Kyoto 602-8566, Japan

AIMS AND SCOPE

World Journal of Gastroenterology (*World J Gastroenterol*, *WJG*, print ISSN 1007-9327, online ISSN 2219-2840, DOI: 10.3748) is a peer-reviewed open access journal. *WJG* was established on October 1, 1995. It is published weekly on the 7th, 14th, 21st, and 28th each month. The *WJG* Editorial Board consists of 642 experts in gastroenterology and hepatology from 59 countries.

The primary task of *WJG* is to rapidly publish high-quality original articles, reviews, and commentaries in the fields of gastroenterology, hepatology, gastrointestinal endoscopy, gastrointestinal surgery, hepatobiliary surgery, gastrointestinal oncology, gastrointestinal radiation oncology, gastrointestinal imaging, gastrointestinal interventional therapy, gastrointestinal infectious diseases, gastrointestinal pharmacology, gastrointestinal pathophysiology, gastrointestinal pathology, evidence-based medicine in gastroenterology, pancreatology, gastrointestinal laboratory medicine, gastrointestinal molecular biology, gastrointestinal immunology, gastrointestinal microbiology, gastrointestinal genetics, gastrointestinal translational medicine, gastrointestinal diagnostics, and gastrointestinal therapeutics. *WJG* is dedicated to become an influential and prestigious journal in gastroenterology and hepatology, to promote the development of above disciplines, and to improve the diagnostic and therapeutic skill and expertise of clinicians.

INDEXING/ABSTRACTING

World Journal of Gastroenterology (*WJG*) is now indexed in Current Contents®/Clinical Medicine, Science Citation Index Expanded (also known as SciSearch®), Journal Citation Reports®, Index Medicus, MEDLINE, PubMed, PubMed Central and Directory of Open Access Journals. The 2017 edition of Journal Citation Reports® cites the 2016 impact factor for *WJG* as 3.365 (5-year impact factor: 3.176), ranking *WJG* as 29th among 79 journals in gastroenterology and hepatology (quartile in category Q2).

NAME OF JOURNAL
World Journal of Gastroenterology

ISSN
ISSN 1007-9327 (print)
ISSN 2219-2840 (online)

LAUNCH DATE
October 1, 1995

FREQUENCY
Weekly

EDITORIAL OFFICE
Ze-Mao Gong, Director
World Journal of Gastroenterology
Baishideng Publishing Group Inc
7901 Stoneridge Drive, Suite 501,
Pleasanton, CA 94588, USA
Telephone: +1-925-2238242
Fax: +1-925-2238243
E-mail: editorialoffice@wjgnet.com
Help Desk: http://www.f6publishing.com/helpdesk
http://www.wjgnet.com

PUBLISHER
Baishideng Publishing Group Inc
7901 Stoneridge Drive, Suite 501,
Pleasanton, CA 94588, USA
Telephone: +1-925-2238242
Fax: +1-925-2238243
E-mail: bpgoffice@wjgnet.com
Help Desk: http://www.f6publishing.com/helpdesk
http://www.wjgnet.com

PUBLICATION DATE
February 28, 2018

INSTRUCTIONS TO AUTHORS
Full instructions are available online at http://www.wjgnet.com/bpg/gerinfo/204

ONLINE SUBMISSION
http://www.f6publishing.com

World Journal of Gastroenterology

Submit a Manuscript: http://www.f6publishing.com

World J Gastroenterol 2018 February 28; 24(8): 877-881

DOI: 10.3748/wjg.v24.i8.877

ISSN 1007-9327 (print) ISSN 2219-2840 (online)

MINIREVIEWS

Regulation of the intestinal immune system by flavonoids and its utility in chronic inflammatory bowel disease

Harald Peter Hoensch, Benno Weigmann

Harald Peter Hoensch, Private Practice Gastroenterology, Marien hospital, Darmstadt 64285, Germany

Benno Weigmann, Department of Medicine 1, University Medical Center, Erlangen 91052, Germany

ORCID number: Harald Peter Hoensch (0000-0002-0741-3911); Benno Weigmann (0000-0002-2398-0844).

Author contributions: Hoensch HP and Weigmann B contributed equally to this work, generated the figures and wrote the manuscript.

Conflict-of-interest statement: No potential conflicts of interest relevant to this article were reported.

Manuscript source: Unsolicited manuscript

Correspondence to: Benno Weigmann, PhD, Senior Scientist, Department of Medicine 1, University Medical Center, Hartmann Str. 14, Erlangen D-91052, Germany. benno.weigmann@uk-erlangen.de
Telephone: +49-9131-8535885
Fax: +49-9131-85355959

Received: October 25, 2017
Peer-review started: October 26, 2017
First decision: November 14, 2017
Revised: December 20, 2017
Accepted: December 27, 2017
Article in press: December 27, 2017
Published online: February 28, 2018

Abstract

Flavonoids are phytochemicals which can regulate the activity of the intestinal immune system. In patients with chronic inflammatory bowel disease (IBD) there is an overexpression and imbalance of the components of the inflammatory immune reactions which are chronically activated. Suppression of inflammation can be achieved by anti-inflammatory drugs which are used in clinical medicine but these can cause serious side effects. Flavonoids can have natural immunosuppressive properties and inhibit the activation of immune cells and its effectors (chemokines, TNF-, cytokines). Phytochemicals such as flavonoids bind to the nuclear Ah (aryl hydrocarbon) -receptor thereby stimulating protective enzyme activities. As shown by clinical evidence in patients and by experimental work some flavonoids (apigenin, epigallocatechin gallate) were effective in the inhibition of inflammation. Instead of or additionally to anti-inflammatory drugs flavonoids can be used in IBD patients to treat the over-reactive immunologic system. This is accomplished by upregulation of the Ah-receptor. Flavonoids interact with toll-like receptors expressing on the surface of immune cells, then they were internalized to the cytosol and transferred into the nucleus, where they were attached to the Ah-receptor. The Ah-receptor binds to the Ah-R nuclear translocator and *via* Ah response element beneficial protective enzymes and cytokines are induced, leading to upregulation of the anti-inflammatory system.

Key words: Flavonoids; Inflammatory bowel disease; Ah-receptor

Core tip: Overview regulation of the intestinal immune system by flavonoids and its utility in chronic

inflammatory bowel disease.

Hoensch HP, Weigmann B. Regulation of the intestinal immune system by flavonoids and its utility in chronic inflammatory bowel disease. *World J Gastroenterol* 2018; 24(8): 877-881 Available from: URL: http://www.wjgnet.com/1007-9327/full/v24/i8/877.htm DOI: http://dx.doi.org/10.3748/wjg.v24.i8.877

INTRODUCTION

Disturbances of the intestinal immune system can lead to chronic inflammatory bowel disease (IBD) including Crohn`s disease and ulcerative colitis (UC)[1,2]. Inappropriate chronic stimulation of the native and adoptive immune-system induces an inflammatory reaction of the epithelial mucosa in the rectum, as well as in small and large bowel. There exists only limited evidence about the cause of this reaction which includes bacterial overproduction, defective barrier function, genetic and environmental aberrations.

PATHOPHYSIOLOGY

While the pathophysiology of the inflammatory changes is quite well explained the level of the immune reaction is not sufficiently delineated. This level might be determined by factors which regulate the degree of the immune reactions. These regulatory factors could be responsible for the activity of the inflammatory immune reaction and should be identified. Phytochemicals and among them polyphenols and flavonoids can influence various components of immune system and thereby determine the disease activity in IBD and in experimental colitis[3,4].

There is a plethora of clinical studies and experimental results on the association between colorectal cancer (CRC)[5] and exposure to phytochemicals especially flavonoids[6]. It is still not yet clear whether these xenobiotics could play a role in the development of intestinal neoplasia. Most studies indicate that dietary components from fruits and vegetables lower the risk of CRC and other tumors[7,8]. Flavonoids among other phytochemicals could prevent CRC[9] and its precursors (colonic adenomas, dysplasia and aberrant crypt foci) by long term preneoplastic dietary exposure. It is now accepted that chronic inflammatory changes of the intestinal mucosa predate neoplasia and that treatment of the inflammation and identification of its etiologic factors are necessary for cancer prevention.

ANTI-INFLAMMATORY EFFECTS OF FLAVONOIDS

In chronic inflammatory reactions the intestinal mucosa and the submucosa contain 2 components which are responsible for immune activation: The innate system and the adoptive system both of which contribute to the degree of activation. Whereas immune cells such as dendritic cells, granulocytes, macrophages, natural killer cells and mast cells belong to the innate immune system the adaptive system includes T-lymphocytes, B-lymphocytes and plasma cells and immunoglobulins. Innate immunocytes are activated into myeloic and plasmacytoid dentritic cells. Naïve lymphocytes are activated into T-helper cells, cytotoxic T-cells, regulatory T-cells and active B-cells. Inflammatory signals are the main factors for immune activation. Flavonoids are natural inhibitors and can prevent the activation of the innate and adaptive immune system[10]. Some flavonoids such as tea flavonoids (apigenin and epigallocathechin gallate) have been found to prevent the activation of immune cells and its effectors (chemokines, TNF-α and cytokines)[11].

In vivo the anti-inflammatory effects were shown by inhibition of transcriptions factors like nuclear factor 'kappa-light-chain-enhancer' of activated B-cells (NF-κB) and by suppression of cyclooxygenase 2 (COX-2) enzymes[12]. In patients with IBD chemokines and chemokine receptors are increased[13]. Phytochemicals have been shown to suppress inflammatory signal transduction systems leading to autophagy and apoptosis[14].

INFLUENCE OF FLAVONOIDS ON THE MICROBIOTA

Dysbalance of the microflora has been found in patients with IBD and chronic diarrhea[15]. The microbiota shows less variability and abundance of certain bacteria such as prevotellaceae and sulfide producing bacteria. Dietetic flavonoids can improve the fecal microbiota and prevent diarrhea. A recent study indicates that in pediatric patients the fecal microflora is related to diet and the composition of the microbiota indicates a pre-inflammatory status of IBD[16].

FLAVONOIDS AND MICROSOMAL ENZYMES

Dietary xenobiotics such as phytochemicals seem to be involved in the pathogenesis and treatment of chronic IBD[17]. Flavonoids are substrates for certain cytochrome P-450 enzymes (including CYP1A1) and are metabolized by components of the proteasome (P), endoplasmic reticulum (ER) and mitochondria (M), called PERM hypothesis[18]. This PERM concept defines the functional structure, which regulates the survival decision of cells under stress situation. Most probably this dynamic system can act as a single master tuner of cellular decisions about life or death, in order to give a chance to the remaining living cells in an organism. The ER consists of cytochrome P-450 and conjugating enzymes which metabolically break down toxic compounds. Human cytochrome 3A4 and

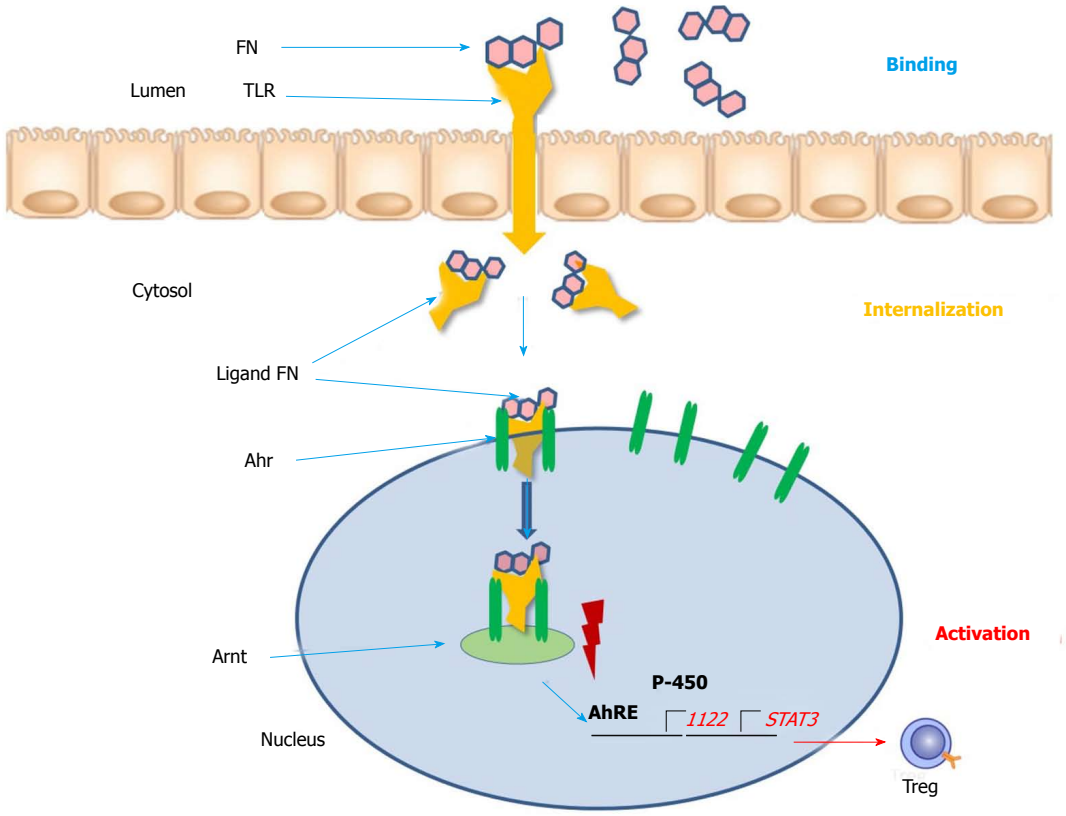

Figure 1 Simplified scheme of the gene regulation by the aryl hydrocarbon receptor. Flavonoids bind to the toll-like receptor in the lumen and get internalized to the cytosol. Then the complex functions as a ligand for the Ah receptor, which results in the release of associated proteins and translocation to the nucleus followed by dimerization with Arnt. The Ahr/Arnt complex binds the AhRE promoting target gene transcription like upregulation of IL-22, cytochrome P-450 and PERM activity as well as downregulation of STAT3 and NF-κB. The ligands can also exert their effects in the cytoplasm through AhR-associated protein kinases to alter the function of a variety of proteins through a cascade of protein phosphorylation. Ahr: Aryl hydrocarbon receptor; Arnt: Ahr nuclear translocator; Ah: Aryl hydrocarbon. FN: Flavonoid;TLR: Toll-like receptor; Ahr: Ah receptor; Arnt: AhR nuclear translocator; AhRE: Ah Response Element.

2C9 enzymes are inhibited by flavonoids *in vitro* but can also be induced *in vivo*[19,20]. These enzymes could be biomarkers for the activity of the PERM system, indicate moderate beneficial induction and a favorable immune status. Flavonoid mediated induction is a positive event for the immune system boosting its anti-inflammatory activity. In the intestine of IBD patients the CYP 1A1 enzymes were upregulated[21].

FLAVONOIDS AND PERM

An intracellular mechanism exists for the detoxification of reactive oxygen radicals, which are taken care of by the proteasome, the ER and the mitochondria[18] acting as PERM system. Flavonoids can activate this system as stressing and signaling molecules and are thereby responsible for the suppression of "pathologic" stress. Patients with IBD could probably benefit from dietary flavonoids supplementation[10,22].

FLAVONOIDS REGULATE THE AH-RECEPTOR

The aryl hydrocarbon receptor (Ahr) functions as intracellular transcription factor for the action of flavonoids and other phytochemicals such as indoles, isothiocyanates, cruciferous plants and cabbage products (Figure 1)[21]. During the passage through the gastrointestinal tract digestion takes place and flavonoids are broken metabolically down into smaller molecules. FN (flavonoids) present in the gut lumen bind to the toll-like receptor of the plasma membrane and are transported into the cytosol. Here as a ligand they are attached to the Ahr and triggers translocation into the cell nucleus. *Via* dimerization with the Ahr nuclear translocator (Arnt) protein the ligand FN-Ahr-Arnt complex binds to the AhRE (Ah response Element) found in the 5 V flanking region of numerous genes. This element activates the target genes which are transcript into cytochrome P-450 and other protective enzymes. Additionally, regulatory T-cells, STAT3 and IL-22 are expressed and upregulated. The Ahr is localized mainly in lymphocytes and dendritic cells of the intestinal mucosa. Interleukin-22 is responsible for the intestinal integrity and the production of mucus and upregulation of beta-defensin-2[23]. The FN ligand is the major immune modulator and induces a beneficial pattern of cytokines and immune cells which counteract the inflammatory alterations of the intestinal mucosa. In contrast to the biologicals these botanicals do not

require an immunosuppressive therapy and constitute natural inducers of the immune system[24]. As plant products (xenobiotica) they could be used as an anti-inflammatory diet and could be beneficial for prevention and as nutritional supplements[10].

EVIDENCE OF INHIBITION OF INTESTINAL INFLAMMATION BY FLAVONOIDS

Diets could be beneficial in the treatment of IBD[25]. Dietary flavonoids could play a prominent role as part of a healthy diet[26]. There are several experimental studies which indicate the utility of flavonoids in models of chronic IBD[27-31]. Especially the effects on the various aspects and consequences of inflammation (barrier integrity and microbiota) have been explained. The therapeutic benefits of cathechins are mediated by glutathione peroxidase, glutathione and by down-regulation of immune cells of the innate and induced system and their related signaling pathways (NF-κB, MAPK`s)[32].

Regular dietary consumption of green tea extract (epigallocathechin gallate) reduces DNA damage and increases the anti-oxidative capacity of blood plasma[33].

In UC chamomile extract (apigenin) given as a nutritional supplement was capable of remission maintenance. This was shown in a placebo controlled prospective trial[34]. In a similar study this could also be found for curcumin (which is a polyphenol) treatment.

Apigenin K was used in two different experimental colitis models and showed intestinal anti-inflammatory activity[35]. Furthermore, apigenin, as a nutritional supplementary flavonoid, can suppress NF-κB regulated expression of anti-apoptotic COX-2 and cFLIP in activated human T cells. Thus, apigenin is a possible interesting potent inhibitor which can be used for autoimmune inflammatory disease therapy, although the problem of bioavailability can be solved in the future[36].

In a study by Najafzadeh *et al*[37] flavonoids, especially quercetin and epicatechin, inhibits the DNA damage potency of H_2O_2 and IQ (quinoline) in lymphocytes isolated from IBD patients[38] *in vitro* experiments to 48% and 43% in comparison to controls. Here a concentration of 250 μg/mL quercetin and 100 μg/mL epicatechin is sufficient, respectively.

CONCLUSION

Flavonoids are able to influence the intestinal immune system and to regulate the strength and the pattern of the immune response in patients with chronic intestinal inflammation. Flavonoids drive the inflammatory cytokines into regression. The transcription factor Ah-R regulates the expression of target genes for the anti-inflammatory activity of the flavonoids.

Clinical trials in patients with IBD with valid end-points to measure the outcome with and without flavonoid treatment are rare and should be done soon.

REFERENCES

1 **Podolsky DK**. Inflammatory bowel disease (1). *N Engl J Med* 1991; **325**: 928-937 [PMID: 1881418 DOI: 10.1056/NEJM199109263251306]

2 **Podolsky DK**. Inflammatory bowel disease (2). *N Engl J Med* 1991; **325**: 1008-1016 [PMID: 1886623 DOI: 10.1056/NEJM199110033251406]

3 **Aldini R**, Micucci M, Cevenini M, Fato R, Bergamini C, Nanni C, Cont M, Camborata C, Spinozzi S, Montagnani M, Roda G, D 'Errico-Grigioni A, Rosini F, Roda A, Mazzella G, Chiarini A, Budriesi R. Antiinflammatory effect of phytosterols in experimental murine colitis model: prevention, induction, remission study. *PLoS One* 2014; **9**: e108112 [PMID: 25268769 DOI: 10.1371/journal.pone.0108112]

4 **Somani SJ**, Modi KP, Majumdar AS, Sadarani BN. Phytochemicals and their potential usefulness in inflammatory bowel disease. *Phytother Res* 2015; **29**: 339-350 [PMID: 25572840 DOI: 10.1002/ptr.5271]

5 **Kornfeld D**, Ekbom A, Ihre T. Is there an excess risk for colorectal cancer in patients with ulcerative colitis and concomitant primary sclerosing cholangitis? A population based study. *Gut* 1997; **41**: 522-525 [PMID: 9391253 DOI: 10.1136/gut.41.4.522]

6 **Scalbert A**, Zamora-Ros R. Bridging evidence from observational and intervention studies to identify flavonoids most protective for human health. *Am J Clin Nutr* 2015; **101**: 897-898 [PMID: 25832341 DOI: 10.3945/ajcn.115.110205]

7 **Li YH**, Niu YB, Sun Y, Zhang F, Liu CX, Fan L, Mei QB. Role of phytochemicals in colorectal cancer prevention. *World J Gastroenterol* 2015; **21**: 9262-9272 [PMID: 26309353 DOI: 10.3748/wjg.v21.i31.9262]

8 **Schwingshackl L**, Schwedhelm C, Hoffmann G, Knüppel S, Laure Preterre A, Iqbal K, Bechthold A, De Henauw S, Michels N, Devleesschauwer B, Boeing H, Schlesinger S. Food groups and risk of colorectal cancer. *Int J Cancer* 2017 [PMID: 29210053 DOI: 10.1002/ijc.31198]

9 **Hoensch HP**, Kirch W. Potential role of flavonoids in the prevention of intestinal neoplasia: a review of their mode of action and their clinical perspectives. *Int J Gastrointest Cancer* 2005; **35**: 187-195 [PMID: 16110120 DOI: 10.1385/IJGC:35:3:187]

10 **Hoensch HP,** Oertel R. The value of flavonoids for the human nutrition: Short review and perspectives. *Clinical Nutrition Experimental* 2015; **3**: 8-14 [DOI:10.1016/j.yclnex.2015.09.001]

11 **Cialdella-Kam L**, Ghosh S, Meaney MP, Knab AM, Shanely RA, Nieman DC. Quercetin and Green Tea Extract Supplementation Downregulates Genes Related to Tissue Inflammatory Responses to a 12-Week High Fat-Diet in Mice. *Nutrients* 2017; **9**: [PMID: 28753942 DOI: 10.3390/nu9070773]

12 **Ruiz PA**, Braune A, Hölzlwimmer G, Quintanilla-Fend L, Haller D. Quercetin inhibits TNF-induced NF-kappaB transcription factor recruitment to proinflammatory gene promoters in murine intestinal epithelial cells. *J Nutr* 2007; **137**: 1208-1215 [PMID: 17449583 DOI: 10.1093/jn/137.5.1208]

13 **Miyazaki H**, Takabe K, Yeudall WA. Chemokines, chemokine receptors and the gastrointestinal system. *World J Gastroenterol* 2013; **19**: 2847-2863 [PMID: 23704819 DOI: 10.3748/wjg.v19.i19.2847]

14 **Talero E**, Ávila-Roman J, Motilva V. Chemoprevention with phytonutrients and microalgae products in chronic inflammation and colon cancer. *Curr Pharm Des* 2012; **18**: 3939-3965 [PMID: 22632755 DOI: 10.2174/138161212802083725]

15 **Magrone T**, Jirillo E. The interplay between the gut immune system and microbiota in health and disease: nutraceutical intervention for restoring intestinal homeostasis. *Curr Pharm Des* 2013; **19**: 1329-1342 [PMID: 23151182]

16 **Sommer F**, Rühlemann MC, Bang C, Höppner M, Rehman A, Kaleta C, Schmitt-Kopplin P, Dempfle A, Weidinger S, Ellinghaus

E, Krauss-Etschmann S, Schmidt-Arras D, Aden K, Schulte D, Ellinghaus D, Schreiber S, Tholey A, Rupp J, Laudes M, Baines JF, Rosenstiel P, Franke A. Microbiomarkers in inflammatory bowel diseases: caveats come with ca*via*r. *Gut* 2017; **66**: 1734-1738 [PMID: 28733278 DOI: 10.1136/gutjnl-2016-313678]

17 **Lee J**, Choi J, Kim S. Effective suppression of pro-inflammatory molecules by DHCA *via* IKK-NF-κB pathway, in vitro and in vivo. *Br J Pharmacol* 2015; **172**: 3353-3369 [PMID: 25802070 DOI: 10.1111/bph.13137]

18 **Chirumbolo S**, Bjørklund G. PERM Hypothesis: The Fundamental Machinery Able to Elucidate the Role of Xenobiotics and Hormesis in Cell Survival and Homeostasis. *Int J Mol Sci* 2017; **18** [PMID: 28098843 DOI: 10.3390/ijms18010165]

19 **Moon YJ**, Wang X, Morris ME. Dietary flavonoids: effects on xenobiotic and carcinogen metabolism. *Toxicol In Vitro* 2006; **20**: 187-210 [PMID: 16289744 DOI: 10.1016/j.tiv.2005.06.048]

20 **Kimura Y**, Ito H, Ohnishi R, Hatano T. Inhibitory effects of polyphenols on human cytochrome P450 3A4 and 2C9 activity. *Food Chem Toxicol* 2010; **48**: 429-435 [PMID: 19883715 DOI: 10.1016/j.fct.2009.10.041]

21 **Klotz U**, Ammon E. Clinical and toxicological consequences of the inductive potential of ethanol. *Eur J Clin Pharmacol* 1998; **54**: 7-12 [PMID: 9591923 DOI: 10.1007/s002280050412]

22 **Carini F**, Tomasello G, Jurjus A, Geagea A, Al Kattar S, Damiani P, Sinagra E, Rappa F, David S, Cappello F, Mazzola M, Leone A. Colorectal cancer and inflammatory bowel diseases: effects of diet and antioxidants. *J Biol Regul Homeost Agents* 2017; **31**: 791-795 [PMID: 28726358]

23 **Li A**, Gan Y, Wang R, Liu Y, Ma T, Huang M, Cui X. IL-22 Up-Regulates β-Defensin-2 Expression in Human Alveolar Epithelium *via* STAT3 but Not NF-κB Signaling Pathway. *Inflammation* 2015; **38**: 1191-1200 [PMID: 25510212 DOI: 10.1007/s10753-014-0083-z]

24 **Tilg H**, Moschen AR. Food, immunity, and the microbiome. *Gastroenterology* 2015; **148**: 1107-1119 [PMID: 25575570 DOI: 10.1053/j.gastro.2014.12.036]

25 **Sigall-Boneh R**, Levine A, Lomer M, Wierdsma N, Allan P, Fiorino G, Gatti S, Jonkers D, Kierkus J, Katsanos KH, Melgar S, Yuksel ES, Whelan K, Wine E, Gerasimidis K. Research Gaps in Diet and Nutrition in Inflammatory Bowel Disease. A Topical Review by D-ECCO Working Group [Dietitians of ECCO]. *J Crohns Colitis* 2017; **11**: 1407-1419 [PMID: 28961811 DOI: 10.1093/ecco-jcc/jjx109]

26 **Sebastian RS**, Wilkinson Enns C, Goldman JD, Martin CL, Steinfeldt LC, Murayi T, Moshfegh AJ. A New Database Facilitates Characterization of Flavonoid Intake, Sources, and Positive Associations with Diet Quality among US Adults. *J Nutr* 2015; **145**: 1239-1248 [PMID: 25948787 DOI: 10.3945/jn.115.213025]

27 **Vezza T**, Rodríguez-Nogales A, Algieri F, Utrilla MP, Rodriguez-Cabezas ME, Galvez J. Flavonoids in Inflammatory Bowel Disease: A Review. *Nutrients* 2016; **8**: 211 [PMID: 27070642 DOI: 10.3390/nu8040211]

28 **Gil-Cardoso K**, Ginés I, Pinent M, Ardévol A, Blay M, Terra X. Effects of flavonoids on intestinal inflammation, barrier integrity and changes in gut microbiota during diet-induced obesity. *Nutr Res Rev* 2016; **29**: 234-248 [PMID: 27841104 DOI: 10.1017/S0954422416000159]

29 **Dou W**, Zhang J, Ren G, Ding L, Sun A, Deng C, Wu X, Wei X, Mani S, Wang Z. Mangiferin attenuates the symptoms of dextran sulfate sodium-induced colitis in mice *via* NF-κB and MAPK signaling inactivation. *Int Immunopharmacol* 2014; **23**: 170-178 [PMID: 25194678 DOI: 10.1016/j.intimp.2014.08.025]

30 **Mascaraque C**, Aranda C, Ocón B, Monte MJ, Suárez MD, Zarzuelo A, Marín JJ, Martínez-Augustin O, de Medina FS. Rutin has intestinal antiinflammatory effects in the CD4+ CD62L+ T cell transfer model of colitis. *Pharmacol Res* 2014; **90**: 48-57 [PMID: 25281414 DOI: 10.1016/j.phrs.2014.09.005]

31 **Cui L**, Feng L, Zhang ZH, Jia XB. The anti-inflammation effect of baicalin on experimental colitis through inhibiting TLR4/NF-κB pathway activation. *Int Immunopharmacol* 2014; **23**: 294-303 [PMID: 25239813 DOI: 10.1016/j.intimp.2014.09.005]

32 **Fan FY**, Sang LX, Jiang M. Catechins and Their Therapeutic Benefits to Inflammatory Bowel Disease. *Molecules* 2017; **22** [PMID: 28335502 DOI: 10.3390/molecules22030484]

33 **Ellinger S**, Müller N, Stehle P, Ulrich-Merzenich G. Consumption of green tea or green tea products: is there an evidence for antioxidant effects from controlled interventional studies? *Phytomedicine* 2011; **18**: 903-915 [PMID: 21802928 DOI: 10.1016/j.phymed.2011.06.006]

34 **Langhorst J**, Varnhagen I, Schneider SB, Albrecht U, Rueffer A, Stange R, Michalsen A, Dobos GJ. Randomised clinical trial: a herbal preparation of myrrh, chamomile and coffee charcoal compared with mesalazine in maintaining remission in ulcerative colitis--a double-blind, double-dummy study. *Aliment Pharmacol Ther* 2013; **38**: 490-500 [PMID: 23826890 DOI: 10.1111/apt.12397]

35 **Mascaraque C**, González R, Suárez MD, Zarzuelo A, Sánchez de Medina F, Martínez-Augustin O. Intestinal anti-inflammatory activity of apigenin K in two rat colitis models induced by trinitrobenzenesulfonic acid and dextran sulphate sodium. *Br J Nutr* 2015; **113**: 618-626 [PMID: 25654996 DOI: 10.1017/S0007114514004292]

36 **Xu L**, Zhang L, Bertucci AM, Pope RM, Datta SK. Apigenin, a dietary flavonoid, sensitizes human T cells for activation-induced cell death by inhibiting PKB/Akt and NF-kappaB activation pathway. *Immunol Lett* 2008; **121**: 74-83 [PMID: 18812189 DOI: 10.1016/j.imlet.2008.08.004]

37 **Najafzadeh M**, Reynolds PD, Baumgartner A, Anderson D. Flavonoids inhibit the genotoxicity of hydrogen peroxide (H(2)O(2)) and of the food mutagen 2-amino-3-methylimadazo[4,5-f]-quinoline (IQ) in lymphocytes from patients with inflammatory bowel disease (IBD). *Mutagenesis* 2009; **24**: 405-411 [PMID: 19553277 DOI: 10.1093/mutage/gep016]

38 **Boots AW**, Wilms LC, Swennen EL, Kleinjans JC, Bast A, Haenen GR. In vitro and ex vivo anti-inflammatory activity of quercetin in healthy volunteers. *Nutrition* 2008; **24**: 703-710 [PMID: 18549926 DOI: 10.1016/j.nut.2008.03.023]

P- Reviewer: Gheita TAA, Ogata H, Vradelis S **S- Editor**: Chen K
L- Editor: A **E- Editor**: Ma YJ

World Journal of Gastroenterology

Submit a Manuscript: http://www.f6publishing.com

World J Gastroenterol 2018 February 28; 24(8): 882-893

DOI: 10.3748/wjg.v24.i8.882

ISSN 1007-9327 (print) ISSN 2219-2840 (online)

ORIGINAL ARTICLE

Basic Study

Relaxin influences ileal muscular activity through a dual signaling pathway in mice

Eglantina Idrizaj, Rachele Garella, Fabio Francini, Roberta Squecco, Maria Caterina Baccari

Eglantina Idrizaj, Rachele Garella, Fabio Francini, Roberta Squecco, Maria Caterina Baccari, Department of Experimental and Clinical Medicine, Section of Physiological Sciences, University of Florence, Florence 50134, Italy

ORCID number: Eglantina Idrizaj (0000-0002-2756-6552); Rachele Garella (0000-0003-3194-7603); Fabio Francini (0000-0002-9255-1824); Roberta Squecco (0000-0002-6534-3675); Maria Caterina Baccari (0000-0003-4665-1426).

Author contributions: Idrizaj E and Garella R contributed equally to this work. Idrizaj E and Garella R performed the electrophysiological and the functional experiments, respectively; Baccari MC, Squecco R, Idrizaj E and Garella R designed the research study and analyzed the data; Francini F contributed to design the research study and analyzed the data; Baccari MC and Squecco R wrote the paper; Idrizaj E, Garella R, Francini F, Squecco R and Baccari MC critically revised the manuscript.

Supported by University of Florence (ex 60%) ROBERTASQUECCORICATEN15 (to Squecco R).

Institutional animal care and use committee statement: The experimental protocol was designed in compliance with the guidelines of the European Communities Council Directive 2010/63/UE and the recommendations for the care and use of laboratory animals approved by the Animal Care Committee of the University of Florence, Italy, with authorization from the Italian Ministry of Health nr. 787/2016-PR.

Conflict-of-interest statement: No conflicts of interest, financial or otherwise, are declared by the authors.

Data sharing statement: No additional data are available.

Manuscript source: Unsolicited manuscript

Correspondence to: Roberta Squecco, PhD, Research Scientist, Department of Experimental and Clinical Medicine, Section of Physiological Sciences, University of Florence, Viale G.B. Morgagni 63, Florence 50134, Italy. roberta.squecco@unifi.it
Telephone: +39-55-2751600
Fax: +39-55-4379506

Received: October 19, 2017
Peer-review started: October 23, 2017
First decision: November 8, 2017
Revised: November 14, 2017
Accepted: November 28, 2017
Article in press: November 28, 2017
Published online: February 28, 2018

Abstract

AIM

To investigate the signaling pathways involved in the relaxin (RLX) effects on ileal preparations from mice through mechanical and electrophysiological experiments.

METHODS

For mechanical experiments, ileal preparations from female mice were mounted in organ baths containing Krebs-Henseleit solution. The mechanical activity was recorded *via* force-displacement transducers, which were coupled to a polygraph for continuous recording of isometric tension. Electrophysiological measurements were performed in current- and voltage-clamp conditions by a microelectrode inserted in a single smooth muscle cell (SMC) of the ileal longitudinal layer. Both the membrane passive properties and inward voltage-dependent L-type Ca^{2+} currents were recorded using suitable solutions and voltage stimulation protocols.

RESULTS

Mechanical experiments showed that RLX induced a decay of the basal tension and a reduction in amplitude of the spontaneous contractions. The effects of RLX were partially reduced by 1H-[1,2,4]oxadiazolo[4,3-*a*]-quinoxalin-1-one (ODQ) or 9-cyclopentyladenine mesylate (9CPA), inhibitors of guanylate cyclase (GC) and adenylate cyclase (AC), respectively, and were abolished in the concomitant presence of both drugs. Electrophysiological experiments demonstrated that RLX directly influenced the biophysical properties of ileal SMCs, decreasing the membrane conductance, hyperpolarizing the resting membrane potential, reducing the L-type calcium current amplitude and affecting its kinetics. The voltage dependence of the current activation and inactivation time constant was significantly speeded by RLX. Each electrophysiological effect of RLX was reduced by ODQ or 9CPA, and abolished in the concomitant presence of both drugs as observed in mechanical experiments.

CONCLUSION

Our new findings demonstrate that RLX influences ileal muscle through a dual mechanism involving both GC and AC.

Key words: Relaxin; Gastrointestinal motility; Smooth muscle; AC/cAMP; GC/cGMP

Core tip: Up to now relaxin (RLX) was described to act only through the NO/guanylate cyclase (GC)/cGMP/PKG pathway in different gastrointestinal tracts. The results of the present study, achieved on mice ileal preparations and carried out by a combined mechanical and electrophysiological approach, demonstrate for the first time that both GC and adenylate cyclase are involved in the effects of RLX in this intestinal region. The activation of this dual signaling pathway by RLX might represent a reinforcing (redundant) myorelaxant mechanism in the ileum, underlying the physiological importance of the hormone and leading to speculate translational perspectives in the treatment of intestinal dysmotilities.

Idrizaj E, Garella R, Francini F, Squecco R, Baccari MC. Relaxin influences ileal muscular activity through a dual signaling pathway in mice. *World J Gastroenterol* 2018; 24(8): 882-893 Available from: URL: http://www.wjgnet.com/1007-9327/full/v24/i8/882.htm DOI: http://dx.doi.org/10.3748/wjg.v24.i8.882

INTRODUCTION

It is widely recognized that the effects of the peptide hormone relaxin (RLX) are not limited to reproductive organs[1-3]. Receptors of the RLX family peptides have been indeed identified in both reproductive and non-reproductive tissues[4-6], including human and rodent intestine[7-9]. Concerning on the molecular mechanism of action of RLX on the target cells, multiple intracellular signaling systems appear to be engaged[10,11]. In some cells, such as the smooth muscle of reproductive tissue, the effects of the hormone RLX are due to the activation of adenylate cyclase (AC)[12-16] leading to increase of the cyclic adenosine monophosphate (cAMP) levels. However, in some other different preparations, such as in vascular and intestinal smooth muscle, the mechanism of action activated by RLX occurs through the endogenous nitric oxide (NO) synthesis[17-23] and leads to increased levels of cyclic guanosine monophosphate (cGMP).

Particularly, in the gastrointestinal tract of mice, RLX has been reported to modulate gastric and colonic smooth muscle activity through the L-arginine/NO pathway[9,24-26]. NO, synthesized under the catalytic action of nitric oxide synthases (NOS)[27], is known to cause gastrointestinal relaxation[28] and its altered production has been reported to be involved in different motor disorders[29]. However, Bani *et al*[30] raised the possibility that in the ileum, at variance with gastric and colonic preparations, the NO signaling pathway could not be the only one activated by the hormone, suggesting the involvement of additional pathways that have not been fully elucidated yet in this preparation. In this regard, the involvement of AC, in addition to guanylate cyclase (GC), in the effects of RLX has been reported in rat and guinea pig airways[31] as well as in human vascular cells[10].

On these grounds, the present study was designed to investigate for the first time, if AC/cAMP, besides the NO/CG/cGMP, could be a further signaling pathway involved in the effects of RLX on ileal smooth muscle. To evaluate this possibility, we performed experiments by a combined mechanical and electrophysiological approach. Particularly, for the first time we investigated the ability of RLX to induce changes of smooth muscle cell (SMC) biophysical properties in ileal preparations through the electrophysiological technique. Moreover, we studied the effects of RLX on the L-type Ca^{2+} current, $I_{Ca,L}$, that is supposed to be the main voltage-dependent source for Ca^{2+} entry useful for the activation of the SMC contractile machinery[32]. This knowledge may contribute to a better understanding of the mechanisms engaged by the hormone to modulate intestinal motility and may help in the design of further therapeutic strategies for the treatment of motor disorders.

MATERIALS AND METHODS

Animals

Experiments were performed on 8- to 12-wk-old female mice (CD1 Swiss strain; Envigo, Udine, Italy). The animals were kept under the following conditions: 12-h light/12-h dark photoperiod, constant

temperature (21 ± 1 ℃), and standard laboratory feed.

After 1 wk of acclimatization, the mice underwent assessment of the phase of the estrous cycle by light microscopic examination of vaginal smears stained with Papanicolaou stain, according to the method of Austin and Rowlands[33]. Only mice in proestrus or estrus (*i.e.*, the estrogen-dominated phases of the ovarian cycle) entered the experiments. This choice was made because estrogen is known to favor RLX responsiveness of several target organs and tissues[34]. The mice were killed by prompt cervical dislocation to minimize animal suffering. According to the procedure reported in previous paper[30] the mouse abdomen was opened, the distal ileum was removed and its content was cleaned with a physiological solution.

Mechanical experiments

For the functional studies, segments of the distal ileum (within 30 mm from the ileocaecal valve) were isolated and placed in Krebs-Henseleit solution, which consisted of 118 mmol/L NaCl, 4.7 mmol/L KCl, 1.2 mmol/L $MgSO_4$, 1.2 mmol/L KH_2PO_4, 25 mmol/L $NaHCO_3$, 2.5 mmol/L $CaCl_2$, and 10 mmol/L glucose pH 7.4, and bubbled with 95% O_2/5% CO_2. Two whole full-thickness, transversely cut, ileal segments (10 mm in length) were dissected from each animal and placed in 5-mL organ baths containing Krebs-Henseleit solution gassed with 95% O_2/5% CO_2, while the temperature was maintained within a range of 37 ± 0.5 ℃. The preparations were mounted in the direction of the longitudinal muscle layer and the continuous recording of isometric tension was achieved by a force displacement transducer (FT03; Grass Instrument) coupled to a polygraph (7K; Grass Instrument). The preparations were allowed to equilibrate for at least 1 h under an initial load of 1.5 g. During this period, the preparations underwent repeated and prolonged washes with Krebs-Henseleit solution to avoid accumulation of metabolites in the organ baths.

Electrophysiological experiments

For electrophysiological recording a full-thickness ileal strip was distended and pinned to a Sylgard (Dow Corning, Midland, MI, United States)-coated dissecting Petri dish filled with Krebs-Henseleit solution. First, we pinned the mucosal side up to dissect carefully the mucosa and submucosa away under a dissecting microscope. The residual tissue was re-pinned serosal side up and the connective tissue was removed in order to expose the smooth muscle layer. The obtained tissue was finally pinned, serosal side up, in the recording chamber with a Sylgard floor and a glass microelectrodes was inserted in a cell of the longitudinal smooth muscle layer. The tissue was continuously superfused (Pump 33, Harvard Apparatus) at a rate of 1.8 mL min^{-1} with the external solution used.

Conventional high resistance microelectrodes were used according to the previously published procedure[9,35]. Microelectrodes were obtained by using a micropipette vertical puller (Narishige PC-10) from borosilicate glass (GC 100-7.5; Clark) and were filled with the following control physiological solution (mmol/L): KCl 130, NaH_2PO_4 10, $CaCl_2$ 0.2, EGTA 1, MgATP 5 and HEPES/KOH 10. Once filled, the pipette resistance measured 60-70 MΩ. The pH was set to 7.4 with NaOH and to 7.2 with tetraethylammonium (TEA) hydroxide for bath and pipette solution, respectively.

To record RMP in current-clamp and the cell membrane passive properties in voltage-clamp mode we used the extracellular Krebs-Henseleit solution. To record only Ca^{2+} currents we bathed the ileal muscle strip in a Na^+- and K^+-free high-TEA solution (mmol/L): 10 $CaCl_2$, 145 TEABr and 10 HEPES and the microelectrode was filled by the following solution (mmol/L): 150 CsBr, 5 $MgCl_2$, 10 EGTA, 10 HEPES. Nifedipine (10 μmol/L) was used to block L-type Ca^{2+} current, $I_{Ca,L}$. Heptanol (1 mmol/L) was consistently used to block gap junctional currents of the functional syncytium and to record membrane passive properties and ionic currents elicited only from the impaled cell[35,36].

The current amplitude was always normalized to cell linear capacitance C_m (in pA/pF) to consent the evaluation of test current recorded from cells of different size; in fact, C_m is usually considered an index of cell-surface area presuming that membrane-specific capacitance has a constant value of 1 μF/cm^2.

Pulse protocols of stimulation

By using the current clamp mode of our amplifier and stimulus waveform with I = 0 pA we recorded the SMC resting membrane potential, before and after drug stimulation. Protocol of recording consisted of 8 episodes, having a sampling interval of 20 ms and a total duration of 5.29 min. The inter-episode interval was 1 min.

The membrane passive properties, membrane conductance (G_m) and C_m, were consistently estimated in voltage clamp mode by applying two step voltage pulses 75 ms long to -80 and -60 mV starting from a holding potential (HP) of -70 mV. Their values were calculated as detailed in Squecco *et al*[37]. Always in this mode, ionic currents were evoked by the following pulse protocols: $I_{Ca,L}$ activation was evoked on the SMC held at -80 mV, and 1-s long step pulses were applied in 10-mV increments from -70 to 50 mV. For each episode, the first 100 ms of the trace had a sampling interval of 50 μs, and the remaining of 1 s. The interval between episodes was 20 s to allow recovery. $I_{Ca,L}$ inactivation was investigated by a two-pulse protocol with a 1-s pre-pulse to different voltages followed by 1-s test pulse to 10 mV as reported in our previous works[9,35]. When we applied the two-pulse protocol, we used again a 20-s interval between stimulating episodes to allow recovery. Capacitive, linear leak and voltage-independent ionic currents were cancelled on-line using the P/4 procedure.

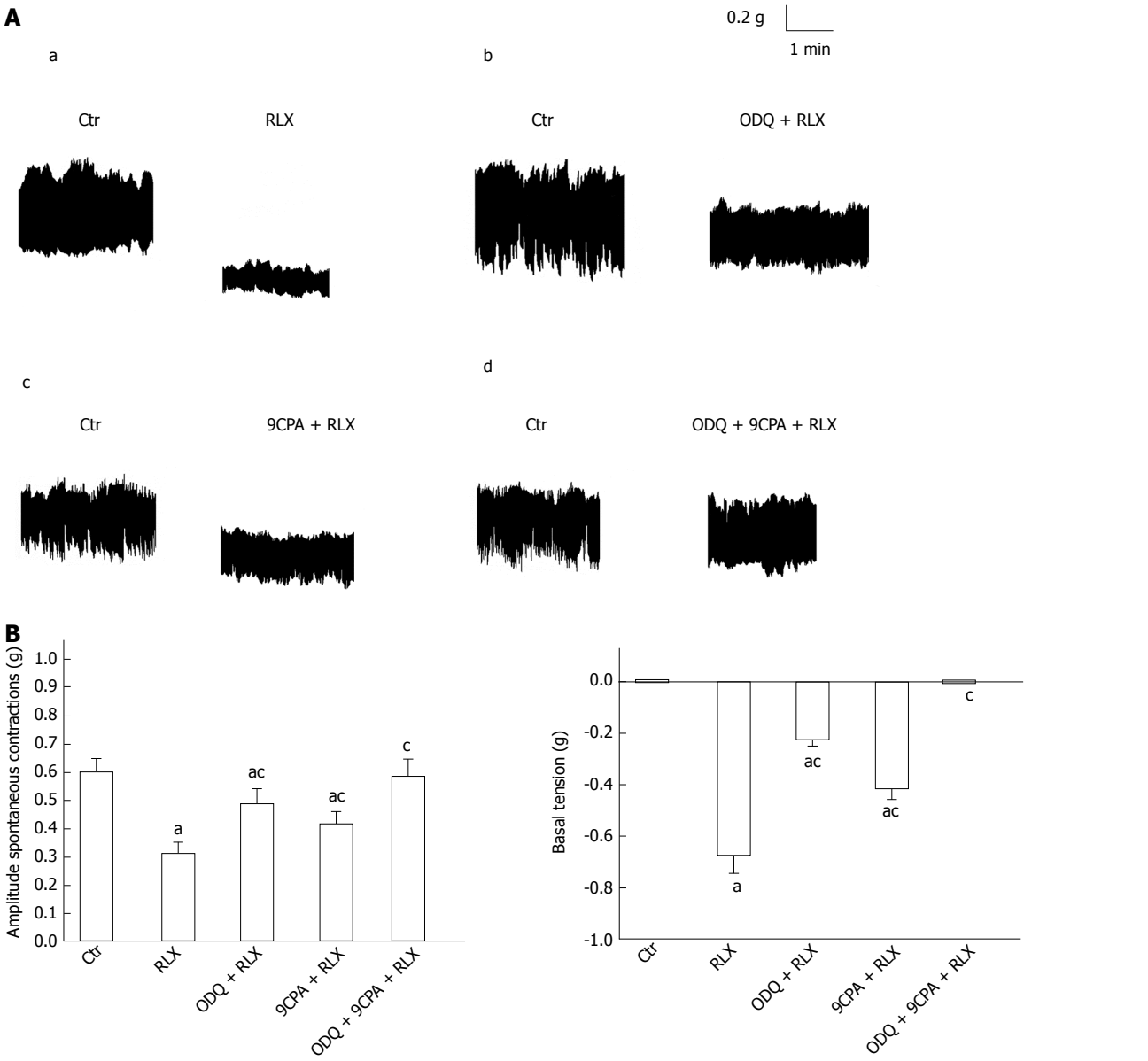

Figure 1 Influence of oxadiazolo[4,3-*a*]-quinoxalin-1-one and 9-cyclopentyladenine mesylate on relaxin effects on the mechanical activity of the mouse ileum. A: Typical tracings showing the spontaneous activity of the ileal segments (Ctr, left hand recordings of each panel). RLX (50 nmol/L), 30 min from its application to the bath medium, causes a decrease in amplitude of the spontaneous contractions and a decay of the basal tension (a, right trace) compared to its control (a, left trace). Both these effects are reduced when RLX is added to the bath medium in the presence of 1 μmol/L ODQ (b, right trace) or 100 μmol/L 9CPA (c, right trace) and abolished in the presence of ODQ plus 9CPA (d, right trace). Data of each panel (a-d) are obtained from different preparations; B: Bar charts showing the influence of ODQ and 9CPA on RLX effects on the mean amplitude of spontaneous contractions (left hand histogram) and basal tension (right hand histogram) with respect to the control. All values are means ± SE of 6 preparations from 3 mice. $^{a}P < 0.05$ *vs* Ctr; $^{c}P < 0.05$ *vs* RLX (one-way ANOVA and Newman-Keuls post-test); RLX: Relaxin; ODQ: Oxadiazolo[4,3-a]-quinoxalin-1-one; 9CPA: 9-cyclopentyladenine.

To evaluate the steady-state ionic current activation through the voltage dependent channels we used the following equation:

$I_a(V) = G_{max} (V-V_{rev})/\{1 + \exp[(V_a-V)/k_a]\}$ and the following was used for the steady-state current inactivation: $I_h(V) = I/\{1 + \exp[-(V_h-V)/k_h]\}$, where G_{max} represents the maximal conductance for I_a; V_{rev} is the apparent reversal potential; V_a and V_h are the voltages causing the half-maximal activation and inactivation, respectively; k_a and k_h are steepness factors.

Drugs

We used tetrodotoxin (TTX, 1 μmol/L), nifedipine (10 μmol/L), 1H-[1,2,4] oxadiazolo[4,3-α]-quinoxalin-1-one (ODQ, 1 μmol/L), 9-cyclopentyladenine mesylate (9CPA, 100 μmol/L) and relaxin (RLX, 50 nmol/L). All drugs were obtained from Sigma Chemical (St. Louis, MO, United States), except for highly purified porcine RLX (2500-3000 U/mg) that was generously provided by Dr. O. D. Sherwood (University of Illinois, Urbana, IL, United States). Solutions were prepared on the day of the experiment, except for TTX, for which a stock solution was kept stored at -20 ℃. Drugs concentrations are given as final bath concentrations. The concentration of porcine RLX used was in the range of that formerly demonstrated to be effective in murine gastrointestinal preparations[9,30,38-40]. The choice of GC

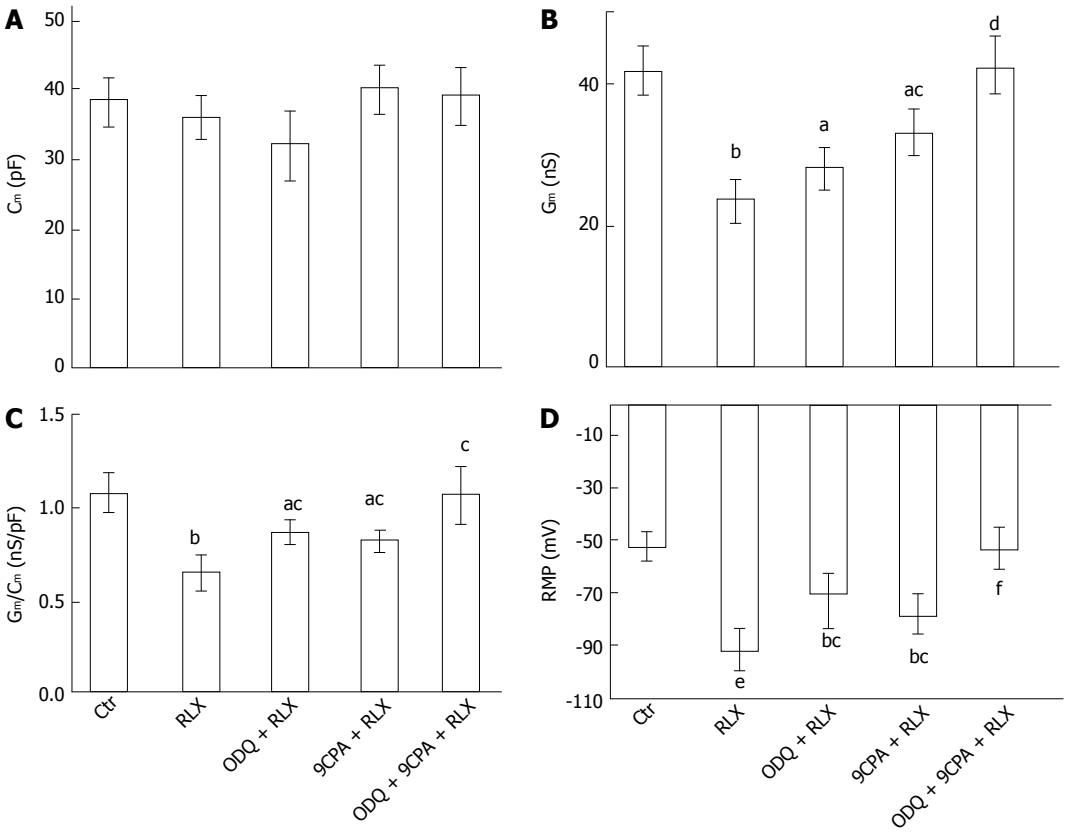

Figure 2 Effect of relaxin on smooth muscle cell membrane passive properties and resting membrane potential (RMP) of the mouse ileum. Influence of relaxin on Cm (A), Gm (B), Gm/Cm (C) and RMP (D) alone (RLX) or in the presence of ODQ (ODQ + RLX), 9CPA (9CPA + RLX) or both of them (ODQ + 9CPA + RLX). $^{a}P < 0.05$, $^{b}P < 0.01$, $^{e}P < 0.001$ *vs* control SMC (Ctr); $^{c}P < 0.05$, $^{d}P < 0.01$, $^{f}P < 0.001$ *vs* RLX. In each experimental condition, data are mean ± SE from $n = 22$ cells (11 strips from 5 mice) (one-way ANOVA and Newman-Keuls post-test), RLX: Relaxin; ODQ: Oxadiazolo[4,3-a]-quinoxalin-1-one; 9CPA: 9-cyclopentyladenine.

and AC inhibitors was based on previous literature[9,41] and their related concentration was in the range of that previously proven to be effective[9,42].

Data analysis and statistical tests

As previously reported[30,38], in the mechanical experiments, amplitude of spontaneous contractions and variations in basal tension are expressed as grams.

For electrophysiological experiments, mathematical and statistical analysis of data was performed by SigmaPlot (Jandel Scientific) and pClamp9 (Axon Instruments). Statistical analysis was performed by Student's *t*-test to compare two experimental groups or one-way ANOVA followed by Newman-Keuls post-test for multiple comparisons. The number of muscle preparations/cells is designated by n in the results. Results are means ± SE. $P \leqslant 0.05$ was considered statistically significant.

RESULTS

Mechanical experiments

Effects of relaxin on the mechanical activity: At basal tension, ileal preparations ($n = 24$, from 12 mice) showed spontaneous and rhythmic phasic contractions (mean amplitude 0.60 ± 0.03 g) (Figure 1), that were unaffected by 1 μmol/L TTX (mean amplitude 0.61 ± 0.03 g), indicating their myogenic nature, and reduced by 10 μmol/L nifedipine (0.35 ± 0.05 g).

Addition of RLX (50 nmol/L) to the bath medium ($n = 18$, from 9 mice) caused a clear-cut decay of the basal muscle tension (62.3% ± 2.2%) and a reduction in amplitude (36.1% ± 1.8%) of the spontaneous contractions (Figure 1). The action of the hormone on basal tension and on spontaneous activity was just evident 10 min and 20 min, respectively, after its addition to the bath medium. The influence of RLX on ileal motility was long lasting, because its effects could still be revealed 1 h after the peptide addition to the organ baths (longer time not observed). The effects of the hormone on basal muscle tension and spontaneous contractions were unaffected by TTX (60% ± 3.1% and 37.2% ± 1.5%, respectively) whereas they were no longer detectable 10 min after the addition of nifedipine ($P > 0.05$ in respect to nifedipine alone) to the bath medium.

Addition of the GC inhibitor ODQ (1 μmol/L) to the bath medium did not induce significant effects ($P > 0.05$). In the presence of ODQ (1 μmol/L) both spontaneous contractions and muscle basal tension were only reduced by 50 nmol/L RLX (Figure 1), thus suggesting the contribution of other signaling paths in the hormone action. We therefore tested the possible involvement of the AC pathway, employing the AC

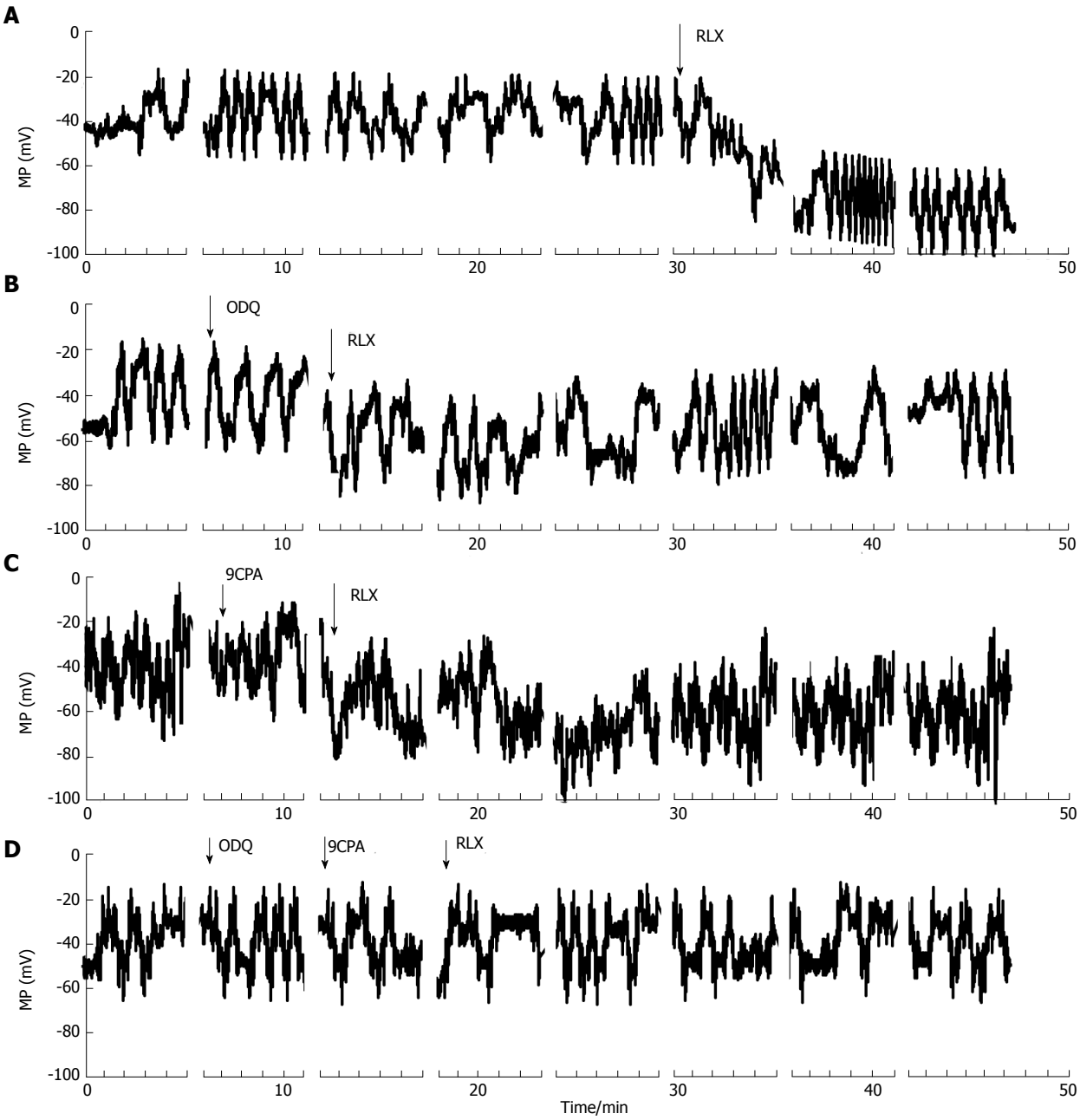

Figure 3 Effects of relaxin, in the absence or in the presence of oxadiazolo[4,3-a]-quinoxalin-1-one and 9-cyclopentyladenine, on membrane potential recorded from smooth muscle cell of the mouse ileum. Typical tracings of membrane potential from four different single ileal SMCs. A-D: Irregular waves of MP recorded in control condition. RLX addition (arrow) induced a persistent hyperpolarization occurring right after about 2 min from its application (A); The hyperpolarization caused by RLX was reduced in the presence of ODQ (B), 9CPA (C) and was abolished when both blockers were concomitantly present in the bath solution (D). Breaks in X-axis (and consequently in the MP traces) indicate the end of each episode, RLX: Relaxin; ODQ: Oxadiazolo[4,3-a]-quinoxalin-1-one; 9CPA: 9-cyclopentyladenine.

inhibitor 9CPA (100 μmol/L): 9CPA had not "per se" significant effects ($P > 0.05$) but reduced the actions of RLX although it was unable to completely restore the control mechanical activity (Figure 1). RLX added to the bath medium in the presence of ODQ plus 9CPA had no longer effects on both muscle tension and spontaneous contractions (Figure 1).

Electrophysiological experiments

Influence of relaxin on the smooth muscle cell membrane passive properties: To further test the possible direct action of RLX on ileal SMC, we investigated the effects of the hormone on the SMC resting membrane properties. RLX did not alter significantly C_m (Figure 2A) but decreased G_m and the specific conductance (G_m/C_m) values (Figure 2B-C). Addition of ODQ (1 μmol/L) or 9CPA (100 μmol/L) to the external recording medium did not affect significantly the membrane passive properties compared to the untreated control ($P > 0.05$). The effects of RLX on G_m and G_m/C_m were partially inhibited when was added in the presence of ODQ or 9CPA, and were completely abolished in their concomitant presence, reaching values similar to those observed in

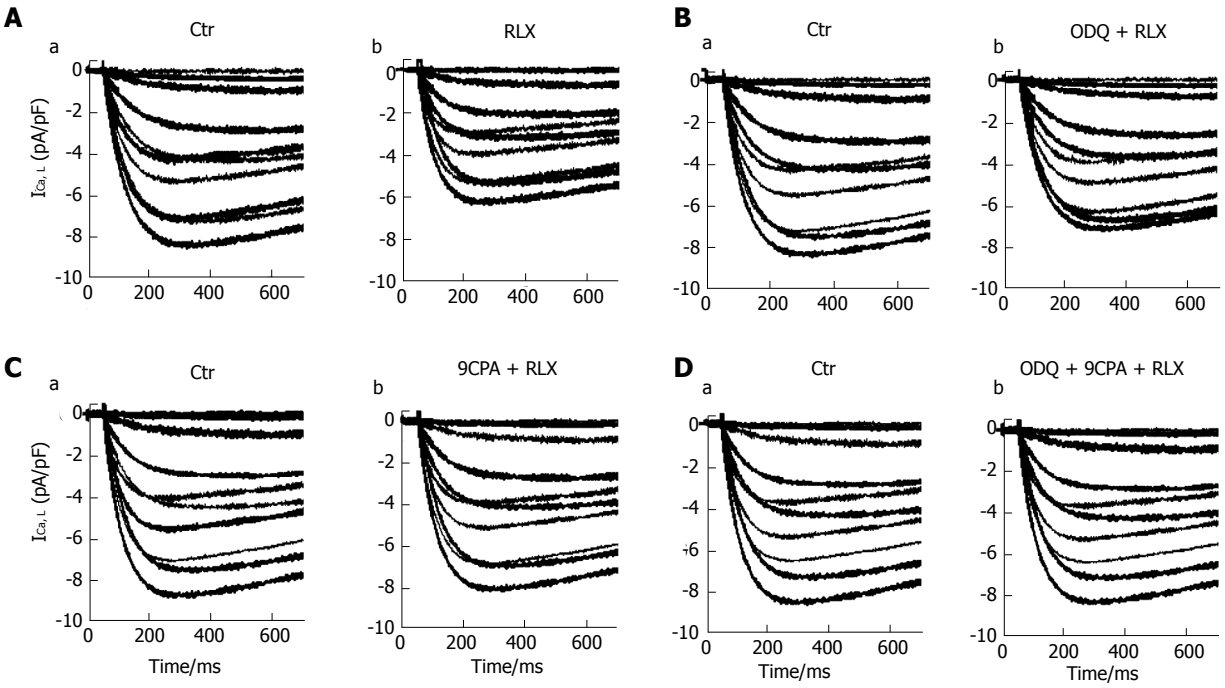

Figure 4 Relaxin affects L-type Ca^{2+} currents in smooth muscle cell of the mouse ileum. A: Representative time course of L-type Ca^{2+} currents ($I_{Ca,L}$) recorded in the high TEA-Ca^{2+} solution from a control cell (a) and after RLX addition (b); B-D: ICa,L tracings in the control (a) and in the presence of RLX (b) added 15 min after ODQ (B) or 9CPA(C) or both ODQ + 9CPA (D). Current records shown in the different panels (A-D) are obtained from four different SMCs. The first 700 ms of the current response are displayed.

control condition (Figure 2B and C).

Effects of relaxin on smooth muscle cell resting membrane potential: We then evaluated the RLX effects on resting membrane potential (RMP) of SMCs, to test its role on cell excitability. In control condition, the membrane potential showed spontaneous irregular slow waves (n = 22 cells; 11 strips from 5 mice) (Figure 3). These waves of the membrane potential lasted 0.4-1.1 min and showed alternating periods of very low (0.5 ± 0.1 wave/min) and higher (1.1 ± 0.2 wave/min) frequencies lasting 5-6 and 15 min, respectively. The maximal hyperpolarization value of the waves was considered as the RMP. The mean amplitude of the irregular waves was 37.5 ± 8 mV.

After RLX addition to the bath solution, the irregular waves were still recorded but the membrane potential showed a hyperpolarization trend that was already appreciable 1-3 min after its application (Figure 3A). The irregular waves were always recorded during the hyperpolarization due to RLX, and maintained a similar amplitude, duration and frequency.

The statistical analysis of the RMP values is reported as histograms in Figure 2D for each experimental condition. Noteworthy, the mean value of control RMP was -53.4 ± 7 mV and it reached -91.1 ± 12 mV in the presence of RLX, clearly indicating a statistically significant hyperpolarization. Furthermore, being the size of the irregular wave similar to the control value (41.5 ± 8 mV), the positive peak of the waves was different in RLX compared to control (Figure 3): it reached a mean value of -20 ± 5 (range from -30 to -12) mV in control and -49.6 ± 16 (range from -75 to -25 mV) mV after RLX addition. This observation indicates that RLX does not influence the amplitude and the frequency of the slow potentials and suggests that RLX may hamper the probability to reach a depolarized voltage threshold suitable for ion channels activation. Consequently, since the slow voltage waves arise from a voltage value that is under threshold for the voltage-dependent L-type Ca^{2+} current activation (see below) and their amplitude in this hyperpolarized state is not altered, we could deduce that they are not due to voltage-dependent channels opening.

In order to investigate the possible effectors involved in these RLX effects, we used the GC and AC inhibitors also in this set of experiments. Again, addition of ODQ or 9CPA alone to the external solution did not modify significantly the wave amplitude, duration, frequency and the resting membrane potential compared to the untreated control (Figure 3) (P > 0.05). RLX added at least 5 min after ODQ or 9CPA, hyperpolarized the RMP to a lesser extent (Figure 3B and C) compared to RLX alone, suggesting the involvement of both GC and AC pathways. Once again, in agreement with the mechanical results, RLX added in the presence of both inhibitors was no more able to induce hyperpolarization (Figures 2D and 3D).

Influence of relaxin on the voltage-dependent Ca^{2+} current: The effects of the hormone were then evaluated on the inward voltage-dependent

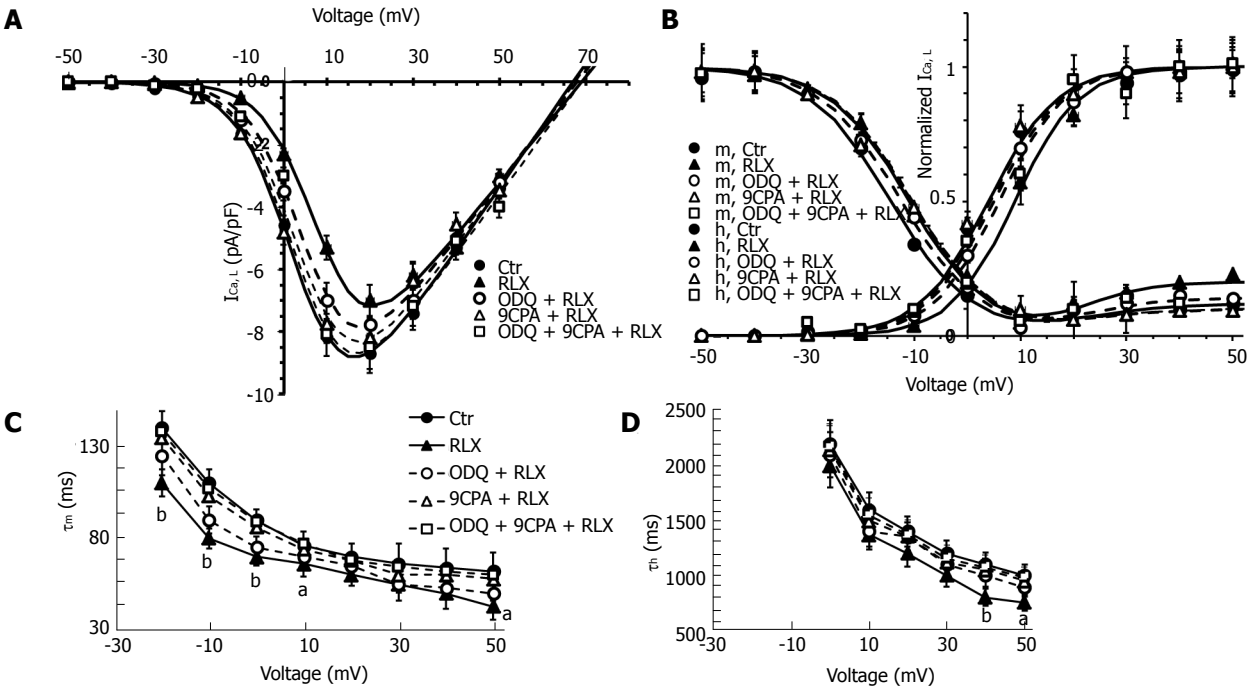

Figure 5 Relaxin affects $I_{Ca,L}$ voltage dependence and kinetics in smooth muscle cell of the mouse ileum. A: *I-V* plots of L-type Ca^{2+} currents ($I_{Ca,L}$) recorded in Ctr (filled circles), RLX (filled up triangles), ODQ + RLX (open circles), 9CPA + RLX (open up triangles) and ODQ+9CPA + RLX (open squares) from experiments as in Figure 4. Statistical significance not shown in the plot for clarity; B: Steady-state $I_{Ca,L}$ activation (m) and inactivation curves (h) in all the conditions tested; the best fit to the inactivation data is obtained by the sum of two Boltzmann terms. A and B: The Boltzmann fits for Ctr and RLX are superimposed to the experimental data as continuous lines, those related to ODQ, 9CPA and ODQ + 9CPA as dashed lines. Data are mean ± SE. Boltzmann parameters, statistical analysis and number of analyzed cells are listed in Table 1. Current values are normalized to cell capacitance (pA/pF). C and D: Voltage dependence of the time constant of $I_{Ca,L}$ activation (τm) and inactivation (τ h). $^{a}P < 0.05$ and $^{b}P < 0.01$ RLX *vs* control SMC (Ctr). $P < 0.05$ for 9CPA + RLX and for 9CPA + ODQ + RLX *vs* RLX alone for the -20, -10 and 0 mV (τm data); $P < 0.05$ for 9CPA + RLX, ODQ + RLX and 9CPA + ODQ + RLX *vs* RLX alone for +40 and +50 mV (τ h data). Statistical significance for the inhibitors not shown in the panels for clarity (one-way ANOVA and Newman-Keuls post-test), RLX: Relaxin; ODQ: Oxadiazolo[4,3-a]-quinoxalin-1-one; 9CPA: 9-cyclopentyladenine.

Ca^{2+} currents, supposed to be the chief path for Ca^{2+} entry useful to trigger the contractile machinery in intestinal SMCs. Notably, in our experiments we did not consistently record TTX-sensitive Na^{+} current. Accordingly, to better put in evidence the appearance of voltage-dependent Ca^{2+} currents, we used appropriate filling pipette solution and a bath recording high TEA-Ca^{2+} solution (see Materials and Methods section). The time course of typical current traces recorded from a control cell and after RLX addition is shown in Figure 4 (Aa and Ab, respectively). Since this kind of current had a high voltage threshold (about -30 mV), a slow activation and inactivation, and was blocked by nifedipine we assumed that it was an L-type Ca^{2+} current ($I_{Ca,L}$). No T-type Ca^{2+} current was revealed in our preparations. It can be clearly seen (Table 1, Figures 4A and 5A) that RLX reduced the maximal peak current amplitude ($P < 0.05$) and the time to peak (t_p) ($P < 0.01$). Moreover, the hormone shifted the mean voltage eliciting the maximal peak current size (from 17.5 ± 2 to 20.1 ± 2 mV).

To evaluate the general behavior of the phenomenon, we plotted our experimental data related to all the experiments done in the *I-V* relationship, reporting the normalized mean $I_{Ca,L}$ maximal amplitude for any voltage step applied (Figure 5A). The analysis of the *I-V* plot confirmed that RLX caused the decrease of current amplitude and a shift of the V_a and V_h values towards more positive potential (Table 1). The ODQ or 9CPA pre-treatment did not completely abolish the effect of RLX, but slightly reduced the size decrease (Figure 4) and the alteration of the V_a and V_h values. These parameters completely recovered the control values in the presence of ODQ plus 9CPA (Table 1, Figure 5C and D).

The voltage dependence of the current activation time constant, τ_m, (Figure 5C) as well as that of inactivation, τ_h, (Figure 5D) was significantly speeded by RLX. Particularly, the ODQ pre-treatment did not entirely eliminate the effects of RLX on τ_m, that did not result significantly different to that recorded in the presence of RLX alone, whereas 9CPA resulted more effective in counteracting RLX effects (Figure 5C) which were abolished in the concomitant presence of the inhibitors. Instead, the action of RLX on τ_h was similarly prevented by each of the inhibitors (Figure 5D).

The effects of RLX and those of the effector inhibitors on $I_{Ca,L}$ voltage dependence were analyzed by the steady-state activation and inactivation curves (Figure 5B): RLX shifted the activation and inactivation curves towards more positive potentials making this latter more U-shaped for depolarized voltages. All the Boltzmann parameters were only partially reverted to control values when RLX was added after ODQ or

Table 1 Boltzmann parameters of $I_{Ca,L}$ activation and inactivation in a smooth muscle cell in control (Ctr), in the presence of relaxin (RLX) alone or RLX with ODQ (ODQ + RLX), 9CPA (9CPA + RLX) and ODQ + 9CPA (ODQ + 9CPA + RLX)

Parameters	Ctr	RLX	ODQ + RLX	9CPA + RLX	ODQ + 9CPA + RLX
$I_{Ca,L}/C_m$ (pA/pF)	8.8 ± 0.5	7.2 ± 0.7[a]	7.9 ± 0.6	8.2 ± 0.6	8.7 ± 0.6[c]
V_p (mV)	17.5 ± 2	20.1 ± 2	17.9 ± 2	18.1 ± 1	17.5 ± 1.9
t_p (ms)	270.8 ± 22	194.1 ± 19[b]	230.8 ± 15[a,c]	244.8 ± 22[c]	259.8 ± 24[c]
V_a (mV)	4.0 ± 0.3	8.9 ± 0.6[e]	6.0 ± 0.6[b,c]	4.9 ± 0.5[a,d]	4.3 ± 0.4[d]
k_a (mV)	6.5 ± 0.4	6.0 ± 0.5	6.2 ± 0.4	6.4 ± 0.4	6.4 ± 0.4
V_{rev} (mV)	67.2 ± 4	68.8 ± 4	68.1 ± 5	67.5 ± 4	67.8 ± 4
V_h (mV)	-14.4 ± 2	-10.9 ± 1[a]	-12.4 ± 1	-12.6 ± 2	-14.0 ± 1[c]
k_h (mV)	7.6 ± 0.5	7.5 ± 0.5	7.6 ± 0.6	7.6 ± 0.7	7.6 ± 0.6
I_{2h} (Norm)	0.09 ± 0.02	0.23 ± 0.02[b]	0.14 ± 0.01[a,d]	0.13 ± 0.03[d]	0.09 ± 0.03[f]
V_{2h} (mV)	22.0 ± 2	22.3 ± 1.9	21.8 ± 2.1	21.5 ± 2	21.9 ± 1.8
k_{2h} (mV)	8.0 ± 0.7	6.3 ± 0.6[a]	7.1 ± 0.7	7.5 ± 0.3[c]	7.9 ± 0.2[c]

In the U shaped inactivation curves (h) the best fit to the data is obtained by the sum of two Boltzmann terms whose parameters are indicated with the subscript h for the term at negative potential, and 2h for the term at positive potential; the amplitude of the normalized second term, I_{2h} (Norm), was evaluated at 50 mV. [a]$P < 0.05$, [b]$P < 0.01$ and [e]$P < 0.001$ RLX compared to the related control; [c]$P < 0.05$, [d]$P < 0.01$ and [f]$P < 0.001$ compared to RLX. Data for Ctr (n = 67 cells, 25 strips from 12 mice), for RLX (n = 20 cells, 10 strips from 5 mice), for ODQ + RLX (n = 18 cells, 9 strips from 5 mice), for 9CPA + RLX (n = 15 cells, 8 strips from 5 mice) and for ODQ + 9CPA + RLX (n = 16 cells, 9 strips from 5 mice), RLX: Relaxin; ODQ: Oxadiazolo[4,3-a]-quinoxalin-1-one; 9CPA: 9-cyclopentyladenine.

9CPA and recovered when the hormone was applied in the concomitant presence of both the inhibitors. ODQ or 9CPA added alone to the bath solution did not cause appreciable differences in current records compared to control records ($P > 0.05$). The best fit parameters, statistical analysis and number of analyzed cells are reported in Table 1.

DISCUSSION

The present mechanical and electrophysiological results indicate, for the first time, that the hormone RLX is able to influence the ileal smooth muscle activity from female mice acting through a dual pathway, where both CG and AC activity are involved.

We previously observed in the same kind of preparation[30] that RLX increased the expression of both inducible and endothelial nitric oxide synthases but its depressant effects were not completely abolished by the NO synthesis inhibitor L-NNA. These observations indicated that the inhibitory effects of the hormone mainly occurred through the activation of intrinsic NO biosynthesis but, at the same time, suggested the involvement of additional signaling pathways. Accordingly, the mechanical results of the present study show that the decay of the muscular tension and the decrease in amplitude of the spontaneous contractions caused by RLX are reduced not only by ODQ but also by 9CPA leading to the novel finding that, other than GC, AC too is involved in the effects of the hormone on ileal motility. The involvement of other signaling pathways, besides the NO/cGMP, may account for the site-related actions of RLX in the modulation of the activity of the different GI tract in mice[26]. In this view, regional differences among mouse small intestine tracts concerning the nitrergic mechanisms mediating inhibitory control of longitudinal SMC contraction have been reported: the effects of NO donors were indeed completely abolished by ODQ in jejunum but only partially eliminated in ileum, suggesting the involvement of an additional pathway[43].

Another novel aspect of this research is represented by the electrophysiological results demonstrating, for the first time in ileal preparations, that RLX was able to act directly on the SMC, by influencing its biophysical membrane features and the voltage-dependent L-type Ca^{2+} channels properties. Regarding to the biophysical properties, the observations that RLX decreases the total and specific membrane conductance and hyperpolarizes the membrane potential definitely strengthen each other, since the decrease of the resting membrane conductance can indicate the reduction of aspecific cationic influxes that, in turn, hampering the entrance of positive charges may favor RMP hyperpolarization. They are also in good agreement with the depressant mechanical effects observed in this study, since changes of the RMP value lead to the reduction of the contractile activity that strictly depends on membrane potential (electro-mechanical coupling)[44]. However, the signaling cascade associated to membrane hyperpolarization is complicated and still debated; the GC/cGMP/PKG- and AC/cAMP/PKA-mediated smooth muscle hyperpolarization is also controversial[44-46]. In the present experiments, the observation that RLX was able to induce hyperpolarization and that both ODQ and 9CPA prevented this effect actually supports the involvement of GC and AC paths on the RMP modulation.

A remarkable consequence of changes in RMP can be relayed on L-type Ca^{2+} channels activation, since a greater depolarization is necessary to reach their activation voltage threshold. In this view, it could be hypothesized that the rhythmic spontaneous slow waves of the membrane potential, mainly due to voltage independent channels, only allow a slight number of SMC to reach the voltage threshold for L-type Ca^{2+} current, useful for contractile activation whereas most of the cells remain relaxed because

their RMP is too negative for the achievement of the electro-mechanical coupling. In fact, the mean positive membrane value of the waves observed in the presence of RLX resulted significantly more negative than that recorded in control condition. Hence, this RLX effect could also have a role in the control of RMP when the SMC reaches depolarized potentials at which L-type Ca^{2+} channels can be activated: in this case, any reduction of Ca^{2+} influx through membrane channels can facilitate the setting of negative charges in the inner side of the membrane and thus the hyperpolarization. In addition, whenever the channel can be activated, its activation would be reduced by RLX, since it also modified its voltage-dependence. The consequent reduction of Ca^{2+} influx caused by RLX fits well with its depressant actions on the mechanical activity, since L-type Ca^{2+} channels are a chief path through which Ca^{2+} can enter into the cell and trigger the contractile machinery in intestinal SMCs. Therefore, their modulation represents an effective mechanism playing a role in SMC relaxation. Noteworthy, these voltage-gated Ca^{2+} channels can be modulated by several signaling systems such as cyclic nucleotides cascades and, even if data about this item are sometimes contradictory[47], in general it is accepted that cAMP and cGMP inhibit L-type Ca^{2+} channels. Our results actually support this clue in the ileum: L-type Ca^{2+} channels resulted inhibited by RLX treatment and either ODQ or 9CPA reduced the effect of RLX, thus indicating that RLX exerts its effects through the activation of both NO/GC/cGMP and AC/cAMP signaling pathways. Since we observed that the blockade of the synthesis of each cyclic nucleotide seems to prevent a full RLX action also through the other pathway, we also suggest a sort of cross-talk mechanism between the two pathways, as previously proposed in vascular[44] and uterine smooth muscle[48].

In conclusion, the bulk of the above results indicate that RLX can be considered an efficient intestinal motility modulator since it is able to induce significant changes in smooth muscle mechanical and electrical activity of ileal preparations. In particular, we found that RLX reduces the basal tension and the amplitude of the spontaneous contractions. These effects fit well with the observed decrease of the resting conductance, the membrane hyperpolarization and the diminished Ca^{2+} influx through L-type channels. All of these actions are exerted by RLX through a dual signaling pathway involving both GC and AC, as reported in other tissues[10,31].

From a physiological point of view, it could be speculated that the dual signaling pathway may represent a reinforcing and cross-talking (redundant) mechanism for RLX aimed to guarantee its actions and to prolong its modulatory effects in the small intestine. Furthermore, the observation that two pathways are engaged by RLX to cause myorelaxation may create the basis for identifying new therapeutic targets, offering stimulating translational perspectives in the treatment of those intestinal dysmotilities characterized by hypermotility.

In conclusion, this study shows for the first time that RLX exerts its relaxant effects on ileal smooth muscle through the involvement of both GC and AC and suggests a cross-talk between GC/cGMP and AC/cAMP pathways.

ARTICLE HIGHLIGHTS

Background

Relaxin (RLX) has been reported to modulate gastrointestinal smooth muscle activity in mice through the L-arginine/NO pathway. However, the possibility that the depressant effects of RLX in ileal preparations could involve additional pathways, not fully elucidated yet, was raised. On these grounds, the present study was designed to investigate the signaling pathways involved in the effects of RLX on ileal preparations. To this aim, we performed experiments using a combined mechanical and electrophysiological approach.

Research frontiers

The actions of RLX occur through a dual signaling pathway that, from a physiological point of view, might represent a reinforcing and cross-talking mechanism for the hormone aimed to guarantee and to prolong its myorelaxant effects in the small intestine.

Innovations and breakthroughs

This study shows, for the first time in ileal preparations, that RLX is able to influence the smooth muscle mechanical and electrophysiological activity through a dual signaling pathway.

Applications

The activation of both adenylate cyclase and guanylate cyclase pathways by RLX underlines the physiological importance of the hormone to relax ileal smooth muscle. In this view, it could be speculated that RLX may represent a potential therapeutic tool in those intestinal dysfunctions characterized by hypermotility states.

Terminology

The modulation of gastrointestinal smooth muscle activity by hormones may be investigated *"in vitro"* by recording either the mechanical responses or the electrophysiological properties. In ileal preparations, the hormone RLX has been shown to exert a modulatory role by depressing spontaneous contractions and by influencing the electrophysiological activity.

ACKNOWLEDGMENTS

The Authors thank Adrio Vannucchi for preparation of Figure 1.

REFERENCES

1 **Bani D**. Relaxin: a pleiotropic hormone. *Gen Pharmacol* 1997; **28**: 13-22 [PMID: 9112071 DOI: 10.1016/S0306-3623(96)00171-1]
2 **Baccari MC**, Calamai F. Relaxin: new functions for an old peptide. *Curr Protein Pept Sci* 2004; **5**: 9-18 [PMID: 14965317 DOI: 10.2174/1389203043486928]
3 **Sherwood OD**. Relaxin's physiological roles and other diverse actions. *Endocr Rev* 2004; **25**: 205-234 [PMID: 15082520 DOI: 10.1210/er.2003-0013]
4 **Bathgate RA**, Halls ML, van der Westhuizen ET, Callander GE, Kocan M, Summers RJ. Relaxin family peptides and their receptors. *Physiol Rev* 2013; **93**: 405-480 [PMID: 23303914 DOI:

10.1152/physrev.00001.2012]
5 **Halls ML**, Bathgate RA, Sutton SW, Dschietzig TB, Summers RJ. International Union of Basic and Clinical Pharmacology. XCV. Recent advances in the understanding of the pharmacology and biological roles of relaxin family peptide receptors 1-4, the receptors for relaxin family peptides. *Pharmacol Rev* 2015; **67**: 389-440 [PMID: 25761609 DOI: 10.1124/pr.114.009472]
6 **Yamasato K**, Tsai PS, Davis J, Yamamoto SY, Bryant-Greenwood GD. Human relaxins (RLNH1, RLNH2), their receptor (RXFP1) and fetoplacental growth. *Reproduction* 2017; **154**: 67-77 [PMID: 28468839 DOI: 10.1530/REP-17-0039]
7 **Hsu SY**, Kudo M, Chen T, Nakabayashi K, Bhalla A, van der Spek PJ, van Duin M, Hsueh AJ. The three subfamilies of leucine-rich repeat-containing G protein-coupled receptors (LGR): identification of LGR6 and LGR7 and the signaling mechanism for LGR7. *Mol Endocrinol* 2000; **14**: 1257-1271 [PMID: 10935549 DOI: 10.1210/mend.14.8.0510]
8 **Scott DJ**, Layfield S, Riesewijk A, Morita H, Tregear GW, Bathgate RA. Identification and characterization of the mouse and rat relaxin receptors as the novel orthologues of human leucine-rich repeat-containing G-protein-coupled receptor 7. *Clin Exp Pharmacol Physiol* 2004; **31**: 828-832 [PMID: 15566402 DOI: 10.1111/j.1440-1681.2004.04075.x]
9 **Squecco R**, Garella R, Idrizaj E, Nistri S, Francini F, Baccari MC. Relaxin Affects Smooth Muscle Biophysical Properties and Mechanical Activity of the Female Mouse Colon. *Endocrinology* 2015; **156**: 4398-4410 [PMID: 26360621 DOI: 10.1210/en.2015-1428]
10 **Sarwar M**, Samuel CS, Bathgate RA, Stewart DR, Summers RJ. Serelaxin-mediated signal transduction in human vascular cells: bell-shaped concentration-response curves reflect differential coupling to G proteins. *Br J Pharmacol* 2015; **172**: 1005-1019 [PMID: 25297987 DOI: 10.1111/bph.12964]
11 **Summers RJ**. Recent progress in the understanding of relaxin family peptides and their receptors. *Br J Pharmacol* 2017; **174**: 915-920 [PMID: 28447360 DOI: 10.1111/bph.13778]
12 **Braddon SA**. Relaxin-dependent adenosine 6',5'-monophosphate concentration changes in the mouse pubic symphysis. *Endocrinology* 1978; **102**: 1292-1299 [PMID: 217619 DOI: 10.1210/endo-102-4-1292]
13 **Cheah SH**, Sherwood OD. Target tissues for relaxin in the rat: tissue distribution of injected 125I-labeled relaxin and tissue changes in adenosine 3',5'-monophosphate levels after in vitro relaxin incubation. *Endocrinology* 1980; **106**: 1203-1209 [PMID: 6244145 DOI: 10.1210/endo-106-4-1203]
14 **Sanborn BM**, Kuo HS, Weisbrodt NW, Sherwood OD. The interaction of relaxin with the rat uterus. I. Effect on cyclic nucleotide levels and spontaneous contractile activity. *Endocrinology* 1980; **106**: 1210-1215 [PMID: 6244146 DOI: 10.1210/endo-106-4-1210]
15 **Sanborn BM**, Sherwood OD. Effect of relaxin on bound cAMP in rat uterus. *Endocr Res Commun* 1981; **8**: 179-192 [PMID: 6174316 DOI: 10.3109/07435808109045738]
16 **Hsu CJ**, McCormack SM, Sanborn BM. The effect of relaxin on cyclic adenosine 3',5'-monophosphate concentrations in rat myometrial cells in culture. *Endocrinology* 1985; **116**: 2029-2035 [PMID: 2985368 DOI: 10.1210/endo-116-5-2029]
17 **Bani D**, Baccari MC, Nistri S, Calamai F, Bigazzi M, Sacchi TB. Relaxin up-regulates the nitric oxide biosynthetic pathway in the mouse uterus: involvement in the inhibition of myometrial contractility. *Endocrinology* 1999; **140**: 4434-4441 [PMID: 10499496 DOI: 10.1210/endo.140.10.7055]
18 **Novak J**, Ramirez RJ, Gandley RE, Sherwood OD, Conrad KP. Myogenic reactivity is reduced in small renal arteries isolated from relaxin-treated rats. *Am J Physiol Regul Integr Comp Physiol* 2002; **283**: R349-R355 [PMID: 12121847 DOI: 10.1152/ajpregu.00635.2001]
19 **Schlossmann J**, Feil R, Hofmann F. Signaling through NO and cGMP-dependent protein kinases. *Ann Med* 2003; **35**: 21-27 [PMID: 12693609 DOI: 10.1080/07853890310004093]
20 **Conrad KP**, Novak J. Emerging role of relaxin in renal and cardiovascular function. *Am J Physiol Regul Integr Comp Physiol* 2004; **287**: R250-R261 [PMID: 15271674 DOI: 10.1152/ajpregu.00672.2003]
21 **Samuel CS**, Du XJ, Bathgate RA, Summers RJ. 'Relaxin' the stiffened heart and arteries: the therapeutic potential for relaxin in the treatment of cardiovascular disease. *Pharmacol Ther* 2006; **112**: 529-552 [PMID: 16814863 DOI: 10.1016/j.pharmthera.2005.05.012]
22 **Baccari MC**, Bani D. Relaxin and nitric oxide signalling. *Curr Protein Pept Sci* 2008; **9**: 638-645 [PMID: 19075752 DOI: 10.2174/138920308786733921]
23 **Leo CH**, Jelinic M, Ng HH, Marshall SA, Novak J, Tare M, Conrad KP, Parry LJ. Vascular actions of relaxin: nitric oxide and beyond. *Br J Pharmacol* 2017; **174**: 1002-1014 [PMID: 27590257 DOI: 10.1111/bph.13614]
24 **Baccari MC**, Bani D, Bigazzi M, Calamai F. Influence of relaxin on the neurally induced relaxant responses of the mouse gastric fundus. *Biol Reprod* 2004; **71**: 1325-1329 [PMID: 15215200 DOI: 10.1095/biolreprod.104.029579]
25 **Baccari MC**, Nistri S, Quattrone S, Bigazzi M, Bani Sacchi T, Calamai F, Bani D. Depression by relaxin of neurally induced contractile responses in the mouse gastric fundus. *Biol Reprod* 2004; **70**: 222-228 [PMID: 14522837 DOI: 10.1095/biolreprod.103.018374]
26 **Garella R**, Squecco R, Baccari MC. Site-related Effects of Relaxin in the Gastrointestinal Tract Through Nitric Oxide Signalling: An Updated Report. *Curr Protein Pept Sci* 2017; **18**: 1254-1262 [PMID: 28606038 DOI: 10.2174/1389203718666170612104719]
27 **Moncada S**, Palmer RM, Higgs EA. Nitric oxide: physiology, pathophysiology, and pharmacology. *Pharmacol Rev* 1991; **43**: 109-142 [PMID: 1852778 DOI: 10.1080/07853890310004093]
28 **Groneberg D**, Voussen B, Friebe A. Integrative Control of Gastrointestinal Motility by Nitric Oxide. *Curr Med Chem* 2016; **23**: 2715-2735 [PMID: 27528058 DOI: 10.2174/0929867323666160812150907]
29 **Vallance P**. Nitric oxide: therapeutic opportunities. *Fundam Clin Pharmacol* 2003; **17**: 1-10 [PMID: 12588625 DOI: 10.1046/j.1472-8206.2003.00124.x]
30 **Bani D**, Baccari MC, Quattrone S, Nistri S, Calamai F, Bigazzi M, Bani Sacchi T. Relaxin depresses small bowel motility through a nitric oxide-mediated mechanism. Studies in mice. *Biol Reprod* 2002; **66**: 778-784 [PMID: 11870086 DOI: 10.1095/biolreprod66.3.778]
31 **Lam M**, Royce SG, Donovan C, Jelinic M, Parry LJ, Samuel CS, Bourke JE. Serelaxin Elicits Bronchodilation and Enhances β-Adrenoceptor-Mediated Airway Relaxation. *Front Pharmacol* 2016; **7**: 406 [PMID: 27833558 DOI: 10.3389/fphar.2016.00406]
32 **Bolton TB**, Prestwich SA, Zholos AV, Gordienko DV. Excitation-contraction coupling in gastrointestinal and other smooth muscles. *Annu Rev Physiol* 1999; **61**: 85-115 [PMID: 10099683 DOI: 10.1146/annurev.physiol.61.1.85]
33 **Austin CR,** Rowlands JW. Mammalian reproduction. The IAT Manual of Laboratory Animal Practice and Technique. 2nd edn, ed. Short DJ Woodnott DP. Bungay, UK: Lockwood. **1969**: 340-349 [DOI: 10.1038/223652b0]
34 **Mercado-Simmen RC**, Bryant-Greenwood GD, Greenwood FC. Relaxin receptor in the rat myometrium: regulation by estrogen and relaxin. *Endocrinology* 1982; **110**: 220-226 [PMID: 6274617 DOI: 10.1210/endo-110-1-220]
35 **Squecco R**, Garella R, Luciani G, Francini F, Baccari MC. Muscular effects of orexin A on the mouse duodenum: mechanical and electrophysiological studies. *J Physiol* 2011; **589**: 5231-5246 [PMID: 21911618 DOI: 10.1113/jphysiol.2011.214940]
36 **Squecco R**, Garella R, Francini F, Baccari MC. Influence of obestatin on the gastric longitudinal smooth muscle from mice: mechanical and electrophysiological studies. *Am J Physiol Gastrointest Liver Physiol* 2013; **305**: G628-G637 [PMID: 23989009 DOI: 10.1152/ajpgi.00059.2013]
37 **Squecco R**, Sassoli C, Garella R, Chellini F, Idrizaj E, Nistri

S, Formigli L, Bani D, Francini F. Inhibitory effects of relaxin on cardiac fibroblast-to-myofibroblast transition: an electrophysiological study. *Exp Physiol* 2015; **100**: 652-666 [PMID: 25786395 DOI: 10.1113/EP085178]

38 **Baccari MC**, Nistri S, Vannucchi MG, Calamai F, Bani D. Reversal by relaxin of altered ileal spontaneous contractions in dystrophic (mdx) mice through a nitric oxide-mediated mechanism. *Am J Physiol Regul Integr Comp Physiol* 2007; **293**: R662-R668 [PMID: 17522128 DOI: 10.1152/ajpregu.00214.2007]

39 **Vannucchi MG**, Garella R, Cipriani G, Baccari MC. Relaxin counteracts the altered gastric motility of dystrophic (mdx) mice: functional and immunohistochemical evidence for the involvement of nitric oxide. *Am J Physiol Endocrinol Metab* 2011; **300**: E380-E391 [PMID: 21081707 DOI: 10.1152/ajpendo.00375.2010]

40 **Baccari MC**, Traini C, Garella R, Cipriani G, Vannucchi MG. Relaxin exerts two opposite effects on mechanical activity and nitric oxide synthase expression in the mouse colon. *Am J Physiol Endocrinol Metab* 2012; **303**: E1142-E1150 [PMID: 22932783 DOI: 10.1152/ajpendo.00260.2012]

41 **Ibrahimi A**, Abumrad N, Maghareie H, Golia M, Shoshani I, Désaubry L, Johnson RA. Adenylyl cyclase P-site ligands accelerate differentiation in Ob1771 preadipocytes. *Am J Physiol* 1999; **276**: C487-C496 [PMID: 9950777 DOI: 10.1152/ajpcell.1999.276.2.C487]

42 **Boland BB**, Alarcón C, Ali A, Rhodes CJ. Monomethylated-adenines potentiate glucose-induced insulin production and secretion via inhibition of phosphodiesterase activity in rat pancreatic islets. *Islets* 2015; **7**: e1073435 [PMID: 26404841 DOI: 10.1080/19382014.2015.1073435]

43 **Ueno T**, Duenes JA, Zarroug AE, Sarr MG. Nitrergic mechanisms mediating inhibitory control of longitudinal smooth muscle contraction in mouse small intestine. *J Gastrointest Surg* 2004; **8**: 831-841 [PMID: 15531236 DOI: 10.1016/j.gassur.2004.06.004]

44 **Morgado M**, Cairrão E, Santos-Silva AJ, Verde I. Cyclic nucleotide-dependent relaxation pathways in vascular smooth muscle. *Cell Mol Life Sci* 2012; **69**: 247-266 [PMID: 21947498 DOI: 10.1007/s00018-011-0815-2]

45 **Omori K**, Kotera J. Overview of PDEs and their regulation. *Circ Res* 2007; **100**: 309-327 [PMID: 17307970 DOI: 10.1161/01.RES.0000256354.95791.f1]

46 **He XD**, Goyal RK. CaMKII inhibition hyperpolarizes membrane and blocks nitrergic IJP by closing a Cl(-) conductance in intestinal smooth muscle. *Am J Physiol Gastrointest Liver Physiol* 2012; **303**: G240-G246 [PMID: 22538403 DOI: 10.1152/ajpgi.00102.2012]

47 **McDonald TF**, Pelzer S, Trautwein W, Pelzer DJ. Regulation and modulation of calcium channels in cardiac, skeletal, and smooth muscle cells. *Physiol Rev* 1994; **74**: 365-507 [PMID: 8171118 DOI: 10.1152/physrev.1994.74.2.365]

48 **Sanborn BM**. Hormones and calcium: mechanisms controlling uterine smooth muscle contractile activity. The Litchfield Lecture. *Exp Physiol* 2001; **86**: 223-237 [PMID: 11429639 DOI: 10.1113/eph8602179]

P- Reviewer: Chiba T, Grizzi F **S- Editor**: Chen K **L- Editor**: A **E- Editor**: Ma YJ

World Journal of Gastroenterology

Submit a Manuscript: http://www.f6publishing.com

World J Gastroenterol 2018 February 28; 24(8): 894-904

DOI: 10.3748/wjg.v24.i8.894

ISSN 1007-9327 (print) ISSN 2219-2840 (online)

ORIGINAL ARTICLE

Basic Study

Gas chromatography/mass spectrometry based metabolomic study in a murine model of irritable bowel syndrome

Lei-Min Yu, Ke-Jia Zhao, Shuang-Shuang Wang, Xi Wang, Bin Lu

Lei-Min Yu, Ke-Jia Zhao, Shuang-Shuang Wang, Bin Lu, Department of Gastroenterology, First Affiliated Hospital of Zhejiang Chinese Medical University, Hangzhou 310006, Zhejiang Province, China

Lei-Min Yu, Ke-Jia Zhao, Shuang-Shuang Wang, First Clinical Medical College of Zhejiang Chinese Medical University, Hangzhou 310053, Zhejiang Province, China

Xi Wang, Key Laboratory of Digestive Pathophysiology of Zhejiang Province, First Affiliated Hospital of Zhejiang Chinese Medical University, Hangzhou 310053, Zhejiang Province, China

ORCID number: Lei-Min Yu (0000-0001-8436-9232); Ke-Jia Zhao (0000-0002-7127-5736); Shuang-Shuang Wang (0000-0003-4265-7003); Xi Wang (0000-0003-4861-0441); Bin Lu (0000-0002-6247-571X).

Author contributions: Yu LM, Zhao KJ, Wang SS, Wang X and Lu B designed the study; Yu LM and Zhao KJ collected and analyzed the data; Yu LM drafted and wrote the manuscript; Lu B revised the manuscript critically for intellectual content; all authors gave intellectual input to the study and approved the final version of the manuscript.

Supported by the National Natural Science Foundation of China, No. 81470814 and No. 81400594; and Zhejiang Provincial Natural Science Foundation of China, No. LQ14H160014.

Institutional review board statement: This study was approved by the Ethics Committee of the Zhejiang Chinese Medical University. All procedures in the animal studies were performed in accordance with the ethical standards of the institution or practice.

Institutional animal care and use committee statement: All procedures were approved by the Animal Care Committee of Zhejiang Chinese Medical University, and all methods were performed in accordance with the relevant guidelines and regulations.

Conflict-of-interest statement: The authors declare that they have no conflict of interest.

Data sharing statement: No additional data are available.

ARRIVE guidelines statement: The authors have read the ARRIVE guidelines, and the manuscript was prepared and revised according to the ARRIVE guidelines.

Manuscript source: Unsolicited manuscript

Correspondence to: Bin Lu, MD, PhD, Doctor, Professor, Department of Gastroenterology, First Affiliated Hospital of Zhejiang Chinese Medicine University, No. 54, Youdian Road, Hangzhou 310006, Zhejiang Province, China. lvbin@medmail.com.cn
Telephone: +86-571-87032028
Fax: +86-571-87077785

Received: December 13, 2017
Peer-review started: December 13, 2017
First decision: December 27, 2017
Revised: January 12, 2018
Accepted: January 20, 2018
Article in press: January 20, 2018
Published online: February 28, 2018

Abstract

AIM

To study the role of microbial metabolites in the modulation of biochemical and physiological processes in irritable bowel syndrome (IBS).

METHODS

In the current study, using a metabolomic approach, we analyzed the key metabolites differentially excreted in the feces of control mice and mice with IBS, with or without *Clostridium butyricum (C. butyricum)* treatment. C57BL/6 mice were divided into control, IBS, and IBS + *C. butyricum* groups. In the IBS and IBS + *C. butyricum* groups, the mice were subjected to water avoidance stress (WAS) for 1 h/d for ten days. Gas chromatography/mass spectrometry (GC-MS) together with multivariate analysis was employed to compare the fecal samples between groups.

RESULTS

WAS exposure established an appropriate model of IBS in mice, with symptoms of visceral hyperalgesia and diarrhea. The differences in the metabolite profiles between the control group and IBS group significantly changed with the progression of IBS (days 0, 5, 10, and 17). A total of 14 differentially excreted metabolites were identified between the control and IBS groups, and phenylethylamine was a major metabolite induced by stress. In addition, phenylalanine metabolism was found to be the most relevant metabolic pathway. Between the IBS group and IBS + *C. butyricum* group, 10 differentially excreted metabolites were identified. Among these, pantothenate and coenzyme A (CoA) biosynthesis metabolites, as well as steroid hormone biosynthesis metabolites were identified as significantly relevant metabolic pathways.

CONCLUSION

The metabolic profile of IBS mice is significantly altered compared to control mice. Supplementation with *C. butyricum* to IBS mice may provide a considerable benefit by modulating host metabolism.

Key words: Irritable bowel syndrome; Metabolite; Gas chromatography/mass spectrometry; *Clostridium butyricum*

Core tip: In this study, we analyzed the key metabolites differentially excreted in the feces of control mice and mice with irritable bowel syndrome (IBS). A total of 14 differentially excreted metabolites were identified, and phenylalanine (a major metabolite induced by stress) was found to be the most relevant of these metabolites. Between the IBS group and IBS + *C. butyricum* group, 10 differentially excreted metabolites were identified, and pantothenate and coenzyme A (CoA) biosynthesis metabolites, as well as steroid hormone biosynthesis metabolites were found to be significantly relevant. Thus, supplementation with *C. butyricum* to IBS mice had beneficial effects through modulation of host metabolism.

Yu LM, Zhao KJ, Wang SS, Wang X, Lu B. Gas chromatography/mass spectrometry based metabolomic study in a murine model of irritable bowel syndrome. *World J Gastroenterol* 2018; 24(8): 894-904 Available from: URL: http://www.wjgnet.com/1007-9327/full/v24/i8/894.htm DOI: http://dx.doi.org/10.3748/wjg.v24.i8.894

INTRODUCTION

Irritable bowel syndrome (IBS) is a functional disorder of the gastrointestinal (GI) tract. Although the pathology is complicated, it is believed that multiple factors such as genetics, visceral hypersensitivity, gastrointestinal motility, dysregulation of the brain-gut axis, levels of neuropeptides and hormones, as well as inflammatory changes all contribute to IBS development[1]. Recent emerging evidence has demonstrated certain disorders that alter fecal microbiota profiles may cause IBS[2-7]. The adult human intestinal tract contains a high density of microbes (typically 10^{11}-10^{12} microbes/mL of luminal content)[8], which are predominantly obligate anaerobes[3]. The gut microbiota not only enhances host digestion, nutrient absorption, and energy turnover, but also substantially regulates metabolism, protects against pathogens, and modulates the host immune response[9]. Probiotics are defined as "living nonpathogenic microorganisms that benefit the health of the host by modifying intestinal flora"[10]. A recent study found that both probiotics and symbiotics can benefit host health by improving the body's nitrogen metabolism[11].

Microbial metabolites positively influence biochemical and physiological processes. Thus, studying the impact of the microbiota on host–microbial interactions is more important than identifying the microbial species present. The metabolome, a complete collection of all metabolites in a biological specimen, is the end-product of the complex interactions between the genome, transcriptome, proteome, and the environment. Metabolomics is defined as "the nonbiased identification and quantification of all metabolites in a biological system"[12]. The metabolome amplifies the metabolic changes caused by a certain biological perturbation[13]. Fecal samples are ideal biospecimen for metabolomics analysis, due to the non-invasive nature of sample collection. Fecal metabolic compositions and variations not only reflect the status of the intestinal microbiota, but also bridge the relationship between symbiotic microbes and host health[14-16]. Thus, the metabonomics signature of IBS fecal samples will be useful to study the IBS pathological process.

The gas chromatography/mass spectrometry (GC-MS) platform presents a unique tool with high sensitivity, high reproducibility, and available spectral libraries. In this study, we investigated the changes of the fecal metabolome in IBS pathology using a murine water-avoidance stress (WAS) model of IBS. The purpose of this study was to compare and verify important metabolites and key pathway alterations between IBS mice and control mice, as well as

between IBS mice with and without *C. butyricum* treatment.

MATERIALS AND METHODS

Probiotic strains

C. butyricum (S20020015) was kindly provided by Shandong Kexing Bioproducts Co. Ltd. (China). Freeze-dried *C. butyricum* powder contained both viable bacteria [5.6 × 10^9 colony-forming units (CFU)/g] and spores (4.4 × 10^9 CFU/g). Before use, the probiotic powder was reconstituted in sterile saline at 37 ℃ for 15 min. The final concentration of *C. butyricum* was 1.25 × 10^9 CFU/mL.

Animals and experimental design

Female C57BL/6 mice (n = 18, aged 5-6 wk) were purchased from the Experimental Animal Center of Zhejiang Province (Zhejiang, China), and housed in the animal maintenance facility at the Zhejiang Chinese Medical University. Mice were randomly divided into three groups (control, IBS, and IBS + *C. butyricum*), with six mice in each group. Mice in the IBS and IBS + *C. butyricum* groups were exposed to water-avoidance stress (WAS) for 1 h every day for ten days to induce IBS. All procedures were performed between 8:00 and 10:00 AM to minimize the bias of the circadian rhythm. Briefly, mice were placed on a small platform (3 cm × 6 cm) in a plastic container (56 cm × 50 cm) with warm water (25 ℃) 1 cm below the platform. After the ten-day WAS period, mice in the IBS and IBS + *C. butyricum* groups were given sterile saline (0.4 mL) and *C. butyricum* (0.4 mL, 5 × 10^8 CFU), respectively, by gastric gavage daily for a seven-day treatment period. All procedures were approved by the Animal Care Committee of Zhejiang Chinese Medical University, and all methods were performed in accordance with the relevant guidelines and regulations.

Assessment of stool features and visceral sensitivity

Fecal features were evaluated through visual inspection performed by two investigators blinded to the randomization. Presence of semisolid, pasty, or watery stools was considered abnormal[17]. Fresh fecal pellets were collected from all mice in individual metabolic cages within 2 h on days 0, 5, 10, and 17. All fecal samples were then stored at -80 ℃ until further analysis. The visceral sensitivity of mice was evaluated by measuring the abdominal withdrawal reflex (AWR) in response to colorectal distension (CRD)[18]. Semi-quantitative AWR scores (0-4) were used to grade pain responses at various magnitudes of CRD (20, 40, 60, and 80 mmHg)[17,19,20]. Two investigators blinded to the randomization recorded the AWR scores at each pressure five times to improve accuracy.

Metabolite extraction

Fecal samples were collected in 2 mL microfuge tubes, and were extracted with extraction liquid (0.3 mL; methanol: chloroform at 3:1). L-2-chlorophenylalanine (20 μL; 1 mg/mL stock in dH_2O) was added as an internal standard. The mixture was vortexed for 30 s and homogenized in a ball mill for 4 min at 45 Hz, and then exposed to ultrasound for 5 min on ice. The supernatant (0.2 mL) was transferred into a fresh 2 mL GC-MS glass vial, and 4 μL from each sample was used to generate a quality control (QC) pooled sample.

Derivatives of metabolites

Fecal samples were dried in a vacuum concentrator without heating. Methoxyamination hydrochloride (70 μL; 20 mg/mL in pyridine) was added and the mixture was incubated at 80 ℃ for 30 min, followed by addition of the bis(trimethylsilyl)trifluoroacetamide regent (80 μL; 1% trimethylchlorosilane, v/v) to the sample aliquots, which were further incubated for 2 h at 70 ℃. A standard mixture of fatty acid methyl esters (10 μL; C8-C16: 1 mg/mL; C18-C24: 0.5 mg/mL in chloroform) was added to the QC sample. Samples were then cooled to room temperature and mixed well prior to GC-MS analysis.

GC-MS analysis

GC-MS analysis was performed using an Agilent 7890 gas chromatograph system coupled with a Pegasus HT time-of-flight mass spectrometer. The system utilized a DB-5MS capillary column coated with 5% diphenyl cross-linked with 95% dimethylpolysiloxane. An aliquot of the analyte (1 μL) was injected in a splitless mode according to the instructions from the kit. The carrier gas was helium, the front inlet purge flow was 3 mL/min, and the gas flow rate through the column was 1 mL/min. The initial temperature for 1 min was 50 ℃. The temperature was then raised to 305 ℃ at a rate of 12 ℃/min, and maintained for 7.75 min at 305 ℃. The energy was -70 eV in electron impact mode. The mass spectrometry data were acquired in full-scan mode with the mass-to-charge (m/z) range of 50-500 at a rate of 20 spectra per sec after a solvent delay of 6.1 min.

Metabolic profiling analysis

Chroma TOF 4.3× software from LECO Corporation and the LECO-Fiehn Rtx5 database were used for metabolic profiling analysis as described previously[21]. The RI (retention time index) method was used for peak identification, and the RI tolerance was 5000. The metabolic features detected in < 50% of QC samples were removed[22]. Raw GC-MS data were exported to mzData format using MassHunter Workstation Software (Version B.06.00, Agilent Technologies) and subsequently sent to the XCMS package under the R Project. In addition, an internal standard normalization method was used for the analysis of these data. The resulting three-dimensional data involving the peak number, sample name, and normalized peak area were submitted to SIMCA14.1 software package (V14.1, MKS

Table 1 Assessment of fecal features

Fecal feature	Control	IBS	IBS + *C. butyricum*
After WAS exposure Normal/Abnormal (*n*)	6/0	0/6[b]	0/6[b]
After treatment Normal/Abnormal (*n*)	6/0	0/6[a]	5/1[c]

The presence of semisolid, pasty, or watery stools was considered abnormal. [b]$P < 0.01$: control *vs* IBS or IBS + *C. butyricum*; [c]$P < 0.05$, IBS *vs* IBS + *C. butyricum*; [a]$P < 0.05$, control *vs* IBS. *C. butyricum*: *Clostridium butyricum*; IBS: Irritable bowel syndrome; WAS: Water avoidance stress.

Data Analytics Solutions, Umea, Sweden) for principal component analysis (PCA) and orthogonal projections to latent structures-discriminate analysis (OPLS-DA). PCA provided the distribution of origin data. Subsequently, as an effective approach to sift metabolites, the score plot of OPLS-DA was achieved to detect differences and filter variations between the groups. The quality of the models was assessed by the R^2 and Q^2 values in OPLS-DA, which represented the variance and the predictability derived from the models. After assessing the data in OPLS-DA, 200 permutations were performed, and the resulting R^2 and Q^2 values were plotted to further assess the model validity. To refine this analysis, the first principal component of variable importance in the projection (VIP) was obtained. A VIP that exceeded 1 with a *P*-value less than 0.05 indicated a changed biomarker. In addition, the Kyoto Encyclopedia of Genes and Genomes (KEGG) database (http://www.genome.jp/kegg/) was utilized to link these metabolites to metabolic pathways. MetaboAnalyst, which uses the high-quality KEGG metabolic pathway as the backend knowledge base, as well as integrated enrichment analysis and pathway topology analysis were used to identify the most relevant pathways (http://www.metaboanalyst.ca).

Statistical analysis

Differences between groups were analyzed by Student's *t*-test for variables following a normal distribution or Wilcoxon two-sample test for variables without following a normal distribution. A χ^2 test was used in the analysis of contingency tables. Data are presented as mean ± SD. A *P*-value < 0.05 was considered statistically significant. Statistical analyses were conducted using SPSS 22.0 (Chicago, IL, United States) and GraphPad Prism 6.0 software (San Diego, CA, United States).

RESULTS

Impact of C. butyricum treatment on IBS mice

At day 10 following WAS exposure, all 12 IBS mice (IBS and IBS + *C. butyricum* groups) demonstrated increased mean AWR scores at CRD pressures of 20, 40, 60, and 80 mmHg compared to the six control mice (Figure 1A). A higher proportion of IBS mice showed abnormal stool features and a consistently increased number of fecal pellets compared with control mice (Table 1 and Figure 1B). These results suggested that WAS exposure established an appropriate model of IBS with symptoms of visceral hyperalgesia and diarrhea. Interestingly, when *C. butyricum* was given for 7 d to WAS-exposed mice, the AWR scores were significantly reduced (Figure 1C), and the stool features and number of pellets were improved (Table 1 and Figure 1B), suggesting that *C. butyricum* treatment could relieve IBS symptoms in WAS-exposed mice.

Metabolomic profiles

Fecal metabolite profiles in the control and IBS groups were carefully compared. A heat map analysis revealed that metabolomics could be used to distinguish between the control and IBS groups (Figure 2). With the progression of time (days 0, 5, 10, and 17), the differences in the metabolite profiles between these two groups were significant. When comparing the fecal metabolite profiles of the control group with those of the IBS model group on day 17, PCA revealed that metabolites were distinguishable between the groups (Figure 3A). OPLS-DA was used to examine the metabolites that contributed to the group separation (Figure 3B). Permutation testing performed on the OPLS-DA model revealed remarkable positive slopes (Figure 3C), indicating statistical significance in the separation of these two groups. A total of 14 differentially excreted metabolites were distinguishable in the IBS model group compared to the control group, including myristic acid, arachidic acid, octadecanol, N-acetyl-D-galactosamine 1,1-hexadecanol, phenylethylamine, 2-furoic acid, 4,2′,4′-trihydroxychalcone, 24,25-dihydrolanosterol, androsterone 1, chlorogenic acid 1, cysteinylglycine 2, alpha-tocopherol, and 4-hydroxybenzoic acid. Table 2 summarizes the metabolite differences between the IBS model and control samples.

To further explore the biological significance associated with IBS morbidity, we used MetaboAnalyst to detect the key relevant pathways influenced by IBS. This pathway analysis revealed that phenylalanine metabolism was the most relevant pathway influenced by IBS with an impact value of 0.222 (Figure 3D).

To test whether the metabolomic profile could be used to distinguish the IBS + *C. butyricum* group from the IBS group, we performed a comparison of metabolomic profiles in these two groups. PCA revealed that the metabolomics were significantly different between these two groups (Figure 4A). OPLS-DA was used to examine the metabolites that contributed to the separation (Figure 4B). Permutation testing performed on the OPLS-DA model revealed significantly positive slopes (Figure 4C), indicating statistical significance for these two groups. The ten differentially excreted metabolites between the IBS and IBS + *C. butyricum*

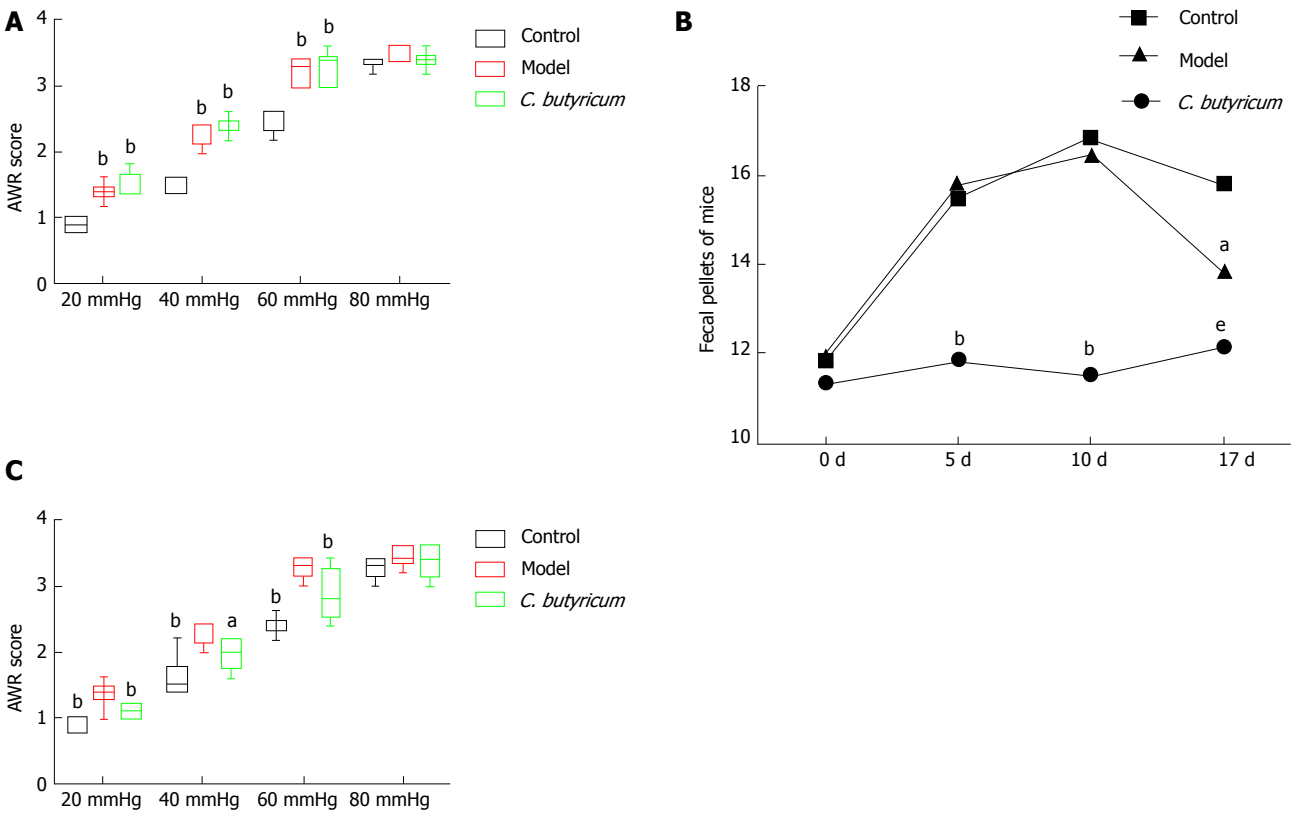

Figure 1 Impact of *Clostridium butyricum* treatment on irritable bowel syndrome mice. A: Comparison of AWR scores between control and IBS groups, as well as between IBS and IBS + *C. butyricum* groups after WAS exposure (n = 6 per group). $^{a}P < 0.05$; $^{b}P < 0.01$. B: Fecal pellets at various time points during the experiment (n = 6 per group). $^{a}P < 0.05$: IBS *vs* IBS + *C. butyricum*; $^{b}P < 0.01$: control *vs* IBS, control *vs* IBS + C. buyricum; $^{e}P < 0.001$: control *vs* IBS. C: Comparison of AWR scores between control and IBS groups, as well as between IBS and IBS + *C. butyricum* groups following the *C. butyricum* treatment period (n = 6 per group) $^{a}P < 0.05$; $^{b}P < 0.01$. AWR: Abdominal withdrawal reflex; *C. butyricum*: Clostridium butyricum; IBS: Irritable bowel syndrome; WAS: Water avoidance stress.

groups were pantothenic acid, cysteinylglycine 2, d-arabitol, arbutin, 3-hydroxyphenylacetic acid, 4-hydroxybenzaldehyde 2, 1-hexadecanol, octadecanol, 5,6-dihydrouracil 1, and androsterone 1 (Table 3).

To explain the biological significance associated with *C. butyricum* administration, we applied MetaboAnalyst to test the important relevant pathways influenced by IBS and IBS + *C. butyricum* treatment. Pantothenate, coenzyme A (CoA) biosynthesis, and steroid hormone biosynthesis were found to be involved in the most relevant pathways influenced by *C. butyricum* treatment with impact values of 0.077 and 0.013, respectively (Figure 4D).

DISCUSSION

In this study, we studied the fecal metabolic profile in a mouse model of IBS, and investigated the impact of *C. butyricum* on metabolic changes using the GC-MS technique. A total of 14 differentially excreted metabolites were identified in the control and IBS groups, and phenylalanine metabolism was the significant metabolic pathway identified in the IBS group. We found that even 7 d following WAS termination, the metabolites in the IBS group were still distinct from those in the control group. The AWR scores, and the number and features of the fecal pellets were also still abnormal in the IBS group compared to the control group, indicating that the pathological processes resulting in IBS-like symptoms did not immediately stop upon stress termination. Of note, phenylethylamine, which is involved in the key metabolism pathway of phenylalanine, was significantly increased in the IBS model group. Interestingly, treatment of IBS mice with *C. butyricum* decreased the fecal pellet number and AWR scores, and restored the fecal features. A total of ten differentially expressed metabolites were identified in the IBS + *C. butyricum* and IBS model groups. Among these, pantothenic acid and androsterone 1 were increased in the IBS + *C. butyricum* group. Both pantothenic acid and androsterone 1 are implicated in the key metabolic pathways of pantothenate and CoA biosynthesis, as well as steroid hormone biosynthesis. Therefore, *C. butyricum* could change metabolic pathways and reduce visceral sensitivity and diarrhea symptoms in IBS mice.

The digestive tract of the host is colonized with a highly complex array of microorganisms composed mainly of bacteria, with numbers increasing progressively from the proximal to the distal colon[23]. The microbiome includes more than five million genes. Many genes encode biosynthetic enzymes, proteases, and glycosidases to enlarge the host's biochemical and metabolic capabilities[24]. Such interactions were

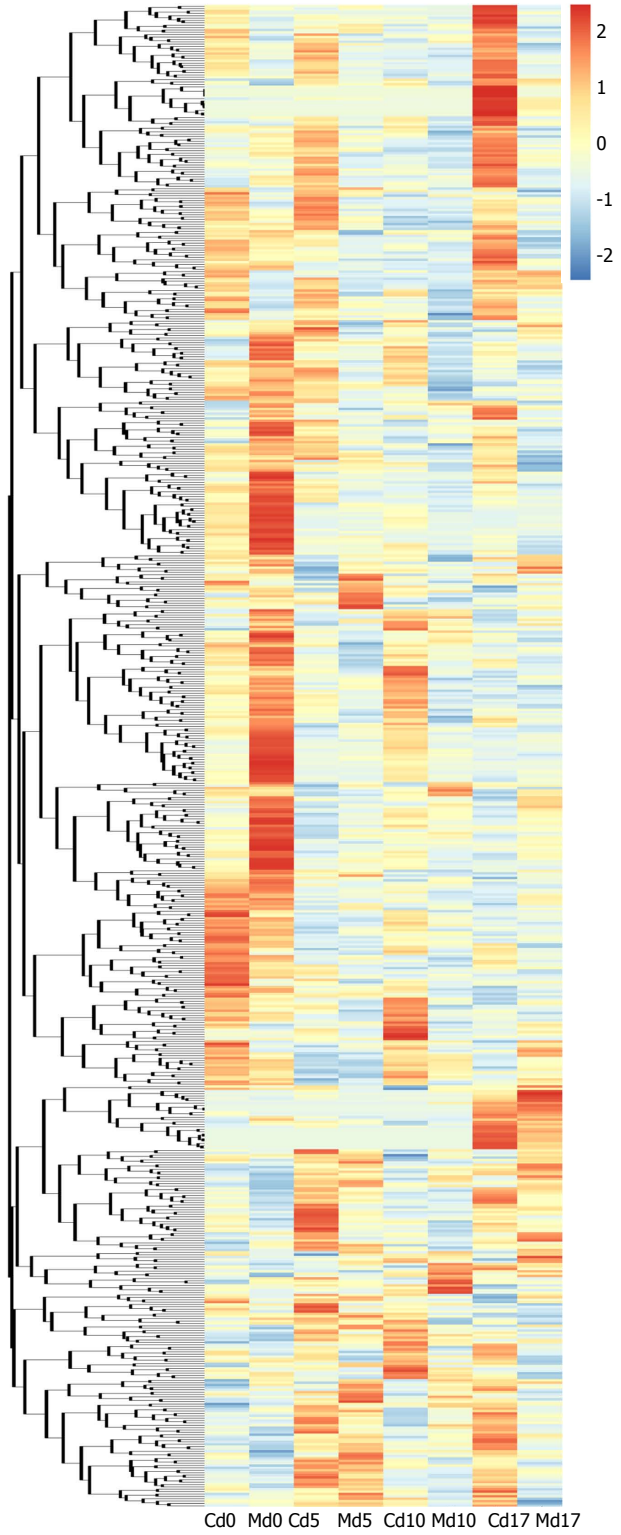

Figure 2 Heatmap of hierarchical clustering analysis for irritable bowel syndrome group *vs* control group at various time points. The colors at different positions indicate the relative expression of the corresponding metabolites. C: Control group; M: Model (IBS) group. IBS: Irritable bowel syndrome.

termed the "microbial-mammalian metabolic axis", which was defined as "the multi-way exchange and co-metabolism of compounds between the host organism and the gut microbiome resulting in transgenically-regulated secondary metabolites, which have biological activity on both host and microbial compartments"[25,26]. Intestinal bacteria primarily influence the metabolism of amino acids, fatty acids, steroid hormone biosynthesis, and oxidative stress pathways. Any changes in the gut microbiota, such as the diversity, the number, or the stability, could affect metabolic end-products and lead to disease development. These metabolites can harm the host through[27]: (1) toxic and/or carcinogenic metabolites produced directly; (2) disturbances of the homeostatic energy balance, resulting in changes to host physiology; (3) increased proliferation of other potentially harmful bacteria *via* syntrophy; and (4) direct interaction with intestinal epithelial cells. Gall *et al*[28] have used proton nuclear magnetic resonance metabolite profiling of fecal extracts to separate IBS patients from healthy controls, and indicated that the gut microbial metabolites were important factors implicated in the pathogenesis of IBS. Dietary probiotics have been shown to improve the health of the host[29]. A recent study found that probiotics altered a diversity of pathways including amino acid metabolism, methylamines, and short-chain fatty acids (SCFA)[30]. Martin *et al*[31] also found that the application of *Lactobacillus paracasei* into the intestine of germ free mice changed the concentration of amino acids, anti-oxidants, and creatine in the jejunum and ileum of these mice.

Amino acids are major nutrients in the diet and the basic units of protein. The host uses amino acids as metabolic fuel, and gut bacteria are linked to host energy metabolism. Proportions of arginine, proline, and phenylalanine were shown to be high in *Streptococcus spp*[32]. As an essential aromatic amino acid, phenylalanine is utilized for protein synthesis by cells throughout the body. Peripheral phenylalanine is elevated in phenylketonuria disease, which can lead to mental retardation, seizures, and neurological and psychiatric dysfunctions[33]. Phenylalanine has also been linked to inflammation. Klassen *et al*[34] have found that the phenylalanine level was increased in patients during the acute phase of dengue fever, suggesting that infection may alter amino acid metabolism. In our study, we found increased phenylethylamine in fecal extracts of IBS mice compared with healthy control mice, indicating that the increased stress in mice led to higher phenylethylamine levels. Phenylethylamine is an endogenous neuroamine that promotes energy and elevates mood[35], and it is a potential mediator of stress[36] . We speculated that the fecal metabolic changes could be associated with increased energy metabolism induced by stress in IBS mice to accommodate the extra energy demand due to muscle hyper-contractility and inflammation. These findings were consistent with a study by Martin *et al*[37], in which they also indicated that post-infectious IBS was related to changes in energy metabolic intermediates, as well as lipid and amino acid metabolism, to meet the energy demand of intestinal muscular hyper-

Table 2 Metabolites distinguishing irritable bowel syndrome mice from control mice

Compound	Formula	Similarity	RT (min)	VIP value	*P* value	Fold change	Trend compared with controls
N-acetyl-D-galactosamine 1	$C_8H_{15}NO_6$	886	17.1523,0	1.167810623	0.002673237	2.665558179	Down
Myristic acid	$C_{14}H_{28}O_2$	878	15.2969,0	1.454697623	0.033949959	2.405282471	Down
Arachidic acid	$C_{20}H_{40}O_2$	837	19.8283,0	2.030221054	0.033823382	0.555519799	Up
1-Hexadecanol	$C_{16}H_{34}O$	761	16.2434,0	2.137279002	0.03239841	3.735617796	Down
Octadecanol	$C_{18}H_{38}O$	632	17.7928,0	1.226172539	0.039254153	3.503198671	Down
Phenylethylamine	$C_8H_{11}N$	764	12.6834,0	1.844742352	0.040836128	0.234956253	Up
2-Furoic acid	$C_5H_4O_3$	710	7.80292,0	1.057850377	0.044324108	1.829643584	Down
4,2',4'-Trihydroxychalcone	$C_{15}H_{12}O_4$	245	22.6862,0	1.871154718	0.049356394	0.502503451	Up
24,25-Dihydrolanosterol	$C_{30}H_{52}O$	593	25.186,0	2.237217404	0.041969612	0.449343275	Up
Androsterone 1	$C_{19}H_{30}O_2$	476	20.6021,0	1.51415211	0.031210567	2.125877191	Down
Chlorogenic acid 1	$C_{16}H_{18}O_9$	402	23.8786,0	1.950369158	0.016252537	3.264118801	Down
Cysteinylglycine 2	$C_{10}H_{18}N_4O_6S_2$	393	16.5878,0	2.464379346	0.003149634	11.06227902	Down
Alpha-tocopherol	$C_{29}H_{50}O_2$	305	24.0995,0	1.25237824	0.040967864	0.406678915	Up
4-Hydroxybenzoic acid	$C_7H_6O_3$	811	13.2781,0	1.348316951	0.0129929	2.36224644	Down

IBS: Irritable bowel syndrome; RT: Retention time; VIP: Variable importance in the projection.

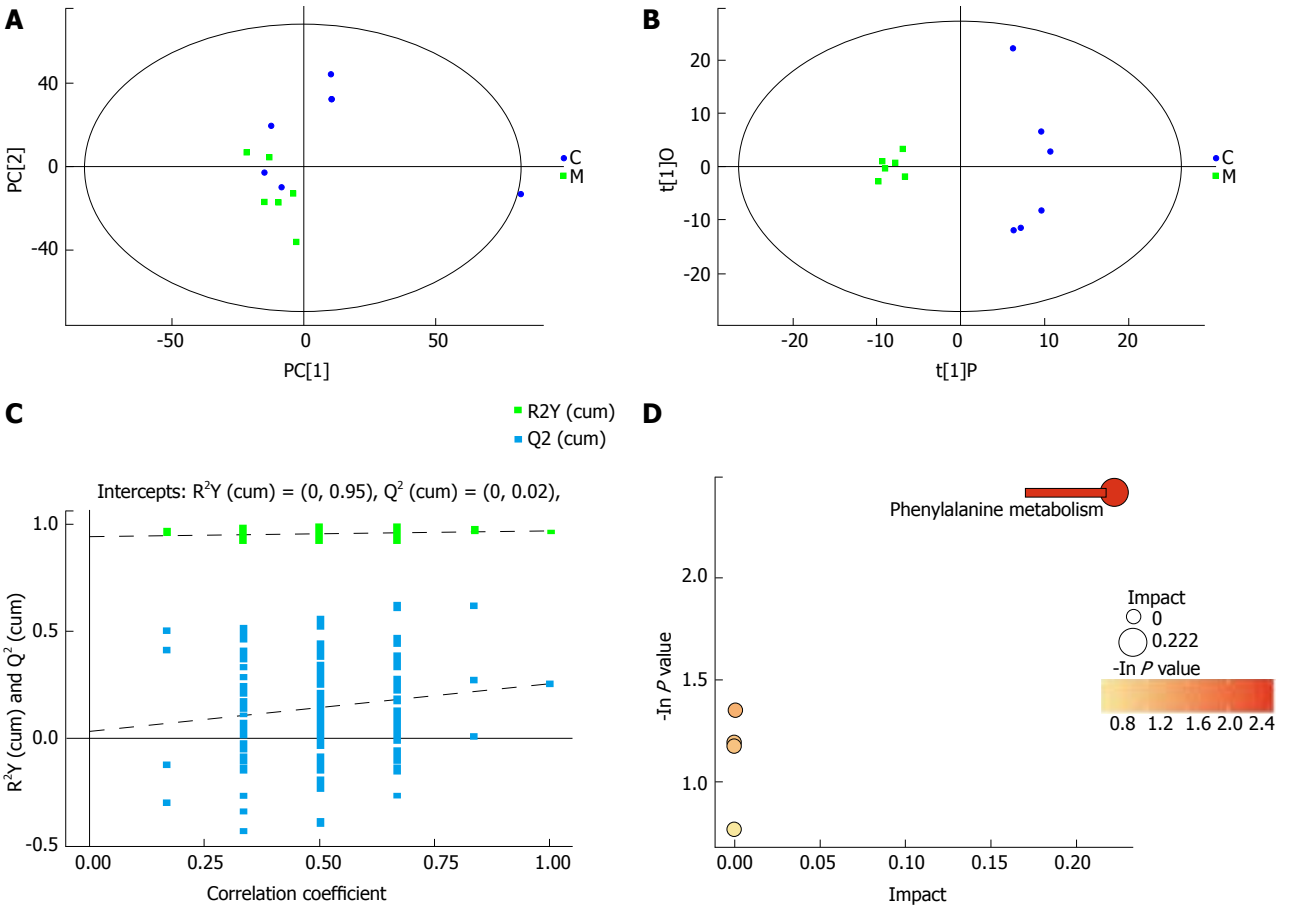

Figure 3 Separating the irritable bowel syndrome group from the control group by metabolic profiling analysis. A: Score scatter plot of PCA model for IBS group *vs* control group; B: Score scatter plot of OPLS-DA model for model group *vs* control group; C: Permutation test of OPLS-DA model for model group *vs* control group; D: Pathway analysis for IBS group *vs* control group. C: Control group; M: Model (IBS) group; PCA: Principal component analysis; OPLS-DA: Orthogonal projections to latent structures-discriminant analysis; IBS: Irritable bowel syndrome; *C. butyricum: Clostridium butyricum*.

contractility[37]. In another study, Ponnusamy *et al*[38] found that amino acids and phenolic compounds were increased in IBS patients. This metabolic signature is similar to that observed in humans experiencing stress and trauma. Therefore, it is likely that there exists an energy metabolism disorder induced by stress in the IBS pathological processes. In our study, we also found that alpha-tocopherol was increased in the feces of IBS mice, likely resulting from its poor absorption due to diarrhea. Alpha-tocopherol was shown to be an important anti-oxidant metabolite with anti-inflammatory activity[39]. Therefore, its poor absorption

Table 3 Differentially excreted metabolites in response to *Clostridium butyricum*

Compound	Formula	Similarity	RT (min)	VIP value	*P*-value	Fold change	Trend compared with IBS mice
Pantothenic acid	$C_9H_{17}NO_5$	844	16.4657,0	1.387200939	0.016130158	0.408462268	Up
Cysteinylglycine 2	$C_{10}H_{18}N_4O_6S_2$	393	16.5878,0	1.498082744	0.047913423	0.166509123	Up
D-Arabitol	$C_5H_{12}O_5$	807	14.118,0	2.6949064	0.04068909	2511115.131	Down
Arbutin	$C_{12}H_{16}O_7$	569	20.5587,0	1.693255625	0.019486947	0.467550145	Up
3-Hydroxyphenylacetic acid	$C_8H_8O_3$	545	13.0677,0	1.462693364	0.014333152	0.467960253	Up
4-Hydroxybenzaldehyde 2	$C_7H_6O_2$	798	11.9397,0	1.38788733	0.01853018	0.376921771	Up
1-Hexadecanol	$C_{16}H_{34}O$	761	16.2434,0	2.206799293	0.049776549	0.311045618	Up
Octadecanol	$C_{18}H_{38}O$	632	17.7928,0	1.352431526	0.033517221	0.308621946	Up
5,6-Dihydrouracil 1	$C_4H_6N_2O_2$	512	11.8596,0	1.260961668	0.022218939	0.600255286	Up
Androsterone 1	$C_{19}H_{30}O_2$	476	20.6021,0	1.62619412	0.04838445	0.494710622	Up

IBS: Irritable bowel syndrome; RT: Retention time; VIP: Variable importance in the projection.

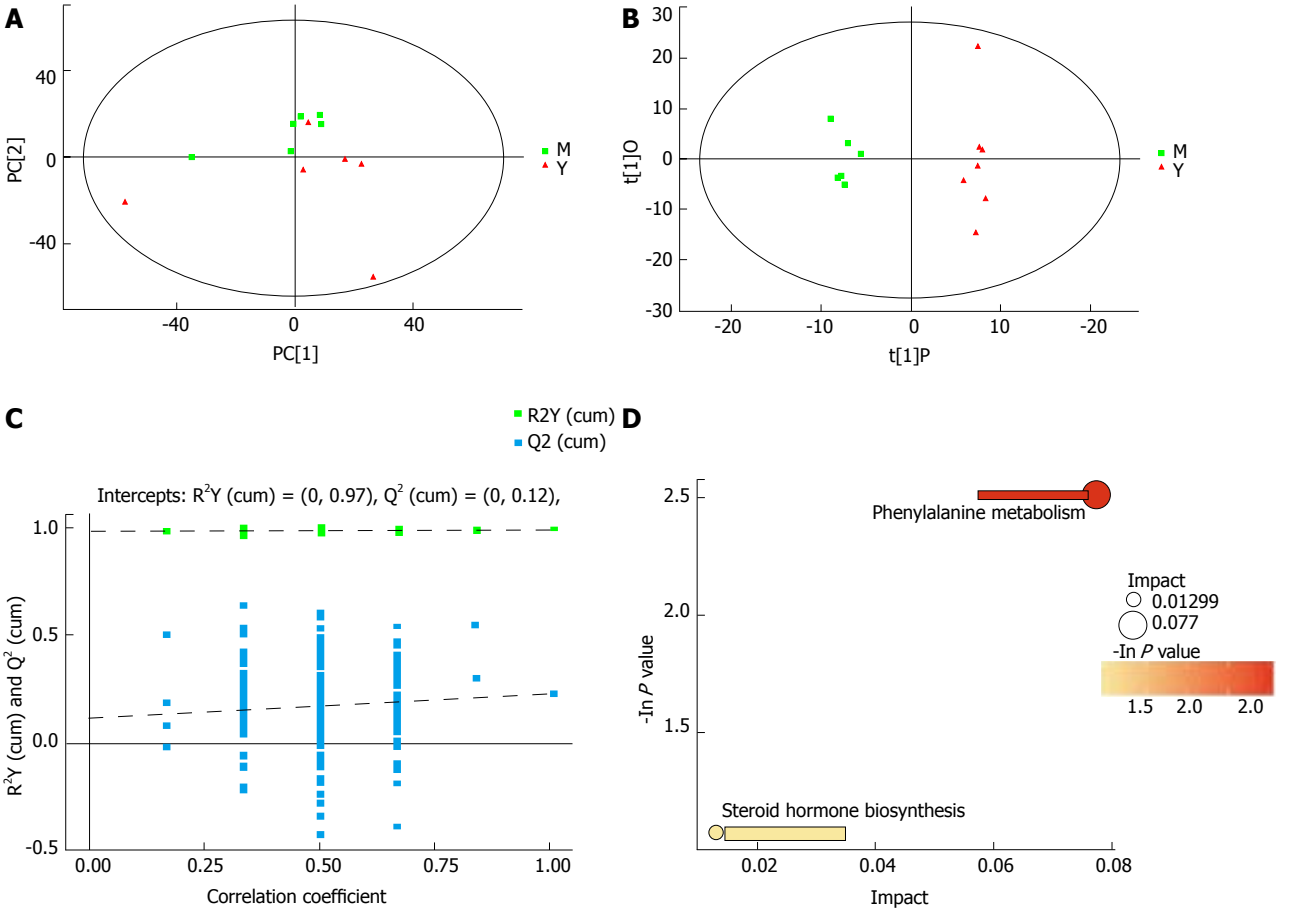

Figure 4 Separating the group treated with *Clostridium butyricum* from the irritable bowel syndrome only group by metabolic profiling analysis. A: Score scatter plot of PCA model for IBS group *vs* IBS + *C. butyricum* group; B: Score scatter plot of OPLS-DA model for IBS group *vs* IBS + *C. butyricum* group; C: Permutation test of OPLS-DA model for IBS group *vs* IBS + *C. butyricum* group; D: Pathway analysis for IBS group *vs* IBS + *C. butyricum* group. M: Model (IBS) group; Y: IBS + *C. butyricum* group; PCA: Principal component analysis; OPLS-DA: Orthogonal projections to latent structures-discriminant analysis; IBS: Irritable bowel syndrome; *C. butyricum*: *Clostridium butyricum*.

would further deteriorate the state of IBS. Vitamins are micronutrients that serve as precursors to many important enzymes necessary for vital biochemical reactions in all living cells, and vitamin metabolism has been shown to be important in all types of gut microbiomes[40]. Pantothenic acid is widely distributed in foods, and interestingly, *Escherichia coli* secretes 15-fold more pantothenic acid than that required for maintaining intracellular CoA biosynthesis[41]. The precursor of CoA is pantothenic acid, and CoA is necessary for 4% of known enzymatic reactions[42]. CoA is involved in cellular functions and mitochondrial energy production associated with fatty acids, cholesterol, heme synthesis, and acetylcholine, and also takes part in mitochondrial aerobic respiration (tricarboxylic acid (TCA) cycle)[42,43]. Increased levels of CoA contribute to cellular repair by diminishing lipid peroxidation and potentiating the synthesis of membrane phospholipids.

Even *et al*[44] found that pantothenic acid had a protective effect by improving the muscular response in a mouse model of muscular dystrophy. Tumors in animals have been found to have low CoA levels[45], which were related to increased glycolytic metabolism but less associated with oxidative phosphorylation and the TCA cycle. In our study, we found that the *C. butyricum* treatment increased the level of pantothenic acid, suggesting that *C. butyricum* likely modulates energy metabolism in IBS mice by up-regulating the pantothenate and CoA biosynthesis pathways. Martin *et al*[46] found that probiotics could improve fecal excretion of glutamine, branched-chain amino acids, glutamate, glycine, and alanine, and therefore suggested that IBS could be treated with probiotics. An additional study has also shown that probiotics could regulate microbial proteolytic activity, and bacterial metabolism of amino acids, SCFAs, and methylamines[47]. In addition, Hong *et al*[48] revealed a significant increase of acetate, butyrate, and glutamine, together with a decrease of trimethylamine in the feces of lactic acid bacteria (LAB) + dextran sulfate sodium (DSS)-treated mice when compared to DSS-only mice. Thus, it is possible that probiotic treatment is beneficial to energy metabolism, and could help to relieve gut microbial disturbances. The normal intestinal microbiota is involved in sex hormone metabolism of the enterohepatic circulation. Some *Clostridium* species can convert cortisol to androgen[49]. Our study demonstrated that treatment with *C. butyricum* increased androsterone 1 in fecal samples, thereby influencing the pathway of steroid hormone biosynthesis. These results suggested that *C. butyricum* might change the intestinal microbiota and enterohepatic circulation to restore gut homeostasis in IBS mice. IBS is a common disorder in both children and adults. The pathogenesis and pathophysiology of IBS result from multifactorial and multisystemic alterations. The biopsychosocial model describes IBS as a dysfunction of the gut-brain axis that is influenced by genetic susceptibility, as well as physiological, psychological, and environmental variables, in addition to individual coping mechanisms[50]. In the future, we will perform fecal metabolomic studies in IBS patients to explore the gut metabolites in humans.

In summary, this study demonstrated the potential of metabolomic studies to provide new insights into the etiology of IBS. Supplementation with probiotics may provide great future prospects for the treatment of IBS. However, the findings of this study were limited in that the metabolites were only detected by GC-MS. Thus, liquid chromatography (LC)-MS analysis should be considered for future studies.

ARTICLE HIGHLIGHTS

Research background

The prevalence of irritable bowel syndrome (IBS) in Western societies is approximately 10%-20%, and the pathology of IBS is complicated. It is believed that multiple factors such as genetics, visceral hypersensitivity, gastrointestinal motility, dysregulation of the brain-gut axis, levels of neuropeptides and hormones, as well as inflammatory changes all contribute to IBS development.

Research motivation

Microbial metabolites regulate biochemical and physiological processes. Certain disorders that alter fecal microbial profiles may cause IBS. Thus, the key topic we wanted to address in this study is the impact of the microbiota on host–microbial interactions. Fecal metabolic compositions and variations not only reflect the status of the intestinal microbiota, but also bridge the relationship between symbiotic microbes and host health.

Research objectives

The study of fecal metabolomics offers a unique insight to investigate IBS. In the present study, differentially expressed metabolites and key metabolic pathways were found in fecal samples from IBS mice, when compared to the control group. The metabolomic profile in the IBS group was significantly altered following *Clostridium butyricum* treatment.

Research methods

Fecal samples were analyzed using gas chromatography-mass spectrometry (GC-MS) method. The resulting three-dimensional data involving the peak number, sample name, and normalized peak area were submitted to SIMCA14.1 software package for principal component analysis (PCA) and orthogonal projections to latent structures-discriminate analysis (OPLS-DA). MetaboAnalyst was used to identify the most relevant pathways (http://www.metaboanalyst.ca).

Research results

In this study, we found differentially expressed metabolites between the control and IBS groups. *C. butyricum* administration modulated metabolic profiles and reduced visceral sensitivity and diarrhea symptoms in IBS mice. This study demonstrated the impact of metabolomic studies on the etiology of IBS. Supplementation with probiotics may provide great prospects for the treatment of IBS. In the future, we will focus fecal metabolomic studies in IBS patients to explore the prevalent pathways and mechanisms in humans.

Research conclusions

Based on the GC-MS analysis, we found that fecal metabolites were changed during the pathological process of IBS. IBS mice demonstrated disorders in fecal microbial profiles, which led to fecal metabolic changes that may affect the development of IBS. This study also demonstrated the potential of metabolomic studies to provide new insights into the etiology of IBS. Probiotics can be used to improve the symptoms of IBS and alter fecal metabolites, and therefore may be used to treat IBS.

Research perspectives

Intestinal microbiota metabolites are very complex. In the future, our research will focus on fecal metabolites in IBS patients to explore the pathophysiological mechanisms in humans. GC-MS combined with liquid chromatography (LC)-MS analysis should be considered for future studies.

REFERENCES

1 **Ohman L**, Simrén M. New insights into the pathogenesis and pathophysiology of irritable bowel syndrome. *Dig Liver Dis* 2007; **39**: 201-215 [PMID: 17267314 DOI: 10.1016/j.dld.2006.10.014]

2 **Madden JA**, Hunter JO. A review of the role of the gut microflora in irritable bowel syndrome and the effects of probiotics. *Br J Nutr* 2002; **88** Suppl 1: S67-S72 [PMID: 12215182 DOI: 10.1079/BJN2002631]

3 **Malinen E**, Rinttilä T, Kajander K, Mättö J, Kassinen A, Krogius L, Saarela M, Korpela R, Palva A. Analysis of the fecal microbiota of irritable bowel syndrome patients and healthy controls with real-time PCR. *Am J Gastroenterol* 2005; **100**: 373-382 [PMID: 15667495 DOI: 10.1111/j.1572-0241.2005.40312.x]

4 **Si JM**, Yu YC, Fan YJ, Chen SJ. Intestinal microecology and quality of life in irritable bowel syndrome patients. *World J*

Gastroenterol 2004; **10**: 1802-1805 [PMID: 15188510 DOI: 10.3748/wjg.v10.i12.1802]
5 **Noor SO**, Ridgway K, Scovell L, Kemsley EK, Lund EK, Jamieson C, Johnson IT, Narbad A. Ulcerative colitis and irritable bowel patients exhibit distinct abnormalities of the gut microbiota. *BMC Gastroenterol* 2010; **10**: 134 [PMID: 21073731 DOI: 10.1186/1471-230X-10-134]
6 **Bonfrate L**, Tack J, Grattagliano I, Cuomo R, Portincasa P. Microbiota in health and irritable bowel syndrome: current knowledge, perspectives and therapeutic options. *Scand J Gastroenterol* 2013; **48**: 995-1009 [PMID: 23964766 DOI: 10.3109/00365521.2013.799220]
7 **Krogius-Kurikka L**, Lyra A, Malinen E, Aarnikunnas J, Tuimala J, Paulin L, Mäkivuokko H, Kajander K, Palva A. Microbial community analysis reveals high level phylogenetic alterations in the overall gastrointestinal microbiota of diarrhoea-predominant irritable bowel syndrome sufferers. *BMC Gastroenterol* 2009; **9**: 95 [PMID: 20015409 DOI: 10.1186/1471-230X-9-95]
8 **Palmer C**, Bik EM, DiGiulio DB, Relman DA, Brown PO. Development of the human infant intestinal microbiota. *PLoS Biol* 2007; **5**: e177 [PMID: 17594176 DOI: 10.1371/journal.pbio.0050177]
9 **Nicholson JK**, Holmes E, Wilson ID. Gut microorganisms, mammalian metabolism and personalized health care. *Nat Rev Microbiol* 2005; **3**: 431-438 [PMID: 15821725 DOI: 10.1038/nrmicro1152]
10 **Sengül N**, Aslím B, Uçar G, Yücel N, Işik S, Bozkurt H, Sakaoğullari Z, Atalay F. Effects of exopolysaccharide-producing probiotic strains on experimental colitis in rats. *Dis Colon Rectum* 2006; **49**: 250-258 [PMID: 16362802 DOI: 10.1007/s10350-005-0267-6]
11 **Bergen WG**, Wu G. Intestinal nitrogen recycling and utilization in health and disease. *J Nutr* 2009; **139**: 821-825 [PMID: 19282369 DOI: 10.3945/jn.109.104497]
12 **Ellis DI**, Dunn WB, Griffin JL, Allwood JW, Goodacre R. Metabolic fingerprinting as a diagnostic tool. *Pharmacogenomics* 2007; **8**: 1243-1266 [PMID: 17924839 DOI: 10.2217/14622416.8.9.1243]
13 **Bertini I**, Calabrò A, De Carli V, Luchinat C, Nepi S, Porfirio B, Renzi D, Saccenti E, Tenori L. The metabonomic signature of celiac disease. *J Proteome Res* 2009; **8**: 170-177 [PMID: 19072164 DOI: 10.1021/pr800548z]
14 **Vanden Bussche J**, Marzorati M, Laukens D, Vanhaecke L. Validated High Resolution Mass Spectrometry-Based Approach for Metabolomic Fingerprinting of the Human Gut Phenotype. *Anal Chem* 2015; **87**: 10927-10934 [PMID: 26451617 DOI: 10.1021/acs.analchem.5b02688]
15 **Zeng H**, Grapov D, Jackson MI, Fahrmann J, Fiehn O, Combs GF. Integrating Multiple Analytical Datasets to Compare Metabolite Profiles of Mouse Colonic-Cecal Contents and Feces. *Metabolites* 2015; **5**: 489-501 [PMID: 26378591 DOI: 10.3390/metabo5030489]
16 **Saric J**, Wang Y, Li J, Coen M, Utzinger J, Marchesi JR, Keiser J, Veselkov K, Lindon JC, Nicholson JK, Holmes E. Species variation in the fecal metabolome gives insight into differential gastrointestinal function. *J Proteome Res* 2008; **7**: 352-360 [PMID: 18052033 DOI: 10.1021/pr070340k]
17 **Chen B**, Zhu S, Du L, He H, Kim JJ, Dai N. Reduced interstitial cells of Cajal and increased intraepithelial lymphocytes are associated with development of small intestinal bacterial overgrowth in post-infectious IBS mouse model. *Scand J Gastroenterol* 2017; **52**: 1065-1071 [PMID: 28679338 DOI: 10.1080/00365521.2017.1342141]
18 **Jones RC 3rd**, Otsuka E, Wagstrom E, Jensen CS, Price MP, Gebhart GF. Short-term sensitization of colon mechanoreceptors is associated with long-term hypersensitivity to colon distention in the mouse. *Gastroenterology* 2007; **133**: 184-194 [PMID: 17553498 DOI: 10.1053/j.gastro.2007.04.042]
19 **Yang B**, Zhou X, Lan C. Changes of cytokine levels in a mouse model of post-infectious irritable bowel syndrome. *BMC Gastroenterol* 2015; **15**: 43 [PMID: 25886744 DOI: 10.1186/s12876-015-0272-8]
20 **Yu YB**, Zuo XL, Zhao QJ, Chen FX, Yang J, Dong YY, Wang P, Li YQ. Brain-derived neurotrophic factor contributes to abdominal pain in irritable bowel syndrome. *Gut* 2012; **61**: 685-694 [PMID: 21997550 DOI: 10.1136/gutjnl-2011-300265]
21 **Kind T**, Wohlgemuth G, Lee DY, Lu Y, Palazoglu M, Shahbaz S, Fiehn O. FiehnLib: mass spectral and retention index libraries for metabolomics based on quadrupole and time-of-flight gas chromatography/mass spectrometry. *Anal Chem* 2009; **81**: 10038-10048 [PMID: 19928838 DOI: 10.1021/ac9019522]
22 **Dunn WB**, Broadhurst D, Begley P, Zelena E, Francis-McIntyre S, Anderson N, Brown M, Knowles JD, Halsall A, Haselden JN, Nicholls AW, Wilson ID, Kell DB, Goodacre R; Human Serum Metabolome (HUSERMET) Consortium. Procedures for large-scale metabolic profiling of serum and plasma using gas chromatography and liquid chromatography coupled to mass spectrometry. *Nat Protoc* 2011; **6**: 1060-1083 [PMID: 21720319 DOI: 10.1038/nprot.2011.335]
23 **Macfarlane GT**, Macfarlane S. Bacteria, colonic fermentation, and gastrointestinal health. *J AOAC Int* 2012; **95**: 50-60 [PMID: 22468341 DOI: 10.5740/jaoacint.SGE_Macfarlane]
24 **Sommer F**, Bäckhed F. The gut microbiota--masters of host development and physiology. *Nat Rev Microbiol* 2013; **11**: 227-238 [PMID: 23435359 DOI: 10.1038/nrmicro2974]
25 **Martin FP**, Dumas ME, Wang Y, Legido-Quigley C, Yap IKS, Tang H, Zirah S, Murphy GM, Cloarec O, Lindon JC, Sprenger N, Fay LB, Kochhar S, van Bladeren P, Holmes E, Nicholson JK. A top-down systems biology view of microbiome-mammalian metabolic interactions in a mouse model. *Mol Syst Biol* 2007; **3**: 112 [PMID: 17515922 DOI: 10.1038/msb4100153]
26 **Nicholson JK**, Holmes E, Lindon JC, Wilson ID. The challenges of modeling mammalian biocomplexity. *Nat Biotechnol* 2004; **22**: 1268-1274 [PMID: 15470467 DOI: 10.1038/nbt1015]
27 **Scanlan PD**, Shanahan F, Clune Y, Collins JK, O'Sullivan GC, O'Riordan M, Holmes E, Wang Y, Marchesi JR. Culture-independent analysis of the gut microbiota in colorectal cancer and polyposis. *Environ Microbiol* 2008; **10**: 789-798 [PMID: 18237311 DOI: 10.1111/j.1462-2920.2007.01503.x]
28 **Le Gall G**, Noor SO, Ridgway K, Scovell L, Jamieson C, Johnson IT, Colquhoun IJ, Kemsley EK, Narbad A. Metabolomics of fecal extracts detects altered metabolic activity of gut microbiota in ulcerative colitis and irritable bowel syndrome. *J Proteome Res* 2011; **10**: 4208-4218 [PMID: 21761941 DOI: 10.1021/pr2003598]
29 **Madsen K**, Cornish A, Soper P, McKaigney C, Jijon H, Yachimec C, Doyle J, Jewell L, De Simone C. Probiotic bacteria enhance murine and human intestinal epithelial barrier function. *Gastroenterology* 2001; **121**: 580-591 [PMID: 11522742 DOI: 10.1053/gast.2001.27224]
30 **Martin FP**, Collino S, Rezzi S, Kochhar S. Metabolomic applications to decipher gut microbial metabolic influence in health and disease. *Front Physiol* 2012; **3**: 113 [PMID: 22557976 DOI: 10.3389/fphys.2012.00113]
31 **Martin FP**, Wang Y, Sprenger N, Holmes E, Lindon JC, Kochhar S, Nicholson JK. Effects of probiotic Lactobacillus paracasei treatment on the host gut tissue metabolic profiles probed via magic-angle-spinning NMR spectroscopy. *J Proteome Res* 2007; **6**: 1471-1481 [PMID: 17316039 DOI: 10.1021/pr060596a]
32 **Dai ZL**, Wu G, Zhu WY. Amino acid metabolism in intestinal bacteria: links between gut ecology and host health. *Front Biosci* (Landmark Ed) 2011; **16**: 1768-1786 [PMID: 21196263 DOI: 10.2741/3820]
33 **Berry MD**. The potential of trace amines and their receptors for treating neurological and psychiatric diseases. *Rev Recent Clin Trials* 2007; **2**: 3-19 [PMID: 18473983 DOI: 10.2174/157488707779318107]
34 **Klassen P**, Fürst P, Schulz C, Mazariegos M, Solomons NW. Plasma free amino acid concentrations in healthy Guatemalan adults and in patients with classic dengue. *Am J Clin Nutr* 2001; **73**: 647-652 [PMID: 11237944]

35 **Sabelli HC**, Javaid JI. Phenylethylamine modulation of affect: therapeutic and diagnostic implications. *J Neuropsychiatry Clin Neurosci* 1995; **7**: 6-14 [PMID: 7711493 DOI: 10.1176/jnp.7.1.6]

36 **Snoddy AM**, Heckathorn D, Tessel RE. Cold-restraint stress and urinary endogenous beta-phenylethylamine excretion in rats. *Pharmacol Biochem Behav* 1985; **22**: 497-500 [PMID: 4039452 DOI: 10.1016/0091-3057(85)90054-1]

37 **Martin FP**, Verdu EF, Wang Y, Dumas ME, Yap IK, Cloarec O, Bergonzelli GE, Corthesy-Theulaz I, Kochhar S, Holmes E, Lindon JC, Collins SM, Nicholson JK. Transgenomic metabolic interactions in a mouse disease model: interactions of Trichinella spiralis infection with dietary Lactobacillus paracasei supplementation. *J Proteome Res* 2006; **5**: 2185-2193 [PMID: 16944930 DOI: 10.1021/pr060157b]

38 **Ponnusamy K**, Choi JN, Kim J, Lee SY, Lee CH. Microbial community and metabolomic comparison of irritable bowel syndrome faeces. *J Med Microbiol* 2011; **60**: 817-827 [PMID: 21330412 DOI: 10.1099/jmm.0.028126-0]

39 **Reiter E**, Jiang Q, Christen S. Anti-inflammatory properties of alpha- and gamma-tocopherol. *Mol Aspects Med* 2007; **28**: 668-691 [PMID: 17316780 DOI: 10.1016/j.mam.2007.01.003]

40 **LeBlanc JG**, Milani C, de Giori GS, Sesma F, van Sinderen D, Ventura M. Bacteria as vitamin suppliers to their host: a gut microbiota perspective. *Curr Opin Biotechnol* 2013; **24**: 160-168 [PMID: 22940212 DOI: 10.1016/j.copbio.2012.08.005]

41 **Jackowski S**, Rock CO. Regulation of coenzyme A biosynthesis. *J Bacteriol* 1981; **148**: 926-932 [PMID: 6796563]

42 **Hutschenreuther A**, Birkenmeier G, Bigl M, Krohn K, Birkemeyer C. Glycerophosphoglycerol, Beta-alanine, and pantothenic Acid as metabolic companions of glycolytic activity and cell migration in breast cancer cell lines. *Metabolites* 2013; **3**: 1084-1101 [PMID: 24958267 DOI: 10.3390/metabo3041084]

43 **Depeint F**, Bruce WR, Shangari N, Mehta R, O'Brien PJ. Mitochondrial function and toxicity: role of the B vitamin family on mitochondrial energy metabolism. *Chem Biol Interact* 2006; **163**: 94-112 [PMID: 16765926 DOI: 10.1016/j.cbi.2006.04.014]

44 **Even PC**, Decrouy A, Chinet A. Defective regulation of energy metabolism in mdx-mouse skeletal muscles. *Biochem J* 1994; **304** (Pt 2): 649-654 [PMID: 7999003 DOI: 10.1042/bj3040649]

45 **Leonardi R**, Zhang YM, Rock CO, Jackowski S. Coenzyme A: back in action. *Prog Lipid Res* 2005; **44**: 125-153 [PMID: 15893380 DOI: 10.1016/j.plipres.2005.04.001]

46 **Martin FP**, Sprenger N, Yap IK, Wang Y, Bibiloni R, Rochat F, Rezzi S, Cherbut C, Kochhar S, Lindon JC, Holmes E, Nicholson JK. Panorganismal gut microbiome-host metabolic crosstalk. *J Proteome Res* 2009; **8**: 2090-2105 [PMID: 19281268 DOI: 10.1021/pr801068x]

47 **Martin FP**, Wang Y, Sprenger N, Yap IK, Lundstedt T, Lek P, Rezzi S, Ramadan Z, van Bladeren P, Fay LB, Kochhar S, Lindon JC, Holmes E, Nicholson JK. Probiotic modulation of symbiotic gut microbial-host metabolic interactions in a humanized microbiome mouse model. *Mol Syst Biol* 2008; **4**: 157 [PMID: 18197175 DOI: 10.1038/msb4100190]

48 **Hong YS**, Ahn YT, Park JC, Lee JH, Lee H, Huh CS, Kim DH, Ryu DH, Hwang GS. 1H NMR-based metabonomic assessment of probiotic effects in a colitis mouse model. *Arch Pharm Res* 2010; **33**: 1091-1101 [PMID: 20661720 DOI: 10.1007/s12272-010-0716-1]

49 **Bokkenheuser VD**, Morris GN, Ritchie AE, Holdeman LV, Winter J. Biosynthesis of androgen from cortisol by a species of Clostridium recovered from human fecal flora. *J Infect Dis* 1984; **149**: 489-494 [PMID: 6725987 DOI: 10.1093/infdis/149.4.489]

50 **Chogle A**, Mintjens S, Saps M. Pediatric IBS: an overview on pathophysiology, diagnosis and treatment. *Pediatr Ann* 2014; **43**: e76-e82 [PMID: 24716562 DOI: 10.3928/00904481-20140325-08]

P- Reviewer: Chuah SK, Soares R **S- Editor**: Gong ZM
L- Editor: Wang TQ **E- Editor**: Ma YJ

World Journal of Gastroenterology

Submit a Manuscript: http://www.f6publishing.com

World J Gastroenterol 2018 February 28; 24(8): 905-916

DOI: 10.3748/wjg.v24.i8.905

ISSN 1007-9327 (print) ISSN 2219-2840 (online)

ORIGINAL ARTICLE

Retrospective Cohort Study

Colonoscopy surveillance for high risk polyps does not always prevent colorectal cancer

Mohamad A Mouchli, Lidia Ouk, Marianne R Scheitel, Alisha P Chaudhry, Donna Felmlee-Devine, Diane E Grill, Shahrooz Rashtak, Panwen Wang, Junwen Wang, Rajeev Chaudhry, Thomas C Smyrk, Ann L Oberg, Brooke R Druliner, Lisa A Boardman

Mohamad A Mouchli, Lidia Ouk, Donna Felmlee-Devine, Shahrooz Rashtak, Brooke R Druliner, Lisa A Boardman, Division of Gastroenterology and Hepatology, Mayo Clinic, Rochester, MN 55905, United States

Marianne R Scheitel, Knowledge and Delivery Center, Mayo Clinic, Rochester, MN 55905, United States

Alisha P Chaudhry, Biostatistics and Bioinformatics, Health Sciences Research, Mayo Clinic, Rochester, MN 55905, United States

Diane E Grill, Ann L Oberg, Division of Biomedical Statistics and Informatics, Health Sciences Research, Mayo Clinic, Rochester, MN 55905, United States

Panwen Wang, Junwen Wang, Biostatistics and Bioinformatics, Health Science Research, Center for Individualized Medicine Mayo Clinic, Scottsdale, AZ 85259, United States

Junwen Wang, Department of Biomedical Informatics, Arizona State University, Scottsdale, AZ 85259, United States

Rajeev Chaudhry, Primary Care Internal Medicine, Mayo Clinic, Rochester, MN 55905, United States

Rajeev Chaudhry, Center for Innovation, Mayo Clinic, Rochester, MN 55905, United States

Thomas C Smyrk, Department of Laboratory Medicine and Pathology, Mayo Clinic, Rochester, MN 55905, United States

ORCID number: Mohamad A Mouchli (0000-0002-5343-2427); Lidia Ouk (0000-0003-3688-7101); Marianne R Scheitel (0000-0002-8826-6916); Alisha P Chaudhry(0000-0003-2678-407X); Donna Felmlee-Devine(0000-0002-7650-9335); Diane E Grill(0000-0002-8677-1724); Shahrooz Rashtak (0000-0002-1875-6012); Panwen Wang (0000-0002-4614-8970); Junwen Wang (0000-0002-4432-4707); Rajeev Chaudhry (0000-0003-1249-5656); Thomas C Smyrk (0000-0001-6194-7853); Ann L Oberg (0000-0003-2539-9807); Brooke R Druliner (0000-0001-9254-8097); Lisa A Boardman (0000-0002-1330-2054).

Author contributions: Boardman LA developed study design; Mouchli MA, Grill DE and Boardman LA participated in the writing of the paper and did the statistical analysis; Mouchli MA, Ouk L, Scheitel MS, Chaudhry AP, Felmlee-Devine D and Boardman LA reviewed medical records and data; Basu N, Ouk L, Scheitel MS, Chaudhry AP, Aletto Felmlee-Devine D, Rashtak S, Wang P, Wang J, Chaudhry R, Smyrk TC, Oberg AL and Druliner BR edited the manuscript.

Supported by the National Cancer Institute, No. CA170357; and the Mayo Clinic Center for Cell Signaling in Gastroenterology, NIDDK Mo. P30DK084567.

Institutional review board statement: Two IRB approved protocols were used for this study including IRB 622-00 which had original approval date of April 4, 2000 and IRB 12-000182 which was approved on February 1, 2012.

Informed consent statement: The Mayo Clinic IRB Reviewer approved waver of informed consent and HIPAA authorization in accordance with applicable regulations for data collected under IRB 622-00.

Conflict-of-interest statement: There are no conflicts of interest to report for any of the authors.

Data sharing statement: We plan to share research resources and materials taking into account the NIH Grant Policy on Sharing of Unique Research Resources, including the Sharing of Biomedical Research Resources Principles and Guidelines for recipients of NIH Grants and Contracts issued in December 1999. In preparing human data for data-sharing, we will de-identify human phenotypic data to ensure that the identities of research subjects cannot be readily ascertained. We will strip the data of identifiers according to the Health Insurance Portability and Accountability Act (HIPAA) Privacy Rule.

Manuscript source: Unsolicited manuscript

Correspondence to: Lisa A Boardman, MD, Full Professor, Staff Physician, Division of Gastroenterology and Hepatology, Mayo Clinic, 200 First Street SW, Rochester, MN 55905, United States. boardman.lisa@mayo.edu
Telephone: +1-507-2664338
Fax: +1-507-2660350

Received: August 3, 2017
Peer-review started: August 5, 2017
First decision: August 30, 2017
Revised: November 17, 2017
Accepted: December 5, 2017
Article in press: December 5, 2017
Published online: February 28, 2018

Abstract

AIM

To determine the frequency and risk factors for colorectal cancer (CRC) development among individuals with resected advanced adenoma (AA)/traditional serrated adenoma (TSA)/advanced sessile serrated adenoma (ASSA).

METHODS

Data was collected from medical records of 14663 subjects found to have AA, TSA, or ASSA at screening or surveillance colonoscopy. Patients with inflammatory bowel disease or known genetic predisposition for CRC were excluded from the study. Factors associated with CRC developing after endoscopic management of high risk polyps were calculated in 4610 such patients who had at least one surveillance colonoscopy within 10 years following the original polypectomy of the incident advanced polyp.

RESULTS

84/4610 (1.8%) patients developed CRC at the polypectomy site within a median of 4.2 years (mean 4.89 years), and 1.2% (54/4610) developed CRC in a region distinct from the AA/TSA/ASSA resection site within a median of 5.1 years (mean 6.67 years). Approximately, 30% (25/84) of patients who developed CRC at the AA/TSA/ASSA site and 27.8% (15/54) of patients who developed CRC at another site had colonoscopy at recommended surveillance intervals. Increasing age; polyp size; male sex; right-sided location; high degree of dysplasia; higher number of polyps resected; and piecemeal removal were associated with an increased risk for CRC development at the same site as the index polyp. Increasing age; right-sided location; higher number of polyps resected and sessile endoscopic appearance of the index AA/TSA/ASSA were significantly associated with an increased risk for CRC development at a different site.

CONCLUSION

Recognition that CRC may develop following AA/TSA/ASSA removal is one step toward improving our practice efficiency and preventing a portion of CRC related morbidity and mortality.

Key words: Colon cancer; Rectal Cancer; Advanced adenoma; Sessile serrated adenoma; High risk polyps; Post-polypectomy colorectal cancer

Core tip: Screening colonoscopy reduces colorectal cancer morbidity and mortality risks through detection and treatment of precursor lesions. However, screening colonoscopy has a 3.5% false negative rate for detection of colorectal cancer (CRC) resulting in 17% of patients who had undergone colon screening within 3 years being diagnosed with CRC. We report that 3% of patients with advanced polyps in a surveillance program developed interval CRC. Recognition that CRC could develop following advanced polyp removal despite adherence to guidelines is one step toward improving our practice efficiency and preventing a portion of CRC related morbidity and mortality.

Mouchli MA, Ouk L, Scheitel MR, Chaudhry AP, Felmlee-Devine D, Grill DE, Rashtak S, Wang P, Wang J, Chaudhry R, Smyrk TC, Oberg AL, Druliner BR, Boardman LA. Colonoscopy surveillance for high risk polyps does not always prevent colorectal cancer. *World J Gastroenterol* 2018; 24(8): 905-916 Available from: URL: http://www.wjgnet.com/1007-9327/full/v24/i8/905.htm DOI: http://dx.doi.org/10.3748/wjg.v24.i8.905

INTRODUCTION

Colorectal cancer (CRC) is the second leading cause of cancer-related death in the United States[1-4]. Colonoscopy with removal of premalignant lesions has contributed to a recent decline in CRC incidence and the number of deaths from this disease; nevertheless 5%-9% of patients diagnosed with CRC have undergone screening colonoscopy within the 3 years prior to detection of cancer[5]. Than *et al*[3] reported that colonoscopy has a 3.5% false negative rate for detection of CRC since 17% of patients with newly diagnosed CRC had been investigated with bowel-specific investigations within the previous 3 years. Winawer *et al*[6] reported that 6% of patients with advanced adenomas (AA) are missed by colonoscopy. The development of CRC despite colonoscopy may

reflect missed superficial depressed lesions (cancer or high risk adenoma), incompletely resected adenomas[7], de novo cancer[8], or delayed diagnosis because of failed biopsy detection[9,10].

Adenomatous polyps are the most common neoplastic finding at colonoscopy[11]. These neoplastic polyps have malignant potential and are classified histologically as villous, tubulovillous, or tubular adenomas[12]. The malignant potential of these polyps correlates with type, size, and degree of dysplasia of the polyp. Advanced adenomas (AA) are those which are larger than 10 mm, have tubulovillous or villous architecture, or have high grade dysplasia[13].

The term "serrated adenoma" was introduced by Longacre *et al*[14] to describe polyps with dysplastic (adenomatous) cytology and serrated crypt architecture. Later, Torlakovic *et al*[15] coined the term sessile serrated adenoma to describe a different lesion, one with serrated crypts and characteristic architectural changes but usually no cytologic dysplasia. In order to avoid (or at least minimize) confusion, the Longacre lesion was renamed "traditional serrated adenoma." Despite the shared terminology, SSA and TSA are not necessarily related lesions[16]. After a few more terminology modifications, the current World Health Organization classification for serrated polyps is: hyperplastic polyp, sessile serrated polyp (SSP) without dysplasia; sessile serrated adenoma (SSA) with cytological dysplasia, and traditional serrated adenoma[17]. The risk of developing CRC from a serrated lesion correlates with larger size (> 10 mm), presence of dysplasia and higher number of synchronous polyps.

Surveillance is recommended by the United States Preventive Services Task Force (USPSTF) 3 years after removal of AA, TSA, or advanced SSA[11] while the European guidelines recommend surveillance at 1 years for high risk polyps (≥ 20 mm) but three years for intermediate risk polyps(10 mm to < 20 mm)[18]. Despite frequent colonoscopy, CRC has been shown to develop at an incidence rate of 1.2/1000[19]. Though several large studies have illustrated the rates of post colonoscopy CRC to be low[20], we were particularly interested in how often CRC develops in the highest risk patients, namely those who have AA, TSA, or advanced SSA.

MATERIALS AND METHODS

Study population

In this IRB-approved nested case cohort study (IRB 622-00), we reviewed the colonoscopy database and pathology reports for patients who were seen at Mayo Clinic, Rochester, Minnesota for colonoscopy related to any indication and found to have high-risk AA (villous architecture; high grade dysplasia and/or size > 10 mm), TSA, or Advanced SSA (any dysplasia and/or size > 10 mm), then identified 4160 patients who had at least one surveillance exam following the index polypectomy for their AA/TSA/ASSA. Surveillance exams were performed only for follow up and were not done in response to clinical symptoms. Colonoscopy reports prior to the incident advanced polyp lesion were not available in the electronic medical record on most patients and thus were not included in this study.

We included all patients ≥ 18 years of age diagnosed with either AA between January 1990 to December 2010 or ASSA/TSA between January 2000 to December 2010. Patients were followed through August 2016. Patients with a diagnosis of a polyposis syndrome, inflammatory bowel disease, or a known genetic predisposition for CRC were excluded from the study. We identified all patients from this cohort who had developed CRC (n = 84) and then randomly selected 252 patients who had an AA, TSA, or ASSA at index colonoscopy but who had not developed CRC. Clinical and pathological features of high-risk polyps (*i.e.*, size, histology, site, and degree of dysplasia, time of index polypectomy), number and timing of surveillance colonoscopies and post polypectomy CRC (*i.e.*, size, site, grade and stage) were collected via chart abstraction for this cohort of patients. Subjects who had not developed post-polypectomy CRC were randomly selected from a pool of 10 patients matched to the post-polypectomy CRC group based on polyp histology and size (< or ≥ 20 mm), degree of dysplasia and decade that the index polyp was removed. ASSA was classified as being at higher risk for malignant transformation if the polyp was > 10 mm, had dysplasia or higher number of synchronous polyps (≥ 3 polyps in small polyps measuring < 10 mm or ≥ 2 large polyps measuring > 10 mm)[17].

Post-polypectomy CRC was classified as same site cancer if the cancer arose in the region of the colon in which the high risk polyp had been removed. Since our surveillance intervals and time from index AA/TSA/ASSA to cancer development extended beyond three years in some cases, we did not use the term interval cancer[21], but rather post-polypectomy cancer. We acknowledge that it is impossible to know if the development of CRC in the same region as the high risk polyp that had prompted surveillance, we would anticipate that this high risk polyp would be the most likely source for the cancer.

Though these cases spanned from 1990 to 2010 for the AA and from 2000 to 2010 for the TSA and ASSA, we applied the most current USPSTF guidelines to all of these cases in order to assess the ability of these recommendations for polyp management of these high risk patients[11]. We similarly assessed using the European surveillance guidelines distinguishing intermediate versus high risk AA/TSA/ASSA based on polyp size. A polyp was classified as persistent if polyp clearance was not achieved on any of the surveillance procedures and as recurrent if the polyp had been

Table 1 Clinical and demographic characteristics of patients who developed colorectal cancer at the index AA/TSA/ASSA resection site *n* (%)

Characteristics	Developed CRC (*n* = 84)	No CRC (*n* = 252)	*P* value[1]
Demographics			
Male sex	56 (66.7)	138 (54.8)	0.06
Age, yr (≥ 70)	40 (47.6)	85 (33.7)	0.02
Time interval from first treatment for advanced adenoma till cancer or last surveillance colonoscopy in years (median, IQR)	4.24 (1.51-7.23)	6.0 (4.05-9.35)	< 0.01
Number of colonoscopies between first polypectomy and cancer (mean ± SD)	1.65 ± 2.30	1.47 ± 1.6	0.83
Adenoma size (1-2 cm)	31 (42.5)	146 (58.2)	0.03
Adenoma size (> 2 cm)	20 (27.4)	27 (10.8)	0.0007
Flat/sessile	76 (91.6)	161 (66.8)	< 0.01
Degree of dysplasia			
High grade	28 (33.3)	66 (26.2)	0.18
Low grade/no dysplasia	56 (66.7)	186 (73.8)	0.18
Number of attempts to remove the polyp (mean ± SD)	2.05 ± 1.62	1.26 ± 0.60	< 0.01
Number of polyps resected (> 3 polyps)	14 (16.7)	21 (8.3)	0.03
Polypectomy device used			
Hot snare	19 (24.1)	41 (16.3)	0.11
Cold snare	5 (6.3)	26 (10.3)	0.11
Snare NOS	60 (75.9)	185 (73.4)	0.11
Additional treatments			
Piecemeal removal	21 (27.6)	30 (13.1)	< 0.01
Mucosal lift	13 (17.1)	23 (10.0)	0.10
Polyp location			
Right colon	63 (75.0)	110 (43.7)	< 0.01
Left colon	8 (9.52)	106 (42.1)	< 0.01
Rectum	13 (15.5)	36 (14.3)	< 0.01

[1]*P*-values for continuous variables were obtained using the Kruskal-Wallis Test; Pearson's χ^2 test was used for discrete variables. CRC: Colorectal cancer.

successfully treated, not detected on at least one subsequent colonoscopy but recurred at the tattooed site of the original AA/TSA/ASSA.

Statistical analysis

The data are reported as mean (± SD), median (interquartile range, IQR), ranges, and categorical variables by counts and percentages as appropriate. We included only cancers occurring at least one year after polypectomy to minimize the risk of detection bias and misclassification. Patients with a past history of CRC diagnosed were included in our study. Estimates of the rate of cancer for the entire cohort were determined by using the Kaplan-Meier survival curve with log-rank test. To identify risk factors associated with development of cancer, we performed univariate time-to-event analysis with Cox proportional regression models that accounted for the case-cohort design by using case weights to account for the sampling frame and robust estimates of variance[22-24]. Variables with $P < 0.05$ on univariate analysis were included in a multivariate Cox proportional hazard analysis to identify independent risk factors associated with malignancy. Finally, penalized regression models were run using Lasso regression, with 10-fold cross validation, to provide robust estimates of the model coefficients, which should provide better predictions when used with external data[25]. All statistical analyses were conducted using JMP version 10 for Windows (SAS Institute Inc., Cary, NC, United States), SAS (version 9) or R (version 3.2.3).

RESULTS

AA/TSA/ASSA were detected in 14633 patients at incident colonoscopy. Of those, 1261 were excluded since they were found to have incident CRC at the time of AA/TSA/ASSA detection. After excluding patients who did not undergo a surveillance colonoscopy after this index polypectomy, 4610 patients were evaluated. Thirty- one of the 1390 (1.67%) of the TSA and ASSA were found to have subsequent CRC, and 107/3406 (3.14%) of the AA patients developed subsequent CRC ($P = 0.11$) (Figure 1).

Post-polypectomy CRC at the AA/TSA/ASSA resection site

Sixty-three patients with history of AA (41 villous, 22 tubular), two with TSA and 19 with ASSA (15 without dysplasia and 4 with dysplasia) who developed CRC at the same site as the index polyp were identified. These 84 patients were compared to a randomly selected cohort of 252 of the AA/TSA/ASSA patients who did not develop post-polypectomy CRC. Patients who developed CRC at the index polypectomy site were significantly older (47.6% *vs* 33.7%, $P = 0.02$); had larger index polyps (15.5% *vs* 7.1%, $P = 0.02$); had an increased number of synchronous polyps at time of polypectomy (16.7% *vs* 8.3%, $P = 0.03$) and were more likely to have AA/TSA/ASSA in the right

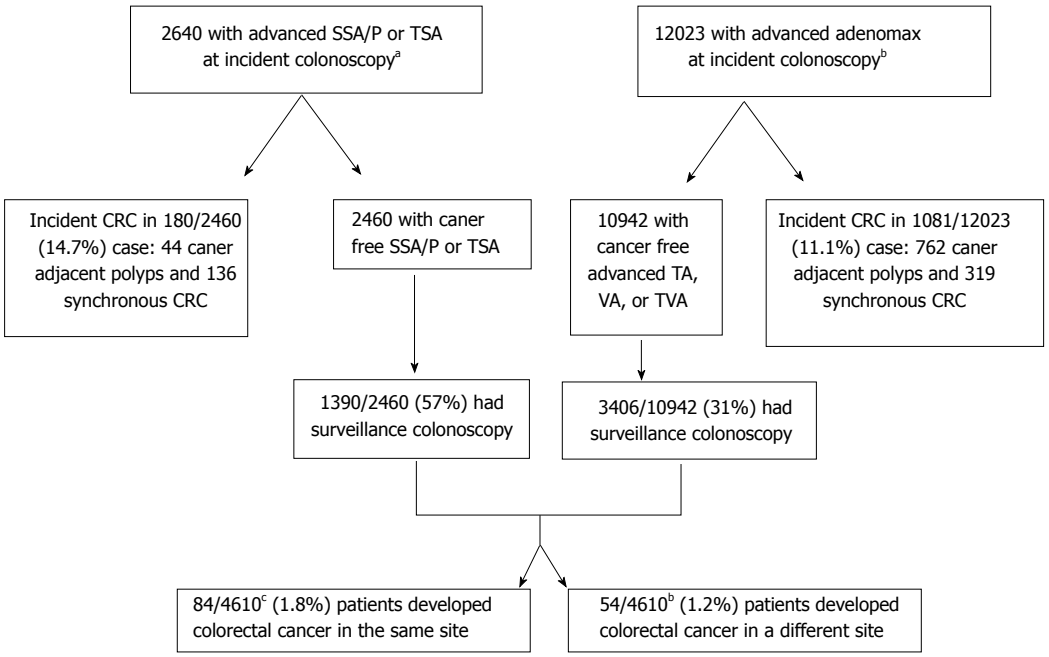

Figure 1 Selection of patients included in the determination of colorectal cancer development despite surveillance colonoscopy. [a]Polyp removal between 1/1/2000 12/31/2010 for SSA and TSA for TA, TVA and VA between 1/1/1990 12/31/2010 with follow up complete through 12/31/2016. [b]186 developed both of sessile/traditional serrated and AA. [c]Patients with advanced developed a denoma have at least one the these features (histology with villous component, > 1 cm, or high grade dysplasis). SSA: Sessile serrated adenoma; SSP: Sessile serrated polyp; TSA: Traditional serrated adenoma; TA: Tubular adenoma; VA: Villous adenoma; TVA: Tubulovillous adenoma.

colon (75% *vs* 43%; $P < 0.01$) than the patients who did not develop post-polypectomy CRC. Patients with smaller polyps (> 10 mm and < 20 mm) that would be categorized by EU guidelines were less likely to develop post-polypectomy CRC ($P = 0.03$). Other findings are shown in Table 1.

CRC developed over a median follow-up of 2.31 years (IQR: 0.58-4.27). The most common site of post- polypectomy CRC was the cecum (33.3%) followed by the ascending colon (20.2%). Mean tumor size was 3.25 ± 2.0 cm. The proportion of patients with stage 1-2 and stage 3-4 were 38.1% and 53.6%, respectively. Altogether, 6 patients (7.1%) were diagnosed with metastatic disease.

The most common causes associated with post-polypectomy CRC development were non-adherence to recommended surveillance interval (27.4%), incomplete resection of high risk polyp (25.0%), and unknown causes (30%) (Supplementary table 1). Notably, the median time from the index polypectomy to post-polypectomy cancer development ranged from 0.7 years for patients with persistent or recurrent polyps at the index polypectomy site to 3.5 years for patient who developed CRC but had at least one negative surveillance colonoscopy done after the index polypectomy. Patients who had their surveillance colonoscopy later than recommended or who were recommended by their healthcare providers to have follow up of their index AA/TSA/ASSA later than guideline recommendations developed CRC at a median of 6 years after treatment for the index AA/TSA/ASSA (Supplementary table 1). The 1-, 5-, and 10- year cumulative incidences of cancer were 0.3%, 1.1%, and 1.6%, respectively (Figure 2A).

By multivariate analysis, patient age ⩾ 70 at time of polypectomy (HR = 2.31, 95%CI: 1.04-5.12, $P = 0.04$), male sex (HR = 2.87, 95%CI: 1.14-6.81, $P = 0.03$), polyp size ⩾ 20 mm (HR = 3.70, 95%CI: 1.07-12.77, $P = 0.04$); degree of dysplasia (High *vs* Low) (HR = 2.59, 95%CI: 1.09-6.18, $P = 0.03$), higher number of polyps resected (HR = 5.94, 95%CI: 1.98-17.79, $P < 0.01$), and piecemeal compared to en bloc resection (HR = 5.42, 95%CI: 1.82-16.20, $P = 0.01$) were all significant factors associated with CRC development. Left *vs* right colon AA/TSA/ASSA location was associated with decreased risk (HR = 0.09, 95%CI: 0.03-0.29, $P < 0.01$) (Table 2).

CRC at site distinct from the index AA/TSA/ASSA

Forty-four patients with history of AA (27 villous, 17 tubular); three with TSA and seven with ASSA (four with dysplasia) later developed CRC at a site distinct from that of the incident AA/TSA/ASSA. One hundred and sixty-two patients who underwent polypectomy for AA/TSA/ASSA but did not later develop CRC (Table 3) were randomly selected to be the comparison group matched to the control group based on polyp histology and degree of dysplasia.

For the 54 patients who developed CRC at a site distinct from the index polypectomy, the most common sites of the index polyp were the rectum (18.5%) and the transverse colon (18.5%) followed by the ascending colon (16.7%). Forty-eight% of these patients were ⩾ 70, while 32.1% of patients who did not develop CRC

Table 2 Risk factors for colorectal cancer at AA/TSA/ASSA resection site

Risk factors	Univariate analysis, HR (95%CI)	*P* value	Multivariate analysis, HR (95%CI)	*P* value
Male sex (M:F)	1.74 (1.01-2.98)	0.04	2.87 (1.14-6.81)	0.03
Age at polypectomy (≥ 70)	2.51 (1.47-4.27)	< 0.01	2.31 (1.04-5.12)	0.04
Polyp size (≥ 20 mm)	2.60 (1.17-5.78)	0.02	3.70 (1.07-12.77)	0.04
Degree of Dysplasia (High:Low)	1.90 (1.06-3.41)	0.03	2.59 (1.09-6.18)	0.03
Polyp location (Left colon: Right colon)	0.10 (0.04-0.22)	< 0.01	0.09 (0.03-0.29)	< 0.01
Polyp location (Rectum: Right colon)	0.47 (0.22-1.02)	0.06	-	-
Number of polyps resected at polypectomy (> 3 polyps)	2.40 (1.10-5.24)	0.03	5.94 (1.98-17.79)	< 0.01
Polypectomy device used (Hot snare: Cold snare)	1.24 (0.49-3.75)	0.46	-	-
Polyp shape (Flat: Pedunculated)	6.15 (2.67-14.15)	< 0.01	2.79 (0.94-15.23)	0.06
Piecemeal removal (Yes:No)	2.80 (1.44-5.46)	< 0.01	5.42 (1.82-16.20)	0.01
Injection-assisted endoscopic mucosal resection (EMR) (Yes:No)	2.15 (0.98-4.68)	0.06	-	-

EMR: Endoscopic mucosal resection.

Table 3 Clinical and demographic characteristics of patients who developed post-polypectomy colorectal cancer at site distinct from index AA/TSA/ASSA polypectomy *n* (%)

Characteristics	Patients with post-polypectomy CRC (*n* = 54)	Patients who did not develop CRC (*n* = 162)	*P* value[1]
Demographics			
Male sex	27 (50.0)	88 (54.3)	0.58
Age ≥ 70	26 (48.2)	52 (32.1)	0.04
Time interval from first treatment for advanced adenoma till cancer or last surveillance colonoscopy in years (median, IQR)	5.11 (2.67-10.37)	6.8 (4.0-10.26)	0.08
Number of colonoscopies between first polypectomy and cancer (mean ± SD)	1.24 ± 1.58	1.65 ± 1.68	0.03
Adenoma size (10-20 mm)	25 (48.1)	106 (65.8)	0.03
Adenoma size (≥ 20 mm)	9 (17.3)	20 (12.4)	0.51
Flat/sessile	47 (92.2)	91 (58.71)	< 0.01
Degree of dysplasia			
High grade	17 (31.5)	51 (31.5)	-
Low grade/no dysplasia	37 (68.5)	111 (68.5)	-
Number of attempts to remove the polyp (mean ± SD)	1.35 ± 0.68	1.33 ± 0.68	< 0.01
Number of polyps resected at polypectomy (> 3 polyps)	11 (20.4)	15 (9.5%)	0.04
Polypectomy Device used			
Hot snare	12 (22.2)	26 (16.05)	0.63
Cold snare	4 (7.4)	12 (7.0)	0.63
Snare NOS	38 (70.5)	127 (76.5)	0.63
Additional treatments			
Piecemeal removal	9 (16.7)	21 (13.0)	0.5
Injection-assisted EMR	3 (5.6)	16 (10.0)	0.33
Polyp location			
Right colon	31 (57.4)	40 (24.7)	< 0.01
Left colon	13 (24.1)	89 (54.9)	< 0.01
Rectum	10 (18.5)	33 (20.4)	< 0.01

[1]*P*-values for continuous variables were obtained using the Kruskal-Wallis Test; Pearson's Chi-square test was used for discrete variables. CRC: Colorectal cancer.

were ≥ 70 years old (P = 0.04). Fifty percent of these patients with post-polypectomy CRC and 54% of those in the comparison group were male. CRC developed over a median follow-up of 2.64 years (1.0-6.33). Mean tumor size was 4.48 ± 4.81 cm. The most common site of CRC was the transverse colon (22.2%) followed by the cecum (18.5%), the ascending colon (18.5%), and the hepatic flexure (18.5%). The proportion of patients with stage 1-2 and stage 3-4 were 31.5% and 57.4%, respectively. In 10 cases, the patients (18.5%) were diagnosed with metastatic disease. Details of patient characteristics are shown in Table 3.

The most common causes associated with post-polypectomy CRC development at another site were non-adherence to recommended USPSTF surveillance intervals (31.5%), followed by unknown causes (27.8%), and incomplete colonoscopy (26.0%) (Supplementary table 2). The 1-, 5-, and 10- year cumulative incidences of cancer were 0.17%, 0.56%, and 0.87%, respectively (Figure 2A). The median

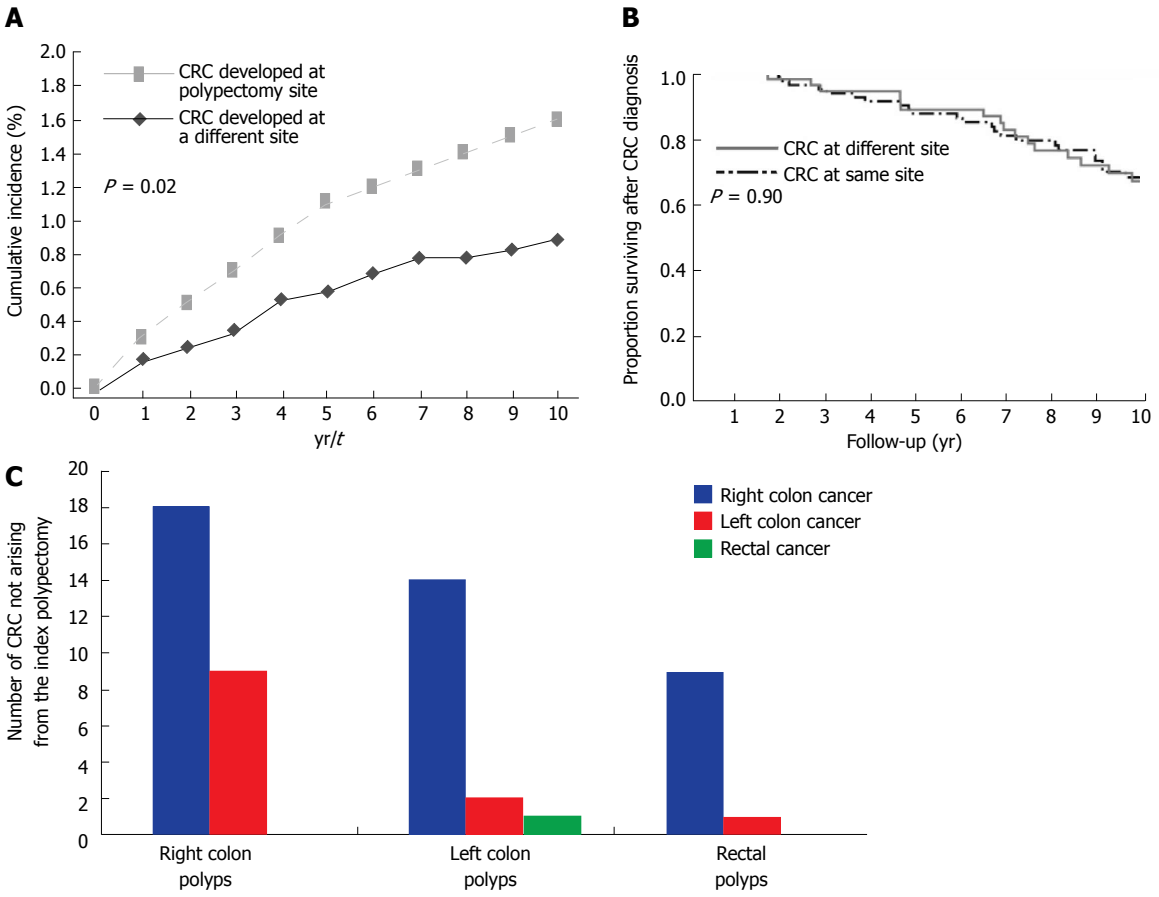

Figure 2 Cumulative incidence of *de novo* cancers after polypectomy in 4610 patients (A). A: Observed cumulative incidence curves of patients who developed CRC at the same site (dashed lines) and a different site (dashed lines) from the index polyp in year 1, 2 and 3 were 0.3, 0.5, and 0.7 *vs* 0.17, 0.24, and 0.33, respectively. B: Survival after CRC diagnosis at the same and different site. Kaplan-Meier Curves for Overall Survival among patients who developed CRC at the same site and a different site distinct from the site of the high risk polyp indicates that there is no significant difference between the two groups. C: Cancer location, as compared to removed polyp location in patients who developed CRC in area distinct from polypectomy site of the high risk polyp. From left to right: right colon polyps, left colon polyps, rectal polyps. On Y axis is the number of right colon cancers (blue); left colon cancer (red) and rectal cancer (green).The figure shows that right sided colon cancer was the most frequent location for a cancer to develop in a site distinct from the index polyp regardless of the location for the index polyp.

survival after CRC development was not significantly different for patients who developed CRC at the same site as compared to those who developed CRC at a different site (15.2 years *vs* 12.7 years, $P = 0.90$)(Figure 2B).

Right-sided post-polypectomy CRC were more common than left-sided CRC ($P < 0.01$) (Figure 2C). By multivariate analysis, patient age ⩾ 70 years at time of polypectomy (HR = 3.02, 95%CI: 1.23-7.41, $P = 0.02$); polyp shape (sessile *vs* pedunculated) (HR = 3.92, 95%CI: 1.10-14.04, $P = 0.04$) and number of polyps resected (HR = 4.05, 95%CI: 1.38-11.90, $P = 0.01$) were significant factors associated with CRC development at another site. Polyp location (left *vs* right) (HR = 0.23, 95%CI: 0.08-0.63, $P < 0.01$) was associated with decreased risk (Table 4).

DISCUSSION

This study showed that there is a persistent risk for post-polypectomy CRC despite surveillance colonoscopy for those polyps known to have the highest risk for malignant transformation. Even under watchful, directed colonoscopic surveillance and management of those polyps with the highest risk, 1.8% of patients developed post polypectomy CRC at the index polyp site and 1.2% developed CRC at a site distinct from the index AA/TSA/ASSA.

Villous and tubular adenomas were the most commonly observed histologies. ASSA/TSA were less common, possibly due to limited recognition of the serrated-cancer pathway during the time frame in this study, but which has improved within the last decade. One-third of patients developed CRC at the polypectomy site despite following appropriate surveillance intervals. This could be secondary to high endoscopic miss rate or rapidly-progressing cancer development. We found that increasing age at the time of polypectomy, number of polyps, polyp size, location, degree of dysplasia, and piecemeal resection were associated with increased CRC risk.

CRC developed at the index AA/TSA/ASSA polypectomy site in 1.8% (84/4610) of patients despite apparent initial complete resection of the high risk

Table 4 Risk factors for post-polypectomy colorectal cancer distinct from index AA/TSA/ASSA site

Risk factors	Univariate analysis, HR (95%CI)	*P* value	Multivariate analysis, HR (95%CI)	*P* value
Male sex (M:F)	0.79 (0.40-1.57)	0.50	-	-
Age at polypectomy (≥ 70)	3.68 (1.82-7.48)	< 0.01	3.02 (1.23-7.41)	0.02
Polyp size (≥ 20 mm)	1.93 (0.77-4.83)	0.16	-	-
Degree of dysplasia (High: Low)	1.41 (0.65-3.08)	0.39	-	-
Polyp location (Left colon: Right)	0.15 (0.07-0.34)	< 0.01	0.23 (0.08-0.63)	< 0.01
Polyp location (Rectum:Right colon)	0.22 (0.07-0.68)	< 0.01	0.23 (0.05-1.00)	0.05
Number of polyps resected at polypectomy (> 3 polyps)	2.94 (1.14-7.54)	0.03	4.05 (1.38-11.90)	0.01
Polypectomy device used (Hot snare:Cold snare)	0.64 (0.22-2.34)	0.24	-	-
Polyp shape (Flat/sessile: Pedunculated)	8.0 (2.62-24.05)	< 0.01	3.92 (1.10-14.04)	0.04
Piecemeal removal (Yes:No)	1.68 (0.67-4.22)	0.27	-	-
Injection-assisted EMR (Yes:No)	0.70 (0.19-2.60)	0.59	-	-

EMR: Endoscopic mucosal resection.

polyp. In 25% of these cases in which CRC developed at the index polypectomy site, the polyp had been found on surveillance colonoscopy either to have persisted or recurred, and subsequently progressed to cancer. It is possible that some polyps were missed, since colonoscopy has a failure rate of 6%-12% in detecting adenomas > 10 mm[26,27]. Alternatively, this could be explained by rapid progression from adenoma to CRC or by de novo CRC formation[28]. In spite of at least one surveillance colonoscopy in which there was no endoscopic evidence of recurrence of the index polyp, CRC was identified at the index polypectomy site on subsequent colonoscopy in nearly one third of those who developed same site post polypectomy CRC.

Polypectomy techniques have been implicated as one potential risk factor for post polypectomy CRC. Endoscopic piecemeal mucosal resection has been reported to be associated with 12.2%-55% rate for recurrence at the polypectomy site[29-33], which is known to be suboptimal for full resection of flat polyps in part because of the difficulty to completely identify, and thus include with the resection, the tissue bordering the polyp. Walsh et al studied 65 patients with large flat polyps treated with piecemeal resection with electrocautery snare. Nearly 14% of the polyps recurred after at least one negative intervening examination, and CRC developed in 17% of the patients after complete resection of the large polyp[30]. In another study, the rate of recurrence after endoscopic mucosal resection (EMR) with mucosal lift was observed in 7% of patients with flat polyps[34]. In our study, CRC occurred in 21 (27.6%) and 13(17.1%) of the patients who received piecemeal resection and en bloc EMR with mucosal lift, respectively. Piecemeal snare excision but not EMR with mucosal lift was an independent risk factor for post polypectomy CRC in this study; but further prospective studies are needed to examine the prognostic utility of EMR with CRC development.

In our study, poor adherence to current surveillance guidelines appeared to contribute to 8.3% of the cases of post-colonoscopy CRC. A previous study showed that delayed surveillance interval was associated with the development of CRC in almost 2% of patients post polypectomy for advanced adenoma[35]. Risk factors for pent surveillance was associated with a colonoscopist's having finished colonoscopy training prior to 1990; presently being in training; practicing in a non-academic setting, and performing a low life time number of colonoscopies[36].

In our study, we confirmed the finding by Robertson *et al*[37] that patients who are older at the time of polypectomy for AA are more likely to develop post-polypectomy CRC. Toll et al reported that CRC developed in 7% of patients with large polyps with high grade dysplasia over an average of 7 mo[38]. We also found that patients with right-sided AA/TSA/ASSA are more likely than those left-sided high risk polyps to develop same site post-polypectomy CRC, possibly due to the fact that flat polyps are more likely to arise in the right-side of the colon and are more easily missed[39]. Our study, like other studies, have implicated large (≥ 20 mm) polyps as particularly high risk and in need of a follow-up colonoscopy relatively soon after initial resection because the residual polyp could persist or recur with subsequent progression to CRC after polypectomy[40]. In this group of patients with persistent or recurrent high risk polyps, markers that predict whether a polyp needs to be removed with a colon resection to prevent CRC have yet to be identified. The clinical or molecular clues that distinguish the three quarters of patients with recurrent AA/TSA/ASSA who are able to be successfully treated with colonoscopic therapy from the ¼ of patients in whom the recurrent polyps will progress to cancer need to be expanded beyond the current features that declare a polyp as "high risk".

Our study highlights the risk of missing additional adenomas or cancers at a surveillance colonoscopy for follow up of an index AA/TSA/ASSA. Recognition that post-polypectomy CRC can happen at a site distinct from the index polypectomy even in individuals undergoing more intensive surveillance may be leveraged to improve the success rates of surveillance colonoscopy. It is possible that by expanding the proceduralist's attention beyond evaluation of the target lesion - in addition to utilizing each opportunity

at the surveillance colonoscopy to perform a thorough examination of the entire colon - may decrease the unanticipated and undesired outcome of CRC developing in spite of repeated surveillance. Adenoma miss rates during colonoscopic surveillance have been reported to range from 6% to 27%[41]. Bressler *et al*[2] reported that the rates for new/missed colon cancer which developed within 6-36 mo after colonoscopy were approximately 6.0% in the right colon; 5.5% in the transverse colon; 2.0% in the descending colon; and 2.3% in the rectosigmoid colon[2]. Positive screening tests such as Cologuard™ could improve colonoscopy performance. Johnson et al found that endoscopists who were aware of the Cologuard™ results spent more time and found more hemorrhagic and precancerous polyps than blinded endoscopists[41]. Features other than colonoscopy adenoma detection and polypectomy skills may contribute to these post-polypectomy CRCs at either the index site or in other areas of the colon.

Our study has several limitations. In addition to the retrospective nature of our study, we were not able to obtain data on all patients who did not develop CRC due to the large size of this cohort. To obtain reliable data would have necessitated manual review of over 4000 patient medical records not available in the electronic medical record to confirm the colonoscopy and pathology data for surveillance colonoscopies done both at Mayo and at other healthcare centers. Therefore, the relatively small number of post-polypectomy CRC cases was compared to a randomly selected portion of patients who did not develop post polypectomy CRC, rather than to the entire cancer free cohort. Another limitation is the relatively low number of TSA or ASSA patients compared to those with AA. We did not account for other confounding factors associated with higher lifetime risks and mortality from CRC such as the patient's BMI, smoking exposure, exercise, use of aspirin or NSAIDs, prior colonoscopy exams, or the adenoma detection rate of the performing colonoscopist[42].

This study shows that the applicability of current evidence-based surveillance guidelines to some patients with AA/TSA/ASSA is limited. There is insufficient data to provide explicit guidance for the follow up of polyps removed using specific treatments such as piecemeal endoscopic resection[11]. Current surveillance guidelines do not incorporate the impact of multiple high-risk features such as the risk of a large AA/TSA/ASSA being more recalcitrant or at higher risk for progressing to cancer if present in the right versus left side of the colon or the age of the patient. Current USPSTF guidelines recommend 3-year surveillance interval following polypectomy of adenoma with high-grade dysplasia but does not account for other features[11,43]. European guidelines stratify intermediate risk polyps as having a lower risk than EU guideline high risk polyps $\geqslant$ 20 mm, and recommend surveillance at 1 year for high risk polyps. Our findings that post-polypectomy CRC was significantly associated with high, but not intermediate risk polyps as classified by EU guidelines supports the need for a one year surveillance colonoscopy for these larger polyps currently not addressed in the USPSTF recommendations. Developing a risk score to optimize risk stratifications of patients with AA/TSA/ASSA might result in better discrimination between low- and high-risk patients. A recent study developed a scoring system based on older age, male sex, adenoma number, size $\geqslant$ 10 mm, villous histology, and proximal location at index colonoscopy; which were found to be independent predictors for detecting AA/TSA/ASSA, but not cancer, at surveillance endoscopy[44]. Having additional tools to risk stratify polyps will assist with making recommendations for surveillance, could identify tissue or molecular features that might be used to improve visualization of polyps, and stratify the risks that a polyp might recur or progress to cancer.

To our knowledge, this is the first study to determine risk factors for incident CRC at the same site or at another site in the colon following polypectomy of advanced lesions. Current guidelines are still limited in detecting such patients. Our study supports Atkin *et al*'s[45] study who recently reported that the incidence of CRC in patients was higher in patients with suboptimal quality colonoscopy, proximal polyps, large or high-grade polyps at baseline. Patients with increasing age and a history of large, multiple, highly dysplastic, right-sided, and difficult to remove adenomas requiring piecemeal resection are a high-risk population for the development of CRC at the same site. Increasing age and the presence of flat and/or right-sided adenomas increased the risk of CRC at another site. A diagnosis of CRC soon after complete colonoscopy may imply the need for shortened surveillance intervals. Understanding risk factors for subsequent CRC development and developing molecular markers predictive of progression to cancer are important for individualizing surveillance recommendations following adenoma removal since colonoscopy is not 100% sensitive tool in the identification or prevention of CRC in this population. In order to better stratify a polyp's risk for recurrence and subsequent CRC will require further research to identify molecular or other features to guide more individualized polyp management.

ARTICLE HIGHLIGHTS

Research background

Screening colonoscopy has a 3.5% false negative rate for detection of colorectal cancer (CRC) resulting in 17% of patients who had undergone colon screening within 3 years being diagnosed with CRC. However, no large studies have assessed the frequency and risk factors for CRC development among individuals following advanced adenoma (AA)/traditional serrated adenoma (TSA)/advanced sessile serrated adenoma (ASSA) removal. Recognition of this group at high-risk for interval CRC is one step toward preventing morbidity and mortality associated with CRC development.

Research motivation

Recognition that CRC could develop following AA/TSA/ASSA removal despite

adherence to guidelines is one step toward improving our practice efficiency and preventing a portion of CRC related morbidity and mortality. Understanding risk factors and developing molecular markers that predict progression may become important in order to individualize surveillance recommendations and recognize those AA/TSA/ASSA patients at high-risk for interval CRC.

Research objectives

To report the frequency of interval CRC development following high-risk polypectomy at the polypectomy site and another site distinct from polypectomy site and to identify risk factors associated with development of cancer. Realizing these objective is critical for future research since current evidence-based surveillance guidelines are limited in predicting CRC risk in these patients.

Research methods

We reviewed medical records of all adult patients (⩾ 18 years of age) who underwent colonoscopy (between January 1990 to December 2010) and were found to have high-risk polyps (either AA between January 1990 to December 2010 or ASSA/TSA between January 2000 to December 2010) to identify 4160 patients who had at least one follow-up surveillance colonoscopy following polypectomy. We excluded patients with IBD, polyposis syndromes or other genetic syndromes predisposing for CRC. Patients with a past history of CRC were not excluded from our study. From this cohort, we identified 84 patients who had developed CRC and matched to 252 patients who had not developed CRC based on polyp histology and size (< or ⩾ 20 mm), degree of dysplasia and decade that the index polyp was removed. Data abstracted included clinical and pathological features of high-risk polyps, number and timing of surveillance colonoscopies and post polypectomy CRC.

The data are reported as mean (± SD), median (interquartile range, IQR), ranges, and categorical variables by counts and percentages as appropriate. Estimates of the rate of cancer for the entire cohort were determined by using the Kaplan-Meier survival curve with log-rank test. We performed univariate time-to-event analysis with Cox proportional regression models to identify risk factors associated with development of cancer. Variables with $P < 0.05$ on univariate analysis were included in a multivariate Cox proportional hazard analysis to identify independent risk factors associated with malignancy. Finally, penalized regression models were run using Lasso regression, with 10-fold cross validation, to provide robust estimates of the model coefficients, which should provide better predictions when used with external data. All statistical analyses were conducted using JMP version 10 for Windows (SAS Institute Inc., Cary, NC, United States), SAS (version 9) or R (version 3.2.3).

Research results

Despite colonoscopic surveillance and management of high-risk polyps, 1.8% of patients developed post polypectomy CRC at or the index polyp site and 1.2% developed CRC at a site distinct from the index AA/TSA/ASSA. About one-third of patients developed CRC at the polypectomy site despite following appropriate surveillance intervals. Increasing age at the time of polypectomy, number of polyps, polyp size, location, degree of dysplasia, and piecemeal resection were associated with increased CRC risk. Current surveillance guidelines are not sufficient since it does not take into account the impact of multiple high-risk features of high-risk polyps for CRC development. This study also highlights the risk of missing additional adenomas or cancers at a surveillance colonoscopy for follow up of an index AA/TSA/ASSA. Resection technique (Piecemeal snare excision) was an independent risk factor for post polypectomy CRC in this study; but further prospective studies are needed to examine the prognostic utility of EMR with CRC development.

Research conclusions

1.8% of patients developed post polypectomy CRC at the index polyp site and 1.2% developed CRC at a site distinct from the index AA/TSA/ASSA despite surveillance colonoscopy. Surveillance colonoscopy for high-risk polyp does not always prevent CRC cancer development. Current surveillance guidelines are not sufficient in predicting CRC risk in some patients. Incorporate the impact of multiple high-risk features of resected polyps in surveillance guidelines. Interval CRC develops after high-risk polyp resection despite being in a surveillance program. We compared patients who had developed interval CRC after high-risk polyp resection at same site and different site and matched to patients who had not developed CRC to identify risk factors associated with CRC development. Patients with increasing age and a history of large, multiple, highly dysplastic, right-sided, and difficult to remove adenomas requiring piecemeal resection are a high-risk population for the development of CRC at the same site. Increasing age and the presence of flat and/or right-sided adenomas increased the risk of CRC at another site. Colonoscopy is not 100% sensitive tool in the identification or prevention of CRC. Shortened surveillance intervals may be needed post-polypectomy in some patients with multiple high-risk features.

Research perspectives

Interval CRC cancer rate after high-risk polyp resection is low yet CRC does develop in spite of post-polypectomy surveillance. We require further research to identify molecular or other features to guide more individualized polyp management. Study molecular features of patients who developed CRC at the polypectomy site despite following appropriate surveillance intervals

ACKNOWLEDGMENTS

We wish to thank our work study collaborators Paige Diedrick and Alexander Leehan for their assistance in reviewing clinical records.

REFERENCES

1 **Simon K**. Colorectal cancer development and advances in screening. *Clin Interv Aging* 2016; **11**: 967-976 [PMID: 27486317 DOI: 10.2147/CIA.S109285]
2 **Bressler B**, Paszat LF, Chen Z, Rothwell DM, Vinden C, Rabeneck L. Rates of new or missed colorectal cancers after colonoscopy and their risk factors: a population-based analysis. *Gastroenterology* 2007; **132**: 96-102 [PMID: 17241863 DOI: 10.1053/j.gastro.2006.10.027]
3 **Than M**, Witherspoon J, Shami J, Patil P, Saklani A. Diagnostic miss rate for colorectal cancer: an audit. *Ann Gastroenterol* 2015; **28**: 94-98 [PMID: 25609386]
4 **Siegel RL**, Miller KD, Fedewa SA, Ahnen DJ, Meester RGS, Barzi A, Jemal A. Colorectal cancer statistics, 2017. *CA Cancer J Clin* 2017; **67**: 177-193 [PMID: 28248415 DOI: 10.3322/caac.21395]
5 **Welch HG**, Robertson DJ. Colorectal Cancer on the Decline--Why Screening Can't Explain It All. *N Engl J Med* 2016; **374**: 1605-1607 [PMID: 27119236 DOI: 10.1056/NEJMp1600448]
6 **Winawer S**, Fletcher R, Rex D, Bond J, Burt R, Ferrucci J, Ganiats T, Levin T, Woolf S, Johnson D, Kirk L, Litin S, Simmang C; Gastrointestinal Consortium Panel. Colorectal cancer screening and surveillance: clinical guidelines and rationale-Update based on new evidence. *Gastroenterology* 2003; **124**: 544-560 [PMID: 12557158 DOI: 10.1053/gast.2003.50044]
7 **Pohl H**, Srivastava A, Bensen SP, Anderson P, Rothstein RI, Gordon SR, Levy LC, Toor A, Mackenzie TA, Rosch T, Robertson DJ. Incomplete polyp resection during colonoscopy-results of the complete adenoma resection (CARE) study. *Gastroenterology* 2013; **144**: 74-80.e1 [PMID: 23022496 DOI: 10.1053/j.gastro.2012.09.043]
8 **Umetani N**, Sasaki S, Masaki T, Watanabe T, Matsuda K, Muto T. Involvement of APC and K-ras mutation in non-polypoid colorectal tumorigenesis. *Br J Cancer* 2000; **82**: 9-15 [PMID: 10638959 DOI: 10.1054/bjoc.1999.0868]
9 **Robertson DJ**, Lieberman DA, Winawer SJ, Ahnen DJ, Baron JA, Schatzkin A, Cross AJ, Zauber AG, Church TR, Lance P, Greenberg ER, Martínez ME. Colorectal cancers soon after colonoscopy: a pooled multicohort analysis. *Gut* 2014; **63**: 949-956 [PMID: 23793224 DOI: 10.1136/gutjnl-2012-303796]
10 **Pohl H**, Robertson DJ. Colorectal cancers detected after colonoscopy frequently result from missed lesions. *Clin Gastroenterol Hepatol* 2010; **8**: 858-864 [PMID: 20655393 DOI: 10.1016/j.cgh.2010.06.028]
11 **Lieberman DA**, Rex DK, Winawer SJ, Giardiello FM, Johnson DA, Levin TR. Guidelines for colonoscopy surveillance after

screening and polypectomy: a consensus update by the US Multi-Society Task Force on Colorectal Cancer. *Gastroenterology* 2012; **143**: 844-857 [PMID: 22763141 DOI: 10.1053/j.gastro.2012.06.001]

12 **Colucci PM**, Yale SH, Rall CJ. Colorectal polyps. *Clin Med Res* 2003; **1**: 261-262 [PMID: 15931318 DOI: 10.3121/cmr.1.3.261]

13 **Bond JH**. Polyp guideline: diagnosis, treatment, and surveillance for patients with colorectal polyps. Practice Parameters Committee of the American College of Gastroenterology. *Am J Gastroenterol* 2000; **95**: 3053-3063 [PMID: 11095318 DOI: 10.1111/j.1572-0241.2000.03434.x]

14 **Longacre TA**, Fenoglio-Preiser CM. Mixed hyperplastic adenomatous polyps/serrated adenomas. A distinct form of colorectal neoplasia. *Am J Surg Pathol* 1990; **14**: 524-537 [PMID: 2186644 DOI: 10.1097/00000478-199006000-00003]

15 **Torlakovic E**, Skovlund E, Snover DC, Torlakovic G, Nesland JM. Morphologic reappraisal of serrated colorectal polyps. *Am J Surg Pathol* 2003; **27**: 65-81 [PMID: 12502929 DOI: 10.1097/00000478-200301000-00008]

16 **Wiland HO 4th**, Shadrach B, Allende D, Carver P, Goldblum JR, Liu X, Patil DT, Rybicki LA, Pai RK. Morphologic and molecular characterization of traditional serrated adenomas of the distal colon and rectum. *Am J Surg Pathol* 2014; **38**: 1290-1297 [PMID: 25127095 DOI: 10.1097/PAS.0000000000000253]

17 **Rex DK**, Ahnen DJ, Baron JA, Batts KP, Burke CA, Burt RW, Goldblum JR, Guillem JG, Kahi CJ, Kalady MF, O'Brien MJ, Odze RD, Ogino S, Parry S, Snover DC, Torlakovic EE, Wise PE, Young J, Church J. Serrated lesions of the colorectum: review and recommendations from an expert panel. *Am J Gastroenterol* 2012; **107**: 1315-29; quiz 1314, 1330 [PMID: 22710576 DOI: 10.1038/ajg.2012.161]

18 **Steele RJ**, Pox C, Kuipers EJ, Minoli G, Lambert R; International Agency for Research on Cancer. European guidelines for quality assurance in colorectal cancer screening and diagnosis. First Edition--Management of lesions detected in colorectal cancer screening. *Endoscopy* 2012; **44** Suppl 3: SE140-SE150 [PMID: 23012117 DOI: 10.1055/s-0032-1309802]

19 **Leung K**, Pinsky P, Laiyemo AO, Lanza E, Schatzkin A, Schoen RE. Ongoing colorectal cancer risk despite surveillance colonoscopy: the Polyp Prevention Trial Continued Follow-up Study. *Gastrointest Endosc* 2010; **71**: 111-117 [PMID: 19647250 DOI: 10.1016/j.gie.2009.05.010]

20 **Atkin WS**, Morson BC, Cuzick J. Long-term risk of colorectal cancer after excision of rectosigmoid adenomas. *N Engl J Med* 1992; **326**: 658-662 [PMID: 1736104 DOI: 10.1056/NEJM199203053261002]

21 **Sanduleanu S**, le Clercq CM, Dekker E, Meijer GA, Rabeneck L, Rutter MD, Valori R, Young GP, Schoen RE; Expert Working Group on 'Right-sided lesions and interval cancers', Colorectal Cancer Screening Committee, World Endoscopy Organization. Definition and taxonomy of interval colorectal cancers: a proposal for standardising nomenclature. *Gut* 2015; **64**: 1257-1267 [PMID: 25193802 DOI: 10.1136/gutjnl-2014-307992]

22 **Barlow WE**. Robust variance estimation for the case-cohort design. *Biometrics* 1994; **50**: 1064-1072 [PMID: 7786988 DOI: 10.2307/2533444]

23 **Binder S**. Hazards of low-level lead exposure recognized. *Am J Public Health* 1992; **82**: 1043-1044 [PMID: 1319118 DOI: 10.2105/AJPH.82.7.1043-a]

24 **Prentice RL**. On the design of synthetic case-control studies. *Biometrics* 1986; **42**: 301-310 [PMID: 3741972 DOI: 10.2307/2531051]

25 **Simon N**, Friedman J, Hastie T, Tibshirani R. Regularization Paths for Cox's Proportional Hazards Model via Coordinate Descent. *J Stat Softw* 2011; **39**: 1-13 [PMID: 27065756 DOI: 10.18637/jss.v039.i05]

26 **Rex DK**, Cutler CS, Lemmel GT, Rahmani EY, Clark DW, Helper DJ, Lehman GA, Mark DG. Colonoscopic miss rates of adenomas determined by back-to-back colonoscopies. *Gastroenterology* 1997; **112**: 24-28 [PMID: 8978338 DOI: 10.1016/S0016-5085(97)70214-2]

27 **Pickhardt PJ**, Choi JR, Hwang I, Butler JA, Puckett ML, Hildebrandt HA, Wong RK, Nugent PA, Mysliwiec PA, Schindler WR. Computed tomographic virtual colonoscopy to screen for colorectal neoplasia in asymptomatic adults. *N Engl J Med* 2003; **349**: 2191-2200 [PMID: 14657426 DOI: 10.1056/NEJMoa031618]

28 **Rembacken BJ**, Fujii T, Cairns A, Dixon MF, Yoshida S, Chalmers DM, Axon AT. Flat and depressed colonic neoplasms: a prospective study of 1000 colonoscopies in the UK. *Lancet* 2000; **355**: 1211-1214 [PMID: 10770302 DOI: 10.1016/S0140-6736(00)02086-9]

29 **Seo GJ**, Sohn DK, Han KS, Hong CW, Kim BC, Park JW, Choi HS, Chang HJ, Oh JH. Recurrence after endoscopic piecemeal mucosal resection for large sessile colorectal polyps. *World J Gastroenterol* 2010; **16**: 2806-2811 [PMID: 20533602 DOI: 10.3748/wjg.v16.i22.2806]

30 **Walsh RM**, Ackroyd FW, Shellito PC. Endoscopic resection of large sessile colorectal polyps. *Gastrointest Endosc* 1992; **38**: 303-309 [PMID: 1607080 DOI: 10.1016/S0016-5107(92)70421-0]

31 **Zlatanic J**, Waye JD, Kim PS, Baiocco PJ, Gleim GW. Large sessile colonic adenomas: use of argon plasma coagulator to supplement piecemeal snare polypectomy. *Gastrointest Endosc* 1999; **49**: 731-735 [PMID: 10343218 DOI: 10.1016/S0016-5107(99)70291-9]

32 **Brooker JC**, Saunders BP, Shah SG, Williams CB. Endoscopic resection of large sessile colonic polyps by specialist and non-specialist endoscopists. *Br J Surg* 2002; **89**: 1020-1024 [PMID: 12153628 DOI: 10.1046/j.1365-2168.2002.02157.x]

33 **Khashab M**, Eid E, Rusche M, Rex DK. Incidence and predictors of "late" recurrences after endoscopic piecemeal resection of large sessile adenomas. *Gastrointest Endosc* 2009; **70**: 344-349 [PMID: 19249767 DOI: 10.1016/j.gie.2008.10.037]

34 **Ferrara F**, Luigiano C, Ghersi S, Fabbri C, Bassi M, Landi P, Polifemo AM, Billi P, Cennamo V, Consolo P, Alibrandi A, D' Imperio N. Efficacy, safety and outcomes of 'inject and cut' endoscopic mucosal resection for large sessile and flat colorectal polyps. *Digestion* 2010; **82**: 213-220 [PMID: 20588036 DOI: 10.1159/000284397]

35 **van Heijningen EM**, Lansdorp-Vogelaar I, Steyerberg EW, Goede SL, Dekker E, Lesterhuis W, ter Borg F, Vecht J, Spoelstra P, Engels L, Bolwerk CJ, Timmer R, Kleibeuker JH, Koornstra JJ, de Koning HJ, Kuipers EJ, van Ballegooijen M. Adherence to surveillance guidelines after removal of colorectal adenomas: a large, community-based study. *Gut* 2015; **64**: 1584-1592 [PMID: 25586057 DOI: 10.1136/gutjnl-2013-306453]

36 **Iskandar H**, Yan Y, Elwing J, Early D, Colditz GA, Wang JS. Predictors of Poor Adherence of US Gastroenterologists with Colonoscopy Screening and Surveillance Guidelines. *Dig Dis Sci* 2015; **60**: 971-978 [PMID: 25366146 DOI: 10.1007/s10620-014-3403-0]

37 **Robertson DJ**, Greenberg ER, Beach M, Sandler RS, Ahnen D, Haile RW, Burke CA, Snover DC, Bresalier RS, McKeown-Eyssen G, Mandel JS, Bond JH, Van Stolk RU, Summers RW, Rothstein R, Church TR, Cole BF, Byers T, Mott L, Baron JA. Colorectal cancer in patients under close colonoscopic surveillance. *Gastroenterology* 2005; **129**: 34-41 [PMID: 16012932 DOI: 10.1053/j.gastro.2005.05.012]

38 **Toll AD**, Fabius D, Hyslop T, Pequignot E, DiMarino AJ, Infantolino A, Palazzo JP. Prognostic significance of high-grade dysplasia in colorectal adenomas. *Colorectal Dis* 2011; **13**: 370-373 [PMID: 20718835 DOI: 10.1111/j.1463-1318.2010.02385.x]

39 **Nawa T**, Kato J, Kawamoto H, Okada H, Yamamoto H, Kohno H, Endo H, Shiratori Y. Differences between right- and left-sided colon cancer in patient characteristics, cancer morphology and histology. *J Gastroenterol Hepatol* 2008; **23**: 418-423 [PMID: 17532785 DOI: 10.1111/j.1440-1746.2007.04923.x]

40 **Nivatvongs S**, Snover DC, Fang DT. Piecemeal snare excision of large sessile colon and rectal polyps: is it adequate? *Gastrointest*

Endosc 1984; **30**: 18-20 [PMID: 6706083 DOI: 10.1016/S0016-5107(84)72287-5]

41 **Ahn SB**, Han DS, Bae JH, Byun TJ, Kim JP, Eun CS. The Miss Rate for Colorectal Adenoma Determined by Quality-Adjusted, Back-to-Back Colonoscopies. *Gut Liver* 2012; **6**: 64-70 [PMID: 22375173 DOI: 10.5009/gnl.2012.6.1.64]

42 **Meester RG**, Doubeni CA, Lansdorp-Vogelaar I, Jensen CD, van der Meulen MP, Levin TR, Quinn VP, Schottinger JE, Zauber AG, Corley DA, van Ballegooijen M. Variation in Adenoma Detection Rate and the Lifetime Benefits and Cost of Colorectal Cancer Screening: A Microsimulation Model. *JAMA* 2015; **313**: 2349-2358 [PMID: 26080339 DOI: 10.1001/jama.2015.6251]

43 **Martínez ME**, Baron JA, Lieberman DA, Schatzkin A, Lanza E, Winawer SJ, Zauber AG, Jiang R, Ahnen DJ, Bond JH, Church TR, Robertson DJ, Smith-Warner SA, Jacobs ET, Alberts DS, Greenberg ER. A pooled analysis of advanced colorectal neoplasia diagnoses after colonoscopic polypectomy. *Gastroenterology* 2009; **136**: 832-841 [PMID: 19171141 DOI: 10.1053/j.gastro.2008.12.007]

44 **van Heijningen EM**, Lansdorp-Vogelaar I, van Hees F, Kuipers EJ, Biermann K, de Koning HJ, van Ballegooijen M, Steyerberg EW; SAP Study Group. Developing a score chart to improve risk stratification of patients with colorectal adenoma. *Endoscopy* 2016; **48**: 563-570 [PMID: 27167762 DOI: 10.1055/s-0042-104275]

45 **Atkin W**, Wooldrage K, Brenner A, Martin J, Shah U, Perera S, Lucas F, Brown JP, Kralj-Hans I, Greliak P, Pack K, Wood J, Thomson A, Veitch A, Duffy SW, Cross AJ. Adenoma surveillance and colorectal cancer incidence: a retrospective, multicentre, cohort study. *Lancet Oncol* 2017; **18**: 823-834 [PMID: 28457708 DOI: 10.1016/S1470-2045(17)30187-0]

P- Reviewer: Augustin G, Chiu CT, Lakatos PL, Perez-Cuadrado-Robles E, Sali L, Zorzi M **S- Editor**: Gong ZM
L- Editor: A **E- Editor**: Ma YJ

World Journal of Gastroenterology

Submit a Manuscript: http://www.f6publishing.com

World J Gastroenterol 2018 February 28; 24(8): 917-928

DOI: 10.3748/wjg.v24.i8.917

ISSN 1007-9327 (print) ISSN 2219-2840 (online)

ORIGINAL ARTICLE

Retrospective Cohort Study

Nationwide cohort study suggests that nucleos(t)ide analogue therapy decreases dialysis risk in Taiwanese chronic kidney disease patients acquiring hepatitis B virus infection

Yi-Chun Chen, Chung-Yi Li, Shiang-Jiun Tsai, Yen-Chun Chen

Yi-Chun Chen, Division of Nephrology, Department of Internal Medicine, Dalin Tzu Chi Hospital, Buddhist Tzu Chi Medical Foundation, Chiayi County 622, Taiwan

Yi-Chun Chen, School of Medicine, Tzu Chi University, Hualien 970, Taiwan

Chung-Yi Li, Department and Graduate Institute of Public Health, College of Medicine, National Cheng Hung University, Tainan 701, Taiwan

Chung-Yi Li, Department of Public Health, College of Public Health, China Medical University, Taichung 404, Taiwan

Shiang-Jiun Tsai, Department of Medical Research, Dalin Tzu Chi Hospital, Buddhist Tzu Chi Medical Foundation, Chiayi County 622, Taiwan

Yen-Chun Chen, Division of Hepato-Gastroenterology, Department of Internal Medicine, Dalin Tzu Chi Hospital, Buddhist Tzu Chi Medical Foundation, Chiayi County 622, Taiwan

ORCID number: Yi-Chun Chen (0000-0003-2153-272X); Chung-Yi Li (0000-0002-0321-8908); Shiang-Jiun Tsai (0000-0002-0644-8223); Yen-Chun Chen (0000-0002-9739-9905)

Author contributions: Chen YC designed the research; Chen YC, Li CY and Tsai SJ performed the research; Chen YC, Li CY, Tsai SJ and Chen YC analyzed the data; Chen YC wrote the paper; Li CY, Tsai SJ, Chen YC critically revised the manuscript for important intellectual content.

Supported by Dalin Tzu Chi Hospital, No. DTCRD 104-I-16.

Institutional review board statement: This study was approved by the institutional review board of the Dalin Tzu Chi Hospital (B10302011).

Informed consent statement: All patients' information was de-identified in the database (LHID2005) and no informed consent was required. This study was exempt from a full ethical review by the institutional review board of the Dalin Tzu Chi Hospital (B10302011).

Conflict-of-interest statement: All authors have no conflict of interests.

Data sharing statement: No additional data are available.

Manuscript source: Unsolicited manuscript

Correspondence to: Yi-Chun Chen, MD, Assistant Professor, Division of Nephrology, Department of Internal Medicine, Dalin Tzu Chi Hospital, Buddhist Tzu Chi Medical Foundation, No. 2, Minsheng Road, Dalin Township, Chiayi County 622, Taiwan. chenyichun0320@yahoo.com.tw
Telephone: +886-5-2648000-5665
Fax: +886-5-2648128

Received: November 4, 2017
Peer-review started: November 4, 2017
First decision: November 22, 2017
Revised: December 10, 2017
Accepted: December 20, 2017
Article in press: December 20, 2017
Published online: February 28, 2018

Abstract

AIM

To investigate the risk of end-stage renal disease (ESRD) in hepatitis B virus (HBV)-infected patients with chronic kidney disease (CKD) with and without nucleos(t)ide analogue (NA) therapy.

METHODS

This nationwide cohort study included 103444 Taiwanese CKD adults without hepatitis C virus infection from the Taiwan Longitudinal Health Insurance Database 2005 between 1997 and 2012. We identified 2916 CKD patients who acquired HBV infection and did not receive NAs (untreated cohort), and they were propensity-matched 1:4 with 11664 uninfected counterparts. We also identified 442 CKD patients who acquired HBV infection and received NAs (treated cohort), and they were propensity-matched 1:3 with 1326 untreated counterparts. The association between HBV infection, NA use, and ESRD was analyzed using competing risk analysis.

RESULTS

Multivariable Cox regression analysis showed a 1.67-fold higher risk ($P < 0.0001$) of ESRD in the untreated cohort (16-year cumulative incidence, 10.1%) than in the matched uninfected cohort (16-year cumulative incidence, 6.6%), which was independent of cirrhosis or diabetes. The treated cohort (16-year cumulative incidence, 2.2%) had an 87% lower ESRD risk ($P < 0.0001$) compared with the matched untreated cohort (16-year cumulative incidence, 11.9%). The number needed to treat for one fewer ESRD after NA use at 12 years was 12. Multivariable stratified analyses verified these associations in all subgroups.

CONCLUSION

This study suggests that untreated HBV infection and NA therapy are associated with increased and decreased risk of ESRD, respectively, in CKD patients. Identification of HBV status and targeted monitoring for ESRD development are important in CKD patients living in HBV-endemic areas.

Key words: Hepatitis B virus; Chronic kidney disease; End-stage renal disease; Nucleos(t)ide analogue; Cohort study

Core tip: This nationwide retrospective cohort study used propensity score-matched and competing risk analyses to evaluate the effect of untreated hepatitis B virus (HBV) infection and nucleos(t)ide analogue (NA) therapy on the development of end-stage renal disease (ESRD) in chronic kidney disease (CKD) patients who acquired HBV infection. We found that untreated HBV infection in CKD patients was associated with an increased risk of ESRD, while NA therapy reduced the risk.

Chen YC, Li CY, Tsai SJ, Chen YC. Nationwide cohort study suggests that nucleos(t)ide analogue therapy decreases dialysis risk in Taiwanese chronic kidney disease patients acquiring hepatitis B virus infection. *World J Gastroenterol* 2018; 24(8): 917-928 Available from: URL: http://www.wjgnet.com/1007-9327/full/v24/i8/917.htm DOI: http://dx.doi.org/10.3748/wjg.v24.i8.917

INTRODUCTION

Hepatitis B virus (HBV) infection, chronic kidney disease (CKD), and end-stage renal disease (ESRD) are global health challenges which impose a major economic burden[1,2]. Emerging clinical and experimental evidence suggests that in addition to liver inflammation and fibrosis, chronic HBV infection may also play a role in the initiation and progression of renal injury. Untreated chronic HBV infection could lead to an annual decline in the estimated glomerular filtration rate[3], and subsequent development of CKD and ESRD in the general population, even in the absence of cirrhosis[4,5]. Sera of patients with chronic HBV infection, even those negative for the presence of HBV-DNA, could induce apoptosis of cultured human renal tubular cells[6]. Chronic HBV infection has also been shown to progress to ESRD in special populations with diabetic nephropathy[7] and HBV-related glomerulonephritis (HBV-GN)[8]. CKD patients were reported to be at increased risk of acquiring HBV infection[1,9,10], more vulnerable to the cytopathic effects of HBV infection, and prone to becoming chronic carriers. This could be because of increased exposure of these patients to blood products, and the immunosuppressive effects of CKD[1,11]. The risk factors for CKD onset in the general population may differ somewhat from those for progression of established CKD[12]. However, there are presently no cohort studies which have addressed the incidence of chronic HBV infection among CKD patients and their renal outcome regardless of etiology.

HBV infection among CKD patients is associated with higher morbidity and mortality rates, and its management remains challenging for clinicians[1,13]. Nucleos(t)ide analogue (NA) therapy effectively suppresses HBV replication by inhibiting HBV polymerase, and thus decreases the levels of serum HBV-DNA[14] and delays progression of cirrhosis[15]. Although NA therapy is recommended for all patients with chronic HBV infection, regardless of any level of renal dysfunction, there is limited information on NA use in CKD patients[13]. Serum HBV-DNA levels were shown to have a positive correlation with the degree of renal injury[16], and lamivudine treatment resulted in a significant reduction in proteinuria, serum HBV-DNA, and ESRD risk[17] in a small number of adult patients with HBV-GN. However, no randomized clinical trials have been conducted to date to examine the effect of NAs on renal outcome among CKD patients regardless of etiology[1]. This issue assumes greater importance

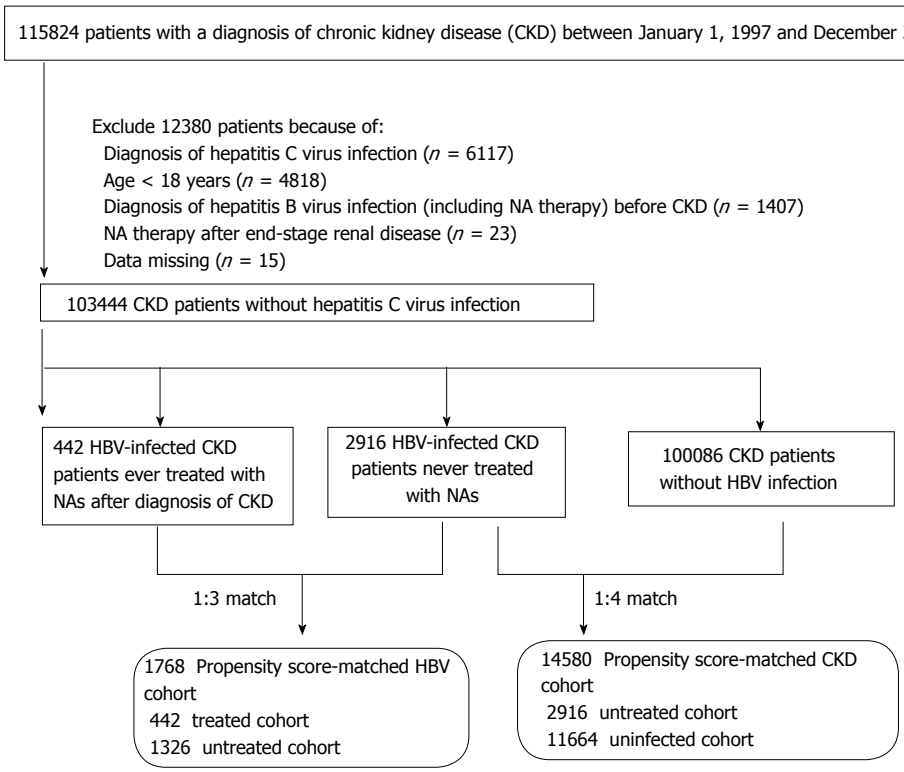

Figure 1 Flow diagram of the enrollment process. NAs: Nucleos(t)ide analogues; HBV: Hepatitis B virus; CKD: Chronic kidney disease.

because of the rising global burden of CKD, ESRD, and HBV infection. The high prevalence of these three diseases in Taiwan makes it a particularly suitable location to evaluate this relationship. Our nationwide cohort study analysed reimbursement claims data from the Taiwan Longitudinal Health Insurance Database 2005 (LHID2005) in order to determine the effect of chronic HBV infection and NA use on the renal outcome of CKD patients, and the number needed to treat (NNT) for one less ESRD development.

MATERIALS AND METHODS

Database

This study evaluated data from LHID2005, a subset of the National Health Insurance Research Database (NHIRD) which is derived from the Taiwan National Health Insurance (NHI) program and released by the National Health Research Institutes for academic research. The NHI program is a compulsory and universal program for all residents of Taiwan, had a coverage rate of more than 99% by the end of 2012, and adopts ICD-9 codes to define diseases. All insurance claims are scrutinized by medical reimbursement specialists and undergo peer review under strict audits and heavy penalties in the reimbursement process in order to ensure accuracy of coding. The LHID2005 includes the data of 1 million randomly sampled subjects who were NHI beneficiaries in 2005[18]. There was no significant difference in age, sex, birth year, or average insured payroll-related amount between the subjects enrolled in the NHI program. As all personal information was anonymous in the LHID2005, no informed consent was required and this study was exempt from a full ethical review by the institutional review board of the Dalin Tzu Chi Hospital (B10302011).

CKD population

The CKD population comprised patients aged > 18 years who received a primary diagnosis of CKD (ICD-9 codes 250.4*, 274.1*, 283.11, 403.*1, 404.*2, 404.*3, 440.1, 442.1, 447.3, 572.4, 580-588, 642.1*, and 646.2*)[19] between January 1, 1997 and December 31, 2012 and did not have catastrophic illness registration cards for ESRD (indicating the need for long-term renal replacement therapy). We excluded subjects who had claim-based diagnoses of hepatitis C virus infection (ICD-9 codes 070.41, 070.44, 070.51, 070.54, and V02.62) between 1997 and 2012, or of HBV infection (ICD-9 codes 070.22, 070.23, 070.32, 070.33, V02.61) before CKD enrolment. A total of 103,444 CKD patients were eligible for analysis (Figure 1). However, the exact stage of CKD cannot be assessed from the LHID2005.

Study cohorts

Based on HBV infection status and NA use including lamivudine, entecavir, telbivudine, and adefovir[20], the eligible CKD patients in this study were divided into three groups: uninfected (n = 100086), untreated (n = 2916), and treated (n = 442) groups. The incidence of CKD patients acquiring HBV infection was 3.2%. The untreated group was defined as the group of CKD

Table 1 Baseline characteristics and renal outcome of the untreated hepatitis B virus-infected and hepatitis B virus-uninfected chronic kidney disease patients (*n* = 103002), 1997-2012

Variable	Overall CKD patients (*n* = 103002)			Propensity score-matched CKD patients (*n* = 14580)		
	Untreated (*n* = 2916)	Uninfected (*n* = 100086)	*P* value	Untreated (*n* = 2916)	Uninfected (*n* = 11664)	*P* value
Sex			< 0.0001			0.45
Men	1713 (58.7)	51592 (51.6)		1713 (58.7)	6762 (58.0)	
Women	1203 (41.3)	48494 (48.4)		1203 (41.3)	4902 (42.0)	
Age (yr, mean ± SD)	48.1 ± 14.4	56.3 ± 17.4	< 0.0001	48.1 ± 14.4	47.7 ± 15.9	0.21
Comorbidity						
Diabetes	749 (25.7)	33023 (33.0)	< 0.0001	749 (25.7)	3049 (26.1)	0.62
Hypertension	884 (30.3)	45139 (45.1)	< 0.0001	884 (30.3)	3420 (29.3)	0.29
Coronary heart disease	316 (10.8)	18668 (18.7)	< 0.0001	316 (10.8)	1152 (9.9)	0.12
Hyperlipidemia	695 (23.8)	29595 (29.6)	< 0.0001	695 (23.8)	2851 (24.4)	0.49
Cirrhosis	139 (4.8)	1528 (1.5)	< 0.0001	139 (4.8)	472 (4.1)	0.08
Urbanization level			0.0003			0.47
Urban	892 (30.6)	27951 (27.9)		892 (30.6)	3595 (30.8)	
Suburban	1351 (46.3)	46163 (46.1)		1351 (46.3)	5498 (47.2)	
Rural	673 (23.1)	25972 (26.0)		673 (23.1)	2571 (22.0)	
Enrolee category			< 0.0001			0.011
1 + 2	1122 (38.5)	29935 (29.9)		1122 (38.5)	4680 (40.1)	
3	1278 (43.8)	47825 (47.8)		1278 (43.8)	4760 (40.8)	
4	516 (17.7)	22326 (22.3)		516 (17.7)	2224 (19.1)	
No. of medical visits (mean ± SD)	26.1 ± 20.8	29.0 ± 22.8	< 0.0001	26.1 ± 20.8	25.7 ± 22.5	0.31
Charlson comorbidity index score (mean ± SD)	1.6 ± 1.9	1.9 ± 2.3	< 0.0001	1.6 ± 1.9	1.5 ± 2.1	0.06
Propensity score (mean ± SD)	0.4 ± 0.2	0.3 ± 0.2	< 0.0001	0.4 ± 0.2	0.4 ± 0.2	1.00
End-stage renal disease						
Follow-up year (mean ± SD)	8.9 ± 3.9	6.9 ± 4.5	< 0.0001	8.9 ± 3.9	7.4 ± 4.5	< 0.0001
Total follow-up (person-year)	26098	689592	< 0.0001	26098	86780	< 0.0001
Event	197 (6.8)	4076 (4.1)	< 0.0001	197 (6.8)	414 (3.6)	< 0.0001

Categorical variables are given as *n* (%); continuous variable given as mean ± SD. CKD: Chronic kidney disease.

patients who did not receive NA therapy over the course of the study period, following the acquisition of HBV infection. The treated group was defined as the group of CKD patients who received NAs throughout the study period. Each treated patient was propensity score (PS)-matched with three untreated patients. The uninfected patients, who were PS-matched 4:1 with their untreated counterparts, comprised CKD patients who never coded for HBV infection. The PS was estimated by logistic regression built on baseline variables including age, sex, comorbidities, urbanization level, enrolee category (EC), number of medical visits, and the Deyo-Charlson comorbidity index (CCI) score. The PS-matched HBV cohort included 1768 CKD patients (442 treated and 1,326 untreated patients). The PS-matched CKD cohort included 14,580 patients (2,916 untreated and 11,664 uninfected patients).

Endpoint and covariates

The index date of the treated cohort was defined as the date of initiation of NA therapy, that of the untreated cohort was defined as the first occurrence of a HBV claim during the entry period, and that of the uninfected cohort was defined as the date of a CKD claim during the entry period. All CKD patients were followed from the index date until the date of ESRD diagnosis, date of death, or the end of 2012, whichever came first. The diagnosis of ESRD was based on the Catastrophic Illness Patient Database, a part of the NHIRD. All Taiwanese patients who develop ESRD and require long-term dialysis are eligible to apply for catastrophic illness registration cards from the NHI Administration, so they have no copayments for healthcare. Censoring resulting from death during CKD progression was regarded as informative and was adjusted by using competing risk methodology[21]. The adjusted covariates comprised sociodemographic and comorbidity factors. The sociodemographic characteristics included age, sex, urbanization level (urban, suburban, and rural), EC [EC1 (highest status)] to EC4 (lowest status), number of medical visits, CCI score, and PS. The comorbidities (ICD-9 codes] investigated in this study were diabetes (250), hypertension (401-405), coronary heart disease (410-414), hyperlipidemia (272-272.4), and cirrhosis (571.2, 571.5, and 571.6).

Statistical analysis

We used a modified Kaplan-Meier method and Gray's method[22] to calculate and compare the cumulative incidence of ESRD in data with competing risk, and tested differences in the full time-to-event distributions between the study cohorts using the log-

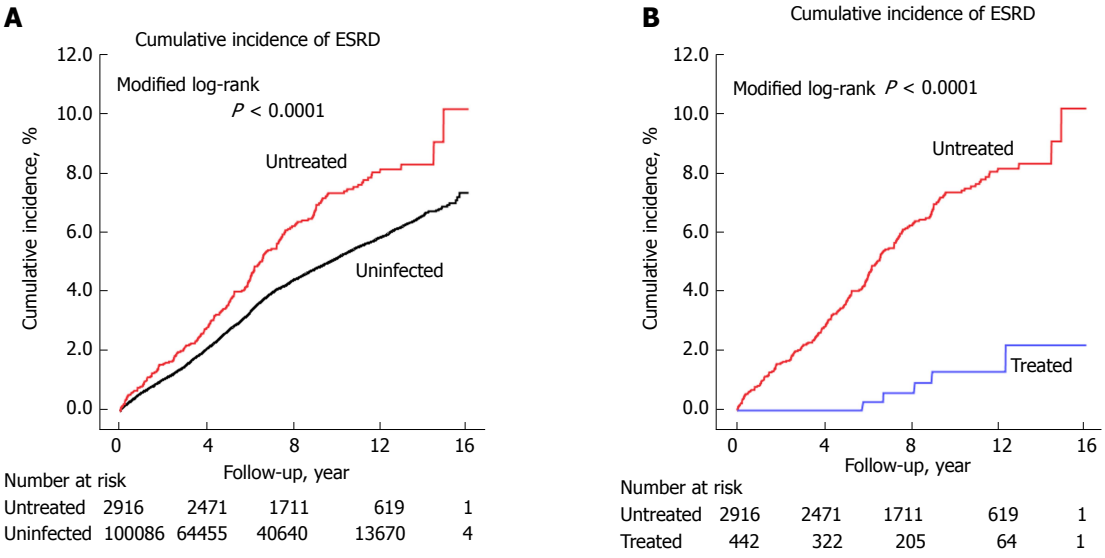

Figure 2 Cumulative incidence of end-stage renal disease after adjustment for competing mortality among (A) propensity score-matched chronic kidney disease cohort and (B) propensity score-matched hepatitis B virus cohort. ESRD: End-stage renal disease.

Table 2 Baseline characteristics and renal outcome of the treated and untreated hepatitis B virus-infected chronic kidney disease patients (*n* = 3358), 1997-2012

Variable	Overall HBV patients (*n* = 3358)			Propensity score-matched HBV patients (*n* = 1768)		
	Treated (*n* = 442)	Untreated (*n* = 2916)	*P* value	Treated (*n* = 442)	Untreated (*n* = 1326)	*P* value
Sex			< 0.0001			0.76
Men	319 (72.2)	1713 (58.7)		319 (72.2)	967 (72.9)	
Women	123 (27.8)	1203 (41.3)		123 (27.8)	359 (27.1)	
Age (yr, mean ± SD)	51.0 ± 13.9	48.1 ± 14.4	< 0.0001	51.0 ± 13.9	51.6 ± 14.7	0.49
Interval to start nucleos(t)ide analogue therapy (yr, mean ± SD)	1.2 ± 1.9	-		1.2 ± 1.9	-	
Nucleos(t)ide analogue therapy duration (yr, mean ± SD)	0.8 ± 0.8	-		0.8 ± 0.8	-	
Comorbidity						
Diabetes	141 (31.9)	749 (25.7)	0.006	141 (31.9)	424 (32.0)	0.98
Hypertension	150 (33.9)	884 (30.3)	0.12	150 (33.9)	457 (34.5)	0.84
Coronary heart disease	59 (13.4)	316 (10.8)	0.12	59 (13.4)	198 (14.9)	0.41
Hyperlipidemia	108 (24.4)	695 (23.8)	0.78	108 (24.4)	334 (25.2)	0.75
Cirrhosis	59 (13.4)	139 (4.8)	< 0.0001	59 (13.4)	135 (10.2)	0.07
Urbanization level			0.45			0.88
Urban	129 (29.2)	892 (30.6)		129 (29.2)	381 (28.7)	
Suburban	199 (45.0)	1351 (46.3)		199 (45.0)	615 (46.4)	
Rural	114 (25.8)	673 (23.1)		114 (25.8)	330 (24.9)	
Enrolee category			0.32			0.61
1 + 2	161 (36.4)	1122 (38.5)		161 (36.4)	460 (34.7)	
3	190 (43.0)	1278 (43.8)		190 (43.0)	606 (45.7)	
4	91 (20.6)	516 (17.7)		91 (20.6)	260 (19.6)	
No. of medical visits (mean ± SD)	26.5 ± 18.2	26.1 ± 20.8	0.75	26.5 ± 18.2	26.3 ± 19.3	0.90
Charlson comorbidity index score (mean ± SD)	1.9 ± 2.1	1.6 ± 1.9	< 0.0001	1.9 ± 2.1	1.9 ± 2.2	0.79
Propensity score (mean ± SD)	1.6 ± 0.7	1.3 ± 0.6	< 0.0001	1.6 ± 0.7	1.5 ± 0.7	0.51
End-stage renal disease						
Follow-up year (mean ± SD)	7.6 ± 4.3	8.9 ± 3.9	< 0.0001	7.6 ± 4.3	8.5 ± 4.0	< 0.0001
Total follow-up (person-year)	3359	26101	< 0.0001	3359	22478	< 0.0001
Event	5 (1.1)	197 (6.8)	< 0.0001	5 (1.1)	108 (8.1)	< 0.0001

Categorical variables are given as *n* (%); continuous variable given as mean ± SD. HBV: Hepatitis B virus.

rank test. The NNT represented the number of patients needed to be treated to yield one fewer ESRD; the NNT was calculated with the inverse of the absolute risk reduction[23]. After ensuring the assumption of

A

	Untreated cohort			Uninfected cohort			Hazard ratio (95% CI)			
	n	PY	ESRD events	*n*	PY	ESRD events	Crude	*P* value	Adjusted[1]	*P* value
Sex										
Men	1713	15002	122	6762	47533	257	1.58 (1.27-1.96)	< 0.0001	1.68 (1.35-2.08)	< 0.0001
Women	1203	11098	75	4902	39282	157	1.72 (1.31-2.27)	0.0001	1.59 (1.20-2.10)	0.0012
Age (yr)										
< 60	2281	21322	148	8987	70363	276	1.82 (1.49-2.22)	< 0.0001	1.78 (1.45-2.18)	< 0.0001
⩾ 60	635	4779	49	2677	16451	138	1.29 (0.94-1.79)	0.12	1.31 (0.94-1.81)	0.11
Men										
< 60 yr	1355	12401	94	5021	37147	173	1.68 (1.31-2.17)	< 0.0001	1.78 (1.37-2.30)	< 0.0001
⩾ 60 yr	358	2602	28	1741	10386	84	1.40 (0.91-2.14)	0.12	1.37 (0.89-2.11)	0.15
Women										
< 60 yr	926	8921	54	3966	33217	103	2.00 (1.44-2.78)	< 0.0001	1.75 (1.25-2.45)	0.001
⩾ 60 yr	277	2177	21	936	6065	54	1.14 (0.69-1.88)	0.6	1.20 (0.72-2.00)	0.49
Diabetes										
No	2167	20232	118	8615	67181	222	1.82 (1.46-2.28)	< 0.0001	1.82 (1.45-2.28)	< 0.0001
Yes	749	5868	79	3049	19634	192	1.43 (1.10-1.85)	0.0081	1.45 (1.12-1.89)	0.006
Hypertension										
No	2032	19535	91	8244	66765	183	1.73 (1.35-2.23)	< 0.0001	1.76 (1.37-2.27)	< 0.0001
Yes	884	6566	106	3420	20050	231	1.49 (1.18-1.87)	0.0008	1.61 (1.27-2.03)	< 0.0001
Coronary heart disease										
No	2600	23477	179	10512	79766	361	1.74 (1.45-2.08)	< 0.0001	1.78 (1.48-2.13)	< 0.0001
Yes	316	2624	18	1152	7049	53	0.99 (0.58-1.69)	0.98	0.97 (0.57-1.65)	0.9
Hyperlipidemia										
No	2221	20602	150	8513	68890	325	1.61 (1.33-1.95)	< 0.0001	1.65 (1.36-2.01)	< 0.0001
Yes	695	5499	47	2851	17925	89	1.75 (1.23-2.48)	0.002	1.72 (1.20-2.47)	0.003
Cirrhosis										
No	2777	25156	191	11192	84543	401	1.65 (1.39-1.96)	< 0.0001	1.67 (1.40-1.99)	< 0.0001
Yes	139	944	6	472	2272	13	1.39 (0.53-3.63)	0.51	1.21 (0.47-3.13)	0.69

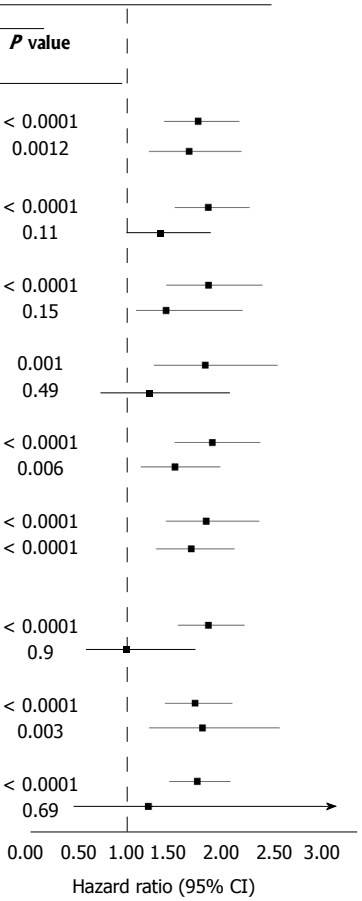

B

	Treated cohort			Untreated cohort			Hazard ratio (95% CI)			
	n	PY	ESRD events	*n*	PY	ESRD events	Crude	*P* value	Adjusted[1]	*P* value
Sex										
Men	319	2347	5	967	8139	74	0.21 (0.09-0.52)	0.0007	0.20 (0.08-0.49)	0.0005
Women	123	1013	0	359	3101	34	-	-	-	-
Age (yr)										
< 60	328	2650	4	935	8439	78	0.15 (0.05-0.40)	0.0002	0.12 (0.05-0.34)	< 0.0001
⩾ 60	114	709	1	391	2800	30	0.12 (0.02-0.87)	0.036	0.10 (0.01-0.80)	0.03
Men										
< 60 yr	246	1928	4	695	6206	55	0.21 (0.08-0.57)	0.002	0.17 (0.06-0.48)	0.0009
⩾ 60 yr	73	418	1	272	1933	19	0.22 (0.03-1.61)	0.13	0.21 (0.03-1.49)	0.12
Diabetes										
No	301	2317	3	902	8156	59	0.16 (0.05-0.51)	< 0.0001	0.15 (0.05-0.47)	0.001
Yes	141	1042	2	424	3084	49	0.11 (0.03-0.45)	0.002	0.10 (0.02-0.43)	0.002
Hypertension										
No	292	2380	2	869	8041	50	0.12 (0.03-0.50)	0.003	0.12 (0.03-0.50)	0.0036
Yes	150	979	3	457	3198	58	0.15 (0.05-0.49)	0.001	0.12 (0.03-0.40)	0.0006
Coronary heart disease										
No	383	2983	4	1128	9671	94	0.13 (0.05-0.34)	< 0.0001	0.11 (0.04-0.31)	< 0.0001
Yes	59	376	1	198	1568	14	0.25 (0.03-1.82)	0.17	0.34 (0.04-2.73)	0.31
Hyperlipidemia										
No	334	2602	4	992	8637	78	0.15 (0.06-0.42)	0.0002	0.14 (0.05-0.38)	0.0001
Yes	108	757	1	334	2602	30	0.10 (0.01-0.75)	0.025	0.10 (0.01-0.75)	0.024
Cirrhosis										
No	383	3031	4	1191	10343	102	0.12 (0.05-0.33)	< 0.0001	0.11 (0.04-0.29)	< 0.0001
Yes	59	329	1	135	896	6	0.39 (0.05-3.19)	0.38	0.79 (0.08-8.10)	0.84

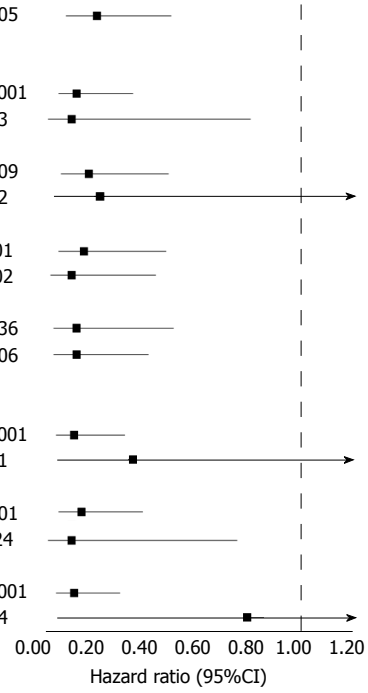

Figure 3 Stratified analyses after adjustment for competing mortality in the (A) propensity score-matched chronic kidney disease cohort and (B) propensity score-matched hepatitis B virus cohort. PY: person-year; ESRD: end-stage renal disease; HBV: Hepatitis B virus; CI: confidence interval. [1]Adjusted for all covariates (age per year, sex, comorbidities, geographic region, urbanization level, enrolee category, number of medical visits, Charlson comorbidity index score, and propensity score) and competing mortality, minus the covariate on which stratified.

Table 3 Hazard ratios for end-stage renal disease in the untreated hepatitis B virus-infected and hepatitis B virus-uninfected chronic kidney disease patients, with adjustment for competing mortality

Variable	Overall CKD patients (n = 103002)				Propensity score-matched CKD patients (n = 14580)			
	Crude		Adjusted[1]		Crude		Adjusted[1]	
	HR (95%CI)	*P* value	HR (95%CI)	*P* value	HR (95%CI)	*P* value	HR (95%CI)	*P* value
CKD patients								
Uninfected	1.00 (Reference)		1.00 (Reference)		1.00 (Reference)		1.00 (Reference)	
Untreated	1.39 (1.20-1.60)	< 0.0001	1.69 (1.47-1.96)	< 0.0001	1.64 (1.38-1.94)	< 0.0001	1.67 (1.40-1.98)	< 0.0001
Sex (Men/Women)	0.94 (0.88-0.99)	0.028	1.38 (1.25-1.51)	< 0.0001	1.24 (1.05-1.46)	0.011	1.65 (1.26-2.16)	0.0003
Age (per year)	1.01 (1.01-1.01)	< 0.0001	0.96 (0.96-0.97)	< 0.0001	1.03 (1.02-1.03)	< 0.0001	0.98 (0.96-0.98)	0.012
Comorbidity (Yes/No)								
Diabetes	2.49 (2.35-2.65)	< 0.0001	1.96 (1.83-2.10)	< 0.0001	2.55 (2.18-2.99)	< 0.0001	1.96 (1.63-2.35)	< 0.0001
Hypertension	2.85 (2.67-3.03)	< 0.0001	2.08 (1.88-2.29)	< 0.0001	3.59 (3.06-4.20)	< 0.0001	2.51 (1.95-3.22)	< 0.0001
Coronary heart disease	1.26 (1.17-1.35)	< 0.0001	0.86 (0.80-1.05)	0.37	1.25 (0.98-1.60)	0.08	0.93 (0.74-1.15)	0.49
Hyperlipidemia	1.16 (1.08-1.24)	< 0.0001	1.01 (0.93-1.08)	0.90	1.07 (0.89-1.30)	0.48	0.84 (0.68-1.03)	0.09
Cirrhosis	0.81 (0.62-1.05)	0.11	8.34 (5.72-12.17)	< 0.0001	0.73 (0.46-1.15)	0.17	4.36 (1.56-12.17)	0.005
Urbanization level								
Urban	1.00 (Reference)		1.00 (Reference)		1.00 (Reference)		1.00 (Reference)	
Suburban	1.01 (0.95-1.08)	0.69	0.93 (0.87-1.00)	0.06	1.10 (0.94-1.28)	0.26	0.99 (0.81-1.19)	0.87
Rural	1.03 (0.97-1.11)	0.35	0.84 (0.77-1.03)	0.07	0.99 (0.82-1.20)	0.94	0.80 (0.63-1.01)	0.06
Enrolee category								
1 + 2	1.00 (Reference)		1.00 (Reference)		1.00 (Reference)		1.00 (Reference)	
3	1.28 (1.21-1.36)	< 0.0001	1.34 (1.23-1.47)	< 0.0001	1.36 (1.16-1.60)	0.0001	1.44 (1.15-1.79)	0.001
4	1.26 (1.18-1.35)	< 0.0001	1.34 (1.21-1.49)	< 0.0001	1.52 (1.27-1.82)	< 0.0001	1.55 (1.21-1.98)	0.0006

[1]Adjusted for all covariates (age per year, sex, comorbidities, urbanization level, enrolee category, number of medical visits, Charlson comorbidity index score, and propensity score) and competing mortality. CKD: Chronic kidney disease.

Table 4 Hazard ratios for end-stage renal disease in the untreated hepatitis B virus-infected and hepatitis B virus-treated chronic kidney disease patients, with adjustment for competing mortality

Variable	Overall HBV patients (n = 3358)				Propensity score-matched HBV patients (n = 1768)			
	Crude		Adjusted[1]		Crude		Adjusted[1]	
	HR (95%CI)	*P* value	HR (95%CI)	*P* value	HR (95%CI)	*P* value	HR (95%CI)	*P* value
HBV cohort								
Untreated	1.00 (Reference)		1.00 (Reference)		1.00 (Reference)		1.00 (Reference)	
Treated	0.17 (0.07-0.41)	< 0.0001	0.15 (0.06-0.36)	< 0.0001	0.14 (0.06-0.34)	< 0.0001	0.13 (0.05-0.31)	< 0.0001
Sex (Men/Women)	1.12 (0.84-1.49)	0.43	0.91 (0.46-1.79)	0.78	0.87 (0.58-1.30)	0.49	0.63 (0.24-1.63)	0.34
Age (per year)	1.02 (1.01-1.02)	0.0002	1.00 (0.98-1.02)	0.86	1.01 (1.00-1.02)	0.20	0.99 (0.96-1.01)	0.34
Comorbidity (Yes/No)								
Diabetes	2.01 (1.52-2.67)	< 0.0001	1.92 (1.33-2.77)	0.0005	1.89 (1.31-2.74)	0.0007	1.77 (1.08-2.91)	0.024
Hypertension	3.09 (2.35-4.06)	< 0.0001	3.90 (2.66-5.72)	< 0.0001	2.59 (1.79-3.74)	< 0.0001	3.52 (2.09-5.95)	< 0.0001
Coronary heart disease	0.85 (0.53-1.36)	0.49	0.51 (0.31-0.84)	0.008	0.93 (0.54-1.60)	0.80	0.59 (0.32-1.09)	0.09
Hyperlipidemia	1.12 (0.81-1.54)	0.51	0.84 (0.58-1.20)	0.33	1.23 (0.81-1.86)	0.33	0.98 (0.61-1.56)	0.91
Cirrhosis	0.57 (0.27-1.22)	0.15	0.35 (0.05-2.61)	0.30	0.53 (0.25-1.14)	0.10	0.30 (0.03-3.32)	0.33
Urbanization level								
Urban	1.00 (Reference)		1.00 (Reference)		1.00 (Reference)		1.00 (Reference)	
Suburban	1.18 (0.90-1.56)	0.24	1.18 (0.85-1.65)	0.33	1.27 (0.88-1.84)	0.20	1.06 (0.68-1.64)	0.80
Rural	1.03 (0.75-1.43)	0.85	1.09 (0.73-1.64)	0.68	0.79 (0.50-1.23)	0.30	0.91 (0.52-1.59)	0.73
Enrolee category								
1 + 2	1.00 (Reference)		1.00 (Reference)		1.00 (Reference)		1.00 (Reference)	
3	0.96 (0.73-1.27)	0.78	1.05 (0.74-1.50)	0.78	0.79 (0.54-1.14)	0.21	0.99 (0.60-1.62)	0.97
4	1.57 (1.14-2.16)	0.006	1.60 (1.06-2.40)	0.024	1.78 (1.19-2.67)	0.005	1.89 (1.10-3.26)	0.022

[1]Adjusted for all covariates (age per year, sex, comorbidities, urbanization level, enrolee category, number of medical visits, Charlson comorbidity index score, and propensity score). HBV: Hepatitis B virus.

proportional hazards, we applied the modified Cox proportional hazard model with adjustment for all covariates and competing risks[24] to determine whether HBV infection and NA use in CKD patients were associated with increased and reduced risk of ESRD, respectively. We also performed stratified analyses to determine the impact of untreated and treated HBV infection on risk of ESRD among PS-matched CKD patients. All data were analyzed with SAS (version 9.3; SAS Institute, Inc., Cary, NC, United States) and a two-sided *P*-value less than 0.05 was considered statistically significant. The statistical methods used in this study were reviewed by co-authors Chung-Yi Li and Shiang-Jiun Tsai.

Table 5 Sensitivity analysis in the propensity-matched chronic kidney disease patients (*n* = 14580) *n* (%)

Model 1: CKD patients without diabetes at baseline (*n* =10782)		
	Uninfected cohort (*n* = 8615)	Untreated cohort (*n* = 2167)
No. of ESRD	222 (2.58)	118 (5.45)
Adjusted HR (95%CI)[1]	1.00 (reference)	1.82 (1.45-2.28)
Model 2: CKD patients without cirrhosis at baseline (*n* = 13969)		
	Uninfected cohort (*n* = 11192)	Untreated cohort (*n* = 2777)
No. of ESRD	401 (3.58)	191 (6.88)
Adjusted HR (95%CI)[1]	1.00 (reference)	1.67 (1.40-1.99)
Model 3: CKD patients without diabetes and cirrhosis at baseline (*n* = 10420)		
	Uninfected cohort (*n* = 8327)	Untreated cohort (*n* = 2093)
No. of ESRD	218 (2.62)	116 (5.54)
Adjusted HR (95%CI)[1]	1.00 (reference)	1.81 (1.44-2.27)

[1]Adjusted for all covariates (age per year, sex, comorbidities, urbanization level, enrolee category, number of medical visits, Charlson comorbidity index score, and propensity score) and competing mortality. ESRD: End-stage renal disease; CKD: Chronic kidney disease.

RESULTS

Patient characteristics

The baseline characteristics of the untreated HBV-infected and HBV-uninfected CKD patients as well as the treated and untreated HBV-infected CKD patients are summarized in Tables 1 and 2, respectively. After matching, there were no significant differences in baseline covariates between the untreated and uninfected cohorts, except for EC, as well as between the treated and untreated cohorts.

16-year cumulative incidence of ESRD

After PS matching, the 16-year cumulative ESRD incidence for the untreated and uninfected cohorts was 10.1% (95%CI: 7.5%-13.2%) and 6.6% (95%CI: 4.7%-9.0%), respectively ($P < 0.0001$) (Figure 2A). The 16-year cumulative ESRD incidence for the treated and matched untreated cohorts was 2.2% (95%CI: 0.7%-5.2%) and 11.9% (95%CI: 8.5%-15.9%), respectively ($P < 0.0001$) (Figure 2B). The NNT associated with one fewer ESRD after 4, 8, and 12 years were 28, 14, and 12, respectively (data not shown).

ESRD risk in untreated vs uninfected CKD patients

After PS matching, 197 (6.8%) untreated and 414 (3.6%) uninfected patients developed ESRD during the study period ($P < 0.0001$) (Table 1). Modified multivariable Cox regression indicated that ESRD was independently associated with untreated HBV infection (adjusted hazard ratio: 1.67; 95%CI: 1.40-1.98; $P < 0.0001$), male gender (1.65; 1.26-2.16; $P = 0.0003$), diabetes (1.96; 1.63-2.35; $P < 0.0001$), hypertension (2.51; 1.95-3.22; $P < 0.0001$), cirrhosis (4.36; 1.56-12.17; $P = 0.005$), EC3 (1.44; 1.15-1.79; $P = 0.001$), and EC4 (1.55; 1.21-1.98; $P = 0.0006$), and inversely associated with advanced age (0.98; 0.96-0.98; $P = 0.012$) (Table 3). The robustness of these data was tested by sensitivity analyses (Table 5). We excluded diabetic or cirrhotic patients or both from both cohorts at baseline, indicating a significantly positive association of untreated HBV with ESRD risk.

ESRD risk in treated vs untreated CKD patients

After PS matching, 5 (1.1%) treated and 108 (8.1%) untreated patients developed ESRD during the study period ($P < 0.0001$) (Table 2). The treated cohort had a significantly lower risk of ESRD than the untreated cohort (0.13; 0.05-0.31; $P < 0.0001$) (Table 4). As expected, diabetes (1.77; 1.08-2.91; $P = 0.024$), hypertension (3.52; 2.09-5.95; $P < 0.0001$), and EC4 (1.89; 1.10-3.26; $P = 0.022$) were associated with a significant risk of ESRD.

Stratified analysis

The untreated cohort exhibited an increased risk of ESRD on all stratified analyses (Figure 3A), except for those with coronary heart disease. This association was more pronounced in patients younger than 60 years (1.78; 1.45-2.18; $P < 0.0001$), men younger than 60 years (1.78; 1.37-2.30; $P < 0.0001$), women younger than 60 years (1.75; 1.25-2.45; $P = 0.001$), and patients without coronary heart disease (1.78; 1.48-2.13; $P < 0.0001$) and cirrhosis (1.67; 1.40-1.99; $P < 0.0001$). The treated cohort exhibited a reduced risk of ESRD on all stratified analyses (Figure 3B). This association was more pronounced in men younger than 60 years (0.17; 0.06-0.48; $P = 0.0009$) and patients without coronary heart disease (0.11; 0.04-0.31; $P < 0.0001$) and cirrhosis (0.11; 0.04-0.29; $P < 0.0001$).

DISCUSSION

After employing PS-matching and competing mortality, this 16-year nationwide cohort study provided three novel insights. First, the incidence of CKD patients acquiring HBV infection was 3.2%. Second, the risk of ESRD was 1.67-fold higher in the untreated cohort than the uninfected CKD cohort, was independent of cirrhosis or diabetes, and was reduced by 87% in the treated cohort compared to the untreated cohort. These associations were consistent in stratified subgroup analyses. Third, the NNT in association with one

patient free of ESRD at 12 years after NA use was 12. These findings implied that HBV infection may have a role in the pathogenesis of renal injury, and that HBV suppression may improve renal outcome among CKD patients. Given the increased risk of exposure to HBV in CKD patients, this information has important clinical implications for the design of surveillance programs that assess HBV status in CKD patients.

To the best of our knowledge, this is the first study to investigate the incidence and renal outcome in CKD patients acquiring chronic HBV infection. This has long been a neglected issue because there is no recommendation in the K/DOQI guidelines[25] on whether HBV serological evaluation should be carried out in CKD patients. The majority (≥ 60%) of CKD patients acquiring chronic HBV infection are known to become chronic carriers because of a deficiency in CD8+ cytotoxic and CD4+ helper T lymphocytes[1,11]; however, the incidence was unknown. Only two hospital-based studies and one community-based study reported that the prevalence of HBV infection was 10.5% in Turkish patients with CKD stages 4-5[26], 3.5% in Turkish patients with CKD stages 3-5[10], and 9.9% in Taiwanese patients with CKD stages 1-5[27]. Only two case-series studies and one population-based study from China reported the potential risk of ESRD in target CKD subpopulations such as patients with primary GN[28] or HBV-GN[8], and those with diabetic nephropathy[7]. However, these studies did not clarify the difference between HBV-untreated *vs* uninfected CKD patients or perform subgroup analyses. The present study indicated that untreated chronic HBV infection was an independent predictor of ESRD risk in CKD patients, suggesting its role in CKD progression. Given the fact that there are 50 million new cases of HBV diagnosed annually[29] and the burden of CKD continues to increase[1], it is conceivable that the burden of ESRD in CKD patients following chronic HBV infection is increasing.

This is also the first study to evaluate the renal effect of NA therapy and its NNT for one fewer ESRD in HBV-infected CKD patients. Previous studies demonstrated the benefit of NA therapy in reducing proteinuria[16,17,30,31], serum HBV-DNA[16,17,31], and risk of ESRD[17] in HBV-GN patients. However, these studies followed small numbers of patients for short periods, did not provide the NNT after NA therapy, and failed to guide NA therapy in HBV-infected CKD patients. In the present study, we did not have information on baseline HBV-DNA or alanine aminotransferase levels. However, based on the fact that reimbursement for NAs in Taiwan's NHI program requires twice-elevated alanine aminotransferase and higher HBV-DNA levels (> 2000 IU/mL)[20,32], it is reasonable to assume that the treated cohort had higher baseline HBV-DNA and alanine aminotransferase levels, or a higher prevalence of liver decompensation than the untreated cohort to be eligible for reimbursement. Our present data showed a higher prevalence of cirrhosis in the treated cohort compared to the untreated cohort. Since higher HBV-DNA levels are associated with a higher risk of renal injury, the higher baseline HBV-DNA levels in the treated cohort may have led to a more conservative estimation of the association of the renoprotective effect of NAs[20,32] and more favorable renal response to NAs[33]. This may explain why NA treatment for HBV-infected CKD patients in our study was associated with an 87% lower risk of ESRD compared to NA-naive HBV-infected CKD patients in a 16-year follow-up. Moreover, we used a large nationwide dataset, which afforded considerable statistical power and allowed long-term tracking of incident ESRD events.

The exact mechanism of how HBV infection and NA therapy are associated with increased and decreased ESRD risk, respectively, is unclear. Our data suggested that this association can be explained by NA-mediated HBV suppression and reduction in serum HBV-DNA levels. Previous studies[6,16,34] have addressed the association between serum HBV-DNA and renal injury. HBV-DNA was identified in renal tissue from 95.3% of HBV-GN patients[34], and the level of HBV-DNA correlated well with the duration of proteinuria. The degree of proteinuria and the extent of pathological injury, which was defined by the glomerular deposition of HBV antigens, also correlated well with the level of serum HBV-DNA in HBV-GN patients[16]. The same study also showed that patients with higher levels of serum HBV-DNA had lower level of serum complement, suggesting a correlation between serum HBV-DNA levels and the deposition of immune complexes, and the existence of a mechanism involving HBV-related immune complexes formed by passive trapping or *in situ* formation. Du *et al*[35] demonstrated that high levels of serum HBV-DNA correlated with the expression of inflammatory factors in renal biopsy specimens from HBV-GN patients. Deposition of immune complexes in the kidney is perceived to play a pivotal role in the pathogenesis of HBV-related nephropathy. Reducing the quantity of viral antigens and thereby reducing immune complexes in the kidney might ameliorate kidney damage. Other researchers postulated other mechanisms for HBV-related renal injury. Sera from adult patients with mild chronic HBV infection, regardless of the presence of HBV-DNA, induced apoptosis of cultured human renal tubular cells *via* up-regulation of Fas gene expression, and the induction of apoptosis correlated well with the level of serum HBV-DNA[6]. Furthermore, sera from patients with chronic HBV infection also had higher levels of transforming growth factor-beta, a growth factor implicated in the development of apoptosis and renal fibrosis. This may explain why the untreated cohort, a proxy for lower serum HBV-DNA levels in the present study, had a higher risk of ESRD compared to the uninfected cohort. Further research is warranted to better understand the mechanism.

In the present study, we used many methods to prevent potential confounders. PS matching was used

to select comparable controls to imitate a randomized clinical trial and competing risk analysis was used to prevent overestimation of nonfatal outcomes in the untreated cohort[36] and during CKD progression[21]. Another strength of our study was that it was designed to reduce selection bias (through the use of a large nationwide and highly representative sample with random sampling)[5,36,37]; reduce environmental effects (because of the availability of socioeconomic indicators for all subjects)[5,36,37]; avoid detection bias (because of the universal availability of medical services)[5,36,37]; and avoid immortal time bias (because the time when patients received NA was chosen as the entry of observation)[9,20]. In addition, the study population was well defined and follow-up was complete because our design relied on the universal coverage of Taiwan's NHI, which fully reimbursed NA therapy for HBV infection and thus minimized disparity in healthcare accessibility or financial status as a determinant for receiving NA therapy. Although unmeasured confounders may still exist, as with any observational study, we believe that the methodology used in the present study is solid and robust.

It is important to note the limitations of this study. First, coding errors are possible in a database. We could not check the accuracy of NA use in the NHIRD. However, the information regarding insurance-paid NAs was accurate because NA prescription was under strict NHI regulations. Second, some patients may have used self-paid NAs and may have therefore been misclassified into the untreated cohort. Some of our controls may have had sub-clinical HBV infection. These potential misclassifications may have led to an underestimation of the association. Third, information about adverse events of NAs was not available from the NHIRD. However, NAs are generally well-tolerated, relatively safe after dosage adjustment, and are the best options for HBV-positive CKD patients[13]. Fourth, the NHIRD lacks information on family history of kidney diseases, lifestyle, and laboratory data (*e.g.*, levels of serum HBV DNA and HBV genotype), which may contribute to ESRD risk. Thus, we could not adjust for these variables in the PS-matching. Nevertheless, it has been shown that HBV genotype is not related to extrahepatic manifestations[38] and does not influence treatment outcome of NAs[15]. Moreover, we added CCI scores into the PS analysis and included the CCI score and PS in the regression analysis to control confounding in healthcare administrative databases[5,36]. This method had been used in previous NHIRD-based research on patients with chronic HBV infection[5,32]. Finally, the PS matching cannot fit well in all treated, untreated, and uninfected groups. The cumulative ESRD incidence of the PS-matched three cohorts warrants further prospective research.

In conclusion, this large cohort study provides evidence that untreated HBV infection and NA therapy are associated with increased and decreased risk of ESRD, respectively, in CKD patients. Our data suggest that clinicians should consider HBV serological evaluation in CKD patients, especially in areas of high HBV endemicity, so that these patients can be closely monitored for development of ESRD. Further research is warranted to explore the pathological mechanism underlying this association.

ARTICLE HIGHLIGHTS

Research background

The evidence on whether HBV infection affects renal outcome in patients with chronic kidney disease (CKD) is limited. Here we retrospectively explored the association between HBV infection with and without nucleos(t)ide analogue use and the risk of end-stage renal disease (ESRD) in patients with CKD.

Research motivation

There is a significant and increasing burden of CKD, ESRD, and HBV infection in Taiwan and worldwide. CKD patients have an increased risk of acquiring chronic HBV infection. However, the effect of HBV infection and nucleos(t)ide analogue use on the risk of ESRD in CKD patients remains unclear. Taiwan provides an ideal setting for studying this relationship because it has a high prevalence of these three conditions.

Research objectives

To investigate the effect of HBV infection with and without nucleos(t)ide analogue use on the ESRD risk in Taiwanese CKD patients.

Research methods

By analyzing the Taiwan Longitudinal Health Insurance Database 2005, the authors used propensity score-matched and competing risk analyses to evaluate the effect of HBV infection with and without nucleos(t)ide analogue therapy on the development of ESRD in CKD patients. The authors used a modified Kaplan-Meier method and Gray's method to calculate and compare the cumulative incidence of ESRD, and a modified Cox proportional hazard model in the presence of competing risk and stratified analyses to determine the ESRD risk between propensity-matched untreated HBV-infected and HBV-uninfected CKD patients as well as propensity-matched untreated and treated HBV-infected CKD patients. The authors also calculated the number of patients needed to be treated to yield one fewer ESRD.

Research results

In the propensity-matched untreated HBV-infected and HBV-uninfected CKD patients, the risk of ESRD was significantly higher in the untreated cohort (16-year cumulative incidence, 10.1%) than in the uninfected cohort (16-year cumulative incidence, 6.6%) with a significant adjusted hazard ratio of 1.67. In the propensity-matched HBV-treated and HBV-untreated CKD patients, the treated cohort (16-year cumulative incidence, 2.2%) had a significantly 87% reduced ESRD risk compared with the untreated cohort (16-year cumulative incidence, 11.9%). The number needed to treat for one fewer ESRD after NA use at 12 years was 12. Multivariable stratified analyses verified these associations in all subgroups. However, the cumulative ESRD incidence of the propensity-matched three cohorts warrants further prospective research because the propensity score matching cannot fit well in all treated, untreated, and uninfected CKD patients.

Research conclusions

To the best of our knowledge, this is the first study to investigate the incidence and renal outcome in CKD patients acquiring chronic HBV infection and to evaluate the renal effect of nucleos(t)ide analogue therapy and the number needed to treat for one fewer ESRD in HBV-infected CKD patients. This has long been a neglected issue because there is no recommendation in the K/DOQI guidelines on whether HBV serological evaluation should be carried out in CKD patients. This large retrospective cohort study suggests that the incidence of CKD patients acquiring HBV infection is 3.2% and that untreated HBV infection and nucleos(t)ide analogue therapy are associated with increased and decreased risk of ESRD, respectively, in CKD patients. These

findings imply that HBV infection may have a role in the pathogenesis of renal injury, and that HBV suppression may improve renal outcome among CKD patients. Our findings will be helpful in the future CKD prevention care program that assesses HBV status in CKD patients.

Research perspectives

Future prospective study is warranted to confirm our findings and better understand the pathological mechanism underlying this association.

REFERENCES

1 **Chacko EC**, Surrun SK, Mubarack Sani TP, Pappachan JM. Chronic viral hepatitis and chronic kidney disease. *Postgrad Med J* 2010; **86**: 486-492 [PMID: 20709771 DOI: 10.1136/pgmj.2009.092775]

2 **Cooke GS**, Lemoine M, Thursz M, Gore C, Swan T, Kamarulzaman A, DuCros P, Ford N. Viral hepatitis and the Global Burden of Disease: a need to regroup. *J Viral Hepat* 2013; **20**: 600-601 [PMID: 23910643 DOI: 10.1111/jvh.12123]

3 **Mauss S**, Berger F, Filmann N, Hueppe D, Henke J, Hegener P, Athmann C, Schmutz G, Herrmann E. Effect of HBV polymerase inhibitors on renal function in patients with chronic hepatitis B. *J Hepatol* 2011; **55**: 1235-1240 [PMID: 21703180 DOI: 10.1016/j.jhep.2011.03.030]

4 **Chen YC**, Su YC, Li CY, Hung SK. 13-year nationwide cohort study of chronic kidney disease risk among treatment-naïve patients with chronic hepatitis B in Taiwan. *BMC Nephrol* 2015; **16**: 110 [PMID: 26199000 DOI: 10.1186/s12882-015-0106-5]

5 **Chen YC**, Su YC, Li CY, Wu CP, Lee MS. A nationwide cohort study suggests chronic hepatitis B virus infection increases the risk of end-stage renal disease among patients in Taiwan. *Kidney Int* 2015; **87**: 1030-1038 [PMID: 25426815 DOI: 10.1038/ki.2014.363]

6 **Deng CL**, Song XW, Liang HJ, Feng C, Sheng YJ, Wang MY. Chronic hepatitis B serum promotes apoptotic damage in human renal tubular cells. *World J Gastroenterol* 2006; **12**: 1752-1756 [PMID: 16586546 DOI: 10.3748/wjg.v12.i11.1752]

7 **Cheng AY**, Kong AP, Wong VW, So WY, Chan HL, Ho CS, Lam CW, Tam JS, Chow CC, Cockram CS, Chan JC, Tong PC. Chronic hepatitis B viral infection independently predicts renal outcome in type 2 diabetic patients. *Diabetologia* 2006; **49**: 1777-1784 [PMID: 16736132 DOI: 10.1007/s00125-006-0294-4]

8 **Lai KN**, Li PK, Lui SF, Au TC, Tam JS, Tong KL, Lai FM. Membranous nephropathy related to hepatitis B virus in adults. *N Engl J Med* 1991; **324**: 1457-1463 [PMID: 2023605 DOI: 10.1056/NEJM199105233242103]

9 **Peters MG**. Special populations with hepatitis B virus infection. *Hepatology* 2009; **49**: S146-S155 [PMID: 19399810 DOI: 10.1002/hep.22965]

10 **Pişkinpaşa S,** Akoğlu H, Özkayar N, Turgut D, Akyel F, Demir M, Çimen K, Turhan T, KOÇ E, ODABAŞ AR, AŞÇIOĞLU S, Dede F. Seroprevalance of the hepatitis B and C in patients with chronic kidney disease without history of renal replacement therapy. *Turk Neph Dial Transpl* 2013; **22**: 171-176 [DOI: 10.5262/tndt.2013.1002.07]

11 **Urbánek P**. Viral hepatitis infections in chronic kidney disease patients and renal transplant recipients. *Kidney Blood Press Res* 2012; **35**: 454-467 [PMID: 22677941 DOI: 10.1159/000338309]

12 **Taal MW**, Brenner BM. Predicting initiation and progression of chronic kidney disease: Developing renal risk scores. *Kidney Int* 2006; **70**: 1694-1705 [PMID: 16969387 DOI: 10.1038/sj.ki.5001794]

13 **Pipili CL**, Papatheodoridis GV, Cholongitas EC. Treatment of hepatitis B in patients with chronic kidney disease. *Kidney Int* 2013; **84**: 880-885 [PMID: 23783238 DOI: 10.1038/ki.2013.249]

14 **Inoue J**, Ueno Y, Shimosegawa T. Management of chronic hepatitis B patients: efficacy & limitation of nucleos(t)ide analogues. *Indian J Med Res* 2011; **133**: 11-13 [PMID: 21321415]

15 **Dienstag JL**. Hepatitis B virus infection. *N Engl J Med* 2008; **359**: 1486-1500 [PMID: 18832247 DOI: 10.1056/NEJMra0801644]

16 **Jiang W**, Liu T, Dong H, Xu Y, Liu LQ, Guan GJ, Liu XC. Relationship Between Serum DNA Replication, Clinicopathological Characteristics and Prognosis of Hepatitis B Virus-associated Glomerulonephritis with Severe Proteinuria by Lamivudine Plus Adefovir Dipivoxil Combination Therapy. *Biomed Environ Sci* 2015; **28**: 206-213 [PMID: 25800445 DOI: 10.3967/bes2015.027]

17 **Tang S**, Lai FM, Lui YH, Tang CS, Kung NN, Ho YW, Chan KW, Leung JC, Lai KN. Lamivudine in hepatitis B-associated membranous nephropathy. *Kidney Int* 2005; **68**: 1750-1758 [PMID: 16164651 DOI: 10.1111/j.1523-1755.2005.00591.x]

18 National Health Insurance Administration, Ministry of Health and Welfare, Taiwan. Available from: URL: http://www.nhi.gov.tw

19 **Kuo HW**, Tsai SS, Tiao MM, Yang CY. Epidemiological features of CKD in Taiwan. *Am J Kidney Dis* 2007; **49**: 46-55 [PMID: 17185145 DOI: 10.1053/j.ajkd.2006.10.007]

20 **Wu CY**, Chen YJ, Ho HJ, Hsu YC, Kuo KN, Wu MS, Lin JT. Association between nucleoside analogues and risk of hepatitis B virus–related hepatocellular carcinoma recurrence following liver resection. *JAMA* 2012; **308**: 1906-1914 [PMID: 23162861 DOI: 10.1001/2012.jama.11975]

21 **Grams ME**, Coresh J, Segev DL, Kucirka LM, Tighiouart H, Sarnak MJ. Vascular disease, ESRD, and death: interpreting competing risk analyses. *Clin J Am Soc Nephrol* 2012; **7**: 1606-1614 [PMID: 22859747 DOI: 10.2215/CJN.03460412]

22 Gray RJ. A class of K-sample tests for comparing the cumulative incidence of a competing risk. *Ann Stat* 1988; **16**: 1141-1154 [DOI: 10.1214/aos/1176350951]

23 **Altman DG**. Confidence intervals for the number needed to treat. *BMJ* 1998; **317**: 1309-1312 [PMID: 9804726 DOI: 10.1136/bmj.317.7168.1309]

24 **Fine JP,** Gray RJ. A proportional hazards model for the subdistribution of a competing risk. *J Am Stat Assoc* 1999; **94**: 496-509 [DOI: 10.1080/01621459.1999.10474144]

25 **National Kidney Foundation**. K/DOQI clinical practice guidelines for chronic kidney disease: evaluation, classification, and stratification. *Am J Kidney Dis* 2002; **39**: S221-S266 [PMID: 11904577]

26 **Sit D**, Kadiroglu AK, Kayabasi H, Yilmaz ME, Goral V. Seroprevalence of hepatitis B and C viruses in patients with chronic kidney disease in the predialysis stage at a university hospital in Turkey. *Intervirology* 2007; **50**: 133-137 [PMID: 17191015 DOI: 10.1159/000098239]

27 **Lee JJ**, Lin MY, Yang YH, Lu SN, Chen HC, Hwang SJ. Association of hepatitis C and B virus infection with CKD in an endemic area in Taiwan: a cross-sectional study. *Am J Kidney Dis* 2010; **56**: 23-31 [PMID: 20400217 DOI: 10.1053/j.ajkd.2010.01.015]

28 **Lai KN**, Lai FM, Chan KW, Chow CB, Tong KL, Vallance-Owen J. The clinico-pathologic features of hepatitis B virus-associated glomerulonephritis. *Q J Med* 1987; **63**: 323-333 [PMID: 3685245]

29 **Patton H**, Tran TT. Management of hepatitis B during pregnancy. *Nat Rev Gastroenterol Hepatol* 2014; **11**: 402-409 [PMID: 24686270 DOI: 10.1038/nrgastro.2014.30]

30 **Zhang Y**, Zhou JH, Yin XL, Wang FY. Treatment of hepatitis B virus-associated glomerulonephritis: a meta-analysis. *World J Gastroenterol* 2010; **16**: 770-777 [PMID: 20135728 DOI: 10.3748/wjg.v16.i6.770]

31 **Yi Z**, Jie YW, Nan Z. The efficacy of anti-viral therapy on hepatitis B virus-associated glomerulonephritis: A systematic review and meta-analysis. *Ann Hepatol* 2011; **10**: 165-173 [PMID: 21502678]

32 **Wu CY**, Lin JT, Ho HJ, Su CW, Lee TY, Wang SY, Wu C, Wu JC. Association of nucleos(t)ide analogue therapy with reduced risk of hepatocellular carcinoma in patients with chronic hepatitis B: a nationwide cohort study. *Gastroenterology* 2014; **147**: 143-151.e5 [PMID: 24704525 DOI: 10.1053/j.gastro.2014.03.048]

33 **Chan TM**. Hepatitis B and Renal Disease. *Curr Hepat Rep* 2010; **9**: 99-105 [PMID: 20461128 DOI: 10.1007/s11901-010-0042-6]

34 **He XY**, Fang LJ, Zhang YE, Sheng FY, Zhang XR, Guo MY. In situ hybridization of hepatitis B DNA in hepatitis B-associated

glomerulonephritis. *Pediatr Nephrol* 1998; **12**: 117-120 [PMID: 9543368 DOI: 10.1007/s004670050417]

35 **Du W**, Zhen J, Zheng Z, Ma S, Chen S. Expression of AIM2 is high and correlated with inflammation in hepatitis B virus associated glomerulonephritis. *J Inflamm* (Lond) 2013; **10**: 37 [PMID: 24325587 DOI: 10.1186/1476-9255-10-37]

36 **Chen YC**, Hwang SJ, Li CY, Wu CP, Lin LC. A Taiwanese Nationwide Cohort Study Shows Interferon-Based Therapy for Chronic Hepatitis C Reduces the Risk of Chronic Kidney Disease. *Medicine* (Baltimore) 2015; **94**: e1334 [PMID: 26266379 DOI: 10.1097/MD.0000000000001334]

37 **Chen YC**, Lin HY, Li CY, Lee MS, Su YC. A nationwide cohort study suggests that hepatitis C virus infection is associated with increased risk of chronic kidney disease. *Kidney Int* 2014; **85**: 1200-1207 [PMID: 24257691 DOI: 10.1038/ki.2013.455]

38 **Cacoub P**, Saadoun D, Bourlière M, Khiri H, Martineau A, Benhamou Y, Varastet M, Pol S, Thibault V, Rotily M, Halfon P. Hepatitis B virus genotypes and extrahepatic manifestations. *J Hepatol* 2005; **43**: 764-770 [PMID: 16087273 DOI: 10.1016/j.jhep.2005.05.029]

P- Reviewer: Kao JT, Kute VB, Nemcsik J, Robles NR
S- Editor: Gong ZM **L- Editor**: Wang TQ **E- Editor**: Ma YJ

World Journal of Gastroenterology

Submit a Manuscript: http://www.f6publishing.com

World J Gastroenterol 2018 February 28; 24(8): 929-940

DOI: 10.3748/wjg.v24.i8.929

ISSN 1007-9327 (print) ISSN 2219-2840 (online)

ORIGINAL ARTICLE

Retrospective Study

Intravoxel incoherent motion diffusion-weighted magnetic resonance imaging for predicting histological grade of hepatocellular carcinoma: Comparison with conventional diffusion-weighted imaging

Shao-Cheng Zhu, Yue-Hua Liu, Yi Wei, Lin-Lin Li, She-Wei Dou, Ting-Yi Sun, Da-Peng Shi

Shao-Cheng Zhu, Yue-Hua Liu, Lin-Lin Li, She-Wei Dou, Da-Peng Shi, Department of Radiology, Henan Provincial People's Hospital, Zhengzhou 450003, Henan Province, China

Yue-Hua Liu, Medical College of Henan University, Kaifeng 475000, Henan Province, China

Yi Wei, Department of Radiology, West China Hospital, Sichuan University, Chengdu 610000, Sichuan Province, China

Ting-Yi Sun, Department of Pathology, Henan Provincial People's Hospital, Zhengzhou 450003, Henan Province, China

ORCID number: Shao-Cheng Zhu (0000-0003-4553-1940); Yue-Hua Liu (0000-0002-8971-5947); Yi Wei (0000-0003-3993-9747); Lin-Lin Li (0000-0003-2245-2983); She-Wei Dou (0000-0002-8434-7751); Ting-Yi Sun (0000-0003-4616-744X); Da-Peng Shi (0000-0002-2561-7475).

Author contributions: All the authors were involved in performing the research; Zhu SC, Liu YH, Wei Y, Li LL and Shi DP participated in the study design; Zhu SC, Liu YH, Wei Y, Li LL and Dou SW conducted the experiments; Zhu SC and Liu YH participated in the MR image analyses; Sun TY analyzed the histopathological images; Zhu SC, Liu YH and Wei Y analyzed the data; Zhu SC and Liu YH prepared the first draft of the manuscript; Zhu SC, Liu YH and Wei Y revised the manuscript. Shao-Cheng Zhu and Yue-Hua Liu contributed equally to this article.

Institutional review board statement: This study was reviewed and approved by the Ethics Committee of the Henan Provincial People's Hospital.

Informed consent statement: The patients were not required to give informed consent for the study because the analysis used anonymous clinical data that were obtained after each patient agreed to the MRI examination by written consent.

Conflict-of-interest statement: All the authors declare no conflicts of interest related to this article.

Manuscript source: Unsolicited manuscript

Correspondence to: Shao-Cheng Zhu, MD, PhD, Chief Doctor, Professor, Department of Radiology, Henan Provincial People's Hospital, No. 7, Weiwu Road, Zhengzhou 450003, Henan Province, China. 104753150948@vip.henu.edu.cn
Telephone: +86-371-65580790

Received: December 21, 2017
Peer-review started: December 21, 2017
First decision: January 3, 2018
Revised: January 11, 2018
Accepted: January 18, 2018
Article in press: January 18, 2018
Published online: February 28, 2018

Abstract

AIM

To compare intravoxel incoherent motion (IVIM)-derived parameters with conventional diffusion-weighted imaging (DWI) parameters in predicting the histological grade of hepatocellular carcinoma (HCC) and to evaluate the correlation between the parameters and the histological grades.

METHODS

A retrospective study was performed. Sixty-two patients with surgically confirmed HCCs underwent diffusion-weighted magnetic resonance imaging with twelve *b* values (10-1200 s/mm^2). The apparent diffusion coefficient (ADC), pure diffusion coefficient (D), pseudo-diffusion coefficient (D*), and perfusion fraction (*f*) were calculated by two radiologists. The IVIM and conventional DWI parameters were compared among the different grades by using analysis of variance (ANOVA) and the Kruskal-Wallis test. Receiver operating characteristic (ROC) analysis was performed to evaluate the diagnostic efficiency of distinguishing between low-grade (grade 1, G1) and high-grade (grades 2 and 3, G2 and G3) HCC. The correlation between the parameters and the histological grades was assessed by using the Spearman correlation test. Bland-Altman analysis was used to evaluate the reproducibility of the two radiologists' measurements.

RESULTS

The differences in the ADC and D values among the groups with G1, G2, and G3 histological grades of HCCs were statistically significant ($P < 0.001$). The D* and *f* values had no significant differences among the different histological grades of HCC ($P > 0.05$). The ROC analyses demonstrated that the D and ADC values had better diagnostic performance in differentiating the low-grade HCC from the high-grade HCC, with areas under the curve (AUCs) of 0.909 and 0.843, respectively, measured by radiologist 1 and of 0.911 and 0.852, respectively, measured by radiologist 2. The following significant correlations were obtained between the ADC, D, and D* values and the histological grades: $r = -0.619$ ($P < 0.001$), $r = -0.628$ ($P < 0.001$), and $r = -0.299$ ($P = 0.018$), respectively, as measured by radiologist 1; $r = -0.622$ ($P < 0.001$), $r = -0.633$ ($P < 0.001$), and $r = -0.303$ ($P = 0.017$), respectively, as measured by radiologist 2. The intra-class correlation coefficient (ICC) values between the two observers were 0.996 for ADC, 0.997 for D, 0.996 for D*, and 0.992 for *f* values, which indicated excellent inter-observer agreement in the measurements between the two observers.

CONCLUSION

The IVIM-derived D and ADC values show better diagnostic performance in differentiating high-grade HCC from low-grade HCC, and there is a moderate to good correlation between the ADC and D values and the histological grades.

Key words: Intravoxel incoherent motion; Diffusion-weighted imaging; Hepatocellular carcinoma; Pathological differentiation grade

Core tip: Intravoxel incoherent motion (IVIM)-based diffusion-weighted imaging (DWI) can yield diffusion and perfusion information simultaneously. The aims of this study were to compare IVIM-derived parameters with conventional DWI parameters for predicting the histological grade of hepatocellular carcinoma (HCC) and to evaluate the correlation between the parameters and the histological grades. Sixty-two patients with surgically confirmed HCC underwent diffusion-weighted magnetic resonance imaging with twelve *b* values. The differences in the ADC and D values among the groups with G1, G2, and G3 histological grades of HCC were statistically significant ($P < 0.001$). The D* and *f* values had no significant differences among the different histological grades of HCC ($P > 0.05$). A significant correlation was obtained between the ADC, D, and D* values and the histological grades ($P < 0.05$). The ROC analyses demonstrated that the D and ADC values had better diagnostic performance in differentiating low-grade HCC from high-grade HCC. These results suggested that the IVIM-DWI parameters might be useful in assessing the differentiation grades of HCC, which might be helpful in predicting the patient prognosis.

Zhu SC, Liu YH, Wei Y, Li LL, Dou SW, Sun TY, Shi DP. Intravoxel incoherent motion diffusion-weighted magnetic resonance imaging for predicting histological grade of hepatocellular carcinoma: Comparison with conventional diffusion-weighted imaging. *World J Gastroenterol* 2018; 24(8): 929-940 Available from: URL: http://www.wjgnet.com/1007-9327/full/v24/i8/929.htm DOI: http://dx.doi.org/10.3748/wjg.v24.i8.929

INTRODUCTION

Hepatocellular carcinoma (HCC) is the most common primary malignant tumor of the liver, accounting for 85% or more of cases[1]. It is the fifth most important cancer worldwide because of its very poor prognosis, with survival rates of 3% to 5% in the United States and developing countries. Therefore, it is the third leading cause of cancer-related death[2-4]. The pathological grade of a hepatocellular carcinoma is heavily associated with the prognosis, and it is one of the independent predictive factors for recurrence and long-term survival after hepatic curative resection in patients with HCC[5,6]. However, it is difficult to define accurate preoperative grade of HCC using routine imaging modalities. The ultrasound (US)-guided biopsy has been used to diagnose HCC, but this approach is limited due to location and complication risk, such as bleeding or needle-tract seeding, which suggests that it should not be performed in routine clinical practice[7]. Computed tomography (CT) is usually used to identify locations and to assess distant metastasis of HCC, and the performance characteristics of CT also allow it to be used for HCC diagnosis or staging. In terms of triphasic dynamic enhanced CT scans and dynamic

contrast-enhanced magnetic resonance imaging (DCE-MRI), the typical imaging feature of an HCC is that the lesion shows arterial hypervascularity and washes out in the early or delayed venous phase, which can be demonstrated for diagnosis[8]. However, both of these imaging techniques failed to provide a prediction of the pathological grade of an HCC.

Diffusion-weighted imaging (DWI) is a noninvasive approach to sensitively evaluate the small-scale motion of water molecules at the microscopic level that allows the diffusion of water to be quantitatively described by the apparent diffusion coefficient (ADC), which represents a mean value of diffusion contributed by the movement of intracellular, extracellular, and vascular water molecules within an image voxel at different *b* values[9,10]. In addition, these motions include the molecular diffusion of water and microcirculation of the blood in the capillary networks (perfusion). Several studies have shown that DWI, along with ADC measurements, is helpful for the detection, characterization, and staging of malignant lesions[11]. However, the ADC value that is derived from DWI is calculated using the mono-exponential model; therefore, it is often higher than expected, which is attributable to the microcirculation of the blood in capillaries[12]. The ADC value ignores the effect of the perfusion fraction in tissue and could be influenced by microcirculation of the blood in capillaries and cannot reflect the true diffusion of water[13]. Thus, it is limited in that the ADC fails to evaluate the water molecular diffusion in tissues precisely. In 1986, some researchers noted the principles of intravoxel incoherent motion (IVIM) and proposed that the relationship between signal attenuation in tissues with increasing *b* values would estimate the quantitative parameters that separately reflect tissue diffusivity and tissue microcapillary perfusion with the IVIM imaging method[14,15]. The IVIM approach uses a bi-exponential function to describe the DWI data and assumes that the measured signal attenuation of the DWI scans consists of a mixture of tissue perfusion and tissue diffusivity effects. Using the IVIM-based analysis, it is possible to obtain additional quantitative parameters that describe water diffusivity, perfusion (pseudodiffusion coefficient), and the perfusion fraction of tissues, which can also be displayed as parametric maps[12].

Recently, IVIM-DWI has been used to investigate the correlation between the parameters involved in the histological grade of HCC[16-18]. However, knowledge of the measurement reproducibility is critical to the level of confidence that can be ascribed to changes in the parameters for disease characterization or response assessment; this technique can also be developed as a potential imaging biomarker[19]. Therefore, it is important to assess the measurement reproducibility of parameters by different observers. The purpose of our study was to compare IVIM-derived parameters with conventional DWI-derived ADC values for determining the histologic grades of HCC and evaluate the correlation between the parameters and the histological grades.

MATERIALS AND METHODS

Patients

The institutional review board of the Henan Provincial People's Hospital approved this study, and written informed consent was obtained from all the patients. This study was conducted in accordance with the Declaration of Helsinki. Between March 2016 and May 2017, 102 consecutive patients suspected of having HCC underwent liver MR imaging. Among these patients, 40 were excluded for the following reasons: (1) the absence of surgery and/or histopathological examination (n = 14); (2) a history of preoperative treatment (radiofrequency ablation or transarterial chemoembolization) before MR imaging (n = 11); (3) liver lesions that were determined not to be HCC by pathological tests (n = 7); (4) low image quality (n = 3); and (5) tumors that were smaller than 1 cm (n = 5). Finally, a total of 62 patients diagnosed with HCC were included for analysis. The patients comprised 50 men and 12 women (mean age, 54.31 ± 9.36 years; range, 30-76 years). Forty-nine patients tested positive for the hepatitis B surface antigen and six for the hepatitis C virus antibody. The remaining seven patients tested negative for both antigens. According to Child-Pugh class, 54 patients had Child-Pugh A5, 6 had Child-Pugh A6, 2 had Child-Pugh B, and nobody had Child-Pugh C. All the tumors were histologically classified according to the major Edmondson-Steiner grade on the final pathologic reports as follows: grade 1 (n = 14), grade 2 (n = 24), grade 3 (n = 24), and grade 4 (n = 0).

MR imaging technique

All the patients were instructed to fast for 6-8 h prior to the MR examination. The studies were carried out by using a 3.0 T MR system (Discovery MR750, GE Healthcare, MI, United States) with an eight-channel phased-array torsion coil (GE Medical System). The routine MR imaging was performed using a fast spin echo (FSE) sequence with respiratory gating. The axial T1 images were obtained using the following parameters: repetition time/echo time (TR/TE), 180/2.1 ms; slice thickness, 7.0 mm with a gap of 1.0 mm; field of view, 38 cm × 34.2 cm; matrix size, 320 × 192; number of excitations (NEX), 1.00. The fat-saturation axial T2 images were obtained using the following parameters: TR/TE, 4000/75.8 ms; slice thickness, 7.0 mm with a gap of 1.0 mm; field of view, 38 cm × 38 cm; matrix size, 320 × 320; NEX, 2.00. The coronal T2 images were obtained using the following parameters: TR/TE, 2625/78.4 ms; slice thickness, 6.0 mm with a gap of 1.0 mm; field of view, 42 cm × 37.8 cm; matrix size, 352 × 288; NEX, 0.55. The total scanning time for each of the routine sequences was approximately 8 min. The IVIM was performed by using fat-suppressed, echo-planner imaging in the axial plane

with respiratory gating. The parallel imaging was used, and the parameters were as follows: TR/TE, 4286/61.2; slice thickness, 7.0 mm with a gap of 1.0 mm; field of view, 38 cm × 28.5 cm; matrix size, 128 × 128. Twelve *b* values ranging from 0 to 1200 s/mm^2 (10, 20, 40, 80, 100, 150, 200, 400, 600, 800, 1000, and 1200) were used, and the NEX for each *b* was 6, 4, 2, 2, 2, 1, 1, 2, 4, 6, 6, and 8. The total scanning time for the IVIM was approximately 10 min.

Image analysis

The data were quantitatively analyzed by using mono-exponential and bi-exponential models. The mono-exponential model that was used to estimate the ADC value was calculated from 12 *b* values and was described by the following equation: S(b)/S(0) = exp(-b × ADC) Where S(b) represents the signal intensity of diffusion sensitization at a given *b* value and S(0) represents the signal intensity of diffusion sensitization for *b* = 0 s/mm^2. IVIM-derived parameters with all *b*-value data on a pixel-by-pixel basis were calculated according to the following equation[15]: S(b)/S(0) = f exp(-b × D*) + (1-f)exp(-b × D) The bi-exponential IVIM model obtained pure diffusion coefficient (D), pseudo-diffusion coefficient (D*), and perfusion fraction (*f*) values. D was the diffusion coefficient that was representative of the pure molecular diffusivity, and D* was the perfusion parameter that was representative of the incoherent microcirculation (pseudodiffusion). The *f* value was the perfusion fraction that was linked to the microcirculation (pseudodiffusion).

All the images were obtained and transferred to a workstation (Advantage workstation 4.6; GE Medical System) and the data analysis was performed by two independent radiologists (Zhu S and Liu Y with 18 and 5 years of experience in reading MR images, respectively) who were blinded to the histopathological results. For each patient, as many of the MR images were selected for the measurement as possible from three consecutive slices of the DWI images, which covered the largest tumor portion, and the regions of interest (ROIs) were placed on the hepatic solid tumor components; the freehand ROI was placed to cover as much of the solid part of the tumor as possible. Exclusion of the areas of hemorrhage and necrosis was achieved by referring to the fat-saturation axial T2 images. The shape, size, and position of the ROIs were the same for each parameter map. The area of the ROIs ranged from 108 to 5202 mm^2 (the mean ROI area was 714 mm^2). The parametric values of the ROIs from the three imaging sections were averaged.

Pathologic examination

All the surgically resected specimens were subjected to hematoxylin and eosin staining of the tissue slices for the pathological evaluation. A pathologist (Sun T, with 21 years of experience reading histopathological slices) identified the pathological differentiation grades of each carcinoma, as well as the size and location of each, without knowing the MR findings. The pathological differentiation grade of each carcinoma was assessed according to the Edmondson and Steiner grading system[20].

Statistical analysis

The differences in the ADC and D among the different grades were analyzed using analysis of variance (ANOVA) and an LSD *t*-test, and the data are expressed as mean ± SD. The Kruskal-Wallis non-parametric test and paired comparisons were used to compare the D* and *f* values among the different grades. The quantitative data are presented as the median (interquartile range). The Spearman rank analysis was used to compare the correlation between the parameters and the histological grades. The correlation coefficient, rho (*r*), was obtained to compare the degree of the correlations as follows: little or no relationship if $r \geqslant 0$ but < 0.25; fair if $r \geqslant 0.25$ but < 0.5; moderate to good if $r \geq 0.5$ but < 0.75; and very good to excellent if $r \geqslant 0.75$. In addition, receiver operating characteristic (ROC) curve analyses were performed to evaluate the diagnostic performance of the parameters in distinguishing the low-grade (G1) and high-grade (G2 and G3) HCC. The areas under the ROC curves were obtained to compare the diagnostic capacities in terms of sensitivity, specificity, and accuracy, which were calculated with the optimal cutoff values being determined by the point of the largest Youden index for each parameter. The reproducibility of the ADCs and the IVIM-derived parameters of HCC was assessed by determination of the intra-class correlation coefficient (ICC), which reflected the differences in reliability between the two independent radiologists. ICC values less than 0.5 were indicative of poor reliability, values between 0.5 and 0.75 indicated moderate reliability, values between 0.75 and 0.9 indicated good reliability, and values greater than 0.90 indicated excellent reliability[21]. Bland-Altman analysis was used to evaluate the agreement between the inter-observer measurements. All statistical analyses were performed using SPSS19.0 software package (SPSS Inc, Chicago, IL, United States). A *P*-value less than 0.05 was considered to indicate statistical significance.

RESULTS

Comparison of the IVIM-DWI and conventional DWI parameters

Table 1 reports the ADC and IVIM parameters for the different histological grades of HCC. The ADC value, determined by both radiologists, of the G1 group was significantly higher than those of the G2 group and the G3 group ($P < 0.01$). For the IVIM parameters, the D value of the G3 group was significantly lower than those of the G2 group and the G1 group ($P < 0.01$). However, neither D* value nor the *f* value showed any statistical significance in distinguishing the three

Table 1 Intravoxel incoherent motion diffusion-weighted imaging parameters of different pathologic grades of hepatocellular carcinoma

Parameter	Observer	Edmondson-Steiner grade			*P* value
		1 (*n* = 14)	2 (*n* = 24)	3 (*n* = 24)	
ADC ($\times 10^{-3}$ mm^2/s)[1]	R1	1.496 ± 0.312	1.210 ± 0.186	1.003 ± 0.247	< 0.001
	R2	1.503 ± 0.306	1.214 ± 0.186	1.001 ± 0.236	< 0.001
D ($\times 10^{-3}$ mm^2/s)[1]	R1	1.186 ± 0.214	0.910 ± 0.151	0.775 ± 0.188	< 0.001
	R2	1.193 ± 0.226	0.910 ± 0.148	0.771 ± 0.187	< 0.001
D* ($\times 10^{-3}$ mm^2/s)[2]	R1	37.400 (43.900)	29.000 (71.700)	7.980 (63.590)	0.057
	R2	32.200 (44.600)	28.400 (74.363)	7.885 (61.640)	0.054
f (%)[2]	R1	27.250 (14.925)	20.675 (11.225)	31.300 (12.267)	0.149
	R2	26.550 (20.200)	21.200 (11.725)	31.550 (11.325)	0.214

[1]Data are mean ± SD, one-way analysis of variance; [2]data are median (interquartile range), Kruskal-Wallis Test. A *P*-value < 0.05 was considered statistically significant. R1: Radiologist 1; R2: Radiologist 2; ADC: Apparent diffusion coefficient; D: Pure diffusion coefficient; D*: Pseudo-diffusion coefficient; *f*: Perfusion fraction.

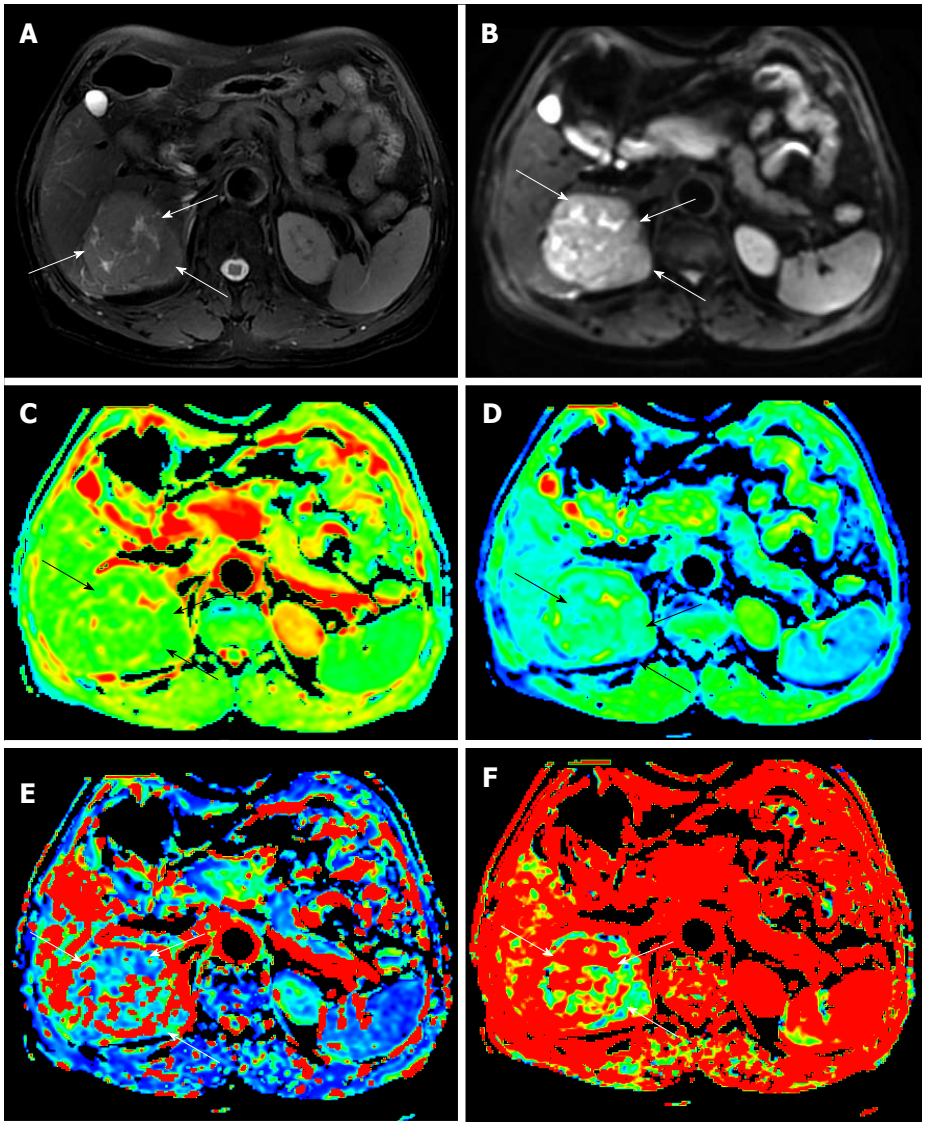

Figure 1 Magnetic resonance images of a 65-year-old man with an 8-cm surgically verified hepatocellular carcinoma with an Edmondson-Steiner grade 1. A: T2-weighted image; B: Diffusion-weighted image with a *b* value of 10 s/mm^2; C-F: Parametric maps (ADC, D, D*, and *f*, respectively) calculated from the IVIM diffusion-weighted imaging data. The tumor (white arrow) demonstrates a slightly high signal intensity on the T2-weighted image and a high signal intensity on the DWI image. The values of ADC, D, D*, and f for the ROIs of the HCC were 1.550 × 10^{-3} mm^2/s, 1.110 × 10^{-3} mm^2/s, 6.55 × 10^{-3} mm^2/s, and 0.387, respectively, which indicated an Edmondson-Steiner grade 1 HCC. HCC: Hepatocellular carcinoma; IVIM: Intravoxel incoherent motion; DWI: Diffusion-weighted imaging.

Table 2 Diagnostic value of intravoxel incoherent motion diffusion-weighted imaging and conventional diffusion-weighted imaging parameters in differentiating the low-grade group (G1) from the high-grade groups (G2 and G3)

Parameter	Observer	AUC (95%CI)	Optimal cutoff value	Youden index	Sensitivity (%)	Specificity (%)	Accuracy (%)
ADC	R1	0.843 (0.718, 0.968)	1.285	0.619	78.6(11/14)	83.3(40/48)	82.3(51/62)
	R2	0.852 (0.730, 0.974)	1.275	0.649	85.7(12/14)	79.2(38/48)	80.6(50/62)
D	R1	0.909 (0.834, 0.985)	0.962	0.741	92.9(13/14)	81.3(39/48)	83.9(52/62)
	R2	0.911 (0.832, 0.990)	0.977	0.804	92.9(13/14)	87.5(42/48)	88.7(55/62)
D*	R1	0.632 (0.489, 0.776)	17.75	0.378	85.7(12/14)	52.1(25/48)	59.7(37/62)
	R2	0.636 (0.495, 0.777)	17.90	0.378	85.7(12/14)	52.1(25/48)	59.7(37/62)
f	R1	0.523 (0.348, 0.698)	0.216	0.182	78.6(11/14)	39.6(19/48)	48.4(30/62)
	R2	0.518 (0.332, 0.704)	0.246	0.173	71.4(10/14)	45.8(22/48)	51.6(32/62)

R1: Radiologist 1; R2: Radiologist 2; ADC: Apparent diffusion coefficient; D: Pure diffusion coefficient; D*: Pseudo-diffusion coefficient; *f*: Perfusion fraction. ADC, D, and D* are in units of × 10^{-3} mm^2/s; f is in units of 100%; 95%CI: 95% confidence intervals.

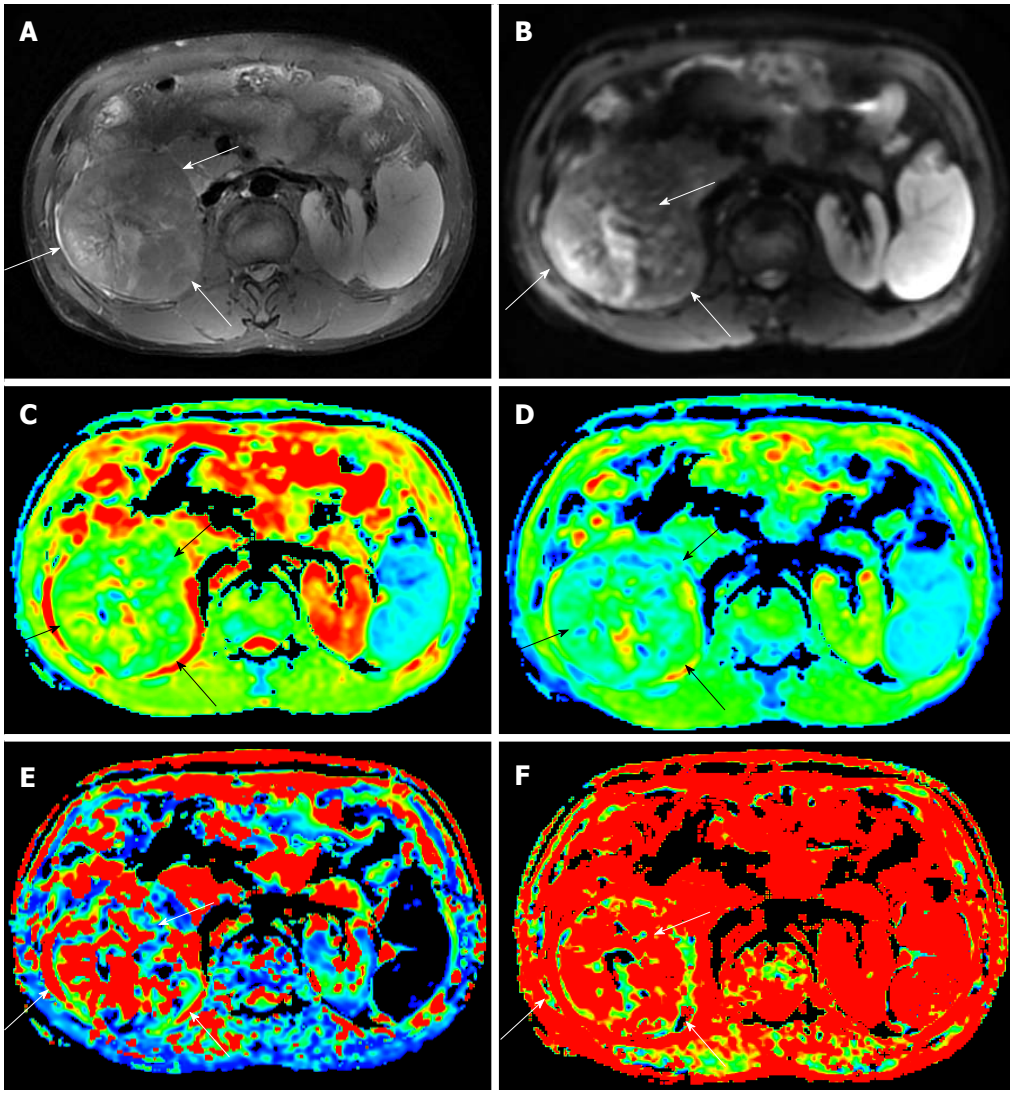

Figure 2 Magnetic resonance images of a 47-year-old man with a 10-cm surgically verified hepatocellular carcinoma of with an Edmondson-Steiner grade 2. A: T2-weighted image; B: Diffusion-weighted image with a *b* value of 10 s/mm^2; C-F: Parametric maps (ADC, D, D*, and *f*, respectively) calculated from the IVIM diffusion-weighted imaging data. The tumor (white arrow) demonstrates a slightly high signal intensity on the T2-weighted image and a high signal intensity on the DWI image. The values of the ADC, D, D*, and f for the ROIs of the HCC were 1.310 × 10^{-3} mm^2/s, 0.885 × 10^{-3} mm^2/s, 27.8 × 10^{-3} mm^2/s, and 0.450, respectively, which indicated an Edmondson-Steiner grade 2 HCC. HCC: Hepatocellular carcinoma; IVIM: Intravoxel incoherent motion; DWI: Diffusion-weighted imaging.

groups (P > 0.05). Figures 1-3 show representative grades 1-3 HCC, respectively. Figure 4 reports the quantitative comparison of the differences in the IVIM and DWI parameters among the three groups.

Table 3 Apparent diffusion coefficient and intravoxel incoherent motion derived parameters: Spearman correlation coefficients of the parameters with the histopathological grades

Spearman correlation			ADC	D	D*	*f*
R1	Grade	Correlation coefficient	-0.619	-0.628	-0.299	0.130
		P-value	< 0.001	< 0.001	0.018	0.313
R2	Grade	Correlation coefficient	-0.622	-0.633	-0.303	0.121
		P-value	< 0.001	< 0.001	0.017	0.349

P-value < 0.05 was considered statistically significant. ADC: Apparent diffusion coefficient; D: Pure diffusion coefficient; D*: Pseudo-diffusion coefficient; *f*: Perfusion fraction.

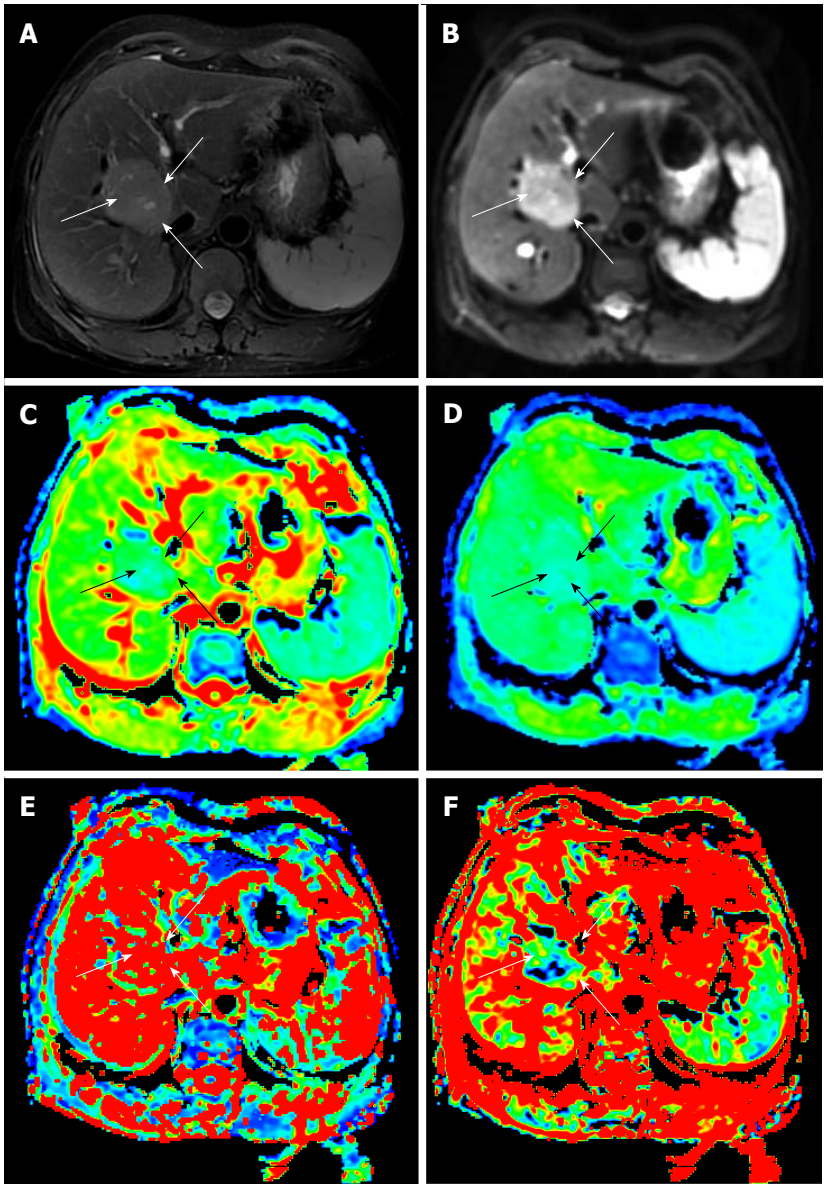

Figure 3 Magnetic resonance images of a 43-year-old woman with a 5-cm surgically verified hepatocellular carcinoma with an Edmondson-Steiner grade 3. A: T2-weighted image, B: Diffusion-weighted image with a *b* value of 10 s/mm^2; C-F: Parametric maps (ADC, D, D*, and *f*, respectively) calculated from the IVIM diffusion-weighted imaging data. The tumor (white arrow) demonstrates a slightly high signal intensity on the T2-weighted image and a high signal intensity on the DWI image. The values of the ADC, D, D*, and *f* for the ROIs of the HCC were 1.060 × 10^{-3} mm^2/s, 0.659 × 10^{-3} mm^2/s, 12.1 × 10^{-3} mm^2/s, and 0.109, respectively, which indicated an Edmondson-Steiner grade 3 HCC. HCC: Hepatocellular carcinomas; IVIM: Intravoxel incoherent motion; DWI: Diffusion-weighted imaging.

ROC analysis for diagnostic performance of the IVIM-DWI and conventional DWI parameters

The ROC curves obtained for differentiating the low-grade group (G1) from the high-grade groups (G2 and G3) are shown in Figure 5. The D showed the largest area under the curve (AUC) of 0.909 (95%CI: 0.834-0.985) obtained by radiologist 1 and 0.911 (95%CI: 0.832-0.990) obtained by radiologist 2. The

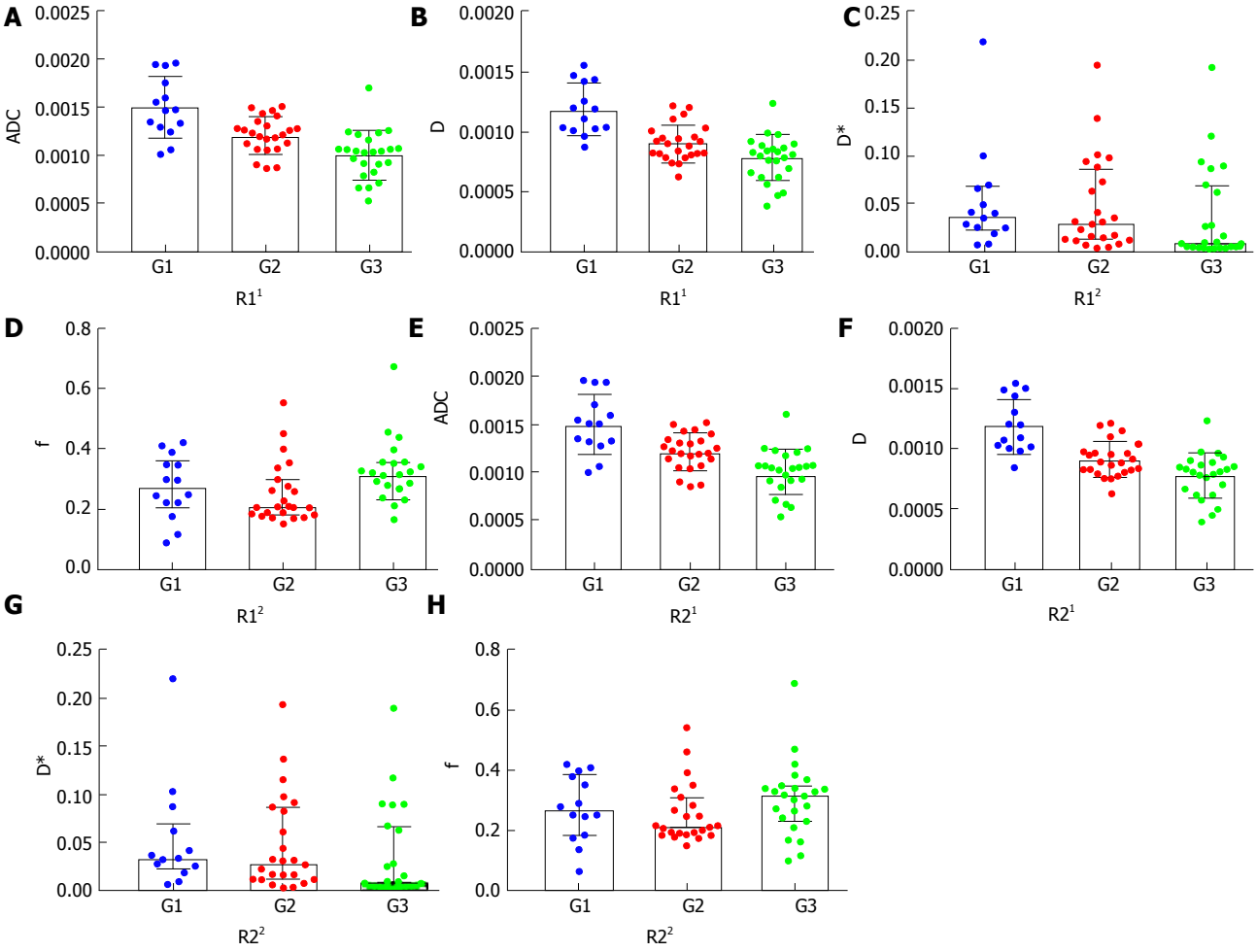

Figure 4 Column and scatter plot diagrams reporting the quantitative comparison of the differences in the intravoxel incoherent motion and conventional diffusion-weighted imaging parameters among the three groups of hepatocellular carcinoma. A-D: Quantitative comparison of the differences among the three groups in the ADC, D, D*, and f values, respectively, by radiologist 1; E and F: Quantitative comparison of the differences among the three groups in the ADC, D, D*, and f values, respectively, by radiologist 2. The differences in the ADC and D values among the different grades were statistically significant ($P < 0.001$); the differences between the G1 and G2, G1 and G3, and G2 and G3 were all statistically significant ($P < 0.05$). No statistical significance was found for the D* or the f values ($P > 0.05$). ADC, D, and D* are in units of mm2/s; f is in unit of 100%. 1Mean with SD; 2median with interquartile range. R1: Radiologist 1; R2: Radiologist 2; HCC: Hepatocellular carcinomas; IVIM: Intravoxel incoherent motion; DWI: Diffusion-weighted imaging, ADC: Apparent diffusion coefficient.

comparisons of the ROC curves of D, ADC, D*, and *f* values for discriminating the low-grade group from the high-grade groups demonstrated that the D and ADC values had similar diagnostic efficacy (AUC: 0.909 *vs* 0.843, respectively, $Z = 1.027$, $P = 0.3043$, measured by radiologist 1; 0.911 *vs* 0.852, respectively, $Z = 0.856$, $P = 0.3920$, measured by radiologist 2), while the D* and *f* values had lower diagnostic efficiency (AUC: 0.632 and 0.523, measured by radiologist 1; 0.636 and 0.518, measured by radiologist 2). No statistically significant differences were observed in the AUC values between the D* and the *f* ($Z = 0.734$, $P = 0.4631$, measured by radiologist 1; $Z = 1.625$, $P = 0.1041$, measured by radiologist 2) values. Table 2 shows the sensitivity, specificity, and accuracy of the IVIM-DWI and conventional DWI parameters at the optimal cutoff values of differentiating the low-grade group from the high-grade groups.

Correlation of IVIM-DWI and conventional DWI parameters with the histopathological results

Table 3 reports the correlation coefficients between the parameters and the histopathological grades. For radiologist 1, the Spearman correlation analysis demonstrated that there was a moderate to good relationship between the pathologically differentiated grade and the ADC ($r = -0.619$, $P < 0.001$), as well as the D ($r = -0.628$, $P < 0.001$) and D*, which demonstrated a fair relationship with the pathologically differentiated grade ($r = -0.299$, $P = 0.018$), but no statistical significance was obtained regarding the correlation between the pathologic grade and the *f* value ($r = 0.130$, $P = 0.313$). Moreover, the correlation coefficients for the ADC ($r = -0.622$, $P < 0.001$), D ($r = -0.633$, $P < 0.001$) and D* ($r = -0.303$, $P = 0.017$) that were obtained by radiologist 2 were also correlated with the pathologically differentiated grade, and the *f* value (*r*

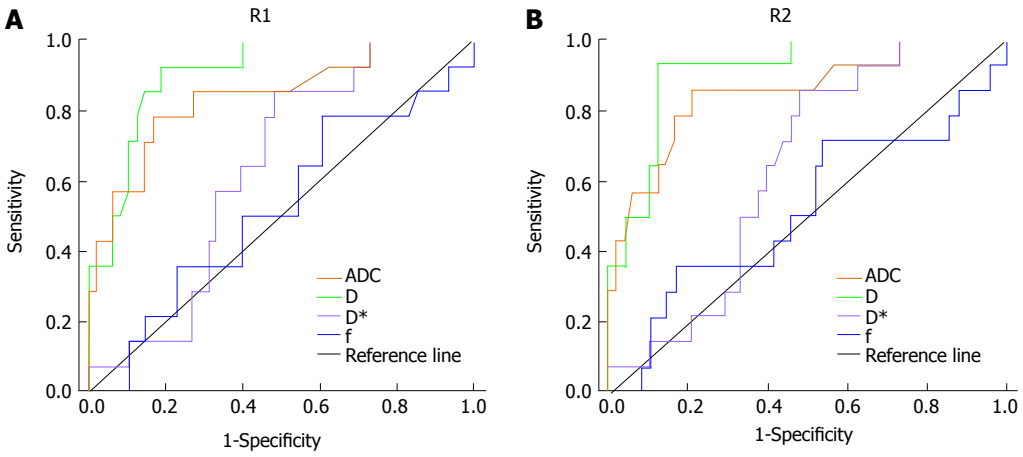

Figure 5 Graphs showing that receiver operating characteristic curves of the intravoxel incoherent motion- diffusion-weighted imaging and conventional diffusion-weighted imaging parameters of hepatocellular carcinoma for differentiating the low-grade group from the high-grade groups, as measured by the two radiologists. A: ROC curves of the parameters of HCC by radiologist 1; B: ROC curves of the parameters of HCC by radiologist 2. The area under curve (AUC) for D was the largest of all the parameters obtained by the two radiologists. R1: Radiologist 1; R2: Radiologist 2; HCC: Hepatocellular carcinomas; IVIM: Intravoxel incoherent motion; DWI: Diffusion-weighted imaging, ADC: Apparent diffusion coefficient; D: Pure diffusion coefficient; D*: Pseudo-diffusion coefficient; *f*: Perfusion fraction.

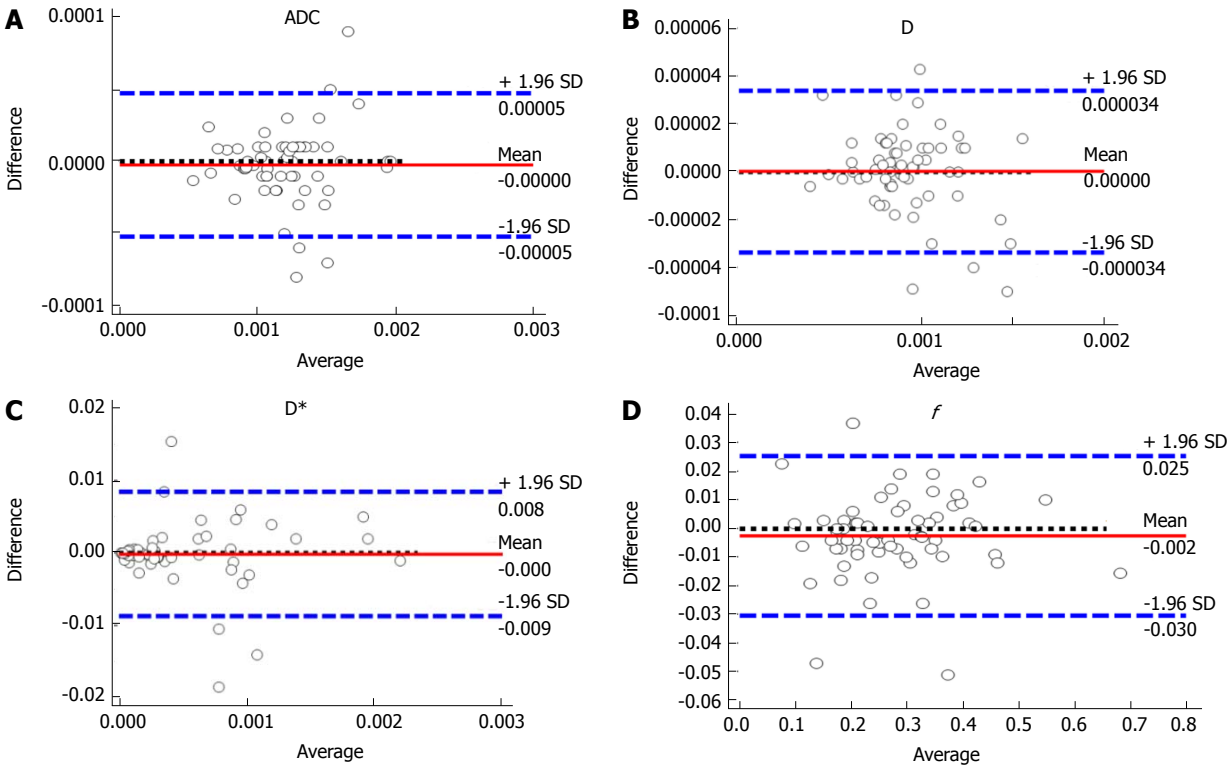

Figure 6 Bland-Altman plots showing the distribution of the differences of the intravoxel incoherent motion diffusion-weighted imaging and conventional diffusion-weighted imaging parameters between the two radiologists. A-D: The distribution of the differences of the ADC, D, D*, and f values, respectively. The differences between measurements by the two radiologists regarding the parameters were relatively small. ±1.95 SD indicates 95% limits of agreement, mean, and mean difference, ADC: Apparent diffusion coefficient.

= 0.121, *P* = 0.349) showed no statistical significance.

Inter-observer reproducibility

The ICCs between the two observers were 0.996 (95%CI: 0.994-0.998) for ADC, 0.997 (95%CI: 0.996-0.998) for D, 0.996 (95%CI: 0.996-0.998) for D*, and 0.992 (95%CI: 0.987-0.995) for the *f* value. The results suggested that there was an excellent agreement between the two observers for all the parameters. Figure 6 shows the reliability of the inter-observer measurements in the IVIM and ADC parameters, as assessed by the Bland-Altman analysis.

DISCUSSION

IVIM-based DWI is a functional and non-contrast-

enhanced MR imaging technique that can obtain diffusion and perfusion information simultaneously. IVIM-DWI has become an evaluation model of tumor microenvironment, showing changes in the microstructure of tissues and of microcirculation. IVIM-DWI may allow cancer to be evaluated more precisely, and it has been used as a diagnostic tool for several organs, including the pancreas, kidney, brain, breast, and liver[22-27]. Recent studies have indicated that accurate differentiation of HCC with different pathological grades is an important issue that should be considered in the planning of treatment strategies and prognostic evaluations[28,29]. Thus, an effective method is needed to evaluate the tumor cell differentiation grade and predict the prognosis.

In this study, both the ADC and D values showed statistically significant differences among the different grades. As the pathological grade increased, the numeric value gradually decreased; the values of the G3 group were lower than those of the G2 and G1 groups. Water mobility is restricted in malignant tissue due to an increase in the cellular density and a decrease in the interstitial space. These results regarding HCC may be attributable to the increased cellular density, nuclear-to-cytoplasmic ratios, and architectural complications when comparing the G3 and G2 groups to the G1 group, which resulted in the decreased ADC and D values[30]. Sungmin Woo *et al*[16] demonstrated that ADC and D values are both significantly lower in high-grade HCC than in low-grade HCC, which is consistent with the current findings. Previous studies in tumors elsewhere in the body also showed similar results[31,32]. The other IVIM-derived parameters, including the D* and *f* values, were not statistically significant in differentiating the G1, G2, and G3 groups. The D* and *f* values are the perfusion parameters, which could be used to reflect the vascularity of the tissue. According to the IVIM theory, D* is defined as the average blood velocity and the mean capillary segment length, and *f* measures the fractional blood volume of the microcirculation[15]. Therefore, the results of the D* and *f* values may be related to the location of the lesion and the feeding artery. Furthermore, previous studies have reported that the D* and *f* values are not accurate in the assessment of the tumor differentiation grades because of their intrinsic instability, poor reproducibility, and lower diagnostic efficiency[33,34]. Nevertheless, Vincenza Granata *et al*[18] demonstrated that the *f* values were significantly different in the HCC groups with G1, G2, and G3 histological grades, and a significant correlation was reported between the *f* value and the histologic grade, which is in disagreement with our results. Thus, the relationship between perfusion parameters and the histological grade remains controversial.

In the present study, the IVIM-derived D and ADC values showed significantly better diagnostic performance than the D* and f values in differentiating low-grade from high-grade HCC, according to the ROC analysis. The AUC values for the D and ADC in differentiating the histologic grades of HCC were not significantly different (AUC: 0.909 *vs* 0.843, respectively, $Z = 1.027$, $P = 0.3043$, by radiologist 1; 0.911 *vs* 0.852, respectively, $Z = 0.856$, $P = 0.3920$, by radiologist 2). Because the higher the *b*-value is, the more sensitive the sequence is to diffusion effects[9], the perfusion effect could be avoided if the mono-exponential fit was performed using high *b* values (> 200 s/mm^2); perfusion may have a small contribution to the ADC value, which leads to the similar results found in the D and ADC values[25]. And, the results were comparable to the values reported in the literature[25]. However, in our study, the D value showed greater AUC, sensitivity, and accuracy than the ADC value. In addition, both the D and ADC values were significantly correlated with the histological grade of HCC, as well as with the D ($r = -0.628$, $P < 0.001$, measured by radiologist 1; $r = -0.633$, $P < 0.001$, measured by radiologist 2) and ADC ($r = -0.619$, $P < 0.001$, measured by radiologist 1; $r = -0.622$, $P < 0.001$, measured by radiologist 2) values, which demonstrated a moderate to good correlation between D and the histological grade, and between ADC and the histological grade.

Our study had several limitations. First, this study was retrospective; thus, there may have been potential bias in the patient selection. Second, the study population was relatively small, and there were no cases of Edmondson-Steiner grade 4. Therefore, further studies with more samples are still needed. Third, the ROIs were mainly selected on the solid parts of the carcinoma; meanwhile, we did not obtain histopathologic verification of the whole tumor. Therefore, we could not examine the exact histological grade of the "solid" region where an ROI was placed, which may have led to selection discordance. Fourth, some of the ROIs were set in the left liver lobe, which is prone to be influenced by adjacent organ functions, such as heart and diaphragm motion or gastrointestinal peristalsis. Finally, further studies to validate the IVIM perfusion parameters are essential to be correlated with the DCE-MRI parameters and reflect the perfusion characteristics of a tumor.

In conclusion, D and ADC values showed better diagnostic performance in differentiating high-grade HCC from low-grade HCC than D* and *f* values, and a moderate to good correlation was observed between the ADC and D values and the histological grades.

ARTICLE HIGHLIGHTS

Research background

Hepatocellular carcinoma (HCC) is the most common primary malignant tumor of the liver. It is the fifth most important cancer worldwide and the third leading cause of cancer-related death. The pathological grade of HCC is heavily associated with the prognosis. However, it is difficult to provide a prediction of accurate preoperative pathological grade of HCC using routine imaging modalities.

Diffusion-weighted imaging (DWI) is a noninvasive approach to sensitively evaluate the small-scale motion of water molecules at the microscopic level. However, it is limited in that the ADC fails to evaluate the water molecular diffusion in tissues precisely. The IVIM approach uses a bi-exponential function to describe the DWI data and it is possible to obtain additional quantitative parameters that describe water diffusivity, perfusion (pseudodiffusion

coefficient), and the perfusion fraction of tissues. Recently, IVIM-DWI has been used to investigate the correlation between the parameters involved in the histologic grade of HCC. This study can determine a new imaging technique to assess the histological grade of HCC and predict the patient's prognosis in clinical practice.

Research motivation

This study investigated the value of the IVIM-derived parameters and conventional DWI-derived parameters for predicting the histological grade of HCC, evaluated the diagnostic efficiency of the parameters in distinguishing the pathological grades of HCC, and assessed the correlation between the parameters and the histological grades. With the help of the parameters, we can determine the pathological grade of HCC without the pathological results of surgery. The pathological grade of HCC is heavily associated with the prognosis. Therefore, we can assess the pathological grade of HCC and predict the patient prognosis, simultaneously.

Research objectives

The present study was to compare IVIM-derived parameters with conventional DWI-derived ADC values for determining the histologic grades of HCC and evaluated the correlation between the parameters and the histological grades. The parameters derived from IVIM-DWI and conventional DWI showed statistical significance in different histologic grades of HCC, and they will have diagnostic value in differentiating the pathological grades, as the correlation was observed between the parameters and grades. The results showed that these parameters are of great significance in the diagnosis of the pathological grades of HCC. DWI-MR will be a new imaging technique to assess the pathological grade of an HCC, which might be helpful in predicting the patient prognosis.

Research methods

A retrospective study was performed. Sixty-two patients (50 men and 12 women; mean age, 54.31 ± 9.36 years; range, 30-76 years) with surgically confirmed HCC underwent diffusion-weighted magnetic resonance imaging with twelve *b* values (10-1200 s/mm^2). All the tumors were histologically classified according to the major Edmondson-Steiner grade on the final pathologic reports as follows: grade 1 (n = 14), grade 2 (n = 24), grade 3 (n = 24), and grade 4 (n = 0). The apparent diffusion coefficient (ADC), pseudo-diffusion coefficient (D*), pure diffusion coefficient (D), and perfusion fraction (f) were calculated by two radiologists. The IVIM and conventional DWI parameters were compared among different grades by using analysis of variance (ANOVA) and the Kruskal-Wallis test. Receiver operating characteristic (ROC) analysis was performed to evaluate the diagnostic efficiency of distinguishing between low-grade (G1) and high-grade (G2 and G3) HCC. The correlations between the parameters and the histological grades were assessed by using the Spearman correlation test. Bland-Altman analysis was used to evaluate the reproducibility of the two radiologists' measurements. The measurement reproducibility between the two observers shows the reliability of parameters, and it makes sure that the results for the study objectives are more persuasive, which is the characteristics and novelty.

Research results

The differences in the ADC and D values among the groups with G1, G2, and G3 histological grades of HCC were statistically significant (P < 0.001). The D* and f values had no significant differences among the different histological grades of HCC (P > 0.05). The ROC analyses demonstrated that the D and ADC values had better diagnostic performance in differentiating the low-grade HCC from the high-grade HCC, with areas under the curve (AUCs) of 0.909 and 0.843, respectively, measured by radiologist 1 and of 0.911 and 0.852, respectively, measured by radiologist 2. The following significant correlations were obtained between the ADC, D, and D* values and the histological grades: r = -0.619 (P < 0.001), r = -0.628 (P < 0.001), and r = -0.299 (P = 0.018), respectively, as measured by radiologist 1; r = -0.622 (P < 0.001), r = -0.633 (P < 0.001), and r = -0.303 (P = 0.017), respectively, as measured by radiologist 2. The intra-class correlation coefficient (ICC) values between the two observers were 0.996 for ADC, 0.997 for D, 0.996 for D*, and 0.992 for the f values, which indicated excellent inter-observer agreement in the measurements between the two observers.

The problem that remains to be solved is that the significance of the perfusion parameters (D* and f) among different histological grades of HCC and the correlation between perfusion parameters and the histological grade are in disagreement with previous results, which remains controversial. At the same time, further studies should investigate the cor relation between the IVIM perfusion parameters and the DCE-MRI parameters to reflect the perfusion characteristics of tumor.

Research conclusions

DWI-MR imaging can be used as a noninvasive quantitative imaging method in discriminating different histological grades of HCC. DWI-MR is a noninvasive approach to sensitively evaluate the small-scale motion of water molecules at the microscopic level, reflect tumor microenvironment, show changes in the microcirculation of tissues, and provide the pathology and physiology information. IVIM-DWI parameters and conventional DWI parameters might be useful in assessing the differentiation grades of carcinoma, which might be helpful in predicting the patient prognosis. The study showed that the perfusion parameters (D* and f) were not statistically significant in differentiating the histological grades of HCC, and showed significant lower diagnostic performance in differentiating low-grade (G1) from high-grade (G2 and G3) HCCs. These results may be related to the location of the lesion and the feeding artery. IVIM-derived parameters and conventional DWI parameters can predict the histological grade of HCC and the correlation was observed between the parameters and the histological grades. The measurement reproducibility of the parameters was excellent between the two radiologists. The measured values of the D* and f existed instability in all patients, and the diagnostic value of the D*and f remains controversial. The IVIM-derived D and ADC values showed better diagnostic performance in differentiating high-grade HCC from low-grade HCC, and a moderate to good correlation was observed between the ADC and D values and the histological grades. IVIM-DWI parameters and conventional DWI parameter might be useful in evaluating the differentiation grades of carcinomas before operation, which might be helpful in predicting the patient prognosis in clinical practice.

Research perspectives

In the MR examination, the total scanning time for the IVIM was related to the respiratory condition of the patient. The faster the breathing, the shorter the scanning time. The total scanning time of all the patients is approximately 8-13 min, and the average time is about 10 min. In the process of the measurement, it should be repeated to ensure the stability and reliability of the parameters. Further studies to validate the IVIM perfusion parameters are essential to be correlated with the DCE-MRI parameters and reflect the perfusion characteristics of tumor. At the same time, the texture information of tumors can be analyzed, which can reflect the essential characteristics of the mass. Radiomics is a new research method for tumors. According to the heterogeneity of tumors, a large number of high dimensional quantitative image features are extracted from MRI, PET, and CT images and analyzed. By extracting and analyzing the characteristics of medical images, it can evaluate the diagnosis and prognosis of patients.

REFERENCES

1 **Kew MC**. Epidemiology of hepatocellular carcinoma. *Toxicology* 2002; **181-182**: 35-38 [PMID: 12505281 DOI: 10.1016/S0300-483X(02)00251-2]

2 **Gomaa AI**, Khan SA, Toledano MB, Waked I, Taylor-Robinson SD. Hepatocellular carcinoma: epidemiology, risk factors and pathogenesis. *World J Gastroenterol* 2008; **14**: 4300-4308 [PMID: 18666317 DOI: 10.3748/wjg.14.4300]

3 **Parkin DM**. Global cancer statistics in the year 2000. *Lancet Oncol* 2001; **2**: 533-543 [PMID: 11905707 DOI: 10.1016/S1470-2045(01)00486-7]

4 **Parkin DM**, Bray F, Ferlay J, Pisani P. Global cancer statistics, 2002. *CA Cancer J Clin* 2005; **55**: 74-108 [PMID: 15761078 DOI: 10.3322/canjclin.55.2.74]

5 **Zhou L**, Rui JA, Wang SB, Chen SG, Qu Q, Chi TY, Wei X, Han K, Zhang N, Zhao HT. Factors predictive for long-term survival of male patients with hepatocellular carcinoma after curative resection. *J Surg Oncol* 2007; **95**: 298-303 [PMID: 17326130 DOI: 10.1002/jso.20678]

6 **Zhou L**, Rui JA, Ye DX, Wang SB, Chen SG, Qu Q. Edmondson-Steiner grading increases the predictive efficiency of TNM staging for long-term survival of patients with hepatocellular carcinoma

after curative resection. *World J Surg* 2008; **32**: 1748-1756 [PMID: 18493820 DOI: 10.1007/s00268-008-9615-8]
7 **Stigliano R**, Marelli L, Yu D, Davies N, Patch D, Burroughs AK. Seeding following percutaneous diagnostic and therapeutic approaches for hepatocellular carcinoma. What is the risk and the outcome? Seeding risk for percutaneous approach of HCC. *Cancer Treat Rev* 2007; **33**: 437-447 [PMID: 17512669 DOI: 10.1016/j.ctrv.2007.04.001]
8 **Bruix J**, Sherman M; Practice Guidelines Committee, American Association for the Study of Liver Diseases. Management of hepatocellular carcinoma. *Hepatology* 2005; **42**: 1208-1236 [PMID: 16250051 DOI: 10.1002/hep.20933]
9 **Kele PG**, van der Jagt EJ. Diffusion weighted imaging in the liver. *World J Gastroenterol* 2010; **16**: 1567-1576 [PMID: 20355235 DOI: 10.3748/wjg.v16.i13.1567]
10 **Baliyan V**, Das CJ, Sharma R, Gupta AK. Diffusion weighted imaging: Technique and applications. *World J Radiol* 2016; **8**: 785-798 [PMID: 27721941 DOI: 10.4329/wjr.v8.i9.785]
11 **Iima M**, Le Bihan D. Clinical Intravoxel Incoherent Motion and Diffusion MR Imaging: Past, Present, and Future. *Radiology* 2016; **278**: 13-32 [PMID: 26690990 DOI: 10.1148/radiol.2015150244]
12 **Koh DM**, Collins DJ, Orton MR. Intravoxel incoherent motion in body diffusion-weighted MRI: reality and challenges. *AJR Am J Roentgenol* 2011; **196**: 1351-1361 [PMID: 21606299 DOI: 10.2214/AJR.10.5515]
13 **Filli L**, Wurnig MC, Luechinger R, Eberhardt C, Guggenberger R, Boss A. Whole-body intravoxel incoherent motion imaging. *Eur Radiol* 2015; **25**: 2049-2058 [PMID: 25576232 DOI: 10.1007/s00330-014-3577-z]
14 **Le Bihan D**, Breton E, Lallemand D, Grenier P, Cabanis E, Laval-Jeantet M. MR imaging of intravoxel incoherent motions: application to diffusion and perfusion in neurologic disorders. *Radiology* 1986; **161**: 401-407 [PMID: 3763909 DOI: 10.1148/radiology.161.2.3763909]
15 **Le Bihan D**, Breton E, Lallemand D, Aubin ML, Vignaud J, Laval-Jeantet M. Separation of diffusion and perfusion in intravoxel incoherent motion MR imaging. *Radiology* 1988; **168**: 497-505 [PMID: 3393671 DOI: 10.1148/radiology.168.2.3393671]
16 **Woo S**, Lee JM, Yoon JH, Joo I, Han JK, Choi BI. Intravoxel incoherent motion diffusion-weighted MR imaging of hepatocellular carcinoma: correlation with enhancement degree and histologic grade. *Radiology* 2014; **270**: 758-767 [PMID: 24475811 DOI: 10.1148/radiol.13130444]
17 **Nakanishi M**, Chuma M, Hige S, Omatsu T, Yokoo H, Nakanishi K, Kamiyama T, Kubota K, Haga H, Matsuno Y, Onodera Y, Kato M, Asaka M. Relationship between diffusion-weighted magnetic resonance imaging and histological tumor grading of hepatocellular carcinoma. *Ann Surg Oncol* 2012; **19**: 1302-1309 [PMID: 21927976 DOI: 10.1245/s10434-011-2066-8]
18 **Granata V**, Fusco R, Catalano O, Guarino B, Granata F, Tatangelo F, Avallone A, Piccirillo M, Palaia R, Izzo F, Petrillo A. Intravoxel incoherent motion (IVIM) in diffusion-weighted imaging (DWI) for Hepatocellular carcinoma: correlation with histologic grade. *Oncotarget* 2016; **7**: 79357-79364 [PMID: 27764817 DOI: 10.18632/oncotarget.12689]
19 **Andreou A**, Koh DM, Collins DJ, Blackledge M, Wallace T, Leach MO, Orton MR. Measurement reproducibility of perfusion fraction and pseudodiffusion coefficient derived by intravoxel incoherent motion diffusion-weighted MR imaging in normal liver and metastases. *Eur Radiol* 2013; **23**: 428-434 [PMID: 23052642 DOI: 10.1007/s00330-012-2604-1]
20 **Edmondson HA**, Steiner PE. Primary carcinoma of the liver: a study of 100 cases among 48,900 necropsies. *Cancer* 1954; **7**: 462-503 [PMID: 13160935]
21 **Koo TK**, Li MY. A Guideline of Selecting and Reporting Intraclass Correlation Coefficients for Reliability Research. *J Chiropr Med* 2016; **15**: 155-163 [PMID: 27330520 DOI: 10.1016/j.jcm.2016.02.012]
22 **Fujima N**, Yoshida D, Sakashita T, Homma A, Tsukahara A, Tha KK, Kudo K, Shirato H. Intravoxel incoherent motion diffusion-weighted imaging in head and neck squamous cell carcinoma: assessment of perfusion-related parameters compared to dynamic contrast-enhanced MRI. *Magn Reson Imaging* 2014; **32**: 1206-1213 [PMID: 25131628 DOI: 10.1016/j.mri.2014.08.009]
23 **Chandarana H**, Lee VS, Hecht E, Taouli B, Sigmund EE. Comparison of biexponential and monoexponential model of diffusion weighted imaging in evaluation of renal lesions: preliminary experience. *Invest Radiol* 2011; **46**: 285-291 [PMID: 21102345 DOI: 10.1097/RLI.0b013e3181ffc485]
24 **Concia M**, Sprinkart AM, Penner AH, Brossart P, Gieseke J, Schild HH, Willinek WA, Mürtz P. Diffusion-weighted magnetic resonance imaging of the pancreas: diagnostic benefit from an intravoxel incoherent motion model-based 3 b-value analysis. *Invest Radiol* 2014; **49**: 93-100 [PMID: 24089021 DOI: 10.1097/RLI.0b013e3182a71cc3]
25 **Liu C**, Liang C, Liu Z, Zhang S, Huang B. Intravoxel incoherent motion (IVIM) in evaluation of breast lesions: comparison with conventional DWI. *Eur J Radiol* 2013; **82**: e782-e789 [PMID: 24034833 DOI: 10.1016/j.ejrad.2013.08.006]
26 **Guo W**, Zhao S, Yang Y, Shao G. Histological grade of hepatocellular carcinoma predicted by quantitative diffusion-weighted imaging. *Int J Clin Exp Med* 2015; **8**: 4164-4169 [PMID: 26064326]
27 **Nishie A**, Tajima T, Asayama Y, Ishigami K, Kakihara D, Nakayama T, Takayama Y, Okamoto D, Fujita N, Taketomi A, Yoshimitsu K, Honda H. Diagnostic performance of apparent diffusion coefficient for predicting histological grade of hepatocellular carcinoma. *Eur J Radiol* 2011; **80**: e29-e33 [PMID: 20619566 DOI: 10.1016/j.ejrad.2010.06.019]
28 **Kim SH**, Lim HK, Choi D, Lee WJ, Kim SH, Kim MJ, Kim CK, Jeon YH, Lee JM, Rhim H. Percutaneous radiofrequency ablation of hepatocellular carcinoma: effect of histologic grade on therapeutic results. *AJR Am J Roentgenol* 2006; **186**: S327-S333 [PMID: 16632696 DOI: 10.2214/AJR.05.0350]
29 **Jonas S**, Bechstein WO, Steinmüller T, Herrmann M, Radke C, Berg T, Settmacher U, Neuhaus P. Vascular invasion and histopathologic grading determine outcome after liver transplantation for hepatocellular carcinoma in cirrhosis. *Hepatology* 2001; **33**: 1080-1086 [PMID: 11343235 DOI: 10.1053/jhep.2001.23561]
30 **Muhi A**, Ichikawa T, Motosugi U, Sano K, Matsuda M, Kitamura T, Nakazawa T, Araki T. High-b-value diffusion-weighted MR imaging of hepatocellular lesions: estimation of grade of malignancy of hepatocellular carcinoma. *J Magn Reson Imaging* 2009; **30**: 1005-1011 [PMID: 19856432 DOI: 10.1002/jmri.21931]
31 **Togao O**, Hiwatashi A, Yamashita K, Kikuchi K, Mizoguchi M, Yoshimoto K, Suzuki SO, Iwaki T, Obara M, Van Cauteren M, Honda H. Differentiation of high-grade and low-grade diffuse gliomas by intravoxel incoherent motion MR imaging. *Neuro Oncol* 2016; **18**: 132-141 [PMID: 26243792 DOI: 10.1093/neuonc/nov147]
32 **Yang DM**, Kim HC, Kim SW, Jahng GH, Won KY, Lim SJ, Oh JH. Prostate cancer: correlation of intravoxel incoherent motion MR parameters with Gleason score. *Clin Imaging* 2016; **40**: 445-450 [PMID: 27133684 DOI: 10.1016/j.clinimag.2016.01.001]
33 **Sun H**, Xu Y, Xu Q, Shi K, Wang W. Rectal cancer: Short-term reproducibility of intravoxel incoherent motion parameters in 3.0T magnetic resonance imaging. *Medicine* (Baltimore) 2017; **96**: e6866 [PMID: 28489784 DOI: 10.1097/MD.0000000000006866]
34 **Luo M**, Zhang L, Jiang XH, Zhang WD. Intravoxel Incoherent Motion Diffusion-weighted Imaging: Evaluation of the Differentiation of Solid Hepatic Lesions. *Transl Oncol* 2017; **10**: 831-838 [PMID: 28866259 DOI: 10.1016/j.tranon.2017.08.003]

P- Reviewer: Mendez-Sanchez N **S- Editor**: Ma YJ
L- Editor: Wang TQ **E- Editor**: Ma YJ

World Journal of Gastroenterology

Submit a Manuscript: http://www.f6publishing.com

World J Gastroenterol 2018 February 28; 24(8): 941-948

DOI: 10.3748/wjg.v24.i8.941

ISSN 1007-9327 (print) ISSN 2219-2840 (online)

ORIGINAL ARTICLE

Clinical Trials Study

Comparison of *TPMT* and *NUDT15* polymorphisms in Chinese patients with inflammatory bowel disease

Hong-Hui Wang, Ying He, Hong-Xian Wang, Cheng-Ling Liao, Yu Peng, Li-Jian Tao, Wei Zhang, Hui-Xiang Yang

Hong-Hui Wang, Ying He, Yu Peng, Hui-Xiang Yang, Department of Gastroenterology, Xiangya Hospital, Central South University, Changsha 410008, Hunan Province, China

Cheng-Ling Liao, Wei Zhang, Department of Clinical Pharmacology, Hunan Key Laboratory of Pharmacogenetics, Xiangya Hospital, Central South University, Changsha 410008, Hunan Province, China

Hong-Xian Wang, Department of Anesthesiology, Kunming Angel Women's & Children's Hospital, Kunming 650000, Yunnan Province, China

Li-Jian Tao, Department of Nephrology, Xiangya Hospital, Central South University, Changsha 410008, Hunan Province, China

ORCID number: Hong-Hui Wang (0000-0003-0438-0234); Ying He (0000-0002-5888-9696); Hong-Xian Wang (0000-0001-7301-2625); Cheng-Ling Liao (0000-0002-0457-4621); Yu Peng (0000-0001-6953-7816); Li-Jian Tao (0000-0003-0816-7588); Wei Zhang (0000-0003-4774-6144); Hui-Xiang Yang (0000-0001-5467-2927).

Author contributions: Wang HH, Yang HX and Tao LJ designed the study; Wang HH, He Y and Wang HX collected the samples; Wang HH, Zhang W and Liao CL performed the DNA extraction and detected the gene polymorphisms; Wang HH, Yang HX, He Y and Wang HX performed follow-up visits; Wang HH, Peng Y, Yang HX and Tao LJ performed the data analysis and interpretation; Wang HH, He Y, Wang HX and Peng Y drafted the manuscript; Yang HX revised the manuscript critically.

Supported by National Natural Science Foundation of China, No. 81370547 and No. 81400642.

Institutional review board statement: The study was reviewed and approved by the Institutional Review Board of Xiangya Hospital, Central South University, Changsha, China.

Clinical trial registration statement: Registration No. ChiCTR-OOC-17010617.

Informed consent statement: Written informed consent was obtained from all the participants.

Conflict-of-interest statement: The authors declare no competing financial interests related to this study.

Manuscript source: Unsolicited manuscript

Correspondence to: Hui-Xiang Yang, PhD, Professor, Department of Gastroenterology, Xiangya Hospital, Central South University, 87 Xiangya Road, Changsha 410008, Hunan Province, China. yang_hx430@csu.edu.cn
Telephone: +86-731-84327106
Fax: +86-731-88879602

Received: December 24, 2017
Peer-review started: December 25, 2017
First decision: January 4, 2018
Revised: January 15, 2018
Accepted: January 18, 2018
Article in press: January 18, 2018
Published online: February 28, 2018

Abstract

AIM

To observe gene polymorphisms of *TPMT* and *NUDT15*, and compare their predictive value for azathioprine (AZA)-induced leukopenia in inflammatory bowel disease (IBD).

METHODS

This study enrolled 219 patients diagnosed with IBD in Xiangya Hospital, Central South University, Changsha, China from February 2016 to November 2017. Peripheral blood of all patients was collected to detect their genotypes of *TPMT* and *NUDT15* by pyrosequencing at the Department of Clinical Pharmacology, Hunan Key Laboratory of Pharmacogenetics, Xiangya Hospital. Eighty patients were treated with AZA according to the disease condition. During the first month, patients who received AZA underwent routine blood tests and liver function tests once a week. The endpoint of the study was leukopenia induced by AZA. By analyzing patient characteristics, genotypes and leukopenia induced by drug use, we found the risk factors associated with AZA-induced leukopenia.

RESULTS

There were 219 patients with IBD (160 men and 59 women), including 39 who were confirmed with ulcerative colitis (UC), 176 with Crohn's disease (CD) and 4 with undetermined IBD (UIBD). There were 44 patients (20.1%) with mutant genotype of *NUDT15* (C/T); among them, 16 received AZA, and 8 (50%) developed leukopenia. There were 175 patients (79.7%) with wild genotype of *NUDT15* (C/C); among them, 64 received AZA, and 11 (17.2%) developed leukopenia. A significant difference was found between *NUDT15* C/T and its wild-type C/C (P = 0.004). There were only 3 patients with *TPMT* mutant genotype of A/G (1.4%) who participated in the research, and 1 of them was treated with AZA and developed leukopenia. The remaining 216 patients (98.6%) were found to bear the wild genotype of TPMT (A/A); among them, 79 patients received AZA, and 18 (22.8%) developed leukopenia, and there was no significant difference from those with A/G (P = 0.071). The frequency of *TPMT* mutation was 1.4%, and *NUDT15* mutation rate was significantly higher and reached 20.1% (P = 0.000). Therefore, *NUDT15* gene polymorphism was obviously a better biomarker than *TPMT* gene polymorphism in the prediction of AZA-induced leukopenia.

CONCLUSION

Mutation rate of *NUDT15* in Chinese IBD patients is higher than that of TPMT. *NUDT15* polymorphism is a better predictor for AZA-induced leukopenia than *TPMT* polymorphism.

Key words: *NUDT15*; *TPMT*; Azathioprine; Leukopenia; Inflammatory bowel disease; Individualized therapy

Core tip: Azathioprine (AZA) plays an important role in the remission maintenance therapy of inflammatory bowel disease (IBD). However, serious drug adverse reactions, especially leukopenia, limit its clinical application. European consensus has identified *TPMT* polymorphism as a predictor of AZA-induced leukopenia. However, the predictive value of *TPMT* is controversial in Asians with low mutation rate and effectiveness. *NUDT15* polymorphism has recently been found to be strongly associated with AZA-induced leukopenia in Asians but there are few data in Chinese populations. This study aimed to observe *TPMT* and *NUDT15* polymorphisms and compare their predictive value for AZA-induced leukopenia in Chinese IBD patients.

Wang HH, He Y, Wang HX, Liao CL, Peng Y, Tao LJ, Zhang W, Yang HX. Comparison of *TPMT* and *NUDT15* polymorphisms in Chinese patients with inflammatory bowel disease. *World J Gastroenterol* 2018; 24(8): 941-948 Available from: URL: http://www.wjgnet.com/1007-9327/full/v24/i8/941.htm DOI: http://dx.doi.org/10.3748/wjg.v24.i8.941

INTRODUCTION

Inflammatory bowel disease (IBD) is a chronic nonspecific intestinal inflammatory disease[1]. The pathogenesis of IBD is still unknown but is possibly related to genetic and environmental factors, as well as intestinal immune dysfunction. IBD mainly includes ulcerative colitis (UC), Crohn's disease (CD) and unclassified IBD (UIBD). During the 21st century, IBD has become a global disease with accelerating incidence in the newly industrialized countries, including Asia, and has caused a huge social and economic burden. An epidemiological study among the ACCESS countries showed an incidence of IBD in China of 3.3 cases per 100000 population, with an increasing trend[2].

The main goal of IBD treatment is to induce and maintain remission and prevent complications[3]. Treatment strategies of IBD include 5-aminosalicylate compounds, steroids, immune modulators and biological agents. Patients with IBD need long-term treatment to maintain remission due to its lifelong relapsing-remitting tendency. Immune modulators, especially azathioprine (AZA), have played an important role in maintaining remission. However, the adverse reactions of AZA, especially leukopenia, seriously limit its clinical application[4]. Research on the metabolic enzymes and adverse reactions of AZA has become popular and controversial. What is the value of these enzymes? How do they influence adverse reactions of AZA?

Thiopurine S-methyltransferase (TPMT), an enzyme of AZA metabolism, has been reported as a risk predictor for AZA-induced leukopenia in Caucasians. The United States Food and Drug Administration has proposed that TPMT status should be assessed before AZA therapy[5]. Researchers[6] have pointed out that AZA should not be used if TPMT activity is deficient because of a high risk of AZA-induced leukopenia. AZA should be used at a lower dose to reduce adverse reactions if TPMT activity is intermediate. However, AZA-induced leukopenia still occurs in patients with normal activity of

TPMT. Moreover, although the mutation rate of *TPMT* is lower in Asians (1%-3%) than that in Caucasians (about 10%), the incidence of AZA-induced leukopenia in Asians (about 35.4%) is higher than that in Caucasians (about 5%)[7]. Thus, the predictive value of *TPMT* polymorphism for AZA-induced leukopenia is uncertain, especially among Asian populations.

Recent studies have revealed that *NUDT15* polymorphism is a better predictor for drug adverse reactions with a higher mutation rate in Asians than *TPMT*[8]. However, little research has been done on the correlation between *NUDT15* polymorphism and AZA-induced leukopenia in Chinese populations. Therefore, our study aimed to observe the gene polymorphism frequency distributions of *TPMT* and *NUDT15*, and compare their value in predicting AZA-induced leukopenia in patients with IBD to help optimize AZA therapy for IBD.

MATERIALS AND METHODS

Patients

We enrolled 219 patients with IBD (160 men and 59 women), including 39 cases of UC, 176 of CD and 4 of UIBD. All of the patients visited Xiangya Hospital, Central South University (Changsha, China) from February 2016 to November 2017. Study inclusion criteria were: (1) diagnosis and disease activity based on the Consensus on Diagnosis and Treatment of Inflammatory Bowel Disease (2012, Guangzhou)[9]; (2) age 16-80 years; and (3) written informed consent obtained before examination. Exclusion criteria were: (1) severe cardiac, hepatic and/or renal insufficiency; (2) mucous biopsy diagnosed as carcinoma or lymphoma; (3) active tuberculosis; (4) active viral hepatitis with an obvious increase in transaminase (> 2 times the upper limit of normal), and/or hepatitis B e antigen(+) with hepatitis B virus DNA > 10^5 copies/mL or hepatitis B e antibody(+) with hepatitis B virus DNA > 10^4 copies/mL; (5) comorbidity such as bacterial or viral infection that had not been controlled effectively; and (6) acute abdominal disease, or other surgical indications (such as complicated fistula and intestinal obstruction caused by fibrosis).

Genotyping

Peripheral blood samples (2-3 mL) were obtained from enrolled patients and total genomic DNA was extracted from peripheral leukocytes. The variants in the *NUDT15* gene of *R139C* (c.415C>T, rs116855232) and the *TPMT* variants of *TPMT*3C* (p.Tyr240Cys, c.719A>G, rs1142345) were genotyped at the Department of Clinical Pharmacology, Hunan Key Laboratory of Pharmacogenetics, Xiangya Hospital, Central South University. Genotyping was performed using pyrosequencing and the results were validated by Sanger sequencing. Pyrosequencing and Sanger sequencing primers were designed with PyroMark Assay Design software 2.0 (Qiagen, Hilden, Germany) and PrimerQuest Tool (IDT, San Jose, CA, United States), respectively. The sequences of the forward, reverse and sequencing primers for rs116855232 were 5′-GTGGGTTCCTTGGGAAGAACTA-3′, 5′-ATCCCACCAGATGGTTCAGATCTT-3′ and 5′-GCTTTTCTGGGGACTG-3′, respectively. The sequences of the forward, reverse and sequencing primers for rs1142345 were 5′-TGGGGAATTGACTGTCTTTTTGA-3′, 5′-TCCATTACATTTTCAGGCTTTAGC-3′ and 5′-GACTGTCTTTTTGAAAAGTT-3′, respectively. Conditions for polymerase chain reaction were 35 cycles of 30 s at 95 ℃ for denaturation, 30 s at 57 ℃ for annealing and 30 s at 72 ℃ for extension.

AZA treatment

Initial dose of AZA was 0.5-1.5 mg/kg daily, based on the Consensus on Diagnosis and Treatment of Inflammatory Bowel Disease (2012, Guangzhou)[9]. Patients who used AZA underwent routine blood tests every week during the first month, then every 2 wk for 2 mo, followed by every month, as well as liver function tests every month. If patients had no adverse reactions, then AZA dose was increased by 0.5 mg/kg daily every month to 1.0-2.0 mg/kg/d. If AZA was effective without adverse reactions, patients should take it for life. If patients developed leukopenia (white blood cell count < 3.5 × 10^9/L or neutrophils < 1.5 × 10^9/L) and/or other severe adverse reactions, such as leukopenia, hepatoxicity, severe gastrointestinal adverse reactions and/or severe hair loss, the treatment was discontinued. The workflow of the study is shown in Figure 1.

Ethics

The study was approved by the ethics committee of the hospital, and written informed consent was obtained before examination.

Statistical analysis

Data such as baseline characteristics including age, sex, disease stage, initial dose and duration of AZA were compared using the χ^2 or Student's *t* test. Combined use of other drugs and the frequency of leukopenia for each genotype were compared by analysis of χ^2 tests. Logistic regression analyses were also performed to identify the associations of leukopenia with each genotype and other factors in multivariate analyses. To study the implication of different genes (*NUDT15* and *TPMT*) in AZA-mediate leukopenia, we calculated relative risk (RR), etiological fraction (EF; if RR > 1) and preventive fraction (PF; if RR < 1). $P < 0.05$ was considered significant. All analyses were performed using SPSS version 18 (SPSS Inc., Chicago, IL, United States).

RESULTS

Mutation rate of NUDT15 was higher than that of TPMT

A total of 219 patients (UC 39, CD 176 and UIBD 4) participated in this study and 80 of them received AZA

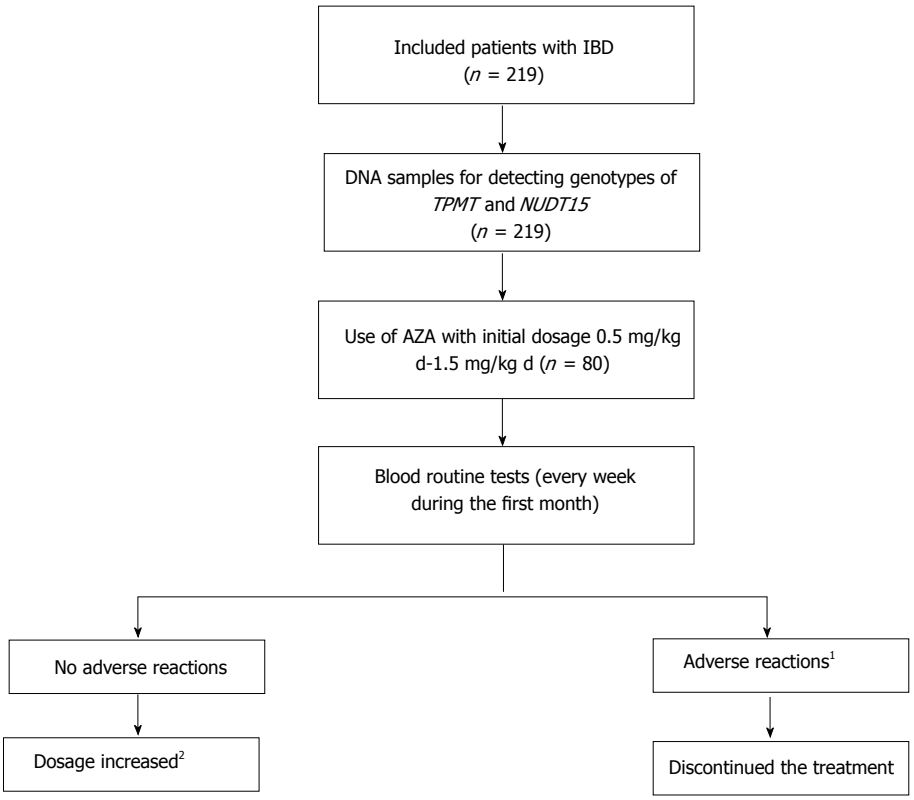

Figure 1 Study design. [1]Adverse reactions included leukopenia (white blood cell count < 3.5 × 10^9/L or neutrophils < 1.5 × 10^9/L), hepatoxicity, severe gastrointestinal adverse reactions and severe hair loss; [2]Drug dose was increased by 0.5 mg/kg daily every month gradually to 1.0-2.0 mg/kg daily. AZA: Azathioprine; IBD: Inflammatory bowel disease.

Table 1 Characteristics of patients

	UC	CD	UIBD	Total
No. of patients (*n*)	39 (17.8)	176 (80.4)	4 (1.8)	219
Age in yr	42.74 ± 13.60	30.51 ± 11.84	45.25 ± 16.62	33.44 ± 13.08
Sex, M/F	27/12	132/44	1/3	161/59
TPMT genotype				
A/A	38 (97.4)	174 (98.9)	4 (100)	216 (98.6)
A/G[a]	1 (2.6)	2 (1.1)	0	3 (1.4)
NUDT15 genotype				
C/C	31 (79.5)	140 (79.5)	4 (100)	175 (79.9)
C/T	8 (20.5)	36 (20.5)	0	44 (20.1)
AZA therapy	3 (7.7)	77 (43.8)	0	80 (36.5)

Data are presented as *n* (%) or mean ± SD. [a]$P < 0.05$ *vs NUDT15 C/T*. CD: Crohn's disease; UC: Ulcerative colitis; UIBD: Undetermined inflammatory bowel disease, AZA: Azathioprine.

therapy. All patients were checked for their genotypes of *NUDT15 R139C* and *TPMT *3C*. The baseline characteristics of the patients are summarized in Table 1. More men than women received AZA treatment. Mutation rate of *TPMT* (1.4%) was significantly lower than that of *NUDT15* (20.1%) ($P = 0.000$), which was in accordance with other studies (Figure 2).

Leukopenia was significantly associated with NUDT15 R139C

Patients characteristics, AZA initial dose, AZA duration, disease stage, adverse events and genotype of *NUDT15* are summarized in Table 2. Sixty-four patients with *NUDT15* C/C (80.0%) and 16 with C/T (20.0%) received AZA therapy. There were no significant differences in the age, sex, disease stage, initial dose of AZA, duration of AZA and combined treatment between these two groups. Eight of 16 patients with *NUDT15* C/T developed leukopenia after receiving AZA therapy, while only 11/64 (11.7%) patients with *NUDT15* C/C had leukopenia; there was a significant difference between the two groups ($P = 0.006$) (Figure 3A). Thus, patients with *NUDT15* C/T had a higher risk of AZA-induced leukopenia than those with *NUDT15* C/C.

We also analyzed *TPMT* gene polymorphism. Most patients (98.75%) were homozygous for the wild allele of *TPMT* (A/A) and 18 (22.8%) developed leukopenia after using AZA, while only 1 patient showed heterozygous *TPMT* (A/G) and then developed leukopenia, with no significant differences between the *TPMT* polymorphism and incidence of leukopenia ($P = 0.071$) (Figure 3B). Based on these results, we suggest that *TPMT* polymorphism does not predict AZA-induced leukopenia efficiently.

AZA-induced leukopenia negatively correlated with corticosteroid usage and female sex

In the logistic regression analysis with age, sex, combined drug use, disease stage, *TPMT* risk allele counts and *NUDT15* risk allele counts, we found that

Table 2 Association analysis of azathioprine and *NUDT15* polymorphism

Genotype of *NUDT15*	C/C	C/T	Total	*P* value
No. of patients (gene frequencies)	64 (90.0)	16 (10.0)	80	-
Age in yr	33.69 ± 11.31	31.13 ± 12.40	33.18 ± 11.50	0.429
Sex, M/F	48/16	11/5	59/21	0.611
Disease stages				
Remission	6 (9.4)	3 (18.8)	9 (11.3)	0.253
Mild activity	10 (15.6)	2 (12.5)	12 (15.0)	
Moderate activity	35 (54.7)	5 (31.3)	40 (50.0)	
Severe activity	13 (20.3)	6 (37.5)	19 (23.8)	
Initial dosage of AZA in mg/kg daily	1.044 ± 0.318	1.241 ± 0.252	1.082 ± 0.441	0.596
Duration of AZA in mo	8.1 ± 11.19	9.3 ± 9.95	8.4 ± 10.90	0.686
Combined with corticosteroids	28 (43.8)	5 (31.3)	33 (41.3)	0.071
Combined with IFX	14 (21.9)	7 (43.8)	21 (26.3)	
Combined with IFX and corticosteroid	0	1 (6.3)	1 (1.3)	
Leukopenia	11 (17.2)	8 (50.0)[a]	19 (23.8)	0.006

Data are presented as *n* (%) or mean ± SD. [a]*P* < 0.05 *vs NUDT15 C/C* developed leukopenia. AZA: Azathioprine; IFX: Infliximab.

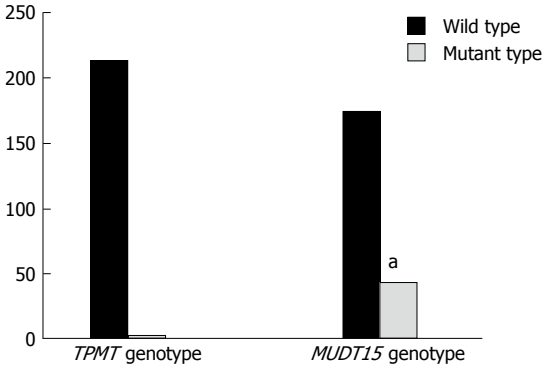

Figure 2 Gene polymorphism frequency distributions of *TPMT* and *NUDT15*. [a]*P* < 0.05 *vs* mutant type of *TPMT* group.

NUDT15 polymorphism was significantly associated with AZA-induced leukopenia (*P* = 0.004, OR = 7.663, 95%CI: 1.893-31.023, RR = 2.909, EF = 0.276). In addition, we found that the incidence of AZA-induced leukopenia negatively correlated with corticosteroid usage and female sex (Table 3). Fewer women than men developed leukopenia after receiving AZA (*P* = 0.039, odds ratio (OR) = 0.146, 95% confidence interval (CI): 0.023-0.909, RR = 0.527, PF = 0.124). Combination with glucocorticoids reduced the risk of AZA-induced leukopenia (*P* = 0.023, OR = 0.201, 95%CI: 0.050-0.798, RR = 0.437, PF = 0.253). We found that age, disease stage, duration of AZA and combination with other drugs were not significantly associated with AZA-induced leukopenia, except for corticosteroids.

DISCUSSION

AZA is an antimetabolic immunosupressor that plays a key role in remission maintenance treatment of IBD. It can be used in patients who are dependent on corticosteroids or in whom corticosteroids are ineffective, as well as in those with fistulas or operations[10]. AZA is metabolized by multiple enzymes through three main pathways[11]. (1) Steps depending on hypoxanthine phosphoribosyl transferase, inosine monophosphate dehydrogenase and GMP synthetase and eventually transferred into 6-thioguanosine triphosphate (6-TGTP). 6-TGTP is an effective form of AZA that is incorporated into double-strand DNA to inhibit its synthesis and trigger apoptosis, as well as causing bone marrow toxicity[12]; (2) Oxidization by xanthine oxidase and conversion into 6-thiouric acid, an inactive product of AZA; and (3) Catalysis by TPMT and conversion into 6-methylmercaptopurine. These three pathways are mutually competitive.

Although AZA is cost-effective, adverse reactions such as leukopenia may lead to severe and life-threatening infections that result in treatment discontinuation. A study by Kakuta *et al*[13] showed that 34 (25.2%) of 135 Japanese patients with IBD developed leukopenia after receiving AZA therapy. Yang *et al*[8] found that 346 (35.4%) of 978 Korean patients with CD developed AZA-induced leukopenia. Consistent with these results, we found that 19 (23.8%) of 80 Chinese patients with IBD discontinued AZA treatment due to leukopenia. So, the incidence of AZA-induced leukopenia is high in Asians and should not be ignored. Research on AZA has found that *TPMT* polymorphism is significantly associated with AZA-induced leukopenia, and > 40 different variant *TPMT* alleles (*TPMT*2-*41*) have been studied[14,15]. Among them, *TPMT*3C* is the most popular variant in Asians, but the gene frequency is low (1%-3%)[16]. Gazouli *et al*[17] have found no association between *TPMT* polymorphisms and the occurrence of AZA-related adverse events. In our study, the variation of *TPMT* (1.4%) was rare and not significantly associated with AZA-induced leukopenia in Chinese patients with IBD, which was consistent with previous reports. Thus, the predictive value of *TPMT* polymorphism is controversial in Asians.

NUDT15 also known as MTH2, is a member of the Nudix hydrolytic enzyme family, which degrades 8-o-dGTP into 8-o-dGMP and prevents DNA from mismatch. Carter *et al*[18] have revealed that *NUDT15*

Table 3 Multivariate association analyses of azathioprine-induced leukopenia

Factor	*P* value	OR (95%CI)	RR	EF/PF
Age	0.714	-	-	-
Sex, female	0.039	0.146 (0.023-0.909)	0.527	0.124
Disease stages	0.509	-		-
Duration of AZA	0.438	-		-
Combined with corticosteroids	0.023	0.201 (0.050-0.798)	0.437	0.253
Combined with IFX	0.339	-	-	-
Combined with IFX and corticosteroid	1.000	-	-	-
TPMT	1.000	-	-	-
NUDT15	0.004	7.663 (1.893-31.023)	2.909	0.276

AZA: Azathioprine; CI: Confidence interval; EF: Etiological fraction; IFX: Infliximab; OR: Odds ratio; PF: Preventive fraction; RR: Relative risk.

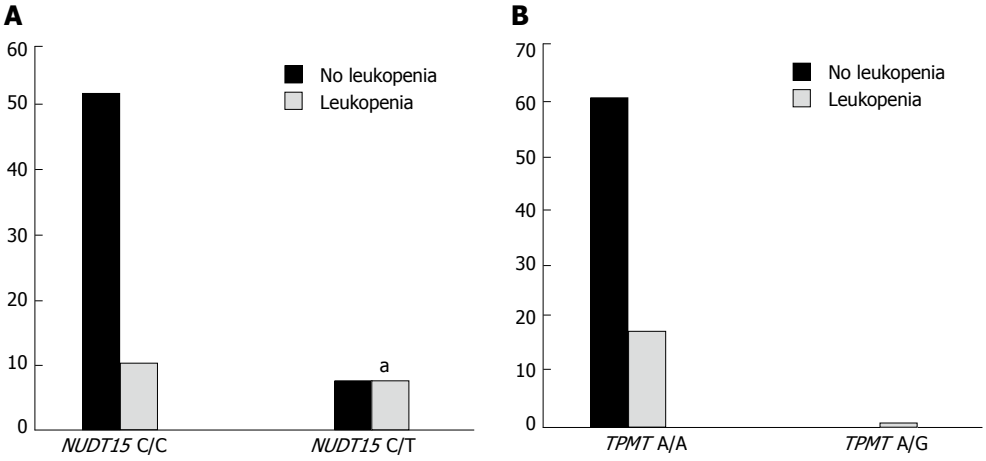

Figure 3 Occurrence of leukopenia with different genotypes of *NUDT15* (A) and *TPMT* (B). [a]*P* < 0.05 *vs NUDT15 C/C* developed leukopenia group.

has a strong effect on dGTP, 6-TGTP and dUTP. It hydrolyzes 6-TGTP into 6-TGMP, decreases the level of AZA active metabolites and prevents AZA-induced leukopenia. Yang *et al*[8] have reported that *NUDT15* polymorphism is strongly associated with thiopurine-induced early leukopenia in Koreans. Zhu *et al*[19] have found in Chinese patients that *NUDT15* has a high mutation rate (22.5%) that is strongly associated with the incidence of AZA-induced leukopenia. A study of Singapore patients with IBD[20] has also revealed that patients with low and intermediate NUDT15 activity have significantly higher risks of developing AZA-induced leukopenia. We verified the same conclusion that the incidence of an aberrant *NUDT15* was 10.0% significantly higher than that of *TPMT* (*P* = 0.000) and *NUDT15* could be an important pharmacogenetic marker for predicting AZA-induced leukopenia in a Chinese cohort (*P* = 0.004, OR = 7.663, 95%CI: 1.893-31.023, RR = 2.909, EF = 0.276).

This is a prospective study that has a lot of clinical value. Our results were significant to optimize AZA therapy for Chinese patients with IBD and helpful to provide more data in Chinese populations and to further multicenter large-scale research. Moreover, we are the first to describe that combined use of corticosteroids is a negative factor for developing AZA-induced leukopenia. Patients who received corticosteroids along with AZA treatment, or those with corticosteroid-induced remission and maintenance by AZA had a lower risk of developing leukopenia (*P* = 0.023, OR = 0.201, 95%CI: 0.050-0.798, RR = 0.437, PF = 0.253). This may be explained by the function of corticosteroids[22] in enhancing bone marrow hematopoiesis and promoting neutrophil release and increasing the number of circulating neutrophils, as well as reducing the infiltration and consumption of neutrophils in the inflammatory regions.

In contrast to the study by Kakuta *et al*[13], which showed that sex was not associated with AZA-induced leukopenia, we found that women were less likely to develop leukopenia after receiving AZA than men (*P* = 0.039, OR = 0.146, 95%CI: 0.023-0.909, RR = 0.527, PF = 0.124). The exact mechanism was unknown. We supposed that might be related to sex differences in pharmacokinetics. More specifically, females may have a lower apparent volume of distributions than males because of the solubility of the drug so that AZA might be removed more quickly in females, which reduces the risk of AZA-induced leukopenia. However, since more men received AZA treatment than women in our study, further study is needed to confirm the relationship between sex and AZA-induced leukopenia.

Our study had a few limitations, including that no patients with *NUDT15*(T/T) participated in our study.

Recent studies have detected additional variants of *NUDT15*, except *R139C*, including Arg139His, Val18Ile and p.Val18_Val19insGlyVal, and defined six haplotype (*1 to *6) combinations of these variants[21], but we have not investigated these in the present study. So, further multicenter studies with larger sample size are warranted in this area.

In conclusion, the mutation rate of *NUDT15* in Chinese patients with IBD is significantly higher than that of *TPMT*. *NUDT15* polymorphism is a better predictor for AZA-induced leukopenia than *TPMT* polymorphism. Combined use of corticosteroids is a potential way to reduce the risk of AZA-induced leukopenia. Males have a higher risk of developing AZA-induced leukopenia and need to be more closely monitored than females. Further research is necessary to verify this relationship and determine the precise mechanism.

ARTICLE HIGHLIGHTS

Research background

Azathioprine (AZA) plays a key role in remission maintenance therapy of inflammatory bowel disease (IBD), although it causes serious adverse reactions, including leukopenia. *TPMT* polymorphism is a predictor of AZA-induced leukopenia in Caucasians. However, the predictive value of *TPMT* is controversial in Asians. *NUDT15* polymorphism is a more effective predictor of AZA-induced leukopenia in Asians, but there are few data in Chinese populations.

Research motivation

The purpose of this study was to observe *TPMT* and *NUDT15* polymorphisms and compare their values in predicting AZA-induced leukopenia in Chinese IBD patients.

Research objectives

To find a more valuable predictor of AZA-induced leukopenia in Chinese patients with IBD, improve our ability to manage these patients more safely, and optimize AZA therapy.

Research methods

A total of 219 patients diagnosed with IBD in Xiangya Hospital, Central South University were enrolled. Peripheral blood of all patients was collected to detect their genotypes of *TPMT* and *NUDT15* by pyrosequencing at the Department of Clinical Pharmacology, Hunan Key Laboratory of Pharmacogenetics, Xiangya Hospital. Eighty patients were treated with AZA according to the disease condition. Patients who received AZA underwent routine blood tests and liver function tests once a week. Data analysis was performed by χ^2 test, Student's *t* test or logistic regression analyses using SPSS version 18.

Research results

We enrolled 219 patients with IBD (160 men and 59 women). There were 44 patients (20.1%) with mutant genotype of *NUDT15* (C/T); among them, 16 received AZA, and 8 (50%) developed leukopenia. There were 175 patients (79.7%) with wild genotype of *NUDT15* (C/C); among them, 64 received AZA, and 11 (17.2%) developed leukopenia. A significant difference was found between *NUDT15* C/T and its wild-type C/C (P = 0.004). There were only 3 patients with *TPMT* mutant genotype of A/G (1.4%) and 1 was treated with AZA and then developed leukopenia. The remaining 216 patients (98.6%) were found to bear the wild genotype of TPMT (A/A); among them, 79 received AZA, and 18 (22.8%) developed leukopenia. There was no significant difference from those with A/Gs (P = 0.071). The frequency of *TPMT* mutation was 1.4%, and *NUDT15* mutation rate was significantly higher and reached 20.1% (P = 0.000). Therefore, *NUDT15* gene polymorphism was obviously a better biomarker than *TPMT* gene polymorphism for prediction of AZA-induced leukopenia. Moreover, combined use of corticosteroids reduced the risk of AZA-induced leukopenia (P = 0.023, odds ratio (OR) = 0.201, 95% confidence interval (CI): 0.050-0.798, relative risk (RR) = 0.437, preventive fraction (PF) = 0.253) and fewer women than men developed leukopenia after receiving AZA (P = 0.039, OR = 0.146, 95%CI: 0.023-0.909, RR = 0.527, PF = 0.124).

Research conclusions

In Chinese patients with IBD, the mutation rate of *NUDT15* is significantly higher than that of *TPMT*. *NUDT15* polymorphism is more strongly associated with AZA-induced leukopenia than *TPMT* is. Detecting *NUDT15* genotype before AZA treatment is more effective at predicting the risk of developing leukopenia than detecting *TPMT* genotype. Combined use of corticosteroids is a potential way to reduce the risk of leukopenia. Males have a higher risk of developing AZA-induced leukopenia and need to be more closely monitored than females. Further research is necessary to verify this relationship and determine the precise mechanism.

Research perspectives

According to our study, *NUDT15* polymorphism may predict AZA-induced leukopenia more effectively than *TPMT* does. Female sex and corticosteroid usage were negatively associated with developing AZA-induced leukopenia. This might be helpful for AZA-induced leukopenia prevention and to optimize AZA therapy for IBD. While the definite relationship was obscure, more research about how they affect AZA metabolism should be carried out in the future. To learn more about the interaction between them, multicenter studies with larger samples and functional genomics technology may be carried out in future research.

REFERENCES

1 **Lakatos PL**. Prevalence, predictors, and clinical consequences of medical adherence in IBD: how to improve it? *World J Gastroenterol* 2009; **15**: 4234-4239 [PMID: 19750566 DOI: 10.3748/wjg.15.4234]

2 **Ng SC**, Tang W, Ching JY, Wong M, Chow CM, Hui AJ, Wong TC, Leung VK, Tsang SW, Yu HH, Li MF, Ng KK, Kamm MA, Studd C, Bell S, Leong R, de Silva HJ, Kasturiratne A, Mufeena MN, Ling KL, Ooi CJ, Tan PS, Ong D, Goh KL, Hilmi I, Pisespongsa P, Manatsathit S, Rerknimitr R, Aniwan S, Wang YF, Ouyang Q, Zeng Z, Zhu Z, Chen MH, Hu PJ, Wu K, Wang X, Simadibrata M, Abdullah M, Wu JC, Sung JJ, Chan FK; Asia-Pacific Crohn's and Colitis Epidemiologic Study (ACCESS) Study Group. Incidence and phenotype of inflammatory bowel disease based on results from the Asia-pacific Crohn's and colitis epidemiology study. *Gastroenterology* 2013; **145**: 158-165.e2 [PMID: 23583432 DOI: 10.1053/j.gastro.2013.04.007]

3 **Bernstein CN**, Eliakim A, Fedail S, Fried M, Gearry R, Goh KL, Hamid S, Khan AG, Khalif I, Ng SC, Ouyang Q, Rey JF, Sood A, Steinwurz F, Watermeyer G, LeMair A; Review Team:. World Gastroenterology Organisation Global Guidelines Inflammatory Bowel Disease: Update August 2015. *J Clin Gastroenterol* 2016; **50**: 803-818 [PMID: 27741097 DOI: 10.1097/MCG.0000000000000660]

4 **Bär F**, Sina C, Fellermann K. Thiopurines in inflammatory bowel disease revisited. *World J Gastroenterol* 2013; **19**: 1699-1706 [PMID: 23555158 DOI: 10.3748/wjg.v19.i11.1699]

5 **Lichtenstein GR**, Sbreu MT, Cohen R, Tremaine W. [American Gastroenterological Association Institute technical review on corticosteroids, immunomodulators, and infliximab in inflammatory bowel disease]. *Rev Gastroenterol Mex* 2006; **71**: 351-401 [PMID: 17140062 DOI: 10.1053/j.gastro.2006.01.048]

6 **Gazouli M**, Pachoula I, Panayotou I, Chouliaras G, Anagnou NP, Chroussos G, Roma E. Thiopurine methyltransferase genotype and thiopurine S-methyltransferase activity in Greek children with inflammatory bowel disease. *Ann Gastroenterol* 2012; **25**: 249-253 [PMID: 24714152 DOI: 10.1016/s1873-9946(12)60248-7]

7 **Lee KM**, Kim YS, Seo GS, Kim TO, Yang SK; IBD Study Group of the Korean Association for the Study of Intestinal Diseases. Use of Thiopurines in Inflammatory Bowel Disease: A Consensus

Statement by the Korean Association for the Study of Intestinal Diseases (KASID). *Intest Res* 2015; **13**: 193-207 [PMID: 26130993 DOI: 10.5217/ir.2015.13.3.193]

8 **Yang SK**, Hong M, Baek J, Choi H, Zhao W, Jung Y, Haritunians T, Ye BD, Kim KJ, Park SH, Park SK, Yang DH, Dubinsky M, Lee I, McGovern DP, Liu J, Song K. A common missense variant in NUDT15 confers susceptibility to thiopurine-induced leukopenia. *Nat Genet* 2014; **46**: 1017-1020 [PMID: 25108385 DOI: 10.1038/ng.3060]

9 **Hu PJ,** Qian JM, Wu KC, Rang ZH. Consensus on Diagnosis and Management of Inflammatory Bowel Disease (2012·Guang Zhou). *Neike Lilun Yu Shijian* 2013; **1**: 62-75 [DOI: 10.3969/j.issn.1673-6087.2013.01.015]

10 **Meijer B**, Mulder CJ, van Bodegraven AA, de Boer NK. How I treat my inflammatory bowel disease-patients with thiopurines? *World J Gastrointest Pharmacol Ther* 2016; **7**: 524-530 [PMID: 27867685 DOI: 10.4292/wjgpt.v7.i4.524]

11 **Fangbin Z**, Xiang G, Liang D, Hui L, Xueding W, Baili C, Huichang B, Yinglian X, Peng C, Lizi Z, Yanjun C, Feng X, Minhu C, Min H, Pinjin H. Prospective Evaluation of Pharmacogenomics and Metabolite Measurements upon Azathioprine Therapy in Inflammatory Bowel Disease: An Observational Study. *Medicine* (Baltimore) 2016; **95**: e3326 [PMID: 27082580 DOI: 10.1097/MD.0000000000003326]

12 **Moriyama T**, Nishii R, Perez-Andreu V, Yang W, Klussmann FA, Zhao X, Lin TN, Hoshitsuki K, Nersting J, Kihira K, Hofmann U, Komada Y, Kato M, McCorkle R, Li L, Koh K, Najera CR, Kham SK, Isobe T, Chen Z, Chiew EK, Bhojwani D, Jeffries C, Lu Y, Schwab M, Inaba H, Pui CH, Relling MV, Manabe A, Hori H, Schmiegelow K, Yeoh AE, Evans WE, Yang JJ. NUDT15 polymorphisms alter thiopurine metabolism and hematopoietic toxicity. *Nat Genet* 2016; **48**: 367-373 [PMID: 26878724 DOI: 10.1038/ng.3508]

13 **Kakuta Y**, Naito T, Onodera M, Kuroha M, Kimura T, Shiga H, Endo K, Negoro K, Kinouchi Y, Shimosegawa T. NUDT15 R139C causes thiopurine-induced early severe hair loss and leukopenia in Japanese patients with IBD. *Pharmacogenomics J* 2016; **16**: 280-285 [PMID: 26076924 DOI: 10.1038/tpj.2015.43]

14 **Appell ML**, Berg J, Duley J, Evans WE, Kennedy MA, Lennard L, Marinaki T, McLeod HL, Relling MV, Schaeffeler E, Schwab M, Weinshilboum R, Yeoh AE, McDonagh EM, Hebert JM, Klein TE, Coulthard SA. Nomenclature for alleles of the thiopurine methyltransferase gene. *Pharmacogenet Genomics* 2013; **23**: 242-248 [PMID: 23407052 DOI: 10.1097/FPC.0b013e32835f1cc0]

15 **Iu YPH**, Helander S, Kahlin AZ, Cheng CW, Shek CC, Leung MH, Wallner B, Mårtensson LG, Appell ML. One amino acid makes a difference-Characterization of a new TPMT allele and the influence of SAM on TPMT stability. *Sci Rep* 2017; **7**: 46428 [PMID: 28462921 DOI: 10.1038/srep46428]

16 **Takatsu N**, Matsui T, Murakami Y, Ishihara H, Hisabe T, Nagahama T, Maki S, Beppu T, Takaki Y, Hirai F, Yao K. Adverse reactions to azathioprine cannot be predicted by thiopurine S-methyltransferase genotype in Japanese patients with inflammatory bowel disease. *J Gastroenterol Hepatol* 2009; **24**: 1258-1264 [PMID: 19682195 DOI: 10.1111/j.1440-1746.2009.05917.x]

17 **Gazouli M**, Pachoula I, Panayotou I, Mantzaris G, Syriopoulou VP, Goutas N, Vlachodimitropoulos D, Anagnou NP, Roma-Giannikou E. Thiopurine S-methyltransferase genotype and the use of thiopurines in paediatric inflammatory bowel disease Greek patients. *J Clin Pharm Ther* 2010; **35**: 93-97 [PMID: 20175817 DOI: 10.1111/j.1365-2710.2009.01041.x]

18 **Carter M**, Jemth AS, Hagenkort A, Page BD, Gustafsson R, Griese JJ, Gad H, Valerie NC, Desroses M, Boström J, Warpman Berglund U, Helleday T, Stenmark P. Crystal structure, biochemical and cellular activities demonstrate separate functions of MTH1 and MTH2. *Nat Commun* 2015; **6**: 7871 [PMID: 26238318 DOI: 10.1038/ncomms8871]

19 **Zhu X**, Wang XD, Chao K, Zhi M, Zheng H, Ruan HL, Xin S, Ding N, Hu PJ, Huang M, Gao X. NUDT15 polymorphisms are better than thiopurine S-methyltransferase as predictor of risk for thiopurine-induced leukopenia in Chinese patients with Crohn's disease. *Aliment Pharmacol Ther* 2016; **44**: 967-975 [PMID: 27604507 DOI: 10.1111/apt.13796]

20 **Sutiman N**, Chen S, Ling KL, Chuah SW, Leong WF, Nadiger V, Tjai M, Choon Kong CS, Schwender BJ, Chan W, Shim HH, Lim WC, Khor CC, Cheung YB, Chowbay B. Predictive role of NUDT15 variants on thiopurine-induced myelotoxicity in Asian inflammatory bowel disease patients. *Pharmacogenomics* 2018; **19**: 31-43 [PMID: 29210335 DOI: 10.2217/pgs-2017-0147]

21 **Chao K**, Wang X, Cao Q, Qian J, Wu K, Zhu X, Yang H, Liang J, Lin L, Huang Z, Zhang Y, Huang Y, Sun Y, Xue X, Huang M, Hu P, Lan P, Gao X. Combined Detection of NUDT15 Variants Could Highly Predict Thiopurine-induced Leukopenia in Chinese Patients with Inflammatory Bowel Disease: A Multicenter Analysis. *Inflamm Bowel Dis* 2017; **23**: 1592-1599 [PMID: 28570428 DOI: 10.1097/MIB.0000000000001148]

22 **Le Jeunne C**. [Pharmacology of glucocorticoids]. *Presse Med* 2012; **41**: 370-377 [PMID: 22341947 DOI: 10.1016/j.lpm.2012.01.007]

P- Reviewer: Gazouli M, Link A, Trifan A **S- Editor**: Ma YJ
L- Editor: Filipodia **E- Editor**: Ma YJ

World Journal of Gastroenterology

Submit a Manuscript: http://www.f6publishing.com

World J Gastroenterol 2018 February 28; 24(8): 949-956

DOI: 10.3748/wjg.v24.i8.949

ISSN 1007-9327 (print) ISSN 2219-2840 (online)

CASE REPORT

Detection of fusion gene in cell-free DNA of a gastric synovial sarcoma

Shinpei Ogino, Hirotaka Konishi, Daisuke Ichikawa, Junichi Hamada, Katsutoshi Shoda, Tomohiro Arita, Shuhei Komatsu, Atsushi Shiozaki, Kazuma Okamoto, Sanae Yamazaki, Satoru Yasukawa, Eiichi Konishi, Eigo Otsuji

Shinpei Ogino, Hirotaka Konishi, Daisuke Ichikawa, Junichi Hamada, Katsutoshi Shoda, Tomohiro Arita, Shuhei Komatsu, Atsushi Shiozaki, Kazuma Okamoto, Eigo Otsuji, Division of Digestive Surgery, Department of Surgery, Kyoto Prefectural University of Medicine, Kamigyo-ku, Kyoto 602-8566, Japan

Sanae Yamazaki, Satoru Yasukawa, Eiichi Konishi, Department of Surgical Pathology, Kyoto Prefectural University of Medicine, Kamigyo-ku, Kyoto 602-8566, Japan

ORCID number: Shinpei Ogino (0000-0001-9867-7623); Hirotaka Konishi (0000-0002-4899-8944); Daisuke Ichikawa (0000-0003-0093-2206); Katsutoshi Shoda (0000-0002-1011-5579); Tomohiro Arita (0000-0001-7127-6504); Shuhei Komatsu (0000-0001-6074-7614); Atsushi Shiozaki (0000-0003-3739-160X); Kazuma Okamoto (0000-0002-8270-4217); Eiichi Konishi (0000-0002-1194-1186); Eigo Otsuji (0000-0002-3260-8155).

Author contributions: Ogino S, Konishi H and Otsuji E analyzed the patient data and were major contributor in writing the manuscript; Ichikawa D, Hamada J, Shoda K, Arita T, Komatsu S, Shiozaki A and Okamoto K performed patient treatment and sample collections; Yamazaki S, Yasukawa S and Konishi E performed the pathological diagnosis; all authors read and approved the final manuscript.

Informed consent statement: The study participant provided informed written consent prior to their treatments and study enrollment.

Conflict-of-interest statement: All authors declare no conflict of interest related to this study or its publication.

CARE Checklist (2013) statement: The authors have read the CARE Checklist (2013), and the manuscript was prepared and revised according to the CARE Checklist (2013).

Manuscript source: Unsolicited manuscript

Correspondence to: Hirotaka Konishi, MD, PhD, Division of Digestive Surgery, Department of Surgery, Kyoto Prefectural University of Medicine, 465 Kajii-cho, Kawaramachi-hirokoji, Kamigyo-ku, Kyoto 602-8566, Japan. h-koni7@koto.kpu-m.ac.jp
Telephone: +81-75-2515527
Fax: +81-75-2515522

Received: December 14, 2017
Peer-review started: December 14, 2017
First decision: January 5, 2018
Revised: January 11, 2018
Accepted: January 20, 2018
Article in press: January 20, 2018
Published online: February 28, 2018

Abstract

Synovial sarcoma (SS) is genetically characterized by chromosomal translocation, which generates *SYT-SSX* fusion transcripts. Although SS can occur in any body part, primary gastric SS is substantially rare. Here we describe a detection of the fusion gene sequence of gastric SS in plasma cell-free DNA (cfDNA). A gastric submucosal tumor was detected in the stomach of a 27-year-old woman and diagnosed as SS. Candidate intronic primers were designed to detect the intronic fusion breakpoint and this fusion sequence was confirmed in intron 10 of *SYT* and intron 5 of *SSX2* by genomic polymerase chain reaction (PCR) and direct sequencing. A locked nucleic acid (LNA) probe specific

to the fusion sequence was designed for detecting the fusion sequence in plasma and the fusion sequence was detected in preoperative plasma cfDNA, while not detected in postoperative plasma cfDNA. This technique will be useful for monitoring translocation-derived diseases such as SS.

Key words: Fusion gene; Gastric synovial sarcoma; Plasma; Cell free DNA

Core tip: Synovial sarcoma (SS) is genetically characterized by *SYT-SSX* fusion transcripts and detection of the fusion gene is necessary for a definitive diagnosis. This study demonstrated the detection of fusion sequence using cfDNA sample. A small gastric SS was detected in the stomach of a 27-year-old woman. Candidate intronic primers were designed and the intronic breakpoint was confirmed by PCR and direct sequencing in frozen tumor sample. A probe specific for fusion sequence was designed and the sequence was detected in preoperative cfDNA and frozen tumor sample. This technique will be useful for monitoring translocation-derived diseases such as SS.

Ogino S, Konishi H, Ichikawa D, Hamada J, Shoda K, Arita T, Komatsu S, Shiozaki A, Okamoto K, Yamazaki S, Yasukawa S, Konishi E, Otsuji E. Detection of fusion gene in cell-free DNA of a gastric synovial sarcoma. *World J Gastroenterol* 2018; 24(8): 949-956 Available from: URL: http://www.wjgnet.com/1007-9327/full/v24/i8/949.htm DOI: http://dx.doi.org/10.3748/wjg.v24.i8.949

INTRODUCTION

Synovial sarcoma (SS), an aggressive soft tissue tumor, accounts for 7% of human soft tissue sarcomas[1]. Although SS frequently arises in large joint capsules in the extremities of young adults, it can occur in any body part, including the digestive tract. SS morphology resembles the developing synovial tissue; however, its origin remains unknown.

SS is genetically characterized by the reciprocal chromosomal translocation between X and 18 t (X; 18) (p11.2; q11.2) chromosomes, which generates *SYT-SSX* fusion transcripts[2,3]. *SYT* (GenBank accession number NC_000018) is normally expressed in human tissues[4], whereas *SSX* expression is limited to normal testis and thyroid, and some variants are found in human malignancies[4-7]. The *SSX* family reportedly comprises nine highly homologous synovial sarcoma X genes (*SSX1-9*)[5]; however, *SSX1* or *SSX2* (GenBank accession number (SSX1) or NC_000023) account for > 90% of t (X;18) translocations and *SSX4* is involved in few cases[7,8]. The breakpoints are frequently found within intron 10 of the *SYT* gene and intron 5 of the *SSX* gene[6-8]. The detection of the *SYT-SSX* fusion gene generally leads to SS diagnosis.

In this time, we could preoperatively diagnose with a primary gastric SS patient by reverse transcription polymerase chain reaction (RT-PCR) of biopsy tissue samples. Although some primary gastric SS cases have been reported, their preoperative diagnosis is rare. Its diagnosis is difficult solely on the basis of clinical or pathological findings[9-11]. Circulating nucleic acids were recently found to reflect the occurrence of cancer or monitoring of many diseases. Regarding SS, the production of the fusion gene *SYT-SSX* is a highly disease-specific alteration, and detecting the fusion gene in the patient's circulation will represent a less-invasive diagnostic tool for this disease.

In this study, we report a detection of the fusion gene sequence in plasma circulating cfDNA.

CASE REPORT

Materials and methods

Case of primary gastric SS: A gastric ulcerated submucosal tumor was detected in the lower stomach of a 27-year-old woman using upper gastrointestinal endoscopy. Endoscopic ultrasound-guided biopsy was performed, and a spindle cell sarcoma compatible with SS was found in biopsy samples. The *SYT-SSX2* fusion gene was detected in tissue RNA of biopsy samples using RT-PCR. Laparoscopic gastrectomy was performed, and the tumor up to 20 mm diameter was pathologically diagnosed with SS. This patient remained disease free during the 6 mo follow-up.

The patient provided informed written consent for specimen collections and biomarker analyses, and the research was conducted with the approval of the ethics committees of the local institution and according to the Helsinki declaration.

Tissue sample collections and tissue DNA and RNA extractions: Tumor tissues and adjacent normal gastric tissues were obtained from operatively resected specimens and stored at -80 ℃ before DNA and RNA extractions. Total DNA and RNA were extracted from frozen samples using the AllPrep® DNA/RNA/miRNA universal kit (Qiagen, Hilden, Germany) according to the manufacturer's instructions. Tissue RNA concentration was determined using a NanoDrop 1000 Spectrophotometer (Thermo Fisher Scientific, Waltham, United States), and the tissue DNA concentration was determined using a Qubit 3.0 fluorometer (Thermo Fisher Scientific).

Plasma sample collections and plasma DNA extractions: Seven-milliliter EDTA blood samples were obtained from the patient at three different times: before operation, 1 mo after the operation, and 6 mo after the operation. Blood samples were also obtained from 10 healthy volunteers. The plasma samples were

Table 1 Overview of primers and probe sequences for all PCR methods

Primers (5'-3')	Sequence	Product size (bp)
Reverse transcription PCR		
SYT-sense	CCAGCAGAGGCCTTATGGA	118
SSX2-antisense	GCACAGCTCTTTCCCATCA	
Genomic PCR		
SYT1-sense	GTAGTTTGACCGGCTGCAGAA	
SYT2-sense	GGTGGTCTGGTTTGTTCACC	
SYT3-sense	GCAAATGTTTATTGAGCAACCA	
SYT4-sense	GGGAGAAATTAAAAGGGTGGA	
SYT5-sense	CACCTGTGAAACCATCAGCA	
SYT6-sense	TTTTCTTTATGGATTATGCTTTTGG	
SYT7-sense	GCTTACTAGGAGTTTCATTGTAATTG	
SYT8-sense	CAGCCTGATAAACTGTATACC	
SYT9-sense	GATTTGAATGCGTGATCACAAG	
SYT10-sense	GATTGGATTCCAGACATTGTG	
SYT11-sense	GCCACCTTGGAATTTGTTAATG	
SYT12-sense	CTGATGATTGAAGAAACCGAG	
SSX2-1-antisense	ACGGAGAATCAGGGTTCTTTGG	
SSX2-2-antisense	TCAGTCTCCACACTGGCAAC	
SSX2-3-antisense	TCAAGGCAACATCCGACTCC	
SSX2-4-antisense	TGGTTTCCAGGGATAGAATGCT	
Real-time PCR		
SYT-specific-sense	CCAGCAACAGTAGTTTACTTTCTATC	106
SSX2-specific-antisense	AAACATAGGGAGGCGACAAA	
SYT-SSX2-FAM probe-sense	ATA+CAA+T+C+CA+G+CAG[1]	

[1] + C, +T, + G = LNA base.

Table 2 Results of rt-PCR analysis by the specific probe and primer sets

Types of DNA	Sample	Ct value 1	Ct value 2	Mean
Genomic	Normal tissue	Undetermined	Undetermined	Undetermined
	Tumor tissue	31.94651	31.30283	31.62467
β-actin	Tumor tissue	28.97511	30.95062	29.96287

Undetermined: No Ct detection till 40 cycles.

instantly separated from the cellular fraction using a three-spin protocol (1500 rpm for 30 min, 3000 rpm for 5 min, and 4500 rpm for 5 min) and stored at -80 ℃.

Circulating cell-free DNA (cfDNA) was isolated from 2 mL of each plasma sample using the QIAamp Circulating Nucleic Acid kit (Qiagen) according to the manufacturer's instructions, and the cfDNA concentration was determined using the Qubit 3.0 fluorometer.

Protocols for RT-PCR and genomic PCR of tissue samples: Reverse transcribed reactions were performed with 400 ng tissue RNA in a 20 μL reaction volume using the high-capacity cDNA reverse transcription kit (Thermo Fisher Scientific) according to the manufacturer's instructions. The complementary DNA was subjected to PCR using AmpliTaq DNA polymerase (Thermo Fisher) and our designed primers (Table 1) with the following conditions: 10 min at 95 ℃, followed by repetitions of 1 min at 95 ℃, 1 min at 60 ℃, and 30 s at 72 ℃ and a final extension step of 30 s at 72 ℃.

Genomic PCR was performed with 10 ng genomic DNA (gDNA) in a 25 μL reaction volume using 1 unit of AmpliTaq DNA polymerase and 0.2 μmol/L of each primer (Table 1). PCR was run using the GeneAmp PCR System 9700 (Thermo Fisher) at the following conditions: 10 min at 95 ℃, followed by repetitions of 1 min at 95 ℃, 1 min at 53 ℃ (40 cycles), and 1 min at 72 ℃ and a final extension step of 30 s at 72 ℃. The accurate length of the PCR products was confirmed using agarose gel electrophoresis. The images were obtained using the BLooK LED transilluminator (BIO-HELIX, Keelung, Taiwan) and a digital camera.

Direct sequencing analysis: The PCR products obtained were subjected to direct sequencing using the BigDye Terminator version1.1 Cycle Sequencing Kit (Thermo Fisher). Samples were run on ABI 3500 genetic analyzer (Applied Biosystems, Foster, United States).

Detection of SYT-SSX2 fusion gene sequence: To detect the fusion gene sequence in tissue and plasma samples, real-time PCR (rt-PCR) was performed in duplicates with 10 ng tissue DNA or 0.5 ng plasma cfDNA using the StepOne real-time PCR systems

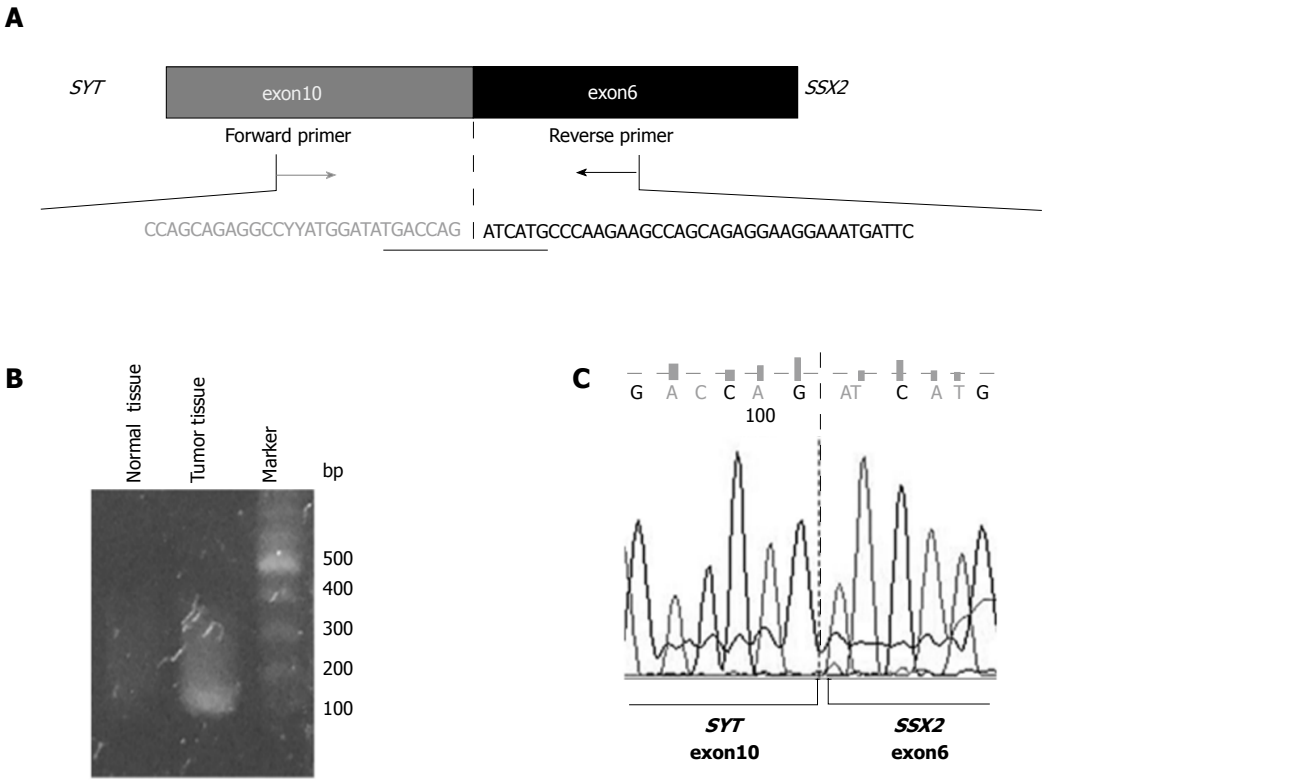

Figure 1 Identification of the *SYT-SSX2* fusion transcript. A: Structure of the *SYT-SSX2* fusion transcript. Exon 10 of the *SYT* gene and exon 6 of the *SSX2* gene are fused together in this transcript. The sequencing of exon is shown. Forward and reverse primers were designed in exon 10 of the *SYT* gene and exon 6 of the *SSX2* gene, respectively; B: The RT-PCR product, including the *SYT-SSX2* fusion site, was obtained from tumor tissue samples only. This analysis was performed more than three times, and a representative result of an electrophoresis is shown; C: The result of direct sequencing of the PCR product is shown. Exon 10 of the *SYT* gene is fused to exon 6 of the *SSX2* gene.

(Thermo Fisher). A pair of primers and specific probes using locked nucleic acid (LNA) bases for detecting the *SYT-SSX2* fusion gene sequence were designed (Table 1; Integrated DNA Technologies, Coralville, United States). The whole rt-PCR mixture (10 μL reaction volume) comprised DNA, Taqman Fast Advanced Master Mix (Thermo Fisher), RNase-free water, 0.5 μmol/L of each primer, and 0.25 μmol/L of probe solution and was performed with the following conditions: 2 min at 50 ℃ and 20 s at 95 ℃, followed by repetitions of 1 s at 95 ℃ and 20 s at 60 ℃ (40 cycles).

Statistical analysis: BLAST software (http://www.ncbi.nlm.nih.gov/BLAST/) was used for sequence data analysis. The detection levels of the fusion gene sequence were compared with those obtained using the ΔΔCt method.

RESULTS

Confirmation of *SYT-SSX2* fusion gene occurrence in tumor tissues: To confirm the fusion of the *SYT* and *SSX2* genes, RT-PCR was performed using total RNA extracted from tumor and adjacent normal tissues. The primer set was designed in exon 10 of the *SYT* gene (SYT-sense) and in exon 6 of the *SSX2* gene (SSX2-antisense) (Figure 1A) for an expected PCR product size of 118 base pairs. The sequence data of this primer sets are shown in Table 1. A PCR product of > 100 base pairs was obtained in tumor tissues only (Figure 1B), and direct sequencing of this PCR product confirmed the fusion between exon 10 of the *SYT* gene and exon 6 of the *SSX2* gene (Figure 1A and C).

Detection of the genomic breakpoint: To detect a genomic breakpoint in intron 10 of the *SYT* gene and intron 5 of the *SSX2* gene, 12 forward primers in *SYT* intron 10 and 3 reverse primers in *SSX2* intron 5 were designed at intervals of approximately 1000 base pairs (Figure 2A and Table 1). Genomic PCR was performed with each forward and reverse primer using gDNA extracted from tumor and normal tissues. The smallest PCR product, approximately 500 base pairs, was detected with the combination of SYT-8 and SSX2-4 primers in tumor tissues only (Figure 2B). The direct sequencing of the obtained PCR product showed a genomic breakpoint within the *SYT* and *SSX2* introns (Figure 2C).

Production of the breakpoint-specific probe: A breakpoint-specific FAM-labeled LNA probe and primer sets for rt-PCR analysis were designed to detect the *SYT-SSX2* fusion sequence in DNA samples (Figure 3A and B, Table 1). Using this specific probe and primer sets, the *SYT-SSX2* fusion sequence was detected in

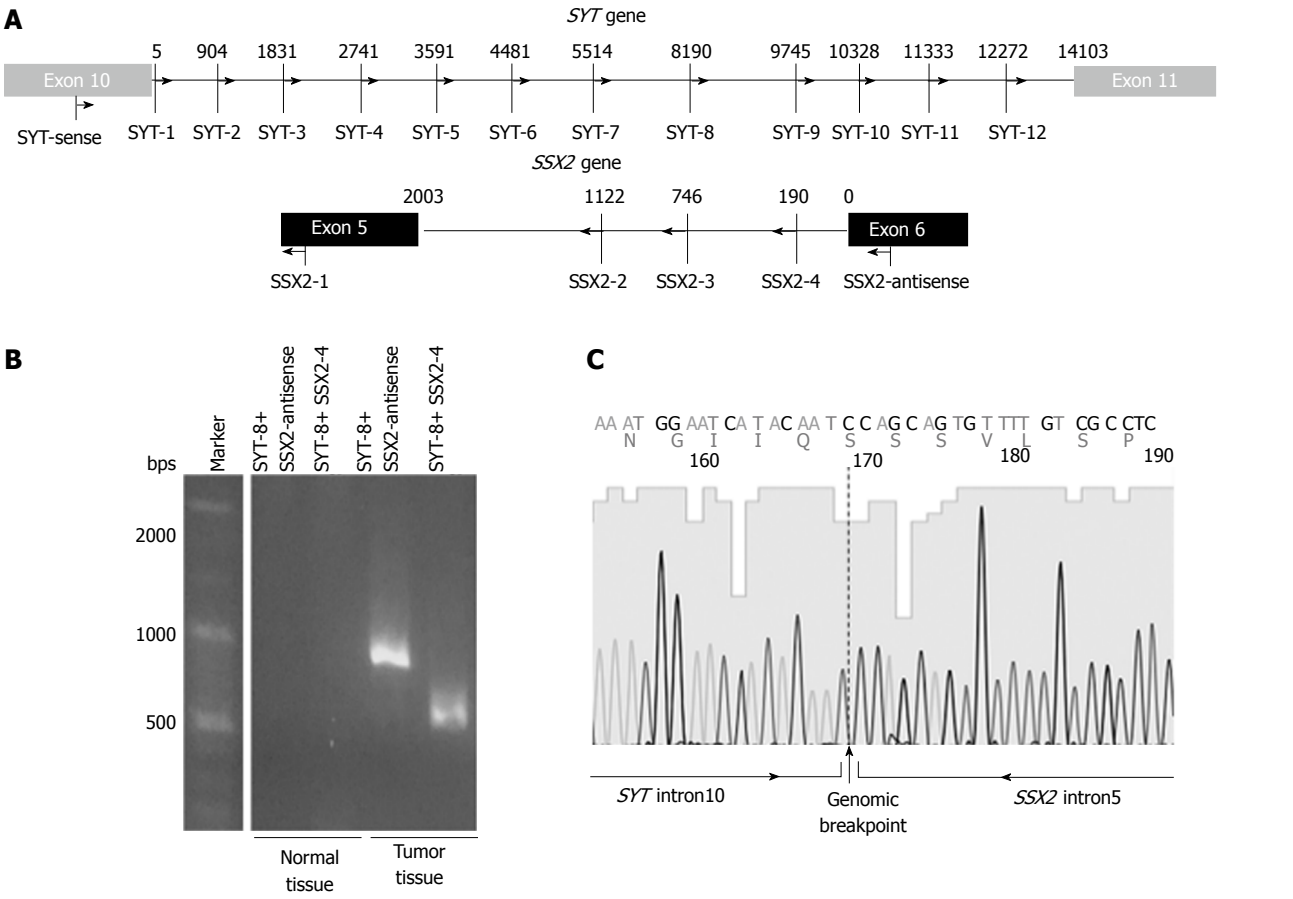

Figure 2 Detection of the *SYT-SSX2* fusion sequence. A: The intronic primer settings in the *SYT* and *SSX2* genes are shown; B: Genomic PCR products were obtained from tumor tissue samples only. This analysis was performed more than two times, and a representative result of an electrophoresis is shown; C: The intronic breakpoint was confirmed by direct sequencing.

10 ng of gDNA extracted from tumor tissues (Ct value; 31.6) (Table 2). Serial dilutions of gDNA extracted from tumor tissue were analyzed by rt-PCR using this specific probe and primer sets to confirm the accurate measurable range. The *SYT-SSX2* fusion sequence was detected proportional to gDNA concentrations from 1 to 0.063 ng (range of Ct value, up to 37, R^2 = 0.974, P = 0.0018) (Figure 4A).

Detection of the *SYT-SSX2* fusion sequence in cfDNA: cfDNA extracted from the plasma was verified by rt-PCR using the specific probe and primer sets. The fusion sequence was detected in the plasma sample collected preoperatively from the patient but not in the plasma sample collected one or six months postoperatively from the patient or in the plasma samples of 10 healthy volunteers (Figure 4B). The Ct value was 35.9 in cfDNA collected preoperatively, whereas it was undetermined in other cfDNA (Not detected till 40 cycles) (Figure 4B).

DISCUSSION

Primary gastric SS is a rare disease, and its diagnosis by clinical or pathological findings is difficult. Detection of the *SYT-SSX* fusion gene using a molecular biological approach is necessary for a definitive diagnosis. In most cases, this fusion gene or fusion sequence was identified from total RNA or DNA of tumor tissues by PCR method. Many alterations, such as microsatellite alteration[12], DNA methylation[13], and some mutations[14], in cancer cells have been recently detected in circulating cfDNA. Regarding translocation-derived diseases such as SS, it may also be possible to detect the fusion sequence in cfDNA. Indeed, Hayashi et al. reported that the *EWS-ETS* fusion gene, specific to Ewing sarcoma, was detected in circulating cfDNA extracted from plasma of a patient with Ewing sarcoma using long-range PCR and digital droplet PCR (ddPCR)[15].

In this study, we developed a highly specific locked nucleic acid (LNA) probe and primer sets for the *SYT-SSX2* fusion gene sequence and detected the sequence in cfDNA extracted from the plasma of a primary gastric SS patient. The translocation causes gene rearrangements in tumor tissues only; therefore, this probe and primer sets specific to the fusion sequence are highly unique to identify the intronic breakpoint. Moreover, the normal PCR method instead of highly accurate and sensitive methods such as ddPCR could detect the objective sequence in a small amount of cfDNA.

Nested PCR[8] or long-range PCR[15] techniques were previously reported for identifying the intronic fusion

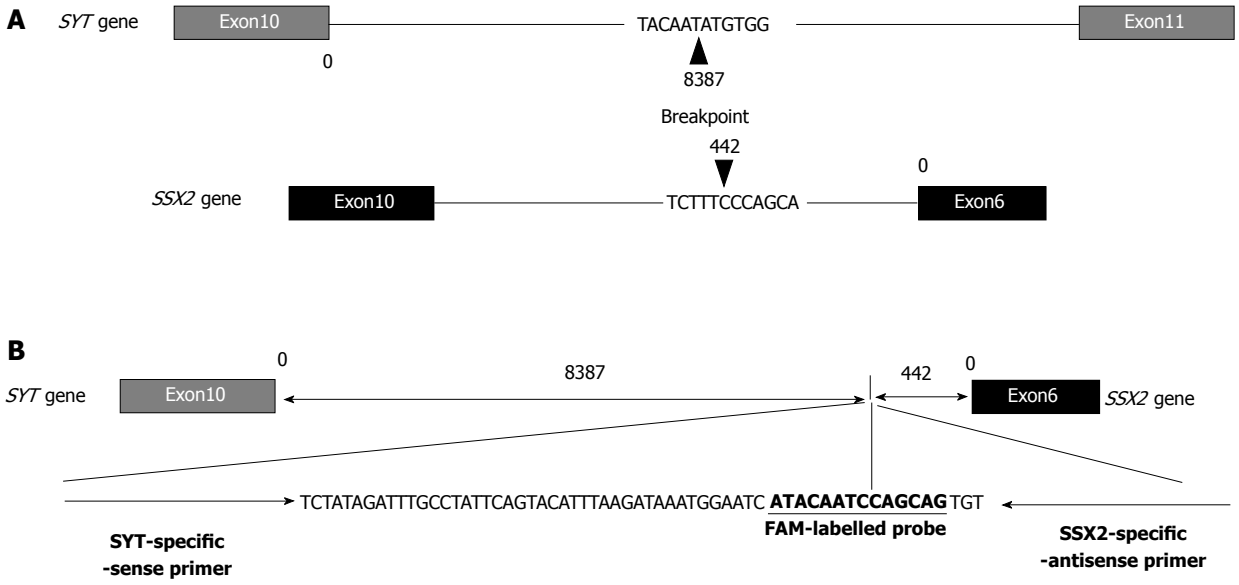

Figure 3 Intronic breakpoint and structure of the fusion sequence with specific probe and primer sets. A: The arrowheads indicate the position and sequence of the intronic breakpoint of the *SYT* and *SSX2* genes; B: The structure and sequence of the FAM-labeled probe and primer sets specific to the intronic breakpoint of the *SYT-SSX* fusion sequence.

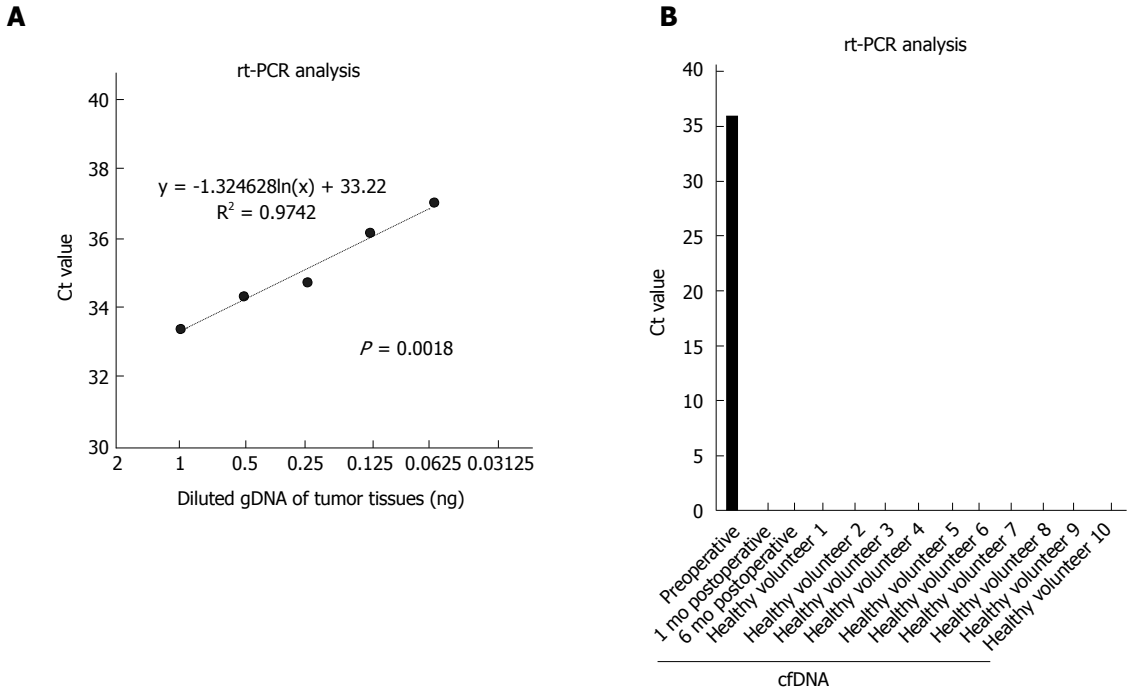

Figure 4 Detection of the fusion gene sequence in cell-free DNA using specific probe and primer sets. A: The range of reproducibility of rt-PCR with the specific probe and primer sets was confirmed. Diluted serial tumor gDNA of 1-0.063 ng was used. The dotted line indicates an approximate curve (R^2 = 0.9742, P = 0.0018); B: cfDNA samples of a patient and 10 healthy volunteers were analyzed using rt-PCR. rt-PCR was performed in duplicate, and mean Ct values are indicated. Standard deviation was calculated from duplicate samples. cfDNA: Cell-free DNA.

sequences of translocation-related diseases. While the detection of *SYT-SSX* fusions in tumor tissues has been previously reported, this is the first report regarding the detection of the fusion sequence in circulating cfDNA. Since the discovery of circulating tumor cfDNA in 1994[16,17], investigations on cfDNA molecules have been proven to be useful for diagnosing or monitoring of disease states[11,18-21]. In this study, the fusion sequence could be detected in preoperative circulating cfDNA only, although the primary lesion was only 20 mm in diameter and undetectable by preoperative computed tomography. We expect the detection method of the *SYT-SSX* fusion sequence in circulating cfDNA to become an effective monitoring tool for SS, because >

90% of SS patients have this reciprocal translocation.

Numerous gene alterations have been recently identified using advanced technologies such as next-generation sequencing, and fusion genes have been reported to contribute to tumorgenesis[22] . For example, recurrent fusions of R-spondin family members RSPO2 and RSPO3, which occur in 10% of colon tumors, have been reported to be involved in the activation of Wnt signaling pathway[23]. NCOA2, a negative growth regulator repressing Wnt signaling pathway, was reported to be disrupted by recurrent fusion with LACTB2 in colorectal cancer[24]. We believe this method can be a less-invasive and personalized monitoring technique with high sensitivity and specificity for translocation-derived diseases, including some cancers.

This technique has some limitations. Sufficient amounts of gDNA from tissue samples need to be obtained to confirm the intronic breakpoint. Frozen tumor samples may be preferred over formalin-fixed tissues to prevent yield decrease because of fragmentation of DNA samples in the latter tissues. Furthermore, although we demonstrated the detection of the fusion sequence in cfDNA of a gastric SS patient, the sensitivity of rt-PCR using cfDNA obtained from 2 mL plasma was not so high (Ct value, 35.9) because of a small amount of cfDNA. A more advanced method to obtain high-quality or large amounts of cfDNA may be more appropriate for this technique in the future regarding a stable application. Finally, while the location of gene fusion is almost same for each disease, the intronic breakpoint may differ in each patient. Thus, a specific probe and primer sets should be designed for each patient per disease. In this regard, if the amounts of collected plasma RNA or sensitivity of the rt-PCR method is improved, a specific probe and primer sets for plasma RNA samples would be more useful and become a valuable diagnostic tool. Large-scale studies will be necessary to confirm the sensitivity and specificity of this method.

In conclusion, we demonstrated the detection of the *SYT-SSX* fusion sequence in the plasma circulating cfDNA of a rare gastric SS patient. In the future, this method may be useful for translocation-derived diseases such as SS or for other cancers which contain translocations.

ARTICLE HIGHLIGHTS

Case characteristics
A 27-year-old woman presented upper abdominal pain.

Clinical diagnosis
Upper abdominal tenderness associated to the gastric tumor.

Differential diagnosis
Stomach tumor including cancer or gastrointestinal stromal tumor.

Laboratory diagnosis
Blood tests ruled out opportunistic infections and severe anemia.

Imaging diagnosis
Upper gastrointestinal endoscopy and ultrasound endoscopy showed a small submucosal tumor less than 20 mm in diameter in the stomach.

Pathological diagnosis
Histological examination of the biopsies showed a spindle cell sarcoma compatible with SS. *SYT-SSX2* fusion gene was detected using biopsy samples by RT-PCR methods.

Treatment
The submucosal tumor was resected by laparosopic and ecdoscopic cooperative surgery.

Related reports
Previous cases of SS whose intronic breakpoints were confirmed using tumor samples have been described.

Term explanation
SYT-SSX fusion gene is SS-specific genetic alternation and detection of SYT-SSX contributes much to the diagnosis of SS.

Experiences and lessons
In patients with SS and other translocation-related diseases, detection of fusion genes specific for those diseases is a powerful diagnostic tool and the detection using liquid sample, such as blood, can be a valuable and less invasive monitoring tool as well.

REFERENCES

1 **Herzog CE**. Overview of sarcomas in the adolescent and young adult population. *J Pediatr Hematol Oncol* 2005; **27**: 215-218 [PMID: 15838394 DOI: 10.1097/01.mph.0000163712.39139.b6]

2 **Turc-Carel C**, Dal Cin P, Limon J, Rao U, Li FP, Corson JM, Zimmerman R, Parry DM, Cowan JM, Sandberg AA. Involvement of chromosome X in primary cytogenetic change in human neoplasia: nonrandom translocation in synovial sarcoma. *Proc Natl Acad Sci USA* 1987; **84**: 1981-1985 [PMID: 3031659 DOI: 10.1073/pnas.84.7.1981]

3 **de Leeuw B**, Balemans M, Olde Weghuis D, Geurts van Kessel A. Identification of two alternative fusion genes, SYT-SSX1 and SYT-SSX2, in t(X;18)(p11.2;q11.2)-positive synovial sarcomas. *Hum Mol Genet* 1995; **4**: 1097-1099 [PMID: 7655467 DOI: 10.1093/hmg/4.6.1097]

4 **Tamborini E**, Agus V, Mezzelani A, Riva C, Sozzi G, Azzarelli A, Pierotti MA, Pilotti S. Identification of a novel spliced variant of the SYT gene expressed in normal tissues and in synovial sarcoma. *Br J Cancer* 2001; **84**: 1087-1094 [PMID: 11308259 DOI: 10.1054/bjoc.2000.1710]

5 **Güre AO**, Wei IJ, Old LJ, Chen YT. The SSX gene family: characterization of 9 complete genes. *Int J Cancer* 2002; **101**: 448-453 [PMID: 12216073 DOI: 10.1002/ijc.10634]

6 **Crew AJ**, Clark J, Fisher C, Gill S, Grimer R, Chand A, Shipley J, Gusterson BA, Cooper CS. Fusion of SYT to two genes, SSX1 and SSX2, encoding proteins with homology to the Kruppel-associated box in human synovial sarcoma. *EMBO J* 1995; **14**: 2333-2340 [PMID: 7539744]

7 **Otsuka S**, Nishijo K, Nakayama T, Aoyama T, Ishibe T, Shibata KR, Shima Y, Nakamura T, Otsuka T, Toguchida J. A variant of the SYT-SSX2 fusion gene in a case of synovial sarcoma. *Cancer Genet Cytogenet* 2006; **167**: 82-88 [PMID: 16682293 DOI: 10.1016/j.cancergencyto.2005.11.012]

8 **Törnkvist M**, Brodin B, Bartolazzi A, Larsson O. A novel type of SYT/SSX fusion: methodological and biological implications. *Mod Pathol* 2002; **15**: 679-685 [PMID: 12065783 DOI: 10.1038/modpathol.3880587]

9 **Torres Rivas HE**, Fernández S, Fresno MF. Primary gastric synovial sarcoma. *Pathology* 2014; **46**: 253-256 [PMID: 24614723 DOI: 10.1097/PAT.0000000000000078]

10 **Michot N**, Robert PE, De Muret A, Marques F, de Calan L, Benchellal Z. Gastric synovial sarcoma: case report and systematic review of literature. *J Gastrointest Cancer* 2014; **45** Suppl 1: 129-131 [PMID: 24595970 DOI: 10.1007/s12029-014-9591-1]

11 **Chen XQ**, Stroun M, Magnenat JL, Nicod LP, Kurt AM, Lyautey J, Lederrey C, Anker P. Microsatellite alterations in plasma DNA of small cell lung cancer patients. *Nat Med* 1996; **2**: 1033-1035 [PMID: 8782463 DOI: 10.1038/nm0996-1033]

12 **Wong IH**, Lo YM, Zhang J, Liew CT, Ng MH, Wong N, Lai PB, Lau WY, Hjelm NM, Johnson PJ. Detection of aberrant p16 methylation in the plasma and serum of liver cancer patients. *Cancer Res* 1999; **59**: 71-73 [PMID: 9892188]

13 **Le Calvez-Kelm F**, Foll M, Wozniak MB, Delhomme TM, Durand G, Chopard P, Pertesi M, Fabianova E, Adamcakova Z, Holcatova I, Foretova L, Janout V, Vallee MP, Rinaldi S, Brennan P, McKay JD, Byrnes GB, Scelo G. KRAS mutations in blood circulating cell-free DNA: a pancreatic cancer case-control. *Oncotarget* 2016; **7**: 78827-78840 [PMID: 27705932 DOI: 10.18632/oncotarget.12386]

14 **Hayashi M**, Chu D, Meyer CF, Llosa NJ, McCarty G, Morris CD, Levin AS, Wolinsky JP, Albert CM, Steppan DA, Park BH, Loeb DM. Highly personalized detection of minimal Ewing sarcoma disease burden from plasma tumor DNA. *Cancer* 2016; **122**: 3015-3023 [PMID: 27351911 DOI: 10.1002/cncr.30144]

15 **Sorenson GD**, Pribish DM, Valone FH, Memoli VA, Bzik DJ, Yao SL. Soluble normal and mutated DNA sequences from single-copy genes in human blood. *Cancer Epidemiol Biomarkers Prev* 1994; **3**: 67-71 [PMID: 8118388]

16 **Vasioukhin V**, Anker P, Maurice P, Lyautey J, Lederrey C, Stroun M. Point mutations of the N-ras gene in the blood plasma DNA of patients with myelodysplastic syndrome or acute myelogenous leukaemia. *Br J Haematol* 1994; **86**: 774-779 [PMID: 7918071 DOI: 10.1111/j.1365-2141.1994.tb04828.x]

17 **Schwarzenbach H**, Hoon DS, Pantel K. Cell-free nucleic acids as biomarkers in cancer patients. *Nat Rev Cancer* 2011; **11**: 426-437 [PMID: 21562580 DOI: 10.1038/nrc3066]

18 **McDermott U**, Downing JR, Stratton MR. Genomics and the continuum of cancer care. *N Engl J Med* 2011; **364**: 340-350 [PMID: 21268726 DOI: /10.1056/NEJMra0907178]

19 **Siravegna G**, Bardelli A. Genotyping cell-free tumor DNA in the blood to detect residual disease and drug resistance. *Genome Biol* 2014; **15**: 449 [PMID: 25222559 DOI: 10.1186/s13059-014-0449-4]

20 **Shoda K**, Ichikawa D, Fujita Y, Masuda K, Hiramoto H, Hamada J, Arita T, Konishi H, Komatsu S, Shiozaki A, Kakihara N, Okamoto K, Taniguchi H, Imoto I, Otsuji E. Monitoring the HER2 copy number status in circulating tumor DNA by droplet digital PCR in patients with gastric cancer. *Gastric Cancer* 2017; **20**: 126-135 [PMID: 26874951 DOI: 10.1007/s10120-016-0599-z]

21 **Seshagiri S**, Stawiski EW, Durinck S, Modrusan Z, Storm EE, Conboy CB, Chaudhuri S, Guan Y, Janakiraman V, Jaiswal BS, Guillory J, Ha C, Dijkgraaf GJ, Stinson J, Gnad F, Huntley MA, Degenhardt JD, Haverty PM, Bourgon R, Wang W, Koeppen H, Gentleman R, Starr TK, Zhang Z, Largaespada DA, Wu TD, de Sauvage FJ. Recurrent R-spondin fusions in colon cancer. *Nature* 2012; **488**: 660-664 [PMID: 22895193 DOI: 10.1038/nature11282]

22 **Yu J**, Wu WK, Liang Q, Zhang N, He J, Li X, Zhang X, Xu L, Chan MT, Ng SS, Sung JJ. Disruption of NCOA2 by recurrent fusion with LACTB2 in colorectal cancer. *Oncogene* 2016; **35**: 187-195 [PMID: 25823027 DOI: 10.1038/onc.2015.72]

23 **Urakami K**, Shimoda Y, Ohshima K, Nagashima T, Serizawa M, Tanabe T, Saito J, Usui T, Watanabe Y, Naruoka A, Ohnami S, Ohnami S, Mochizuki T, Kusuhara M, Yamaguchi K. Next generation sequencing approach for detecting 491 fusion genes from human cancer. *Biomed Res* 2016; **37**: 51-62 [PMID: 26912140 DOI: 10.2220/biomedres.37.51]

24 **Yu J**, Wu WK, Liang Q, Zhang N, He J, Li X, Zhang X, Xu L, Chan MT, Ng SS, Sung JJ. Disruption of NCOA2 by recurrent fusion with LACTB2 in colorectal cancer. *Oncogene* 2016; **35**: 187-195 [PMID: 25823027 DOI: 10.1038/onc.2015.72]

P- Reviewer: Vorobjova T **S- Editor**: Gong ZM **L- Editor**: A **E- Editor**: Ma YJ

Published by **Baishideng Publishing Group Inc**
7901 Stoneridge Drive, Suite 501, Pleasanton, CA 94588, USA
Telephone: +1-925-223-8242
Fax: +1-925-223-8243
E-mail: bpgoffice@wjgnet.com
Help Desk: http://www.f6publishing.com/helpdesk
http://www.wjgnet.com

ISSN 1007-9327